UNIVERSITÀ DEGLI STUDI DI MILANO
Scuola di Dottorato in Terra Ambiente e Biodiversità
Dipartimento di Bioscienze

Dottorato di ricerca in Scienze Naturalistiche e Ambientali
XXV Ciclo

Local and regional distribution of POPs in mountain environments

Evaluation of burden and fluxes in biotic and abiotic matrices

Niccolò Guazzoni

Mat: R08794

Tutor: Dott. Paolo Tremolada

Coordinatore: Prof. Nicola Saino

Anno Accademico: 2011/2012

Index

Chapter I

Introduction

I - General Frame

Obsolescent persistent organic pollutants (POPs), despite the international ban of many of them by the Stockholm convention (2001), still need a high grade of attention and research for two main reason. Firstly they are still present in anthropic and natural environments due to their resistance to degradation, continuing to pone a threat on environmental and human health. Secondly the study of the distribution pattern of old pollutants could be extremely useful to understand also the possible distribution of new pollutant and the development of predictive models could also lead to a better insight on the forces driving chemicals at different spatial scales (from the local scale to the global one). A wide amount of papers have been published about the macro-distribution of chemicals basing on the cornerstone works on the *global fractional distillation* and on the *cold condenser effect* (Wania and Mackay, 1993; Wania and Mackay, 1994; Wania and Mackay, 1996). According to those theories, POPs can be divided into classes of volatility, depending on their chemical and physical properties, that cause a different latitudinal distribution. Generally in areas with high temperatures (low latitudes), there will be mainly volatilization, while in areas with low temperatures (high latitudes or altitude) it will be more deposition and retention.

Soils are the main sink of lipophilic pollutants in terrestrial environments (Mackay, 2001; Meijer et al., 2003) and the distribution in this compartment is driven mainly by temperature and organic matter. Lower temperatures favours condensation and adsorption in soils raising the K_{sa} partition coefficient (that express the concentration ratio at the equilibrium between soil and air; Hippelein and McLachlan, 1998), while otherwise higher temperatures favours volatilization. Since these pollutants are generally highly lipophilic when they reach soils they tend to be adsorbed to the soil organic matter (SOM) fraction (Sweetman et al., 2005). Airborne pollutant could be at vapour phase or associated to atmospheric particulate, depending on their K_{oa} (a

parameter that express the concentration ratio between *n*-octanol and air; Finizio et al., 1997) and could reach soils by dry deposition (direct deposition of vapour phase molecules or deposition of polluted airborne particles; Cousins et al., 1999;) or wet deposition (scavenging of molecules or particles by rain or snow; Lei and Wania, 2004). Another way of deposition for airborne POPs is the *forest filter effect* (Nizzetto et al., 2008), that describes the tendency of airborne pollutant to be scavenged by vegetation. The cuticular waxes that cover leaf surfaces are an excellent solvents in which lipophilic pollutant (that could be coming from the air or re-volatilized from soils) could be retained (Moeckel et al., 2008a). Once POPs are taken up by vegetation, they are then deposited on soils when leaves fall down, giving an over-contamination of forested soils in comparison to that of non forested ones. Partitioning into the vegetal material has been interpreted as a complex system depending on the physical and chemical properties of pollutants, with gaseous deposition and particle deposition dominating the fluxes of pollutants with low and high K_{oa} respectively (McLachlan, 1999). Moreover vegetation is the primary way for POPs to enter into terrestrial food chains (McLachlan, 1993).

POPs tend to bioaccumulate into higher trophic levels and to biomagnify between trophic levels (Armitage and Gobas, 2007). The accumulation of POPs due to contaminated food assumption is also the main source of human contamination (Donato et al., 2006) and cow milk and diary products are responsible for 25-30% of the total intake (Duarte-Davidson and Jones, 1998). Following these observations some attempt have been done to understand the pattern of transfer between vegetation and milk in diary cows, at least in controlled conditions and in feeding experiments (Sweetman et al., 1999), defining the carryover rate (COR) of pollutants in the complex food-cow-milk system evidencing differences in degradability and intake of different pollutants.

Mountainous areas then could surely be regarded as "pollutants condenser" since they are areas (especially at a high altitude) with temperatures colder than their surroundings, favouring deposition and retention of POPs. Moreover, the typical

build-up of slowly mineralizing humus layers, containing high amounts of SOM makes soils of such ecosystems an important global sink for POPs released to the environment (Moeckel et al., 2008b). These observation could be resumed in the concept of the Mountain Contamination Potential (MCP; Daly et al., 2007) that quantifies the accumulation of POPs of a mountain in relation to its surroundings. In general terms mountains are great "natural laboratories" to study the distribution of POPs since they present a wide range of environmental conditions in a small spatial scale. Moreover mountainous environment are affected by a wide temperature range following daily and seasonal cycle. These variations are useful to evaluate the dependence of the distribution from the temperature oscillations, giving the possibility to evaluate in a small spatial and temporal scale the partitive effects that could be observed in macro-scale along the planet profile.

I.1. Outline of the thesis

In this thesis it is summarized the work about the driving forces that determine distribution of POPs at a local and meso-scale in mountain environments. Macro-variability (differences of orders of magnitude) and global distribution model are useful to assess the planetary distribution, but it is also very important to understand the variability (differences within an order of magnitude) that influence the distribution at a local scale.

In chapter II it is reported the situation of the PCBs pollution in soils of the Andossi Plateau (central Italian Alps) and its variability during the spring-summer season, along with micrometeorological and pedological effects that affect the vertical and horizontal distribution of pollutants. These findings could be useful to include the meso and micro-variability into sampling plan and challenge the view of soils as a stable retention compartment for POPs.

In chapter III the data about PCBs pollution in soils are used to validate a distribution model with predictive capacity. The main equation of the model, along with data on SOM and temperature could be used to predict contamination of a whole area with a small number of samplings. Moreover comparing distribution in different date it is possible to use the model to assess contamination net fluxes between different periods of the year.

In chapter IV the relation between pollutants and SOM has been evaluated by dividing SOM into its humic constituents. This work points out the importance of understanding not only the quantity of OM in soils but also its quality to assess the vertical and horizontal distribution patterns of contamination. A relation with the humin fraction is evidenced, pointing out that humin rich soils could be more prone to POPs contamination.

The transfer of pollutants between the soil-air system and the food chains has been analyzed in chapter V and VI. The transfer between soil, vegetation and the milk of cows grazing on the pasture has been assessed and COR values have been calculated in a field experiment without controlled food assumption, which gives a more ecologically realistic picture of the soil-vegetation-cow-milk system.

Finally in chapter VII it is reported a case study of POPs contamination in a mountainous area in Tanzania. This study gives the first contamination data in the soils of that zone and confirms the effects of meteorological and pedological features on POPs distribution in this equatorial environment.

I.2. References

Armitage, J.M., Gobas, F.A.P.C. 2007. A terrestrial food-chain bioaccumulation model for POPs. Environ. Sci. Technol. 41, 4019–4025.

Cousins, I.T., Beck, A.J., Jones, K.C., 1999. A review of the processes involved in the exchange of semi-volatile organic compounds (SVOC) across the air–soil interface. Sci. Total Environ. 228, 5–24.

Daly, G.L., Lei, Y.D., Teixeira, C., Muir, D.C.G., Castillo, L.E., Wania, F., 2007. Accumulation of current-use pesticides in neotropical montane forests. Environ. Sci. Technol. 31, 1118–1123.

Donato, F., Magoni, M., Bergonzi, R., Scarcella, C., Indelicato, A., Carasi, S., Apostoli, P., 2006. Exposure to polychlorinated biphenyls in residents near a chemical factory in Italy: The food chain as main source of contamination. Chemosphere. 64, 1562–1572.

Duarte-Davidson, R., Jones, K.C., 1998. Polychlorinated Biphenils (PCBs) in UK population: Estimated intake, exposure and body burden, Sci. Total. Environ. 151, 131–152

Finizio, A., Mackay, D., Bidleman, T., Harner, T., 1997. Octanol-air partition coefficient as a predictor of partitioning of semi-volatile organic chemicals to aerosols. Atmos. Environ. 31, 2289–2296.

Hippelein, M., McLachlan, M.S., 1998. Soil/air partitioning of semivolatile organic compounds. 1. Method development and influence of physical–chemical properties. Environ. Sci. Technol. 32, 310–316.

Lei, Y.D., Wania, F., 2004. Is rain or snow a more efficient scavenger of organic chemicals?. Atmos. Environ. 38, 3557–3571.

Mackay, D., 2001. Multimedia environmental models: the fugacity approach. Lewis/CRC, Boca Raton, FL.

McLachlan, M.S., 1993. Mass balance of polychlorinated biphenyls and other organochlorine compounds in a lactating cow. J Agr. Food. Chem. 41, 474–480.

McLachlan, M.S., 1999. Framework for the interpretation of measurements of SOCs in Plants. Environ. Sci. Technol. 33, 1799–1804.

Meijer, S.N., Ockenden, W.A., Sweetman, A.J., Breivik, K., Grimalt, J.O., Jones, K.C., 2003. Global distribution and budget of PCBs and HCB in background surface soils: implications for sources and environmental processes. Environ. Sci. Technol. 37, 667–672.

Moeckel, C., Thomas, G.O., Barber, J.L., Jones, K.C., 2008a. Uptake and storage of PCBs by plant cuticles. Environ. Sci. Technol. 42, 100–105

Moeckel, C., Nizzetto, L., Di Guardo, A., Steinnes, E., Freppaz, M., Filippa, G., Camporini, P., Benner, J., Jones, K.C., 2008b. Persistent organic pollutants in boreal and montane soil profiles: distribution, evidence of processes and implications for global cycling. Environ. Sci. Technol. 42, 8374–8380.

Nizzetto, L., Jarvis, A., Brivio, P.A., Jones, K.C., Di Guardo, A., 2008. Seasonality of the air–forest canopy exchange of persistent organic pollutants. Environ. Sci. Technol. 42, 8778–8783.

Stockholm convention, 2001. Stockholm, Sweden. http://chm.pops.int/default.aspx.

Sweetman, A.J., Thomas, G.O., Jones, K.C., 1999. Modelling the fate and the behaviour of lipophilic organic contaminants in lactating dairy cows. Environ. Pollut. 104, 261–270.

Sweetman, A.J., Dalla Valle, M., Prevedouros, K., Jones, K.C. (2005). The role of soil organic carbon in the global cycling of persistent organic pollutants (POPs): Interpreting and modelling field data. Chemosphere. 60, 959–972.

Wania, F., Mackay, D., 1993. Global fractionation and cold condensation of low volatility organochlorine compounds in polar regions. Ambio. 22, 10–18.

Wania, F., Mackay, D., 1994. A global distribution model for persistent organic chemicals. Sci. Total Environ. 160/161, 211–232.

Wania, F., Mackay, D., 1996. Tracking the distribution of persistent organic pollutants. Environ. Sci. Technol. 30, 390–396.

Chapter II

Guazzoni, N., Comolli, R., Mariani, L., Cola, G., Parolini, M., Binelli, A., Tremolada, P., 2011. Meteorological and pedological influence on the PCBs distribution in mountain soils. Chemosphere 83, 186–192.

Chemosphere 83 (2011) 186–192

Contents lists available at ScienceDirect

Chemosphere

journal homepage: www.elsevier.com/locate/chemosphere

Meteorological and pedological influence on the PCBs distribution in mountain soils

Niccolò Guazzoni [a,*], Roberto Comolli [b], Luigi Mariani [c], Gabriele Cola [c], Marco Parolini [a], Andrea Binelli [a], Paolo Tremolada [a]

[a] Department of Biology, University of Milan, Via Celoria 26, 20133 Milan, Italy
[b] Department of Environmental and Land Sciences (DISAT), University of Milan Bicocca, Piazza della Scienza 1, 20126 Milan, Italy
[c] Department of Crop Science, University of Milan, Via Celoria 2, 20133 Milan, Italy

ARTICLE INFO

Article history:
Received 30 June 2010
Received in revised form 3 December 2010
Accepted 9 December 2010
Available online 3 January 2011

Keywords:
PCBs
Alpine soils Seasonal variation Layer effect
Aspect effect Summer volatilisation

ABSTRACT

Polychlorinated biphenyls (PCBs) are a threat to environmental and human health due to their persistence and toxicological effects. In this paper, we analyse some meteorological and organic-matter-related effects on their distribution in the soils of an Alpine environment that is not subject to direct contamination. We collected samples and measured the contamination of 12 selected congeners from three soil layers (O, A1 and A2) and from North-, plain- and South-facing slopes on six different dates spanning the entire snowless portion of the year. We recorded the hourly air and soil temperatures, humidity and rainfall in the study period. We found evidence that PCBs contamination in soils varies significantly, depending on sampling date, layer and aspect. The observed seasonal trend shows an early summer peak and a rapid decrease during June. The layer effect demonstrates higher dry-weight-based concentrations in the O layer, whereas the differences are much smaller for SOM-based concentrations. Different factors caused significantly higher concentrations in northern soils, with a N/S enrichment factor ranging from 1.8 to 1.5 during the season. The southern site has significantly more rapid early-summer re-volatilisation kinetics (half-time of 16 d for South, 25 d for North).

1. Introduction

The continuing threat to human and environment health from PCBs (polychlorinated biphenyls) necessitates maintaining a high level of alert on these compounds (Helyar et al., 2009; Johnson et al., 2009). Mountains are useful and important areas for studying the environmental distribution of POPs (persistent organic pollutants), and many studies have been conducted worldwide (Grimalt et al., 2001; Barra et al., 2005; Nizzetto et al., 2008; Moeckel et al., 2008; Tremolada et al., 2009). It has been estimated that the soil contains the majority of the total environmental burden of POPs (Mackay, 2001; Meijer et al., 2003), and mountain soils in particular have some characteristics that emphasise retention, such as high organic-matter content, efficient snow scavenging (Lei and Wania, 2004), low temperatures and particular wind conditions (anabatic winds) that move contaminants from point sources along the mountain slopes. The total pollutant burden of mountain soils depends on the physical and chemical properties of each pollutant, expressed by biphasic partition coefficients. These parameters are also correlated with temperature because a decrease in temperature tends to lower the air–water partition coefficients (K_{AW}) of POPs (Daly et al., 2007) and raise their soil–air partition coefficients (K_{SA}) (Hippelein and McLachlan, 1998). This effect favours the accumulation of POPs in vegetation and soil at high altitudes. It is possible to identify an annual cycle of pollutant transfer in a mountain area. During the winter season, low temperature and the recurrence of snowy precipitation causes deposition of airborne pollutants and their retention in the snow mantle. The quantity of POPs deposited depends directly on the amount of pollutants in the air. The higher temperatures at lower altitudes (such as plains, in which the majority of pollutants are emitted) favour the volatilisation of compounds (Wania et al., 1998a), and anabatic winds (which blow during daytime) tend to carry polluted air masses up the slopes of mountains. During spring, the snow mantle melts and releases pollutants into the atmosphere or the melting water–soil system. This latter phenomenon drives a particular POP behaviour because hydrophobic pollutants will not flow away and tend to be deposited on soils (Meyer et al., 2006). When the thaw is complete, the soil surface is directly exposed to air, and soil temperatures increase, so PCBs can re-volatilise and deposit elsewhere by the well-known "Grasshopper Effect" (Calamari et al., 1991). Dalla Valle et al. (2005) theorised the concept of a maximum reservoir capacity for soils, which is based on temperature, K_{sa} and organic matter composition. Based on this model, great concentration differences are expected in mountainous areas, which have steep gradients of temperature and soil properties

* Corresponding author. Tel.: +39 02 50314715; fax: +39 02 50314713.
E-mail address: niccolo.guazzoni@unimi.it (N. Guazzoni).

0045-6535/$ - see front matter © 2010 Elsevier Ltd. All rights reserved.
doi:10.1016/j.chemosphere.2010.12.043

(and thus high ΔK_{sa}, which is temperature- and SOM-dependent; Hippelein and McLachlan, 1998). Snowy precipitation interferes with the seasonality by covering the soil and by scavenging airborne pollutants during the winter.

We assume that the POP concentration in European mountain soils is influenced not only by macro-meteorological patterns (e.g., dynamical anticyclones, Atlantic troughs) but also by meso-meteorological (e.g., staü/foehn effects) and micro-meteorological patterns (e.g., mountain/valley breezes) (Barry, 1992). Relief features, such as aspect, slope and landforms, interact with the meteorological patterns, giving rise to peculiar fields of meteorological variables (solar radiation, air and soil temperature, relative humidity, wind and precipitation) that could lead to different POP concentrations. In a previous study, Tremolada et al. (2009) found low POP concentrations in the soil of the southern slope of the Andossi plateau (central Italian Alps), which has higher solar radi-ation and lower soil humidity than the northern side, where condi-tions such as low temperatures favour the deposition and retention of pollutants.

Aside from meteorological effects, POP concentration in soils is also determined by another factor: given their high affinity to soil organic matter (Meijer et al., 2002, 2003; Li et al., 2003), POPs are theoretically present in higher concentrations in soils with a higher percentage of organic matter.

In this paper, we analyse the concentration data of 12 selected PCB congeners obtained from a spring–summer-long sampling campaign of the surface soil horizons of the Andossi plateau (Italy) to understand the importance of seasonality and the solar aspect on PCBs contamination in an alpine environment. Soil samples from three different layers of the superficial soil, in which the majority of soil-bound POPs reside (Moeckel et al., 2008), were also studied to investigate the relation between the organic matter and contamination and between the different layers and environmental features described above. Moreover, this work offers the opportunity to validate on a local scale in a mountain environment the maximum reservoir capacity concept for soil, modelled on a global scale by Dalla Valle et al. (2005).

2. Materials and methods

2.1. Sampling

Soil samples were taken at the Andossi plateau near Splugen Pass in the central Italian Alps during 2008. Soil samples were collected at approximately 1930 m a.s.l. in three nearby sites (less than 100 m distance) but with different aspects (North-, plain- and South-facing). The sampling sites were fenced (5 m × 5 m fences) to prevent the entry of cows that graze on the plateau (a photo of the area and of the fences are reported in the SI). The vegetation present in the Andossi plateau is mainly the result of the anthropic processes of the grazing of cows during the summer, which maintains herbaceous species instead of the upper limit of coniferous woods. The variability of grass species reflects the cows' grazing pressure and the local variability of the pedo-climatic conditions, determined by substrate typology, slope, and solar-radiation exposure. The main vegetational typology of this subalpine area is consistent with the pure or mixed *nardetum*, principally in northern aspects, although other associations are often found (especially in the plan site and in the south aspect), such as *Seslerieto-Semperviretum*, *Poetum* and *Rhodoro-Vaccinietum* (SISS, 2007).

Samples were collected on six dates to cover the entire period in which the soil is free from snow mantle (*T*1 – 06/01/08, *T*2 – 06/27/08, *T*3 – 07/19/08, *T*4 – 08/07/08, *T*5 – 09/09/08, *T*6 – 10/01/08). Within every fence, three cubes (edge 10 cm) of soil were taken and separated into three layers: the O layer (0–1 cm depth), which is very thin in the Alpine grasslands and contains litter and roots in addition to organic-matter-rich soil, the A1 layer (1–4 cm depth) and the A2 layer (4–7 cm depth). The three samples from each layer were homogenised (by manual mixing by site) to reduce the local variability in soil, wrapped in acetone-washed aluminium foil, enclosed in a plastic bag and labelled with the date (*T*1–6), layer and aspect (N, P and S). The samples were stored at −20 °C until analyses were performed.

2.2. Meteorological data

The meteorological monitoring of the study area was performed by three meteorological stations, that measured soil temperature (−0.05 m and −0.1 m), relative soil humidity (−0.05 m) and air temperature (1.80 m), specifically set up in the three experimental sites. The sampling site located at the highest elevation was also provided with a sensor for global solar radiation (2 m). Data were gauged with a time step of 10 min. Rainfall data were collected using totaliser rain gauges. The placement of stations and instruments was carried out following the criteria established by the World Meteorological Organisation (1996).

The first sampling period was not covered by direct meteorological data because data collection started on June 28th. However, the Laboratorio Valchiavenna meteorological station is located approximately 5 km from the sampling sites (Borghetto di Val Febbraro) and provided data for the missing period. Because this latter station is nearly 100 m higher and located in a different geomorphologic context, a linear correlation model between the hourly mean temperatures of the two sites from June 28th to November 1st (R^2 = 0.94) was developed to obtain the missing air–temperature data. These latter data were then used to calculate the soil temperature for the missing period by applying a linear correlation between the soil temperature and the mean air temperature of 2 d earlier. This model, developed on data measured daily, is founded on the robust correlation observed for all soils (−0.05 and −0.1 m for the three sites, with R^2 between 0.84 and 0.90).

2.3. Determination of organic matter

Each soil sample was analysed for organic-C content by an elemental analyser (Flash EA 1112 NC soil, ThermoFisher, Waltham, MA, USA). The organic-matter content was estimated from the organic-C content using a 1.724 multiplier constant, as indicated in Nelson and Sommers (1996).

2.4. PCBs quantification

Samples were lyophilised, extracted in a soxhlet apparatus, digested with sulphuric acid, cleaned on a multilayer column and analysed using GC/MS/MS methodology. Complete information on the PCBs quantification is available in the Supplementary information.

2.5. Statistical analyses

The software SPSS 18.0 was used to perform the Kolmogorov–Smirnov test to verify the data distribution and to obtain linear correlations, conduct generalised linear modelling (GLM) and perform the Bonferroni *post hoc* test.

3. Results

3.1. PCB levels

The PCBs concentration values (ΣPCBs) show large variability (from ∼0.5 ng g^{-1} d.w. to ∼5 ng g^{-1} d.w.) with the highest values

found in the first sampling date (*T*1), in the O layer and in northern samples (see Supplementary information for complete concentration data). The ΣPCBs is consistent with the data obtained in the same area in 2007 (Tremolada et al., 2009). Moreover, the mean concentrations are lower than those observed in forest soils in the Alps (Offenthaler et al., 2009), and this difference can be ex-plained by the absence of the "forest-filter effect" in a grassland (Nizzetto et al., 2006).

The relative abundance of PCBs (calculated for all layers together, Fig. 1) shows very low amounts of 3 Cl and 4 Cl CBs, while the most abundant congeners are CB-153 (26 ± 2.5%, 6 Cl) and CB-138 (20 ± 1.7%, 6 Cl). This relatively high level is higher than the congener abundance in commercial PCB mixtures (Frame et al., 1996; Breivik et al., 2002) and is higher than those found in Aroclor 1254 and 1260 in particular, which are the most heavily used PCB mixtures in Italy (Breivik et al., 2002).

CB-118 is the only dioxin-like CB (the congeners with structure and toxicity comparable to TCDD, Van Den Berg et al., 1998) analysed in this study, and it represents ~5.6% of the ΣPCBs. Observing that a number of dioxin-like PCBs have 5 Cl atoms (Van Den Berg et al., 1998) and that these congeners respond very well to all effects analysed later in this paper, the topic of this work becomes useful for assessing risks for human and environment health. Furthermore, other PCBs have also been shown to have toxic effects (Richthoff et al., 2003; Binelli et al., 2006), and their presence deserves constant attention even if their levels are below Italian legal limits (60 ng g^{-1} d.w. for agricultural soils, DLgs 152/06).

3.2. Meteorological conditions of the experimental period

The climate in the Andossi plateau is typical of an endoalpine area (Barry, 1992), with an annual mean temperature of 2 °C and an annual mean precipitation of 1300 mm (50% snow) with a pluviometric maximum in summer (SISS, 2007). The recorded air temperatures were quite similar in the three sampling sites because of their proximity.

In the study period, the monthly mean temperatures were 5.8 °C in May, 10.2 °C in June, 11.3 °C in July and 6.5 °C in Septem-ber, and these data are in excellent agreement with the 30-year cli-matic normal for the area of study (SISS, 2007). Daily and hourly air and soil records (Fig. 2) highlight the tendency of the soil temper-ature at different sites to significantly diverge during sunny days and during daytime and to re-converge during night time and dur-ing rainy days, showing the effects of energy balance driven by net radiation (Stull, 1997). The monthly amount of rain was higher than the normal value (based on 1971–2000 mean values. SISS, 2007). Finally, the daily humidity of the soils (Fig. 2) shows the different water dynamics of the sites as a consequence of the different behaviour of different terms of water balance (evapotranspiration, runoff, infiltration, etc.).

3.3. Organic matter in soils

The soil in the plain fence is an epileptic cambisol (A-BA-Bw-C horizon sequence) with a topsoil pH_w of 3.6 and a 45-cm thickness over a lithic contact (fractured marble), according to WRB (IUSS Working Group WRB, 2006). The soil in the North fence is also an epileptic cambisol (A-BAw1-BAw2) with a topsoil pH_w of 4.8 and a 42-cm thickness over fractured marble. However, the soil in the South fence is a rendzic phaeozem (A1–A2) with a topsoil pH_w of 5.1 and a 16-cm thickness over a very fractured rock layer (C/R) with weathered marble pockets.

We analysed all soils to assess the organic carbon (SOC) to obtain an estimate of the soil organic-matter (SOM) content (see Supplementary information for organic-matter data). By GLM analysis, we found a highly significant (F = 114.321; d.f. = 2,43; P < 0.001) effect of the layer on the SOM concentration, as was expected. The SOM marginal means for the three layers are 38.4 ± 2.3% for the O layer, 23 ± 2.2% for the A1 layer and 14.2 ± 2.2% for the A2 layer. These high organic-matter levels are due to the slow decomposition that occurs in mountain soils. There is no significant variation in the soil SOM content over the season, and, considering the layers to-gether, there does not seem to be an aspect effect. However, by ana-lysing each layer separately, we found that there is a larger SOM concentration in the O layer in northern soils (N = 40.2 ± 2.6%, S = 31.8 ± 2.6%, P = 0.007 Bonferroni *post hoc* test), and this differ-ence can be explained by the diversity of the N and S soils (Cambisol and Rendzic Phaeozem). The southern soil has a higher pH, more bio-logical activity and faster mineralisation rates, which, together with higher temperatures, lead to lower SOM concentrations. In the A1 layer, there is no significant difference, but we found a higher con-centration in the southern site in the A2 layer (N = 13 ± 0.9%, S = 18.1 ± 0.9%, P < 0.001 Bonferroni *post hoc* test). This difference can be explained by the different soil depths between the sites (42 cm for N, 16 cm for S), which could lead to a larger horizontal radical growth of the grassland plants in the A2 layer.

4. Discussion

4.1. Layer effect

The layer studied has a highly significant effect (F = 28.755; d.f. = 2,43; P < 0.001) on the concentration of ΣPCBs. This layer-dependent effect is evident in Fig. 3, which shows that the highest

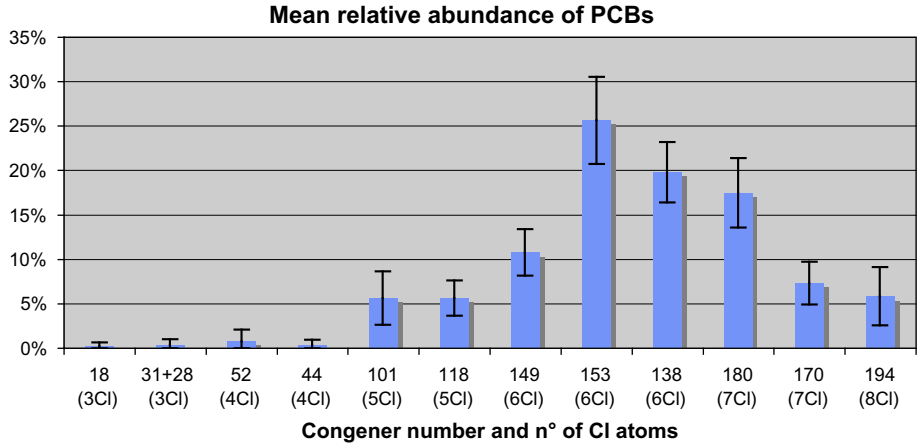

Fig. 1. Mean relative abundance of PCBs (indicated with Ballshmitter number). Bars refer to the 95% confidence interval of the marginal means.

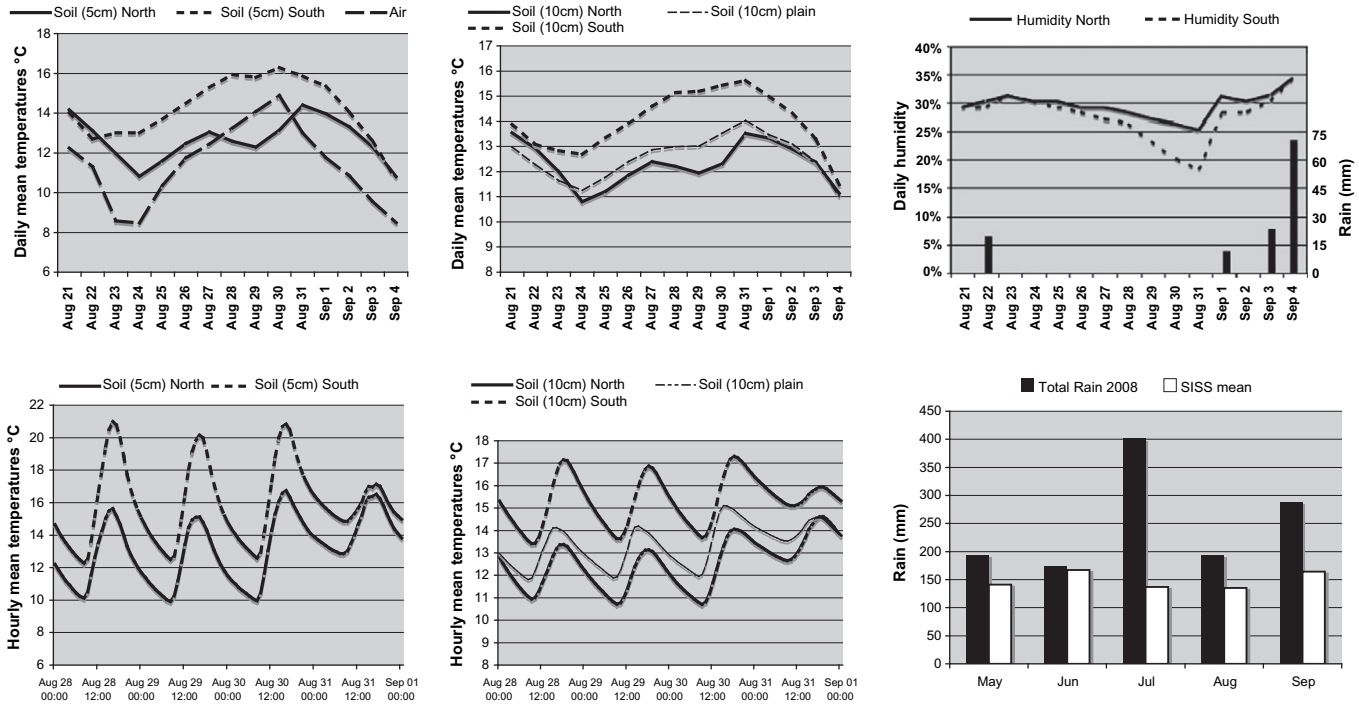

Fig. 2. Examples of the meteorological data collected: daily mean temperatures (−5 and −10 cm) and daily soil humidity (−5 cm, left *y* axis) with rain (right *y* axis); hourly mean soil temperatures (−5 cm and −10 cm); and the total amount of rain during the study period compared with 1971–2000 mean conditions (SISS mean).

ΣPCBs concentration is found in O layer, followed by the A1 and A2 layers. We also found a highly significant correlation between the soil organic matter and the ΣPCBs ($P < 0.001$). The organic matter influence on the PCBs distribution is based on K_{oc}, which is generally high for these hydrophobic pollutants (Girvin and Scott, 1997; Li et al., 2003). The significance of this effect tends to increase with K_{oc} (and thus with the number of Cl atoms), confirming the importance of this parameter in understanding the PCBs distribution in soils.

By introducing the SOM concentration in the GLM as a covariate, we found that, while the O and A2 layers show similar SOM-normalised PCBs concentrations, the A1 layer has the highest contamination ($F = 4.272$; d.f. = 2,42; $P = 0.02$), as shown in Fig. 3. We theorise that the pollutants that reach the A1 layer by bioturbation and diffusion tend to volatilise slowly because they have to recross the superficial O layer. In contrast, this effect is not present in the A2 layer, probably because the A1 layer acts as a filter, retaining the pollutants. By analysing single congeners, we found, in addition to the layer effect, that the higher pollutant concentrations in the A1 layer are of the 5-, 6-, 7- and 8-chlorinated CBs, which have less volatility (Li et al., 2003).

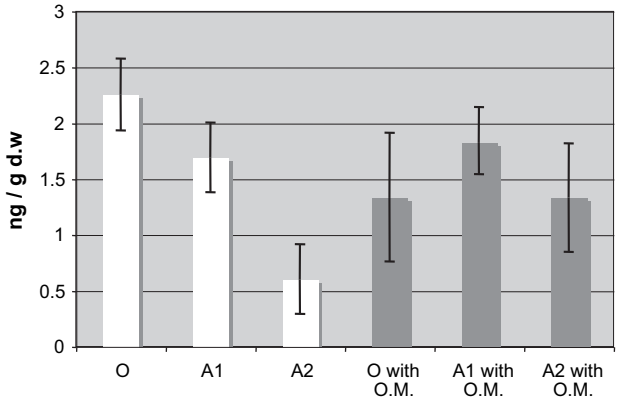

Fig. 3. Mean concentrations (expressed in ng g^{-1} of dry weight) of ΣPCBs without (white columns) and with (black columns) organic matter as a covariate in different layers. Mean concentrations were calculated as marginal means by GLM analysis. Bars refer to the 95% confidence interval of the marginal means.

4.2. Seasonality effect

Soils are considered to be a reservoir of PCBs and usable to obtain historical records about their production and use. Our data suggest a more dynamical behaviour of these contaminants, which causes consistent changes in contamination over different seasons. Fig. 4 shows that the ΣPCBs (calculated for all layers together) are dependent on the sampling date ($F = 11.013$; d.f. = 5,43; $P < 0.001$). The concentration reaches its maximum during the first sampling (06/01/08), which occurred a few days after the complete snowmelt. Next, it decreases rapidly (in the second sampling, the marginal mean of concentration is three times lower than that in the first sampling). Because our study only covers the growing season, we will attempt to explain the relatively high ΣPCBs levels found in *T*1 with two literature-based theories. First, the *T*1 peak could be related to the high scavenging rate of snow precipitation (Lei and Wania, 2004). The hydrophobic pollutants associated to particles retained into the snowpack could then be deposited on soil during the last phase of the thaw (Wania et al., 1998b; Meyer and Wania, 2008). It is also conceivable that post-thaw soils are very cold and able to retain more pollutants than later on in the growing season (following the model of maximum reservoir capacity, Dalla Valle et al., 2005). These two possibilities could also work together to contribute to our observed concentration peak. Between *T*1 and *T*2, PCB concentrations show a consistent decrease, suggesting a relatively fast volatilisation. In this phase, soils (completely snow-free) rapidly become hotter, lowering the K_{sa} and thus enhancing re-volatilisation processes. This rapid loss of PCBs observed between *T*1 and *T*2 (Fig. 4) could be related to the strong wind conditions almost constantly found in the plateau and

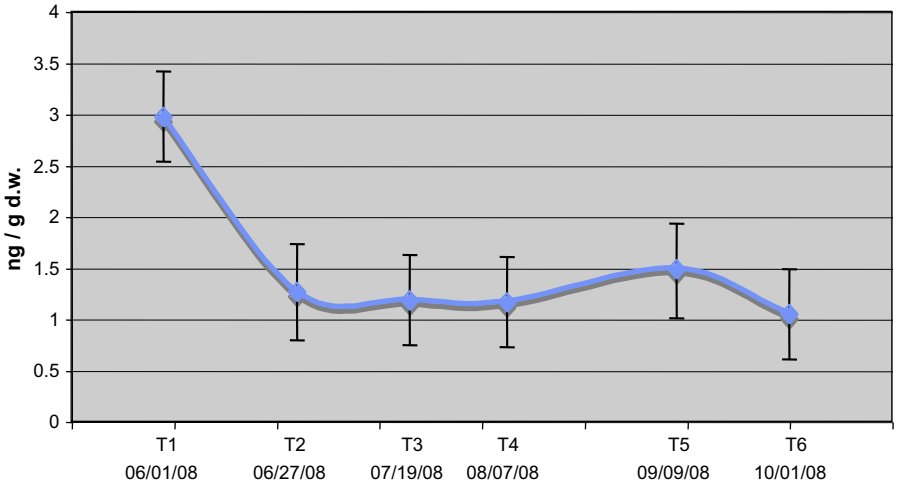

Fig. 4. Seasonal variation of mean ΣPCBs (calculated for all layers together). The mean value at each date is the marginal mean from the GLM analysis. Bars refer to the 95% confidence interval of the marginal means.

neighbouring areas (ARPA, 2010). Strong wind enhances volatilisation, particularly for heavy congeners and in soils with high organic-matter content (Koblizkova et al., 2009). Our data seem to confirm that wind velocity is an important parameter for pollutant volatilisation, and its inclusion in soil–air models is recommended.

From *T*3 to *T*6, there is no significant variation in the total concentration, but a non-significant peak in *T*5 is observable (Fig. 4, a small peak not significant at the Bonferroni *post hoc* test). One possible explanation could be that the heavy rain that fell a few days before the fifth sampling could have increased the air-to-soil fluxes.

Our data show that the PCB concentrations in all analysed layers tend to have great variations (up to 3-fold) during the growth season, with a concentration peak after the thaw followed by a fast decrease, probably by volatilisation. This result clearly shows that mountain soils are reservoirs for these compounds but with consistent fluctuation during the growing season, in agreement with theoretical prevision of Dalla Valle et al. (2005).

The analyses of single CBs indicate that the majority of them show behaviour similar to that found for the ΣPCBs, but the qualitative peak in *T*5 is only evident for congeners that have 5, 6, 7 and 8 Cl atoms, for which the effect of wet scavenging may be more important because of their higher K_{oa} (Li et al., 2003). On the contrary, we found that CB-18 shows no significant dependence on seasonality, remaining in extremely low concentrations. A possible explanation is that this compound could not find environmental conditions suitable for its accumulation on the plateau because CB-18 is the lighter and more volatile congener among the ones analysed (Li et al., 2003).

4.3. Aspect effect and N/S enrichment factor

The meteorological and SOM data show many differences between the northern and southern sampling sites. As expected in a mountain environment, the northern aspect tends to have lower soil temperatures (on long, sunny days ΔT N/S reaches 4–5 °C, Fig. 2), higher humidity (Fig. 2) and less vegetal growth. Moreover, the SOM content on the northern side tends to be higher in the O layer and lower in the A2 layer, while there is no statistically significant difference between the northern and southern SOM concentration in the A1 layer.

In these environmental conditions, we found a significant difference between the ΣPCBs in the northern and southern aspects ($F = 6.693$; d.f. = 2,43; $P = 0.003$), with a mean N/S enrichment factor of 1.8, consistent with those theoretically calculated and measured by Tremolada et al. (2009). This effect seems to be absent for 3-Cl and 4-Cl CBs (which have very low concentrations in every aspect), while all other congeners show a very significant relationship between aspect and concentration. The plain site shows intermediate SOM, temperature and contamination values.

By analysing the N/S factor in different layers, we observed different behaviours. In the O layer, we found that the N/S factor is larger (2.5). Because O is the most superficial layer, it is conceivable that this difference is due to ΔT and ΔSOM, which drives different re-volatilisation rates and different PCB-retaining capabilities between the N and S soils. Differences in temperature (as previously stated, ΔT N/S reaches 4–5 °C in superficial soil) and differences in humidity (southern soils tend to dry faster) lead to changes in the K_{sa} and thus to different levels of volatilisation. Moreover, as it is theorised in Dalla Valle et al. (2005), higher temperatures leads to a lower MRC, and Southern soil could be less able to retain pollutants than Northern soil.

The second observed effect is related to the different SOM contents in the superficial soil. Because PCBs have a high affinity for organic matter, this parameter is relevant to determine the amount of PCBs retainable by soils. To investigate this effect, we normalised the concentration data of the O layer with the level of SOM of each sample and performed GLM analyses on the concentrations (expressed as ng g^{-1} of organic matter). The normalisation leads to a 20% decrease of the N/S factor of the ΣPCBs (from 2.5 to 2.0). This factor decreases because we have removed the ΔSOM part of the aspect effect using normalised concentration data. The use of the normalised value for GLM analyses leads to a slight loss in the degree of significance of the aspect effect (dry weight-based data: $F = 18.792$; d.f. = 2,43 $P = 0.001$; normalised data: $F = 13.937$; d.f. = 2,43; $P = 0.002$), which confirms the temperature interpreta-tion of the N/S enrichment factor.

In the A1 and A2 layers, we found no significant aspect effect (with or without data normalisation), and this finding is probably due to their isolation from air. Pollutants in these layers cannot easily volatilise and instead move through the soil by bioturbation and diffusion. In addition, ΔT is lower for the northern and southern A1 and A2 layers.

4.4. Volatilisation kinetics and enrichment-factor variation

We further analysed the kinetics of the fast decrease that occurs between *T*1 and *T*2. Using the marginal means of the ΣPCBs

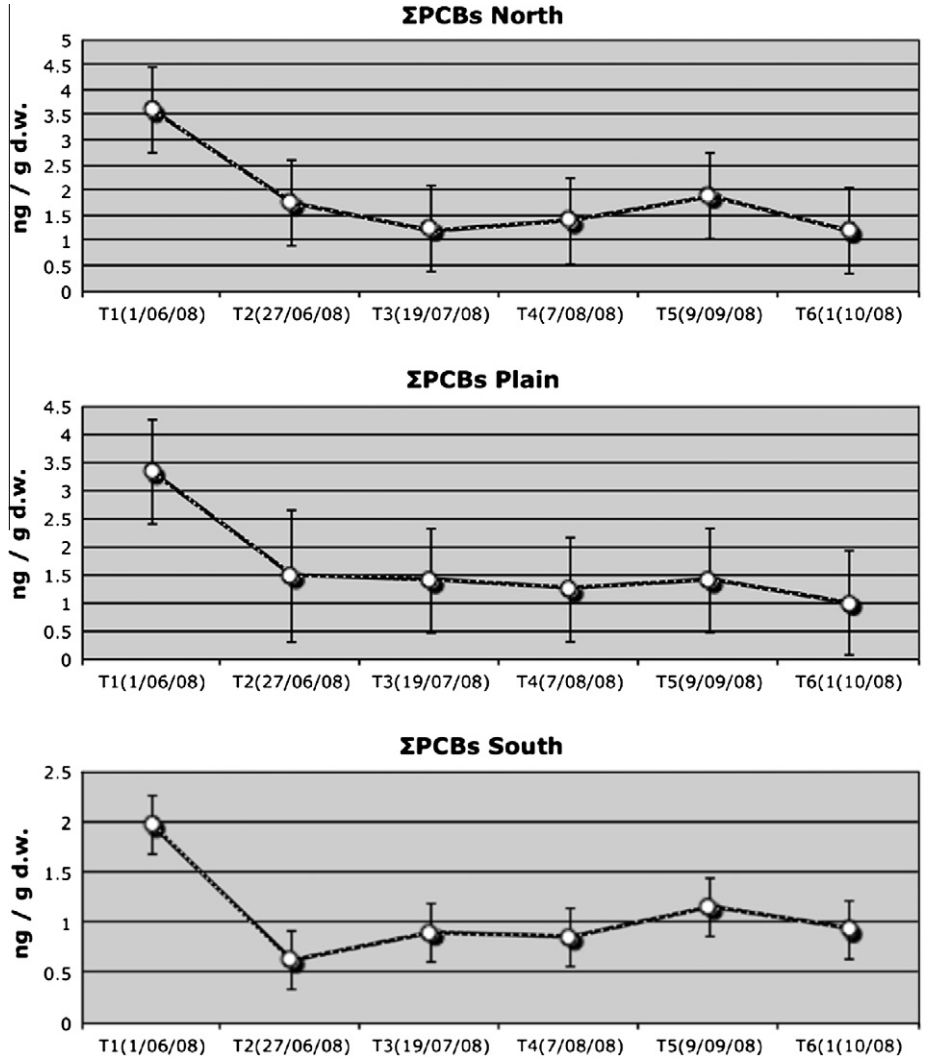

Fig. 5. Seasonal variation in different aspect. The mean value at each date is the marginal mean from the GLM analysis. Bars refer to the 95% confidence interval of the marginal means. *P* values are 0.01 for North-, 0.029 for plain- and <0.001 for South-facing slopes.

(obtained with the GLM) at *T*1 and *T*2, we calculated the PCB half-time in the three sampling sites using an exponential model ($C_1 = C_0 \times e^{-kt}$), as shown in Cousins and Jones (1998). We found a great difference between North, with a half-time during the early summer decrease phase of ~25 d, and South, with a half-time of ~16 d (Fig. 5 and Table 1). The plain site (half-time ~22 d) has kinetics in between those of the northern and southern sites. As previously discussed, strong wind conditions tend to enhance volatilisation, contributing to fast kinetics like those we recorded. The difference between volatilisation fluxes is explainable by the same temperature effects discussed for the N/S enrichment factor. The faster southern kinetics during the *T*1–*T*2 period leads to an increase of the enrichment factor from the first sampling date (1.8) to the second (2.8). Furthermore, the N/S factor remains near 1.5 for the rest of the season. The kinetics found in this study are faster than those recorded by Cousins and Jones (1998), probably because of wind action, and are also faster than those recorded in the same area (Tremolada et al., 2007), but in that study the sampling dates were more distant, dilating the calculated half-times.

Table 1
Mean ΣPCBs (marginal means from GLM, ng g^{-1} d.w.), and half-times (d) of the total PCBs value. *k* is the rate constant used in the exponential model.

Exposition	ΣPCBs (*T*1)	ΣPCBs (*T*2)	*k*	Half-time
North	3.608	1.757	0.028	24.8
Plain	3.336	1.481	0.031	22.4
South	1.974	0.629	0.044	15.8
Mean	2.972	1.262	0.033	21.0

5. Conclusion

In this paper, we demonstrate that PCB concentration in soils tends to vary greatly on a small and relatively homogeneous area during a single growing season. Although most of literature considers soils as a stable compartment, our data suggest a dynamic behaviour of the contamination pattern in this Alpine environment. We report three climatic effects (seasonality, N/S enrichment factor and differential re-volatilisation speed) and an effect related to pedological characteristics (layer effect mainly due to SOM content). The sum of these effects leads to differences in PCB contamination in space and time of up to one order of magnitude. North-facing superficial (0–1 cm) soil sampled just after the thaw can have a PCB concentration ten times higher than South-facing sub-superficial (4–7 cm) soil sampled in the middle of the growing season. Aside from the factors considered in this paper, there are other variability sources that were not considered in this

experiment. For example, the PCB concentration in the analysed soils could be influenced by differences in the vegetation covering the sampling sites, considering both the epigean part (filter effect from air) and the root growth (direct accumulation from soils). However, we considered that differences in vegetation cover are limited because the study area is covered by relatively homogeneous alpine grassland vegetation. Despite several remaining questions (e.g., differences in herbaceous species and macrofauna activity), we believe that our data describe a number of important elements regarding the local time and spatial variability of PCB contamination in a mountain pasture, which are useful for better planning of sampling campaigns and for exposure assessment. The interpretation of the data of this paper offers an experimental demonstration of the maximum reservoir capacity concept.

Acknowledgement

We would like to warmly thank Mr. Donnino Della Bella and 'Consorzio Alpe Andossi' for their hospitality and contributions in setting up the sampling sites and for providing useful information.

We kindly thank Liliana Maria Tato for indispensable help given in laboratory analysis and Dott. Alessio Conforto of Università degli Studi di Milano – Laboratorio Valchiavenna for providing useful meteorological data.

Appendix A. Supplementary material

All concentration data for selected congeners and complete SOM values can be found in supplementary information, together with photos of the area of study. The complete methodology is also described. Supplementary data associated with this article can be found, in the online version, at doi:10.1016/j.chemosphere.2010.12.043.

References

ARPA (Regional agency for environmental protection), Department of Sondrio. <http://ita.arpalombardia.it/ita/dipartimenti/sondrio/index_so.asp>.

Barra, R., Popp, P., Quiroz, R., Bauer, C., Cid, H., Von Tumpling, W., 2005. Persistent toxic substances in soils and waters along an altitudinal gradient in the Laja River Basin, Central Southern Chile. Chemosphere 58, 905–915.

Barry, R.G., 1992. Mountain Weather and Climate, second ed. Routledge, London. 404 pp.

Binelli, A., Ricciardi, F., Riva, C., Provini, A., 2006. New evidences for old biomarkers: effects of several xenobiotics on EROD and AChE activities in Zebra mussel (*Dreissena polymorpha*). Chemosphere 62, 510–519.

Breivik, K., Sweetman, A., Pacyna, J.M., Jones, K.C., 2002. Towards a global historical emission inventory for selected PCB congeners – a mass balance approach. 1. Global production and consumption. Sci. Total Environ. 290, 181–198.

Calamari, D., Bacci, E., Focardi, S., Gaggi, C., Morosini, M., Vighi, M., 1991. Role of plant biomass in the global environmental partitioning of chlorinated hydrocarbons. Environ. Sci. Technol. 25, 1489–1495.

Cousins, I.T., Jones, K.C., 1998. Air–soil exchange of semi-volatile organic compounds (SOCs) in the UK. Environ. Pollut. 102, 105–118.

Dalla Valle, M., Jurado, E., Dachs, J., Sweetman, A.J., Jones, K.C., 2005. The maximum reservoir capacity of soils for persistent organic pollutants: implication for global cycling. Environ. Pollut. 134, 153–164.

Daly, G.L., Lei, Y.D., Teixeira, C., Muir, D.C.G., Castillo, L.E., Wania, F., 2007. Accumulation of current-use pesticides in neotropical montane forests. Environ. Sci. Technol. 41, 1118–1123.

DLgs 152/06. Decreto legislativo: Norme in materia Ambientale. Published in "Gazzetta Ufficiale n. 88 del 14 aprile 2006 – Supplemento Ordinario n. 96".

Frame, G.M., Wagner, R.E., Carnahan, J.C., Brown, J.C., May, R.J., Smullen, L.A., Bedard, D.L., 1996. Comprehensive, quantitative, congener-specific analyses of eight aroclors and complete PCB congener assignments on DB-1 capillary GC columns. Chemosphere 33, 603–623.

Girvin, D.C., Scott, A.J., 1997. Polychlorinated biphenyl sorption by soils: measurement of soil–water partition coefficients at equilibrium. Chemosphere 35, 2007–2025.

Grimalt, J.O., Fernandez, P., Berdie, L., Vilanova, R.M., Catalan, J., Psenner, R., Hofer, R., Appleby, P.G., Rosseland, B.O., Lien, L., Massabuau, J.C., Battarbee, R.W., 2001. Selective trapping of organochlorine compounds in mountain lakes of temperate areas. Environ. Sci. Technol. 35, 2690–2697.

Helyar, S.G., Patel, B., Headington, K., El Assal, M., Chatterjee, P.K., Pacher, P., Mabley, J.G., 2009. PCB-induced endothelial cell dysfunction: role of poly(ADP-ribose) polymerase. Biochem. Pharmacol. 78, 959–965.

Hippelein, M., McLachlan, M.S., 1998. Soil/air partitioning of semivolatile organic compounds. 1. Method development and influence of physical–chemical properties. Environ. Sci. Technol. 32, 310–316.

IUSS Working Group WRB, 2006. World Reference Base for Soil Resources 2006. World Soil Resources Reports No. 103. FAO, Rome.

Johnson, K.E., Knopperb, L.D., Schneider, D.C., Ollson, C.A., Redimer, K.J., 2009. Effects of local point source polychlorinated biphenyl (PCB) contamination on bone mineral density in deer mice (*Peromyscus maniculatus*). Sci. Total Environ. 407, 5050–5055.

Koblizkova, M., Ruzickova, P., Cupr, P., Komprda, J., Holoubek, I., Klanova, J., 2009. Soil burdens of persistent organic pollutants: their levels, fate, and risks. Part IV. Quantification of volatilization fluxes of organochlorine pesticides and polychlorinated biphenyls from contaminated soil surfaces. Environ. Sci. Technol. 43, 3588–3595.

Lei, Y.D., Wania, F., 2004. Is rain or snow a more efficient scavenger of organic chemicals? Atmos. Environ. 38, 3557–3571.

Li, N., Wania, F., Lei, Y.D., Daly, G.L., 2003. A comprehensive and critical compilation, evaluation, and selection of physical–chemical property data for selected polychlorinated biphenyls. J. Chem. Eng. Data. 50, 742–768.

Mackay, D., 2001. Multimedia Environmental Models: The Fugacity Approach. Lewis/CRC, Boca Raton, FL.

Meijer, S.N., Steinnes, E., Ockenden, W.A., Jones, K.C., 2002. Influence of environmental variables on the spatial distribution of PCBs in norwegian and UK soils: implications for global cycling. Environ. Sci. Technol. 36, 2146-2153

Meijer, S.N., Ockenden, W.A., Sweetman, A.J., Breivik, K., Grimalt, J.O., Jones, K.C., 2003. Global distribution and budget of PCBs and HCB in background surface soils: implications for sources and environmental processes. Environ. Sci. Technol. 37, 667–672.

Meyer, T., Lei, Y.D., Wania, F., 2006. Measuring the release of organic contaminants from melting snow under controlled conditions. Environ. Sci. Technol. 40, 3320–3326.

Meyer, T., Wania, F., 2008. Organic contaminants amplification during snowmelt. Water Res. 42, 1847–1865.

Moeckel, C., Nizzetto, L., Di Guardo, A., Steiness, E., Freppaz, M., Filippa, G., Camporini, P., Benner, J., Jones, K.C., 2008. Persistent organic pollutants in boreal and montane soil profiles: distribution, evidence of process and implication for global cycling. Environ. Sci. Technol. 42, 8374–8380.

Nelson, D.W., Sommers, L.E., 1996. Total carbon, organic carbon, and organic matter. In: Page, A.L. et al. (Eds.), Methods of Soil Analysis, 2nd ed., Part 2, Agronomy, vol. 9 Am. Soc. of Agron., Inc., Madison, WI, pp. 961–1010.

Nizzetto, L., Cassani, C., Di Guardo, A., 2006. Deposition of PCBs in mountains: The forest filter effect of different forest ecosystem types. Ecotoxicol. Environ. Saf. 63, 75–83.

Nizzetto, L., Jarvis, A., Brivio, P.A., Jones, K.C., Di Guardo, A., 2008. Seasonality of the air–forest canopy exchange of persistent organic pollutants. Environ. Sci. Technol. 42, 8778–8783.

Offenthaler, I., Bassan, R., Belis, C., Jakobi, G., Kirchner, M., Kräuchi, N., Moche, W., Schramm, K.W., Sedivy, I., Simonc˘ic˘, P., Uhl, M., Weiss, P., 2009. PCDD/F and PCB in spruce forests of the Alps. Environ. Pollut. 157, 3280–3289.

Richthoff, J., Rylander, L., Jonsson, B.A.G., Akesson, H., Hagmar, L., Nilsson-Ehle, P., Stridsberg, M., Giwercman, A., 2003. Serum levels of 2,2′,4,4′,5,5′-hexachlorobiphenyl (CB-153) in relation to markers of reproductive function in young males from the general Swedish population. Environ. Health Perspect. 111, 409–413.

SISS – Società Italiana della Scienze del Suolo, 2007. Escursione scientifica del convegno nazionale: la scienza del suolo nei territori montani e collinari. Milano-Chiavenna, 9-13 Luglio 2007.

Stull, R.B., 1997. An Introduction to Boundary Layer Meteorology. Kluwer Academic Publishers, Dordrecht. 670 pp.

Tremolada, P., Villa, S., Bazzarin, P., Bizzotto, E., Comolli, R., Vighi, M., 2007. POPs in mountain soils from the Alps and Andes: suggestions for a 'precipitation effect' on altitudinal gradients. Water Air Soil Pollut. 188, 93–109.

Tremolada, P., Parolini, M., Binelli, A., Ballabio, C., Comolli, R., Provini, A., 2009. Preferential retention of POPs on the northern aspect of mountains. Environ. Pollut. 157, 3298–3307.

Van Den Berg, M., Birnbaum, L., Bosveld, A.T.C., Brunstrom, B., Cook, P., Freeley, M., Giesy, J.P., Hanberg, A., Hasegawa, R., Kennedy, S.W., Kubiak, T., Christian Larsen, J., Rolaf VanLeeuwen, F.X., Djien Liem, A.K., Nolt, C., Peterson, R.E., Poellinger, L., Safe, S., Schrenk, D., Tillit, D., Tysklind, M., Younes, M., Waern, F., Zacharewski, T., 1998. Toxic equivalency factors (TEFs) for PCBs, PCDDs, PCDFs for humans and wildlife. Environ. Health Perspect. 106, 775–792.

Wania, F., Haugen, J.E., Lei, Y.D., Mackay, D., 1998a. Temperature dependence of atmospheric concentrations of semivolatile organic compounds. Environ. Sci. Technol. 32, 1013–1021.

Wania, F., Hoff, J.T., Jia, C.Q., Mackay, D., 1998b. The effects of snow and ice on the environmental behaviour of hydrophobic organic chemicals. Environ. Pollut. 102, 25–41.

WMO, 1996. Guide to Meteorological Instruments and Methods of Observation (WMO Guide No. 8), sixth ed., loose-leaf; Updated by Supplements When Necessary, Geneva, CH.

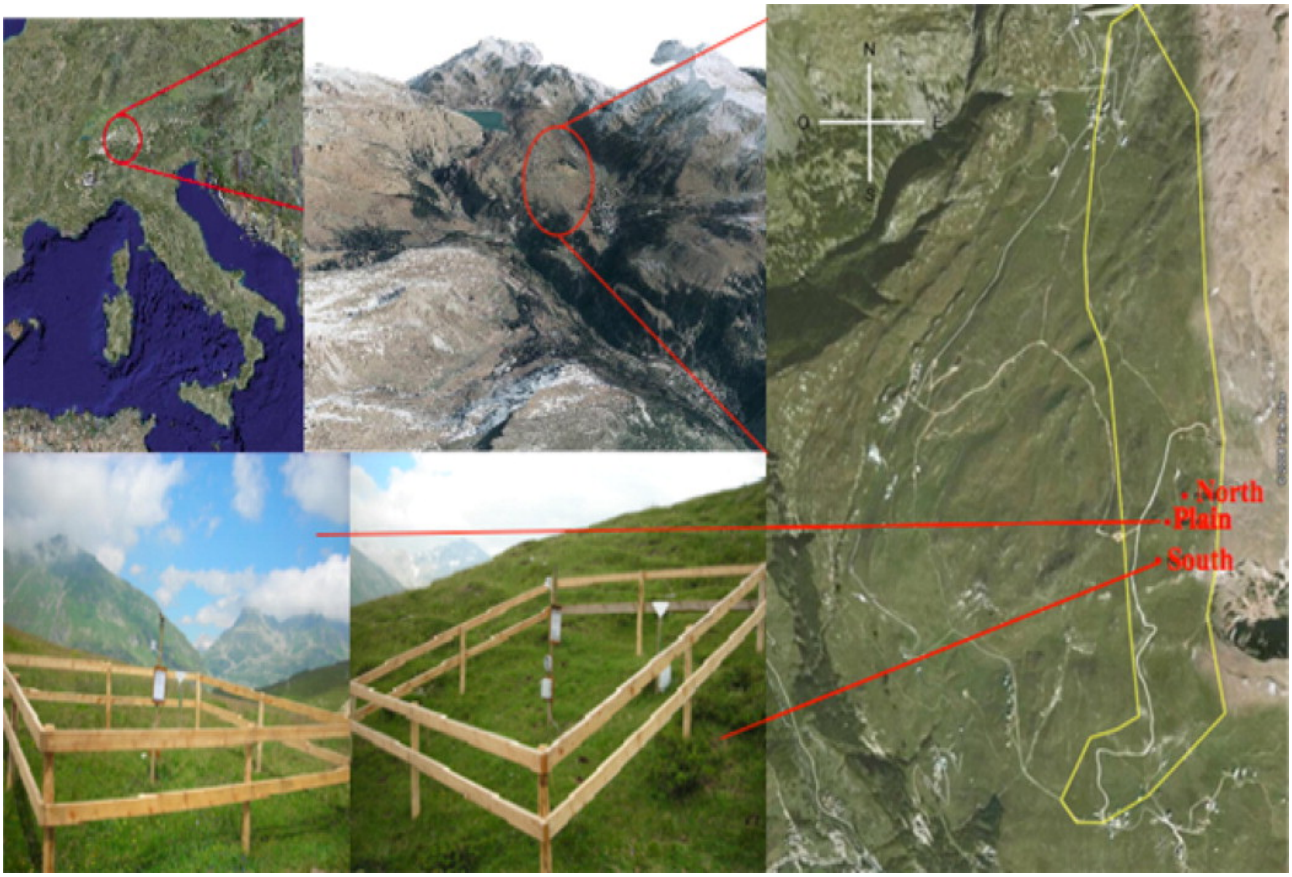

Supplementary Fig. 1 Sampling area. Italian central Alps, Andossi plateau and photos of two of our sampling sites.

Materials and Methods. Supplementary informations.

Chemicals and instruments

All solvents used were pesticide grade. Florisil adsorbent for chromatography (100–200 mesh) was obtained from Fluka (Steinheim, Germany). Silica gel for column chromatography (70–230 mesh) was supplied by Sigma–Aldrich (Steinheim, Germany). The p,p'-DDE D8 (deuterated p,p'-DDE) used as an internal recovery standard was purchased from Dr. Ehrenstorfer (Augsburg, Germany).
A GC chromatograph (TRACE GC, Thermo-Electron, Austin, Texas, USA) equipped with a Programmed Temperature Vaporizer injector (PTV) and an AS 2000 autosampler (Thermo Electron) was used coupled with a PolarisQ Ion Trap mass spectrometer. A Rtx-5MS (Restek, Bellefonte, PA, USA) capillary column (30 m length, 0.25 mm I.D., 0.25 μm film thickness) was used for the chromatographic separation. Helium for gas-chromatographic analyses was purchased from Sapio, Monza, Italy.

Extraction and cleanup procedure

Samples (~20 g) were lyophilised and extracted for 12 h using 100 mL acetone/n-hexane (1:1 v/v) in a soxhlet apparatus (FALC Instruments, Lurano, Italy). Samples were then concentrated to the final volume of 3 mL initially by a rotary evaporator (RV 06-LR, IKA, Staufen, Germany) and then by a gentle nitrogen flow. Organic matter was digested adding 6 mL of sulfuric acid 95% and digesting overnight. The supernatant solution of acetone and hexane was then concentrated with gentle nitrogen flow to the volume of 1 mL.
Cleanup was performed using a multilayer column (40 cm x 1.5 cm I.D.) composed of 10 g of silica gel (activated overnight at 130 °C, then deactivated with water, 5% w/w), followed by 10 g of Florisil (activated for 16 h at 650 °C). The phase-filled columns were washed with n-hexane/acetone/ dichloromethane (8:1:1 v/v). Elution was carried out first by collecting 50 mL of n-hexane and then 50 mL of 1:1 n-hexane/dichloromethane (v/v). 1 mL of isooctane was added to the fractions that were then concentrated by rotary evaporator to 10 mL and then to 1 mL under gentle nitrogen flow.

Quantification conditions

Samples were analysed using GC/MS/MS methodology under the following instrumental conditions: PTV in solvent split mode with split flow of 20 mL min^{-1} and splitless time at 2 min; carrier gas helium at 1 mL min^{-1}; EI mode with standard electron energy of 70 eV; transfer line at 270 °C; damping gas at 1 mL min^{-1} and ion source at 250 °C. Chromatographic separation of the PCB congeners was obtained by the following conditions: initial oven temperature starting at 100 °C and maintained for 1 min, then ramped to 180 °C (no hold time) at 20 °C min^{-1}, to 200 °C (no hold time) at 1.5 °C min^{-1}, to 250 °C (no hold time) at 3 °C min^{-1} and finally to 300 °C (held 5 min) at 30 °C min^{-1}. PCB quantification was performed by external standard calibration curves, ranging from 1 to 100 pg μL^{-1} for each compound.

Quality assurance (QA) and quality control (QC)

Samples and blanks were spiked with 10 μL of the deuterated recovery standard p,p'-DDE D_8 (and so with 5 ng of DDE-D_8) prior to solvent extraction to monitor methodological analyte losses, as in Sarkar *et al*. (2008). Recoveries over 80% were accepted. The suitability and the stability of deuterated standard response were evaluated as in Sarkar *et al*. (2008). A procedural blank was run in parallel with every batch of three samples and then extracted in a manner identical to that of the samples. No significant concentrations of analysed compounds were found in blanks. LODs (limits of detection) were estimated by the signal-to noise ratio (3:1) and ranged between 0.15 and 0.35 pg (injected amount) depending on the compound. Considering 20 g of extracted soil and the ratio 1:1000 or 1:500 of the injected vs. sample volume, LOQs (limits of quantification) are not higher than 0.001 ng g^{-1} d.w. for the considered compounds.

Sample	18	31+28	52	44	101	149	118	153	138	180	170	194	Σ
T1ON	0.008	0.027	0.065	0.03	0.386	0.547	0.312	1.142	0.929	0.954	0.384	0.374	5.158
T1OP	0.012	0.035	0.076	0.032	0.332	0.467	0.32	1.089	0.916	0.647	0.355	0.187	4.468
T1OS	0.004	0.02	0.039	0.018	0.143	0.2	0.128	0.452	0.37	0.295	0.135	0.098	1.902
T1A1N	0.007	0.03	0.078	0.032	0.335	0.487	0.292	1.055	0.789	0.807	0.357	0.361	4.63
T1A1P	0.004	0.025	0.054	0.014	0.246	0.527	0.278	0.964	0.827	0.669	0.298	0.29	4.196
T1A1S	0.005	0.018	0.046	0.013	0.19	0.255	0.187	0.577	0.492	0.446	0.159	0.144	2.532
T1A2N	0.003	0.012	0.023	0.011	0.089	0.094	0.074	0.278	0.198	0.151	0.05	0.052	1.035
T1A2P	0.001	0.012	0.028	0.01	0.09	0.142	0.077	0.352	0.268	0.226	0.077	0.061	1.344
T1A2S	0.004	0.014	0.034	0.012	0.1	0.155	0.097	0.36	0.307	0.226	0.112	0.066	1.487
T2ON	0.022	0.004	0.071	0.044	0.273	0.344	0.2	0.861	0.531	0.518	0.211	0.161	3.24
T2OS	0.004	0.003	0.026	0.009	0.085	0.092	0.051	0.238	0.181	0.139	0.068	0.044	0.94
T2A1N	0.007	0.001	0.006	0.004	0.077	0.166	0.063	0.312	0.255	0.314	0.151	0.127	1.483
T2A1P	<0,001	0.006	0.008	0.005	0.096	0.21	0.135	0.391	0.348	0.416	0.131	0.123	1.869
T2A1S	0.003	0.001	0.005	0.002	0.03	0.085	0.034	0.136	0.104	0.102	0.044	0.042	0.588
T2A2N	0.003	0.001	0.003	0.001	0.032	0.058	0.028	0.144	0.105	0.107	0.045	0.021	0.548
T2A2P	0.001	0.001	0.001	0.001	0.012	0.021	0.008	0.07	0.039	0.039	0.017	0.008	0.218
T2A2S	<0,001	0.004	0.004	0.001	0.017	0.036	0.022	0.093	0.067	0.071	0.018	0.027	0.36
T3ON	0.001	0.001	0.013	0.005	0.149	0.269	0.131	0.535	0.4	0.383	0.176	0.148	2.211
T3OP	0.001	0.001	0.005	0.003	0.113	0.239	0.119	0.441	0.405	0.319	0.129	0.115	1.89
T3OS	0.001	0.001	0.006	0.003	0.084	0.134	0.075	0.268	0.225	0.204	0.083	0.056	1.14
T3A1N	0.001	0.001	0.005	0.001	0.064	0.151	0.056	0.318	0.246	0.213	0.102	0.096	1.254
T3A1P	0.001	0.001	0.003	0.003	0.096	0.231	0.114	0.464	0.399	0.346	0.138	0.15	1.946
T3A1S	0.001	0.001	0.002	0.001	0.048	0.092	0.049	0.229	0.171	0.174	0.074	0.075	0.917
T3A2N	0.001	0.001	0.002	0.001	0.021	0.034	0.014	0.072	0.048	0.044	0.021	0.02	0.279
T3A2P	0.001	0.001	0.001	0.001	0.013	0.039	0.016	0.1	0.073	0.059	0.025	0.023	0.352
T3A2S	0.001	<0,001	0.001	0.001	0.035	0.067	0.027	0.166	0.126	0.121	0.053	0.05	0.648
T4ON	<0,001	0.003	0.005	0.006	0.146	0.243	0.151	0.604	0.528	0.406	0.224	0.209	2.525
T4OP	<0,001	0.002	0.003	0.005	0.124	0.259	0.144	0.594	0.519	0.465	0.226	0.155	2.496
T4OS	<0,001	0.001	0.001	0.003	0.065	0.127	0.085	0.254	0.246	0.176	0.067	0.052	1.077
T4A1N	<0,001	0.001	0.004	0.001	0.078	0.135	0.079	0.302	0.295	0.248	0.097	0.101	1.341
T4A1P	<0,001	0.001	0.001	0.001	0.04	0.092	0.039	0.231	0.211	0.178	0.072	0.063	0.929
T4A1S	<0,001	0.001	0.001	0.001	0.038	0.082	0.072	0.247	0.202	0.2	0.094	0.078	1.016
T4A2N	0.001	0.002	0.002	0.002	0.013	0.027	0.022	0.089	0.066	0.063	0.025	0.009	0.321
T4A2P	0.002	0.001	0.001	0.001	0.011	0.025	0.017	0.089	0.065	0.049	0.016	0.017	0.294
T4A2S	0.003	0.001	0.001	0.001	0.016	0.048	0.032	0.125	0.108	0.081	0.041	0.016	0.473
T5ON	0.011	0.002	0.018	0.004	0.222	0.401	0.174	0.883	0.735	0.641	0.306	0.239	3.636
T5OP	0.004	0.003	0.026	0.008	0.188	0.325	0.163	0.65	0.586	0.32	0.181	0.077	2.531
T5OS	0.001	0.001	0.009	0.003	0.09	0.187	0.074	0.328	0.293	0.209	0.1	0.067	1.362
T5A1N	0.003	0.001	0.005	0.002	0.088	0.181	0.079	0.463	0.381	0.305	0.131	0.125	1.764
T5A1P	0.002	0.001	0.003	<0,001	0.046	0.111	0.052	0.287	0.244	0.214	0.08	0.102	1.142
T5A1S	0.002	0.001	0.005	0.002	0.076	0.171	0.075	0.39	0.345	0.255	0.122	0.099	1.543
T5A2N	0.002	0.001	0.002	0.001	0.014	0.034	0.012	0.088	0.063	0.053	0.016	0.013	0.299
T5A2P	0.001	<0,001	0.003	0.001	0.021	0.054	0.021	0.15	0.116	0.105	0.042	0.017	0.531
T5A2S	<0,001	0.008	0.005	0.005	0.024	0.056	0.029	0.163	0.107	0.092	0.037	0.035	0.561
T6ON	0.002	0.004	0.016	0.004	0.128	0.202	0.093	0.471	0.317	0.234	0.11	0.085	1.666
T6OP	0.002	0.003	0.008	0.006	0.082	0.172	0.076	0.395	0.245	0.247	0.101	0.038	1.375
T6OS	0.002	0.002	0.005	0.002	0.066	0.108	0.05	0.254	0.183	0.147	0.061	0.026	0.906
T6A1N	0.001	0.001	0.004	0.003	0.047	0.148	0.071	0.411	0.263	0.26	0.123	0.113	1.445
T6A1P	0.002	0.002	0.004	0.002	0.021	0.055	0.024	0.132	0.091	0.111	0.036	0.031	0.511
T6A1S	0.001	0.002	0.012	0.003	0.046	0.152	0.08	0.398	0.238	0.234	0.117	0.094	1.377
T6A2N	0.002	0.004	0.003	0.003	0.022	0.041	0.029	0.136	0.106	0.101	0.025	0.025	0.497
T6A2P	0.001	0.003	0.008	0.003	0.038	0.116	0.045	0.342	0.219	0.193	0.117	0.051	1.136
T6A2S	0.002	0.004	0.003	0.003	0.022	0.058	0.029	0.136	0.095	0.101	0.025	0.025	0.503

Complete concentration data for all selected congeners. Values are expressed in ng g^{-1} of dry weight.

Sampling time	Exposition	Layer	Organic Carbon (g / Kg of soil)	Organic Matter (%)
T1	N	O	211.87	36.53
T1	P	O	226.50	39.05
T1	S	O	165.85	28.59
T1	N	A1	166.27	28.67
T1	P	A1	132.19	22.79
T1	S	A1	141.70	24.43
T1	N	A2	83.72	14.43
T1	P	A2	72.33	12.47
T1	S	A2	109.35	18.85
T2	N	O	241.93	41.71
T2	S	O	182.04	31.38
T2	N	A1	145.76	25.13
T2	P	A1	142.73	24.61
T2	S	A1	138.21	23.83
T2	N	A2	78.11	13.47
T2	P	A2	64.77	11.17
T2	S	A2	104.13	17.95
T3	N	O	204.24	35.21
T3	P	O	265.14	45.71
T3	S	O	192.65	33.21
T3	N	A1	121.60	20.96
T3	P	A1	139.75	24.09
T3	S	A1	132.59	22.86
T3	N	A2	69.49	11.98
T3	P	A2	66.22	11.42
T3	S	A2	104.10	17.95
T4	N	O	230.18	39.68
T4	P	O	222.44	38.35
T4	S	O	189.43	32.66
T4	N	A1	108.02	18.62
T4	P	A1	98.75	17.02
T4	S	A1	140.51	24.22
T4	N	A2	63.59	10.96
T4	P	A2	58.93	10.16
T4	S	A2	112.87	19.46
T5	N	O	281.93	48.60
T5	P	O	231.79	39.96
T5	S	O	203.61	35.10
T5	N	A1	126.72	21.85
T5	P	A1	122.91	21.19
T5	S	A1	130.90	22.57
T5	N	A2	81.73	14.09
T5	P	A2	65.06	11.22
T5	S	A2	101.47	17.49
T6	N	O	230.44	39.73
T6	P	O	246.15	42.44
T6	S	O	169.82	29.28
T6	N	A1	146.36	25.23
T6	P	A1	132.79	22.89
T6	S	A1	129.24	22.28
T6	N	A2	75.30	12.98
T6	P	A2	76.42	13.18
T6	S	A2	98.99	17.07

Organic carbon and SOM values for all samples

Chapter III

Ballabio, C., Guazzoni, N., Comolli, R., Tremolada, P., 2012. Highly spatially- and seasonally-resolved predictive contamination maps for Persistent Organic Pollutants: development and validation. Submitted to The science of the total environment

Highly spatially- and seasonally-resolved predictive contamination maps for Persistent Organic Pollutants: development and validation

Cristiano Ballabio[a] , Niccoló Guazzoni[b] , Roberto Comolli[a] , Paolo Tremolada[b]

[a]*Environmental and Land Sciences Dept. - Universitá degli Studi di Milano-Bicocca, Milano, Italy*

[b]*Biology Dept. - Universitá degli Studi di Milano, Milano, Italy*

Submitted to: The science of the total environment

Abstract

The assessment of POPs contamination requires reliable spatial maps for burden and flux assessment. In this work, contamination maps were developed and validated at a space resolution of 1×1 m with a time frame of one day, in an experimental area located in the central Alps, where direct measurements of PCB concentrations in soil and environmental parameters were available for year 2008.

Physical algorithms for temperature and organic carbon estimation along the soil profile and across the year were fitted in order to estimate the horizontal, vertical and seasonal distribution of the contamination potential for PCBs in soil (K_{sa} maps).

The resulting maps were cross-validated with an independent set of PCB contamination data, showing very good result (e.g. for CB-153, $R^2 = 0.80$, p-value $\leq 2.2 \cdot 10^{-06}$). The obtained regression coefficients were used to map the actual soil contamination (concentration maps), taking into account temporal shifts, in soil concentrations, from the equilibrium (as defined by K_{sa} values). These maps offer the opportunity to evaluate burden and fluxes with highly resolved temporal and spatial detail, and therefore with a high degree of ecological realism (emission maps).

A consequent dynamic model of seasonal variation of soil concentrations was able to describe the observed concentrations asymmetries between the discharge stage in summer and the recharge stage in autumn, explaining the observed low autumn PCB concentrations in soil related to the high K_{sa} values of this period.

Key words: persistent organic pollutants, soil organic carbon, differential equations, time models, balance equations, spatial mapping

1. Introduction

The assessment of environmental burdens and inter-compartmental fluxes is essential for the evaluation of pollutants cycling within ecosystems. Many methodologies were proposed for this evaluation, from production and emission inventories (Breivik et al., 2002a;b), to mass balance calculations based on measured concentrations (Meijer et al., 2003b), to model elaboration assisted by GIS-based techniques (Verro et al., 2002; Chattopadhyay et al., 2010). Model elaborations are very useful for extrapolating and complete direct experimental measurements limited in space and time (Wania and Mackay, 1995), while GIS techniques provide a useful tool to integrate and introduce spatial variability in models to produce reliable predictive maps (Verro et al.,c 2002; Dalla Valle et al., 2005). While at a global scale it is not possible to introduce meso- and micro-scale effects in models variables, at regional and local scale taking into account spatial variability becomes essential in order to avoid spatially related uncertainties. Time and spatial fluctuations of environmental variables are impressive also for relatively stable compartments such as soil, as its features may vary greatly at short distances (Guazzoni et al., 2011). Thus it follows that this variability will influence also properties related to soil chemical and physical parameters, such as contamination.

This paper accounts for the spatial and temporal variability of different soil features in order to produce predictive contamination maps for POPs, referred to a specific place and time. We believe that this approach can improve the assessment of contaminant burden and fluxes that vary spatially and temporally, as functions of soil and climatic features. The main soil features considered in this paper are the spatial distribution of the Soil Organic Carbon (SOC) and the spatial and temporal variability of the soil temperature gradient.

POPs contamination in soils depend on two main factors: the proximity in space and time of emission sources (Meijer et al., 2003b) and the capacity of the soil itself to retain POPs once they are deposited, regardless of the deposition mechanism (Cousins et al., 1999a). In not directly contaminated areas, the accumulation capacity of soils is the most important factor determining POPs distribution and concentrations (Meijer et al., 2002; Ribes et al., 2002). This accumulation capacity of soils was globally mapped by Dalla Valle et al. (2005) using the Maximum Reservoir Capacity concept (MRC). MCR maps took into account both spatial variability (world distribution of SOC levels) and seasonal variability.

The accumulation potential in soils of semivolatile organic compounds is described by the soil-air partition coefficient (K_{sa}), which measures the physical partition of a compound between soil and air at the equilibrium. Predictive K_{sa} equations based on SOC fraction, soil density and K_{oa} or K_{ow}/K_{aw}, were developed by different authors (Hippelein and McLachlan,

1998; 2000; Meijer et al., 2003a;c; Daly et al., 2007); temperature also affects K_{sa} values throughout K_{oa} values. Good correlations between measured and predicted concentrations were observed for many POPs, because these compounds have specific properties: they are generally characterized by a sufficient volatility for leaving soils by volatilization (semi-Volatile Organic Compounds (SVOC)), they are highly persistent in soils (recalcitrant to microbial bio-degradation) and they do not easily leave soils by leaching (very low water solubility). For these reasons, their accumulation in soils can be successfully predicted by a simple physical partition parameter like K_{sa} and from the fugacity ratio of the concentrations in air and soil, net deposition or volatilization fluxes of POPs can be quantitatively evaluated, establishing whether out-gassing or incoming fluxes are prevalent (Harner et al., 2001). From the predictive K_{sa} equation by Daly et al. (2007), we were able to produce highly spatially- and seasonally-resolved predictive contamination maps of PCBs for a high altitude pasture plateau in the Central Alps. This area was chosen due to the availability of PCBs contamination data for the year 2008, sampled in different sites and across the period during which (at this altitude) soils are snow free. This data-set offered a good opportunity to perform a cross-validation of the developed contamination maps.

2. Materials and Methods

2.1. Study area

The study area is located on a high altitude pasture plateau, 1 km wide and 5 km long between 1900 and 2100 m a.s.l. (Andossi plateau near the Splügen Pass, Italian Central Alps). The general climatic conditions of the area were estimated from data gathered by a nearby weather station (Stuetta 1850 m a.s.l.) over a 30-year time interval (1971-2000). Average annual precipitation and mean annual temperature are 1170 mm $year^{-1}$ and 2.7 °C, respectively. The peak for both precipitation and temperature occurs in summer. Snow precipitation accounts for 45-50% of total precipitation, and occurs generally from October to May (Mariani, 2007).

2.2. Chemical and Meteorological monitoring during 2008

In the study area, during year 2008, a specific soil sampling program for PCB quantification and a specific meteorological monitoring were performed at three nearby sites (at ~100 m distance). The three sites were characterized by the same altitude (1930 m), but by different aspects (North, plain and South). The different aspects were determined by the presence of small karstic reliefs (around 100 m high and 300 m wide) located irregularly on the plateau. Soil samples were collected in 2008 on six dates, spanning the period in which the soil was snow free (T1: 06/01/08, T2: 06/27/08, T3: 07/19/08, T4: 08/07/08, T5: 09/09/08, T6: 10/01/08). For every

date and site, three soil layers were sampled: 0-1 cm depth (O layer which is very thin in these Alpine grasslands), 1-4 cm depth (A1 layer) and 4-7 cm depth (A2 layer). Details of the soil sampling and chemical analysis are given in Guazzoni et al. (2011).

Meteorological monitoring was performed in the same sites where soil samples for PCBs analyses were took, by means of three meteorological stations. Since June 28th the three stations were measuring soil temperature (at -0.05 and -0.10 m) and air temperature (at 1.80 m), the intermediate station was also provided with a sensor for global solar radiation (2 m). The placement of stations and instruments was carried out following the criteria stated by the WMO (1996).

The first period of 2008 was not covered by direct in-situ measures, data for the missing period (from January 1st to June 27th) was recorded in a weather station (Borghetto) located 5 km afar from the study area and nearly 100 m higher. Due to different topography, meteorological data series were not identical, but highly correlated (Table S1). Both soil temperature and measured solar radiation time series presented some amount of missing data for the sampling sites. To infer the missing data and a multiple imputation algorithm was applied as proposed by Honaker and King (2010). The algorithm uses an Expectation Maximization (EM) approach (Dempster et al., 1977) to infer missing data in a time series from other correlated series (the Borghetto station series), the process is further improved by the use of importance sampling (King et al., 2001) and polynomial functions to model the time related trend (Honaker and King, 2010). The process is highly efficient and a cross-validation between measured and inferred data (Figure S1), shows R^2 between 0.96 and 0.97 (Table S2).

3. Calculation

3.1. Modeling soil organic carbon content

A SOC map of the study area was produced as described by Ballabio et al. (2010, Submitted). The SOC map was derived from an extensive soil survey comprising 140 samples. SOC content have been mapped through its relation with terrain features (Ballabio, 2009) and vegetation cover descriptors derived from Correspondence Analysis using a Regression Kriging (Odeh et al., 1994; Hengl et al., 2004) framework. The idea was to model SOC content in the topsoil as a function of plant cover, as different plant communities reflect different pedo-climatic conditions and produce different amounts and kinds of organic matter, while the associated microbial communities mineralize organic matter at a related speed. Although the map predicts SOC in the study area content with a good approximation, its estimates are referred to the whole topsoil. However SOC gradient in natural soils is very strong within the first few cm; the soil samples for PCBs monitoring revealed that SOC gradient was exponential and consistent with a second-order kinetic of accumulation

(Figure S2). It was thus necessary to model this gradient over the full extent of the study area in order to gain reliable estimates of SOC gradient over the whole area and for the POPs sampling depths.

Using an exponential model, SOC gradient has been calculated for all the study area using an inverse problem approach. Knowing that the SOC content expressed by the existing map is the integral of the exponential gradient function calculated over the topsoil we can derive

$$SOC_s = \int_0^d \alpha + \beta e^{(-\gamma x)} dx \quad (1)$$

Where SOC_s is the measured topsoil SOC content, d is the depth at which the exponential gradient becomes null (calculated from data as equal to 20 cm), α, β are unknown parameters to be estimated and γ, which express curve concavity, was estimated in a second step as equal to 0.36. As SOC_s is know, it is possible to estimate the other parameters as the ones which minimize the squared difference between the left and the right hand terms of Eq. 1. Thus the problem becomes a simple optimization problem solvable for each location of the study area. SOC estimates for the POP sampling depths are, thereafter, calculated from Eq. 1 using the locally fitted parameters.

3.2. Modeling soil temperature

The Sine Wave approach (Hillel, 2004), estimates the soil thermal regime from amplitude and phase differences of soil temperatures measured at two depths, assuming an homogeneous soil media, and a simple sinusoidal diurnal temperature wave describing the temperature T at depth z and time t (details in supplementary data).

$$T(t,z) = \bar{T} + A_0 \sin\left[\omega t - z/d\right] e^{-z/d} \quad (2)$$

Where T is the average soil temperature, A_0 is the amplitude of the sinusoidal at depth 0, ω is the time period, z represents depth and d is the damping depth which is a function of soil thermal conductivity and heat capacity. From Eq. 2 follows that soil temperature variation in time is represented by a sine wave whose amplitude decreases with depth. As temperature oscillates between day and night, heat propagates within the soil in a sequence of depth waning sinusoidal waves, at any fixed time the temperature gradient is represented by the convolution of these wave-fronts. While Eq. 2 is usually solved directly for two depths to derive the ratio between thermal conductivity and heat capacity, it is also possible to perform a direct non-linear fit of the sine series. In this case the amplitude was estimated from as a linear function of air temperature (T_{air}) and incident solar radiation (R_x), whose parameters were estimated by minimizing the difference between measured ($T\,m$) and sine wave estimated temperature at sampling depths z for every aspect a, by finding β_1, β_2, ω and λ which minimize

$$\sum_{\substack{z=5,10 \\ a=N,P,S}} \left[Tm_{a,z} - \left[(\beta_1 T_{air} + \beta_2 R_a)\sin(\omega(t) + \lambda(z))\right] e^{\lambda(z)} \right]^2 \quad (3)$$

Given the absence of a strong altitudinal temperature gradient, air temperature is approximately, uniform for the entire study area. The only spatially varying parameter is local solar radiation, which was derived from station measured and topography based theoretical radiation. Theoretical radiation was modelled using a ray-tracing hourly simulated solar radiation, calculated from the Digital Terrain Model (DTM) of the study area; this model takes into account not only the general terrain aspect and seasonal sun azimuth variation, but also the shadowing effect of topographic features. So, local solar radiation can be expressed as

$$R_x = Rs_x \frac{R_a}{Rs_a} \quad (4)$$

Where R_x, is the actual radiation for a general location x, R_a is the radiation measured at the station's location a, Rs_a is the radiation simulated at location a and Rs_x is the simulated radiation at a general location x, with all values referred to the same given time. Using the parameters estimated from Eq. 4 and R_x it is possible to calculate weekly soil temperatures at any given depth and for all the study area using air temperature, measured solar radiation and local simulated solar radiation.

The parameters of Eq. 2 have been estimated on a weekly basis, using a BFGS (Avriel, 2003) optimization procedure for each different depths and aspect. To improve coefficient reliability, the optimization was implemented in a bootstrap procedure thus reducing the influence of outliers on the model outcome. The resulting average error is generally below 0.1 °C with the exception of the second week of July where the error is around 0.7 °C (Figure S3).

3.3. Modeling soil contamination potential

For SVOC the soil-air partition coefficient, K_{sa} can be considered equal to the ratios between the soil-water partition coefficients (K_{sw}) and the air-water partition coefficients (K_{aw}), where the K_{sw} can be predicted by the Karickhoff's equation ($K_{sw} = f_{oc} \cdot K_{oc} = 0.411 \cdot f_{oc} \cdot \rho \cdot K_{ow}$, where f_{oc}, K_{oc} and ρ are the SOC fraction of a dry soil, the organic carbon-water partition coefficient and the density of the soil solids, respectively). Therefore, K_{sa} can be related to the ratio of K_{ow}/K_{aw} or to the octanol-air partition coefficient (K_{oa}) of chemicals considering the SOC fraction and the density of soils (Hippelein and McLachlan, 1998).

Experimental measurements of K_{sa} of different POPs (Hippelein and McLachlan, 2000) highlighted the importance of soil temperature. Varying the soil temperature between 5 and 60 °C, they evidenced that, as soil temperature decreases, K_{sa} increases (due to the greater effect of temperature on the vapour pressure than on the octanol solubility). In our study, the effect of the temperature was considered by the use of the Clausius-Clapeyron equation.

Including temperature in the evaluation of the soil accumulation capacity, the Daly et al. (2007)'s equation becomes

$$K_{sa} = 0.75 \cdot K_{oa} \cdot f_{oc} \cdot \rho_s \cdot \exp\left[\frac{\Delta U_{sa}}{R}\left(\frac{1}{T} - \frac{1}{298.15}\right)\right] \quad (5)$$

Where:

- K_{sa} = soil-air partition coefficient
- f_{oc} = SOC of the dry soil (g of organic carbon · g of dry soil^{-1})
- ρ_s = density of the soil solids (kg dm^{-3})
- K_{oa} = octanol-air partition coefficient
- ΔU_{sa} = soil-air heat transfer (kJ mol^{-1})
- R = gas constant (kJ mol^{-1} K^{-1})
- T = absolute temperature (K)

This equation takes into account differences among the soils in terms of density, SOC content and temperature. Soil density and SOC can be considered constant at least on a yearly base, while temperature is quite variable even on a daily basis.

Temperature fluctuations affect K_{sa} continuously, but these changes are very fast in comparison to exchange fluxes between the air-soil interface. The daily cycle of the surface temperature, giving an excursion of 5-10 °C, continuously drives the net contaminant flux toward equilibrium conditions, which cannot be reached in such small time, because of exchange limitations. Therefore, soil concentrations are not substantially affected by instant temperatures and not even by daily average soil temperature. Because the half times of emission rates were evaluated, in these conditions, in the order of weeks (Guazzoni et al., 2011), we decided to choose the 15 days averaged soil temperature as the temperature condition able to substantially affect the effective accumulation capability of soils in a mountain area. Therefore, the temperature parameters in Eq. 5 can be better defined as follows:

- T = mean absolute temperature (°K) of a specific soil layer, referred to the interval of 15-days before each sampling date

An additional variability factor derives from the pollutants distribution along the soil profile. Usually, POPs contamination in natural soils is evaluated between depths of 0-5 cm (Meijer et al., 2003b) or 0-10 cm (Čupr et al., 2010), because these contaminants are localized in the surface layers where most of the SOC is accumulated (Sweetman et al., 2005). Several authors studied the distribution profile within the soil (Cousins et al., 1999b; McLachlan et al., 2002; Armitage et al., 2006) evidencing that much of the variability among the concentrations in the different layers is related to the SOC content, while the main transport mechanism which distributes relatively non-volatile and hydrophobic compounds within the soil profile is vertical sorbed phase transport by means of bioturbation, cryoturbation and particle transport via macropores (McLachlan et al., 2002). McLachlan et al. (2002) demonstrated through modeling calculations, that without this mechanisms, CB-101 deposited in the

surface layer (0-1 cm) remains almost entirely therein over a 10-year period. Therefore, it can be assumed that POPs in soils follow the behaviour of the SOC, whose content decreases with depth.

3.4. Modeling the discharge and recharge behaviour

In our measurements, we have experienced that in autumn POPs concentrations are still generally low compared to those expected from time-specific K_{sa}, showing a retard in the recharge time (Tremolada et al., 2009b).

We know that air concentrations at low altitudes follow a typical yearly cycle with winter levels lower than summer ones (4-6 times) (Lee and Jones, 1999; Halsall et al., 1999); the same data showed a great variability also between daily concentrations, but not between the average concentrations of two consecutive periods, because of the high daily variability and the smoothing effect of the average concentrations of multi-day period. An experimental support of this hypothesis came from Nizzetto et al. (2008) data. These authors described an almost constant weekly-averaged air concentration, at least for penta-, hexa- and hepta-chlorinated biphenyls on another high altitude Alpine site during all summer. These high and quite constant air concentrations last until air is warm; in autumn, when air temperature decreases at both high and low altitudes, we can suppose, according to low altitude measurements, that average air concentrations at high altitude decrease too. In this conditions, the low soil concentrations measured in October could be, at least partially, explained by the decrease of PCB air concentrations.

Nevertheless, autumn behaviour is likely due to the fact that, despite the higher K_{sa}, the system is still beginning its recharge stage. A complete recharge was experimentally observed only the year after when soil was again snow free. Between the years 2007 and 2008, the same contamination peak, found in 2007 after the snow melt, was found in 2008, drawing a typical yearly cycle with a minimum of the POPs concentrations in summer (July) and a maximum of the concentrations in May/June (Tremolada et al., 2010). The observed retard of the recharge period, can also be explained by considering POPs accumulation and release as two different processes occurring at different velocities, independently from the variation of the PCB concentrations in air. Therefore, we mathematically tested this hypothesis at constant air levels. In these conditions, the recharge rate is directly proportional only to air concentration, because recharge occurs when soil concentrations are low and K_{sa} is high. On the contrary, the discharge phase happens when soil concentrations are high and K_{sa} is low; therefore the discharge rate depends on the PCB concentration in soil exceeding the equilibrium. Mathematically, POPs balance in soils can be summarized by a time dependent mass conservation equation, whose differential form is

$$\frac{dS_k}{dt} = k_1 A - k_2 S_k \quad (6)$$

where S_k is the mass of PCB exceeding the equilibrium with the atmospheric concentration A as defined by

$$S_k = \Delta Cs(t) = Cs(t) - K_{sa}(t)[A] \quad (7)$$

where $Cs(t)$ is the concentration of the congener in the soil and $K_{sa}(t)$ is the relative partition coefficient at a given time t, respectively. In these conditions, the accumulation term $k_1 A$ is linear while the depletion term $k_2 S_k$ is exponential, depending upon a varying quantity. Whenever the K_{sa} decreases, the excess of PCB in the soil will pass in the gaseous phase and then into atmosphere, this process depends on ΔK_{sa}, if ΔK_{sa} is large the excess of PCB will be lost faster. The process is also function of the concentration of PCB through time: considering that PCB depletion is not instantaneous, depletion will diminish PCB excess with a typical exponential decay. On the other side, accumulation will happen with a first order kinetic approximating atmospheric concentration as constant in time. Eq. 6 can be numerically solved using the Runge-Kutta method (Butcher, 2003).

4. Results and Discussion

4.1. Potential POP reservoir and K_{sa} maps of the study area

Using seasonally resolved soil temperature and SOC gradients maps, it was possible to calculate maps of specific K_{sa} gradients (Figure S10) for each PCB congener with a resolution of 1×1 m for each sampling day (daily resolution). All maps (Figure S4-S9) show clearly the effect of SOC and temperature distribution on K_{sa}, giving time dependent accumulation potential differences of roughly one order of magnitude also at this limited spatial scale. Each group of maps shows lower K_{sa} values for deeper soil layers as their SOC content is significantly lower and a large horizontal variability depending on topography, which accounts for temperature differences at the same date (aspect effect; Tremolada et al., 2009a), and SOC distribution. The difference in the accumulation potential can be evaluated from K_{sa}, which ranges from around $1 \cdot 10^9$ to above $1 \cdot 10^{10}$. The K_{sa} Δ and K_{sa} values are bigger in May, then they become small in July, and later they start to increase again progressively from August to October.

The map of October 2008 (Figure S9) is strikingly different from the other maps as the effect of topography on K_{sa} becomes more relevant. This is due to the increased difference of solar radiation between south and north facing slopes; as the sun azimuth draws near its minimum at the winter solstice, south facing slopes become more exposed to sunlight, while north facing slopes are permanently shadowed: this creates a strong temperature gradient which modifies the spatial distribution of K_{sa} (Table S3-S4) (in October, ΔK_{sa} between North and South aspects, reaches its maximum of exactly 1 order of magnitude). However this effect is likely to be present only at the

beginning of autumn, as during winter solar radiation is too weak to overcome the effect of air temperature on soil's and thereafter snow cover insulates the soil (Figure S11). The increasing effect of topography on soil temperature in October was directly observed by the instrumentation (Figure S11). The Δ of temperature between North and South sites were much larger in September and October than in May, June and July, but a parallel increase in the Δ of the POPs concentrations between the same two sites was not observed (Guazzoni et al., 2011). This apparent contrasting result will be discussed later, considering differences in the recharge and discharge rate of these contaminants toward and from soils.

In general, maps of K_{sa} accord with theoretical consideration and experimental evidences about the effect of physico-chemical properties of the compounds, SOC content and temperatures on POPs contamination in soil (Hippelein and McLachlan, 1998, 2000; Ribes et al., 2002; Meijer et al., 2003b;a). Moreover, the same maps accord with the profile distribution of PCBs in soil (Armitage et al., 2006; Moeckel et al., 2008) which was mainly related to the SOC gradient, and with the seasonal trends of mountain soils found by Tremolada et al. (2009b) and Guazzoni et al. (2011) which highlighted an intense concentration decrease between the first (just after the snow melting when air temperature is high, but the soils are still cold) and the second sampling date (when both soil and air temperatures are high).

The produced maps are also in qualitative agreement with the global MRC elaborated by Dalla Valle et al. (2005). These authors evidenced, a strong reduction of the reservoir capacity of soils in the northern hemisphere from January to July due to higher average temperatures and differences in the soil capacity of more than one order of magnitude due to differences of SOC content. The authors concluded that, at least for lighter PCBs, soils may act as sources or sinks in different areas, or at different times with seasonal flux shifts depending on temperature.

Our maps shows a similar picture of very different equilibrium conditions (K_{sa} values) depending on the site and the time of the year also at local scale. Shift of one order of magnitude in the equilibrium concentrations can occur in soils depending on season and SOC content, so that, even in the absence of changes in the air contamination, net emission fluxes and net deposition fluxes will cycle depending only on soil features (mainly soil temperatures). On this cycle of net PCB discharge (from May to July) and net PCB recharge (from October to May), based only on soil properties, the average air contamination levels play an additional role retarding the recharge period in autumn because of the lower autumn/winter air concentrations (Buehler and Hites, 2002; Lee and Jones, 1999; Halsall et al., 1999).

4.2. Validation of the K_{sa} maps with experimental data on CB-153

The assessment of the prediction made by the K_{sa} maps requires a validation step with external data. This can be done using an independent set of experimentally measured PCBs concentrations. A successful validation means that POP concentrations can be mapped at a very high resolution with good spatial and temporal approximation, on the basis of environmental conditions (soil temperature and SOC).

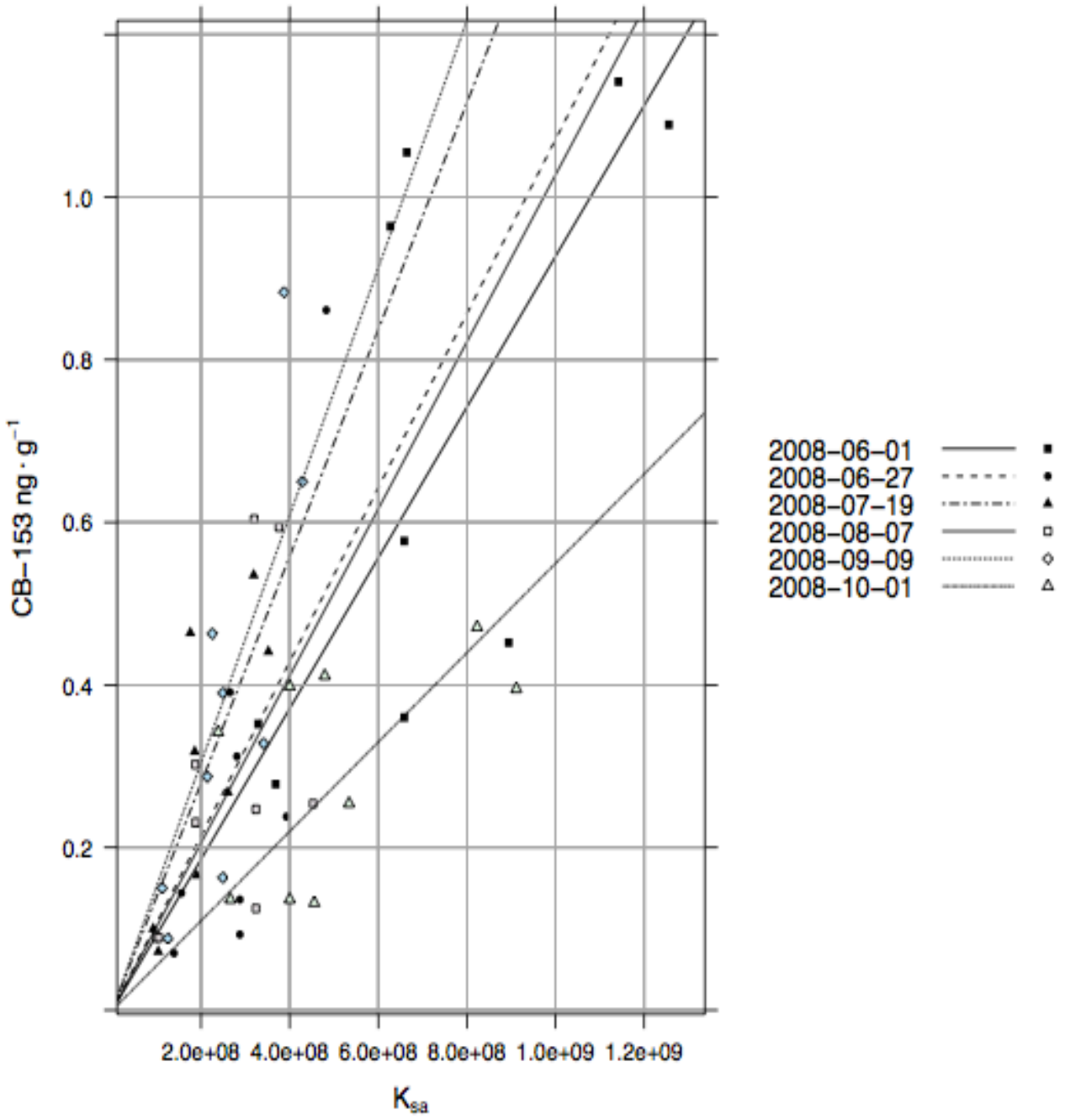

Fig.1: Plot of the measured concentrations versus predicted K_{sa} values for CB-153. Separate linear regression have been fitted for each sampling date and are shown as lines. The graph shows a good correlation between K_{sa} values and CB-153 concentrations (R^2=0.8, p-value=1.19e-09)

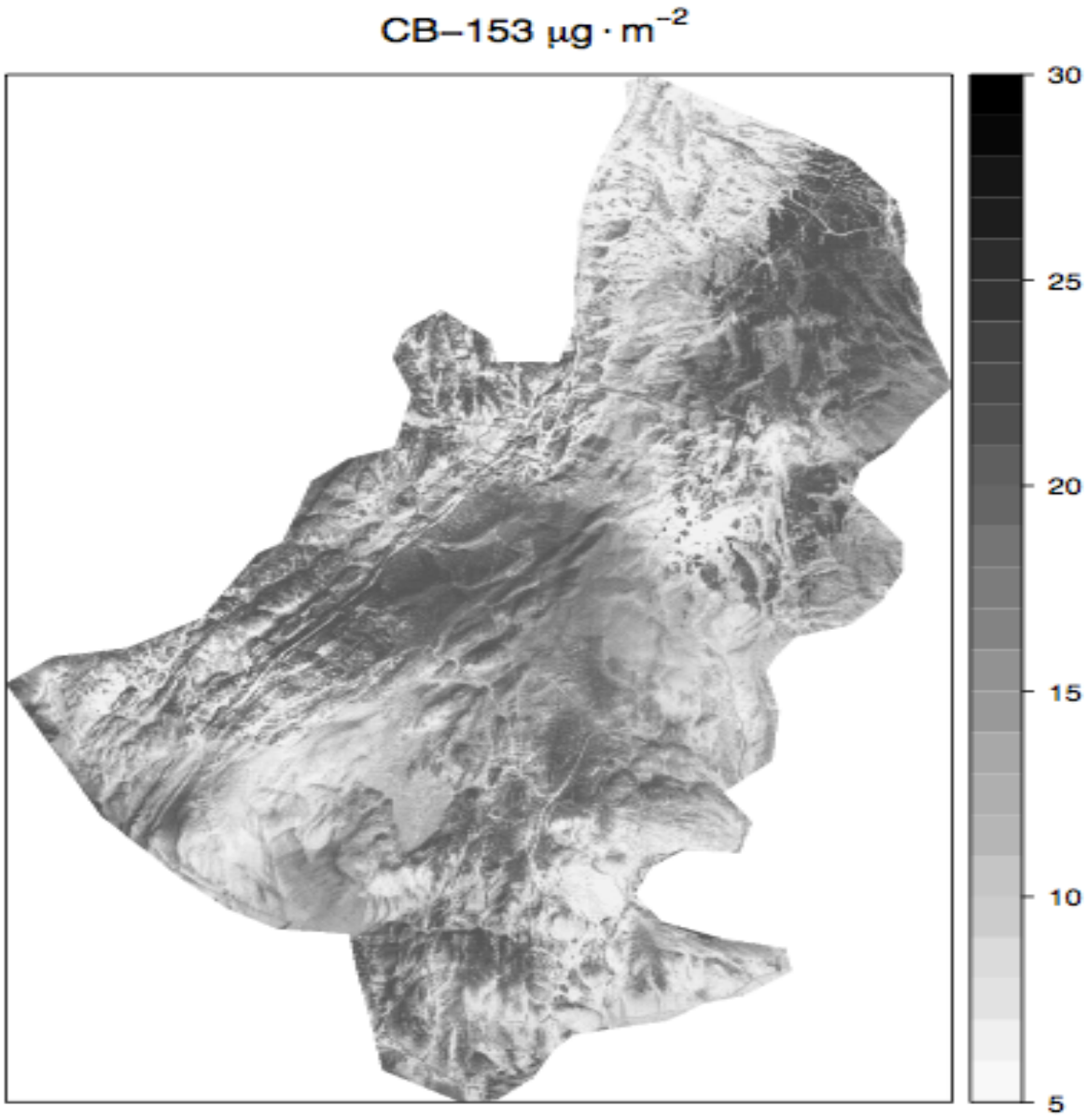

Fig 2: map of the net loss (in µg m^{-2} of CB-153 between May and August. As expected northern slopes are releasing higher quantities of PCB in the atmosphere as the initial concentration was also higher

Therefore the K_{sa} predictions made in the study area for the year 2008 were directly compared with measured data. Detail of the analysis and of the results are given in Guazzoni et al. (2011). Since the different kinetics of recharge and discharge imply a different ratio between K_{sa} and actual POPs concentrations for different periods of the year as well as differences coming from air concentrations levels, a global linear model R^2 is not a suited performance metric. However, it is possible to consider the relationship between a PCB congener and its K_{sa} values in a linear mixed-model with random slopes taking the sampling dates taken as a random effect. In this way we were able to include, in the predicted vs measured comparison, differences due to the possible shifts of soil concentrations from the equilibrium (K_{sa} value) and differences coming from different average PCB air

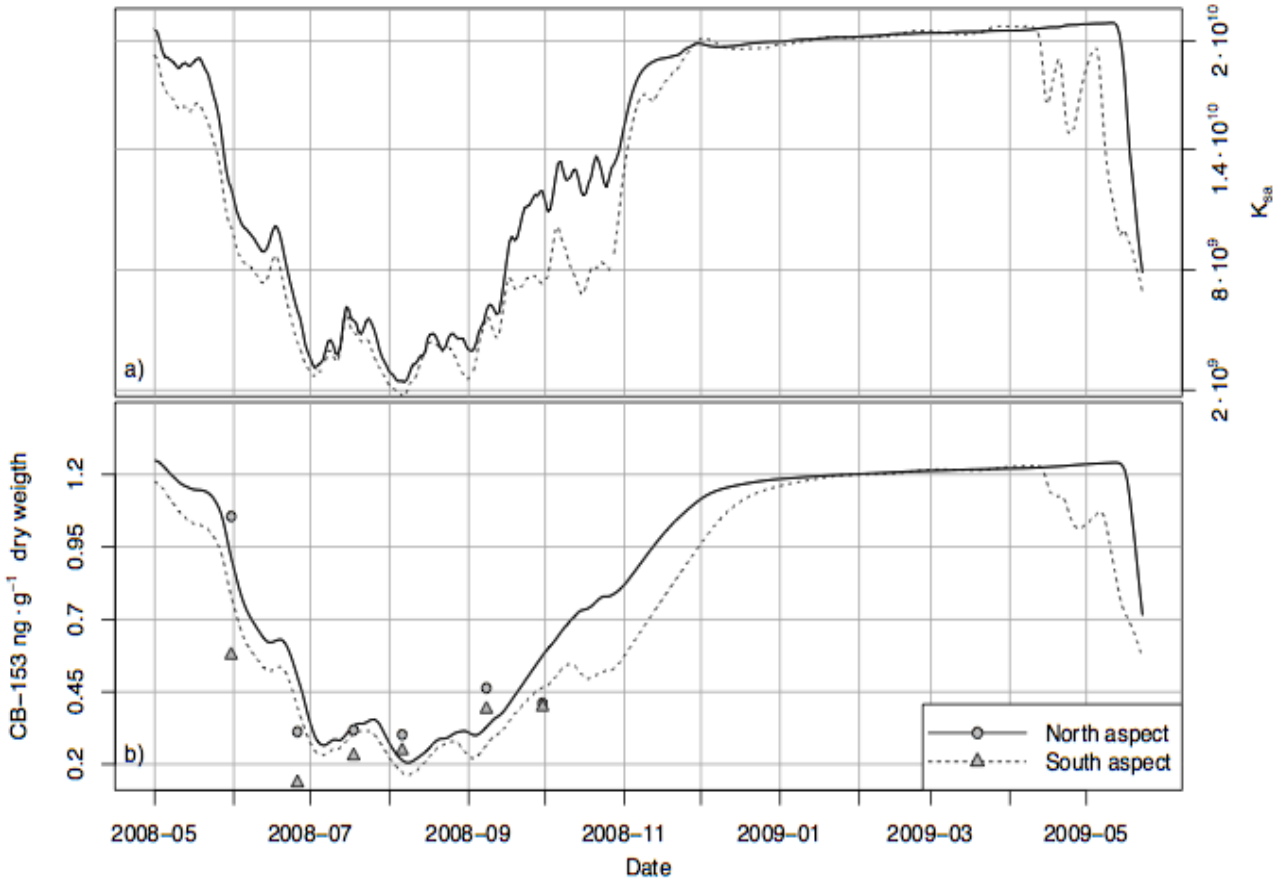

Fig. 3: a) Variation of the K_{sa} at the soil-atmosphere interface for the period between January 2008 and May 2009. b) variation of the concentration for congener CB-153 (ng g^{-1} dry weight) as predicted by the ordinary differential equation (ODE) model. The solid lines show the North aspect behaviour and the dashed lines the South one. Experimental CB-153 concentrations in N and S aspects are shown by circle and triangle marks, respectively.

levels during the considered season. Moreover, as the content of CB-153 must tend to zero for $\boldsymbol{K_{sa} \rightarrow 0}$, it follows that the mixed-model is bound to have zero intercept. Such model is depicted in Fig. 1 for CB-153 where each line is fitted on the data corresponding to the relative date and all the models are constrained to have zero intercept. The model shows a good performance as its overall R^2 is 0.80 and its p-value is strongly significant with a value around $\boldsymbol{2 \cdot 10^{-06}}$. Other congeners show similar prediction performances as show in Tab. S6.

The coefficients of Tab. S5 can be used as empirical parameters in order to seasonally calibrate the model for prediction purposes. Applying these coefficients, a highly spatial resolved concentration map can be obtained for a burden evaluation of the whole area referring to specific periods (predicted concentration maps). Changes in PCB burdens among seasons can be obtained as differences between predicted PCB concentrations for two periods. During the period of decreasing burdens, concentration differences can be interpreted as net emissions, while (during period of increasing burdens) as net depositions. Fig. 2 shows, for CB-153, the net mass

loss over the whole area between the maximum level of the recharge and discharge period. This map can be interpreted as the map of the whole emission, and from it, the amount of the total CB-153 loss can be accurately calculated by integrating punctual emissions over the whole area obtaining a total flux of 11.144 g.

4.3. Recharge and Discharge model

Fig.. 3 shows the outcome of the ordinary differential equation (ODE) model of Eq. 6, the upper graph (a) shows the K_{sa} trend of the CB-153 at the North and South facing sampling points for the period between January 2008 and May 2009, while the lower graph (b) shows the CB-153 concentrations for the same sites and period. Although this model does not take into account other sources of PCB (i.e. particulate and wet deposition) or the effect of snow cover, it is useful to show that the recharge rate is slower than the discharge rate also when constant air concentrations are used. The CB-153 concentration decrease between May and July was faster than the concentration increase between September and November especially for the South facing sampling point, which experienced in autumn the maximum temperature gain due to the aspect effect. In addition, hypothesizing a more realistic situation, other two factors are able to enhance the delay in the recharge phase for both North and South sites: one is the decreasing autumnal temperature which affects diffusion velocity in the air-soil interface; the second one is the expected decrease in air concentrations during autumn and winter.

Air concentrations were considered constant in order to highlight the kinetic aspects of the two phases, but this can be realistic only during summer when temperatures are generally high and measured air concentrations nearly constant (Nizzetto et al., 2008), while in autumn-winter measured air concentration levels are much lower (Růžičková et al., 2008), therefore the air-to-soil transfer retarded. The effect of temperatures on diffusion kinetics will act again in the same way: the release phase occurs mainly in June and July when temperature are at their maximum, while the recharge/accumulation phase happens in autumn when temperature are much lower. The recharge phase starts in autumn as soil temperature begin to decrease (as suggested by the model elaboration) but probably lasts after the snow melting the next year, when air temperature are high but soils are still cold and therefore their K_{sa} are still high.

Following the model predictions (Fig.. 3), CB-153 concentrations in soil are high until the end of May when soil becomes snow free and soil temperature starts to rise. Then in June, the PCB concentrations fall rapidly until the beginning of July. During July and August the PCB concentrations reach their minimum as the soil temperature was at its maximum. During this period, a small concentration increase happens in July due to worsening weather conditions,

causing a small rise of K_{sa}. The PCB concentrations then fall again until a minimum is reached at the beginning of August. Thereafter, concentrations are almost constant during all August, while at the beginning of September soil concentrations begin slowly to rise. During this period, it is interesting to note that K_{sa} increases faster than CB-153 levels which steadily increases with a first order kinetic.

The lower slope of the trend line of Fig.. 1 for October, can be thus explained by the retard in the recharge phase in autumn and by the increased difference of K_{sa} values between north and south facing slopes which increases the spread of the points along the horizontal axis, while the difference in measured CB-153 concentration remains relatively small.

5. Conclusions

The potential contamination maps developed in this work have two main peculiarities: they introduce in the computations the spatial variability of the main soil features (SOC and temperature) together with their vertical gradient along the soil profile. The second element introduced is the seasonal variability of the soil contamination due to the temperature cycle. Each of these elements have required the specific elaboration of spatial maps validated on experimental data available in the experimental area. Both these elements greatly improve the reliability of the overall environmental contaminants burdens at regional scale, which will allow a better prediction accuracy of inter-compartmental fluxes. While the presented contamination and flux maps refer to CB-153, chosen as the most representative of the class because of its abundance in environmental samples and for its intermediate chlorination level (haxa-chlorinated), the same elaborations can be done for any other PCB congener or with other POPs.

The high spatial-temporal resolution of this study evidenced also some interesting findings about PCBs distribution. Autumn spatial distribution of K_{sa} is substantially different from the one of others months, due to a stronger influence of temperature differences, produced by dissimilar amounts of incident solar radiation. While during spring and summer most of the K_{sa} differences among sites derives from differences in SOC.

In additions the increase in K_{sa} calculated in October do not corresponds to an equivalent concentration increase, indicating a possible consistent shift or retard in the equilibrium conditions. This fact was made evident by analysing the potential contamination maps and by the slope of the regressions between K_{sa} and measured data. The reason for this shift of October PCBs concentrations, in relation to their K_{sa} was discussed and, at least partially explained, by a differential equations model which highlights the effect on soil concentrations of the discharge kinetic (interpreted as an exponential process) and of the recharge kinetic (interpreted as first order process). Only the nature

of the process is able to produce the observed rapid discharge between June and July and a relatively slow recharge observed in October.

Considering the possible applications of the developed maps expressing both potential and actual contamination, we can highlight several items:

1. the maps of the potential contamination can shows times and sites more exposed to high contamination due to particular environmental features;
2. maps of the actual concentrations can integrate a limited number of experimental measures to model the contamination of an area;
3. maps of the actual concentrations give the opportunity to evaluate burden and fluxes with highly resolved seasonal and spatial details, therefore they offer a more precise evaluation of such data than referring only to the area average values.

These high-seasonally and -spatially resolved maps offer a very good and environmentally realistic representation of the contamination of an area and are highly suitable at local and regional scale.

References

Armitage, J.M., Hanson, M., Axelman, J., Cousins, I.T., 2006. Levels and vertical distribution of PCBs in agricultural and natural soils from sweden. Science of the Total Environment 371, 344–352.

Avriel, M., 2003. Nonlinear Programming: Analysis and Methods. Dover Publishing.

Ballabio, C., 2009. Spatial prediction of soil properties in temperate mountain regions using support vector regression. Geoderma 151, 338–350.

Ballabio, C., Fava, F., Rosenmund, A., 2010. A plant ecology approach to high-resolution digital soil mapping, in: Global Workshop on Digital Soil Mapping, Rome.

Ballabio, C., Fava, F., Rosenmund, A., Submitted. A plant ecology approach to digital soil mapping, improving the prediction of soil organic carbon content in alpine grasslands. Geoderma .

Breivik, K., Sweetman, A., Pacyna, J.M., Jones, K.C., 2002a. Toward a global historical emission inventory for selected PCB congeners - a mass balance approach. 1. global production and consumption. Science of the Total Environment 290, 181–198.

Breivik, K., Sweetman, A., Pacyna, J.M., Jones, K.C., 2002b. Toward a global historical emission inventory for selected PCB congeners - a mass balance approach. 2. emissions. Science of the Total Environment 290, 199–224.

Buehler, S.S., Hites, R.A., 2002. The great lakes' integrated atmospheric deposition network. Environmental Science & Technology 36, 354–359.

Butcher, J.C., 2003. Numerical methods for ordinary differential equations. John Wiley & Sons.

Chattopadhyay, S., Gupta, S., Saha, R.N., 2010. Spatial and temporal variation of urban air quality: a GIS approach. Journal of Environmental Protection 1, 264–277.

Cousins, I.T., Beck, A.J., Jones, K.C., 1999a. A review of the processes involved in the exchange of semi-volatile organic compounds (SVOC) across the air-soil interface. Science of the Total Environment 228, 5–24.

Cousins, I.T., Gevao, B., Jones, K.C., 1999b. Measuring and modelling the vertical distribution of semi-volatile organic compounds in soils. I:

PCB and PAH soil core data. Chemosphere 39, 2507–2518.

Dalla Valle, M., Jurado, E., Dachs, J., Sweetman, A.J., Jones, K.C., 2005. The maximum reservoir capacity of soils for persistent organic pollutants and implications for their global cycling. Environmental Pollution 134, 153–164.

Daly, G.L., Lei, Y.D., Castillo, L.E., Muir, D.C.G., Wania, F., 2007. Polycyclic aromatic hydrocarbons in costa rican air and soil: a tropical/temperate comparison. Atmospheric Environment 41, 7339–7350.

Dempster, A.P., Laird, N.M., Rubin, D.B., 1977. Maximum likelihood from incomplete data via the em algorithm. Journal of the Royal Statistical Society 39, 1–38.

Guazzoni, N., Comolli, R., Mariani, L., Cola, G., Parolini, M., Binelli, A., Tremolada, P., 2011. Meteorological and pedological influence on the PCBs distribution in mountain soils. Chemosphere 83, 186–192.

Halsall, C.J., Gevao, B., Hoswam, M., Lee, R.G.M., Ockenden, W., Jones, K.C., 1999. Temperature dependence of PCBs in the UK atmosphere. Atmospheric Environment 33, 541–552.

Harner, T., Bidleman, T.F., Jantunen, L.M.M., Mackay, D., 2001. Soil-air exchange model of persistent pesticides in the united states cotton belt. Environmental Toxicology & Chemistry 20, 1612–1621.

Hengl, T., Heuvelink, G.B.M., Stein, A., 2004. A generic framework for spatial prediction of soil variables based on regression-kriging. Geoderma 120, 75–93.

Hillel, D., 2004. Introduction to Environmental Soil Physics. Elsevier Science, London.

Hippelein, M., McLachlan, M.S., 1998. Soil/air partitioning of semivolatile organic compounds. 1. method development and influence of physical-chemical properties. Environmental Science & Technology 32, 310–316.

Hippelein, M., McLachlan, M.S., 2000. Soil/air partitioning of semivolatile organic compounds. 2. influence of temperature and relative humidity. Environmental Science & Technology 34, 3521–3526.

Honaker, J., King, G., 2010. What to do about missing values in time-series cross-section data. American Journal of Political Science 54, 561–581.

King, G., Honaker, J., Joseph, A., Scheve, K., 2001. Analyzing incomplete political science data: An alternative algorithm for multiple imputation. American Journal of Political Science 95, 49–69.

Lee, R.G.M., Jones, K.C., 1999. The influence of meteorology and air masses on daily atmospheric PCB and PAH concentrations at UK location. Environmental Science & Technology 33, 705–712.

Mariani, L., 2007. Caratteristiche climatiche. Società Italiana di Scienze del Suolo, Milano-Chiavenna.

McLachlan, M.S., Czub, G., Wania, F., 2002. The influence of vertical sorbed phase transport on the fate of organic chemicals in surface soils. Environmental Science & Technology 36, 4860–4867.

Meijer, S., Shoeib, M., Jantunen, L., Jones, K., Harner, T., 2003a. Air-soil exchange of organochlorine pesticides in agricultural soils. 1. field measurements using a novel in situ sampling device. Environmental Science & Technology 37, 1292–1299.

Meijer, S.N., Ockenden, W.A., Sweetman, A., Breivik, K., Grimalt, J.O., Jones, K.C., 2003b. Global distribution and budget of PCBs and HCB in background surface soils: implications for sources and environmental processes. Environmental Science & Technology 37, 667–672.

Meijer, S.N., Shoeib, M., Jones, K.C., Harner, T., 2003c. Air-soil exchange of organochlorine pesticides in agricultural soils. 2. laboratory measurements of the soil-air partition coefficient. Environmental Science & Technology 37, 1300–1305.

Meijer, S.N., Steinnes, E., Ockenden, W.A., Jones, K.C., 2002. Influence of environmental variables on the spatial distribution of PCBs in norwegian and u.k. soils: implications for global

cycling. Environmental Science & Technology 36, 2146–2153.

Moeckel, C., Nizzetto, L., Di Guardo, A., Steinnes, E., Freppaz, M., Filippa, G., Camporini, P., Benner, J., Jones, K.C., 2008. Persistent organic pollutants in boreal and montane soil profiles: distribution, evidence of processes and implications for global cycling. Environmental Science & Technology 42, 8374–8380.

Nizzetto, L., Jarvis, A., Brivio, P.A., Jones, K.C., Di Guardo, A., 2008. Seasonality of the air-forest canopy exchange of persistent organic pollutants. Environmental Science & Technology 42, 8778–8783.

Odeh, I.O.A., McBratney, A.B., Chittleborough, D.J., 1994. Spatial prediction of soil properties from landform attributes derived from a digital elevation model. Geoderma 63, 197 – 214.

Ribes, A., Grimalt, J.O., Torres García, C.J., Cuevas, E., 2002. Temperature and organic matter dependence of the distribution of organochlorine compounds in mountain soils from the subtropical atlantic (teide, tenerife island). Environmental Science & Technology 36, 1879–1885.

Růžičková, P., Klánová, J., Čupr, P., Lammel, G., Holoubek, I., 2008. An assessment of air-soil exchange of polychlorinated byphenils and organochlorine pesticides across central and southern europe. Environmental Science & Technology 42, 179–185.

Sweetman, A.J., Dalla Valle, M., Prevedouros, K., Jones, K.C., 2005. The role of soil organic carbon in the global cycling of persistent organic pollutants (POPs): interpreting and modelling field data. Chemosphere 60, 959–972.

Tremolada, P., Comolli, R., Parolini, M., Moia, F., Binelli, A., 2010. One-year cycle of DDT concentrations in high-altitude soils. Water, Air and Soil Pollution 217, 407–419.

Tremolada, P., Parolini, M., Binelli, A., Ballabio, C., Comolli, R., Provini, A., 2009a. Preferential retention of POPs on the northern aspect of mountains. Environmental Pollution 157, 3298–3307.

Tremolada, P., Parolini, M., Binelli, A., Ballabio, C., Comolli, R., Provini, A., 2009b. Seasonal changes and temperature-dependent accumulation of polycyclic aromatic hydrocarbons in high-altitude soils. Science of the Total Environment 407, 4269–4277.

Čupr, P., Bartoš, T., Sáňka, M., Klánová, J., Mikeš, O., Holoubek, I., 2010. Soil burdens of persistent organic pollutants - their levels, fate and risks. part iii. quantification of the soil burdens and related health risks in the czech republic. Science of the Total Environment 408, 486–494.

Verro, R., Calliera, M., Maffioli, G., Auteri, D., Sala, S., Finizio, A., Vighi, M., 2002. GIS-based system for surface water risk assessment of agricultural chemicals. 1. methodological approach. Environmental Science & Technology 36, 1532–1538.

Wania, F., Mackay, D., 1995. A global distribution model for persistent organic chemicals. The Science of the Total Environment 160/161, 211–232.

WMO, 1996. Guide to meteorological instruments and methods of observation. World Meteorological Organization. Geneva, CH. sixth edition. Updated by supplements when necessary.

Table S1: Correlation of data deficient solar radiation time series.

	Borghetto	Andossi	Madesimo	Madesimo.Net
Borghetto	1.00	0.92	0.92	0.91
Andossi	0.92	1.00	0.97	0.94
Madesimo	0.92	0.97	1.00	0.87
Madesimo.Net	0.91	0.94	0.87	1.00

Table S2: Solar radiation time series correlation after bootstrapped multiple imputations (temporal correlation assumed to be polynomial).

	Borghetto	Andossi	Madesimo	Madesimo.Net
Borghetto	1.00	0.97	0.96	0.96
Andossi	0.97	1.00	0.99	0.93
Madesimo	0.96	0.99	1.00	0.91
Madesimo.Net	0.96	0.93	0.91	1.00

Table S3: K_{sa} values for each PCB congener during May 2008.

Cong.	cm	South	Plain	North
CB-28	0.50	7.38e+06	1.00e+07	9.12e+06
	2.50	5.41e+06	5.01e+06	5.31e+06
	5.50	5.41e+06	2.63e+06	2.94e+06
CB-31	0.50	9.12e+06	1.24e+07	1.13e+07
	2.50	6.68e+06	6.19e+06	6.55e+06
	5.50	6.68e+06	3.24e+06	3.64e+06
CB-52	0.50	1.83e+07	2.49e+07	2.26e+07
	2.50	1.34e+07	1.24e+07	1.31e+07
	5.50	1.34e+07	6.51e+06	7.29e+06
CB-101	0.50	6.22e+07	8.44e+07	7.68e+07
	2.50	4.56e+07	4.22e+07	4.47e+07
	5.50	4.56e+07	2.21e+07	2.48e+07
CB-118	0.50	2.97e+08	4.02e+08	3.65e+08
	2.50	2.18e+08	2.01e+08	2.13e+08
	5.50	2.18e+08	1.05e+08	1.18e+08
CB-138	0.50	5.55e+08	7.53e+08	6.84e+08
	2.50	4.07e+08	3.76e+08	3.98e+08
	5.50	4.07e+08	1.97e+08	2.21e+08
CB-153	0.50	3.93e+08	5.31e+08	4.83e+08
	2.50	2.88e+08	2.65e+08	2.81e+08
	5.50	2.88e+08	1.39e+08	1.56e+08
CB-180	0.50	2.03e+09	2.75e+09	2.50e+09
	2.50	1.49e+09	1.37e+09	1.45e+09
	5.50	1.49e+09	7.20e+08	8.07e+08
CB-194	0.50	1.91e+10	2.58e+10	2.34e+10
	2.50	1.40e+10	1.29e+10	1.36e+10
	5.50	1.40e+10	6.75e+09	7.57e+09

Table S4: K_{sa} values for each PCB congener during October 2008.

Cong.	depth	South	Plain	North
CB-28	0.50	8.51e+06	1.57e+07	1.41e+07
	2.50	6.41e+06	7.85e+06	8.19e+06
	5.50	6.41e+06	4.11e+06	4.56e+06
CB-31	0.50	1.05e+07	1.94e+07	1.74e+07
	2.50	7.91e+06	9.70e+06	1.01e+07
	5.50	7.91e+06	5.08e+06	5.64e+06
CB-52	0.50	2.12e+07	3.96e+07	3.54e+07
	2.50	1.60e+07	1.98e+07	2.06e+07
	5.50	1.60e+07	1.04e+07	1.15e+07
CB-101	0.50	7.24e+07	1.36e+08	1.22e+08
	2.50	5.46e+07	6.80e+07	7.09e+07
	5.50	5.46e+07	3.56e+07	3.95e+07
CB-118	0.50	3.49e+08	6.68e+08	5.97e+08
	2.50	2.63e+08	3.34e+08	3.48e+08
	5.50	2.63e+08	1.75e+08	1.94e+08
CB-138	0.50	6.49e+08	1.23e+09	1.10e+09
	2.50	4.90e+08	6.16e+08	6.42e+08
	5.50	4.90e+08	3.23e+08	3.57e+08
CB-153	0.50	4.66e+08	9.08e+08	8.10e+08
	2.50	3.52e+08	4.53e+08	4.72e+08
	4.50	3.52e+08	2.38e+08	2.63e+08
CB-180	0.50	2.40e+09	4.67e+09	4.17e+09
	1.50	1.82e+09	2.33e+09	2.43e+09
	5.50	1.82e+09	1.22e+09	1.35e+09
CB-194	0.50	2.26e+10	4.41e+10	3.93e+10
	2.50	1.71e+10	2.20e+10	2.29e+10
	5.50	1.71e+10	1.15e+10	1.28e+10

Table S5: Regression estimates for each sampling date for the ratio between CB-153 concentration and K_{sa} for a linear mixed model with null intercept. Overall model R^2 is 0.8.

Date	Estimate	Std. Error	t value	Pr(> |t|)
2008-06-01	$2.161 \cdot 10^{-09}$	$1.701 \cdot 10^{-10}$	12.708	$1.332 \cdot 10^{-15}$
2008-07-19	$1.417 \cdot 10^{-09}$	$2.616 \cdot 10^{-10}$	5.419	$3.090 \cdot 10^{-06}$
2008-08-07	$1.293 \cdot 10^{-09}$	$2.384 \cdot 10^{-10}$	5.422	$3.062 \cdot 10^{-06}$
2008-09-09	$1.449 \cdot 10^{-09}$	$1.974 \cdot 10^{-10}$	7.340	$6.329 \cdot 10^{-09}$
2008-10-01	$5.671 \cdot 10^{-10}$	$1.091 \cdot 10^{-10}$	5.200	$6.240 \cdot 10^{-06}$

Table S6: Model fitting performance for different PCB species, R^2: Pearson's coefficient of determination, NRMSE: Normalized root-mean-squared error. Congeners marked with a * have one or more measures below detection limit.

PCB	R^2	NRMSE
18*	0.43	0.156
28/31*	0.32	0.218
101	0.73	0.165
118	0.73	0.183
138	0.81	0.170
153	0.80	0.176
180	0.78	0.155
194	0.74	0.160

Figure S1: a) Original Solar radiation time series with missing data. b) Reconstructed Solar radiation time series bootstrapped multiple imputations.

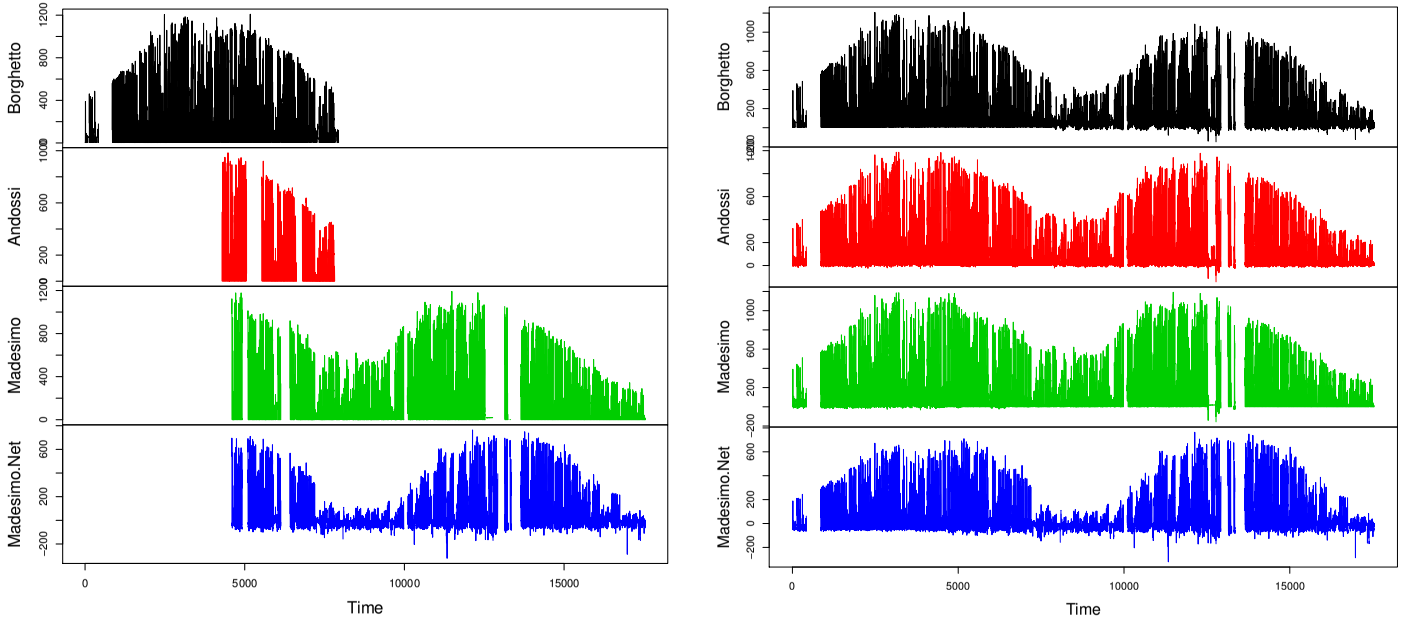

Figure S2: Organic Carbon concentration profiles for each of the three monitoring stations. Measured OC content is displayed by the black dots, the black solid line represents the fitted exponential model and the gray area represents the 0.95 confidence intervals.

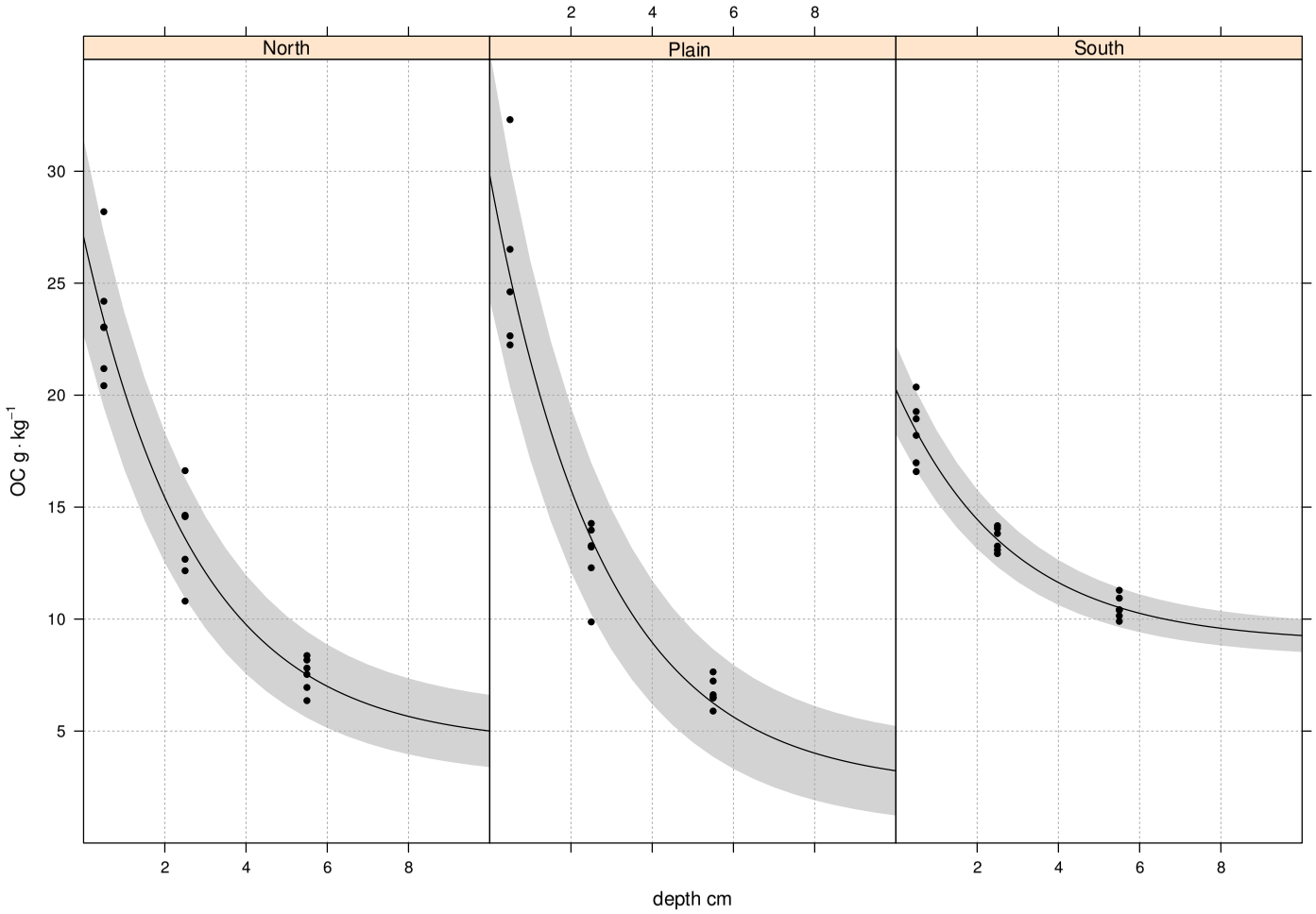

Figure S3: Predicted average temperatures for the three layers (0.5, 2.5, 5.5 cm) for the two weeks preceding the sampling. Temperature in °C is indicated on the vertical axis.

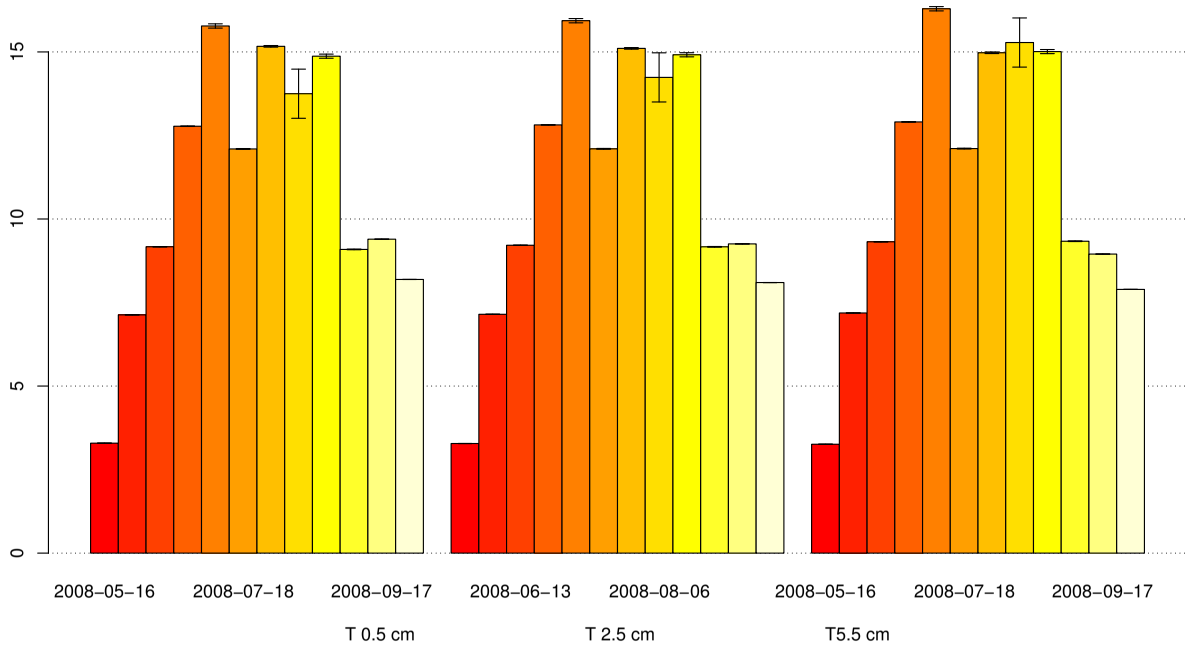

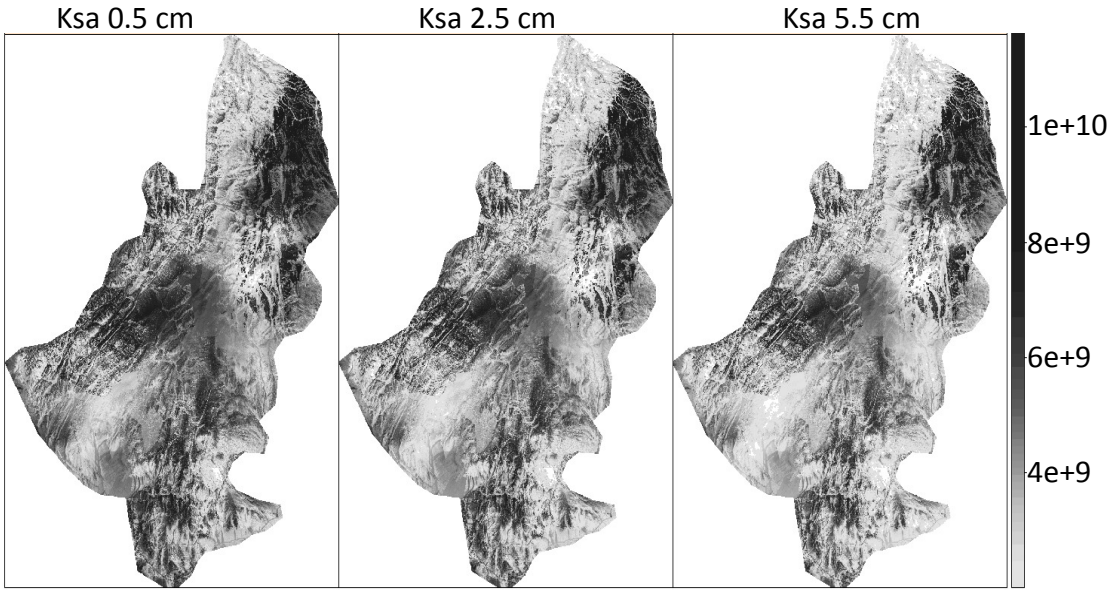

Figure S4: Ksa maps for CB-153 in May for the three sampling depth

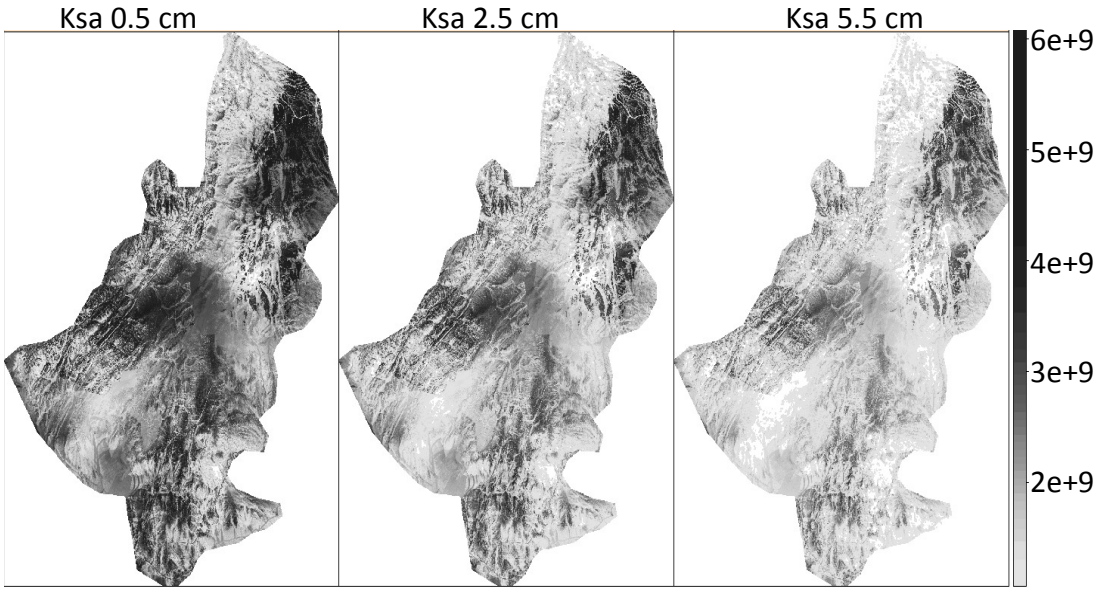

Figure S5: Ksa maps for CB-153 in June for the three sampling depth

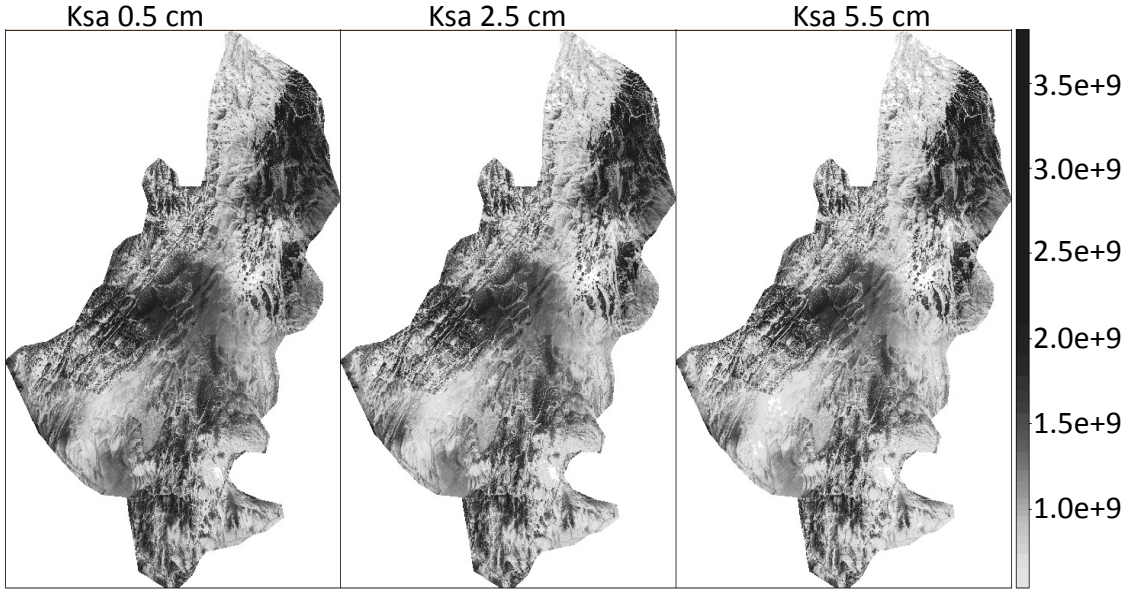

Figure S6: Ksa maps for CB-153 in July for the three sampling depth

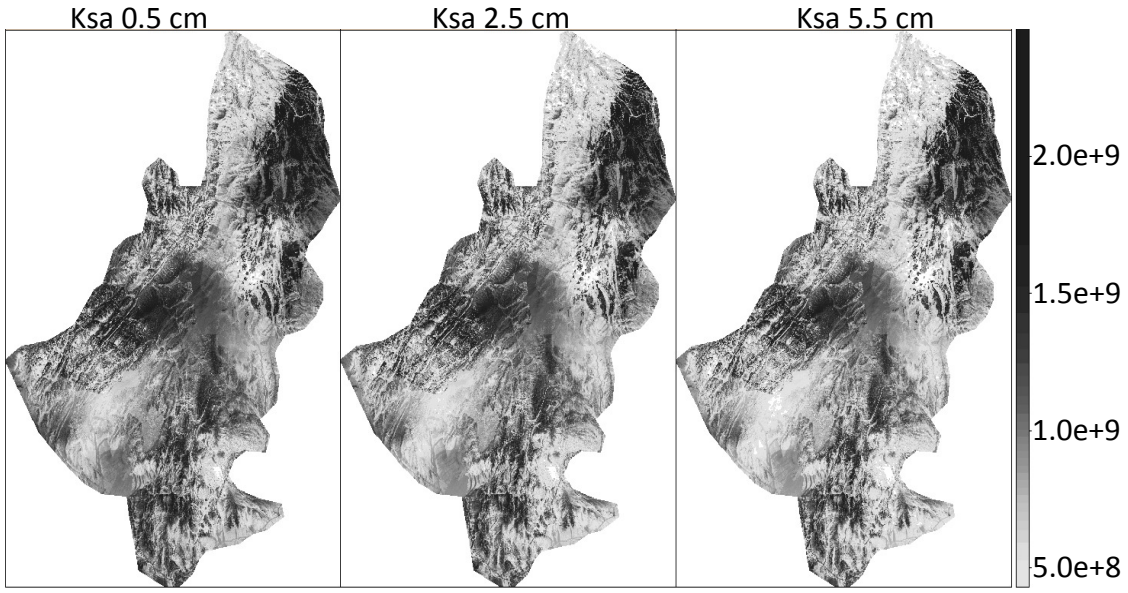

Figure S7: Ksa maps for CB-153 in August for the three sampling depth

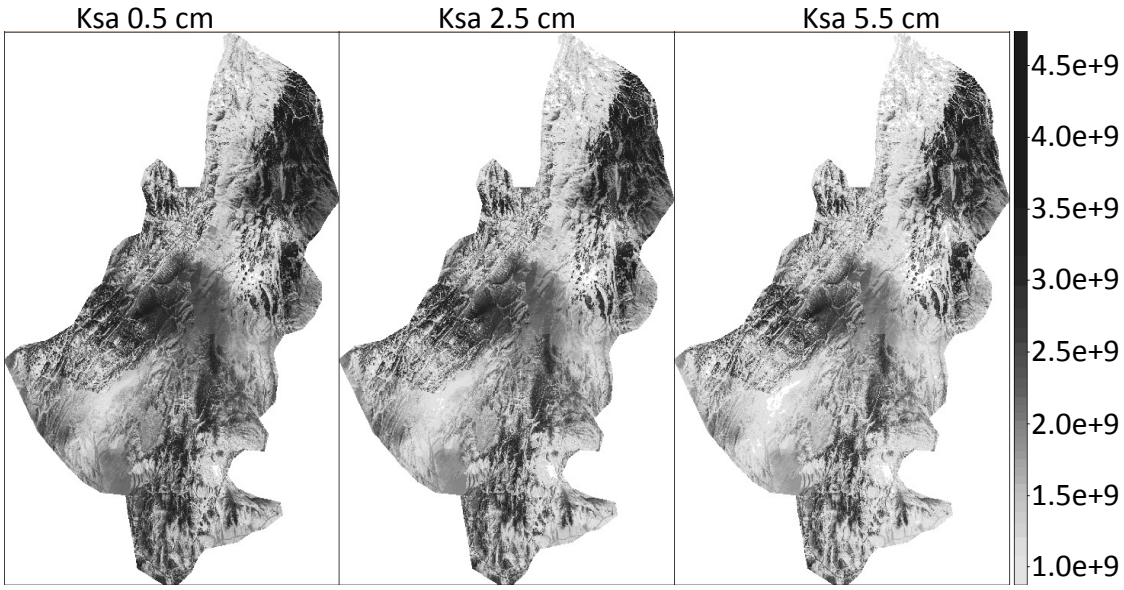

Figure S8: Ksa maps for CB-153 in September for the three sampling depth

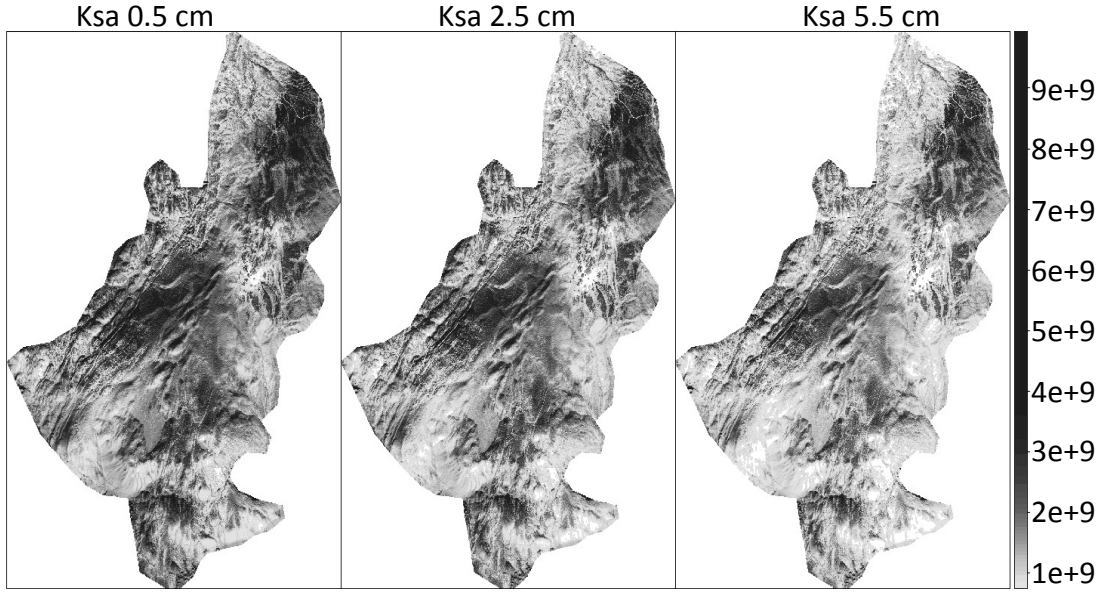

Figure S9: Ksa maps for CB-153 in October for the three sampling depth

Figure S10: a) Depth gradient of CB-153 measured at the three different stations in the different sampling periods. b) calculated K_{sa} for the same stations and the same periods.

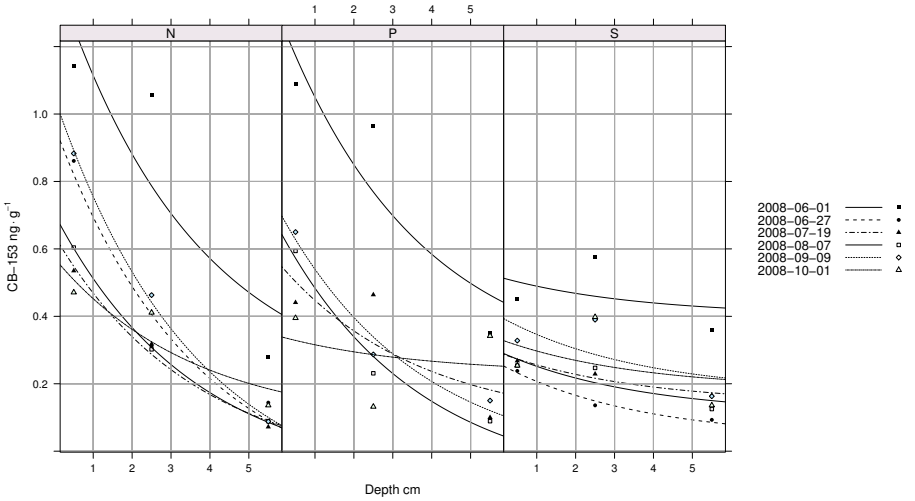

(a)

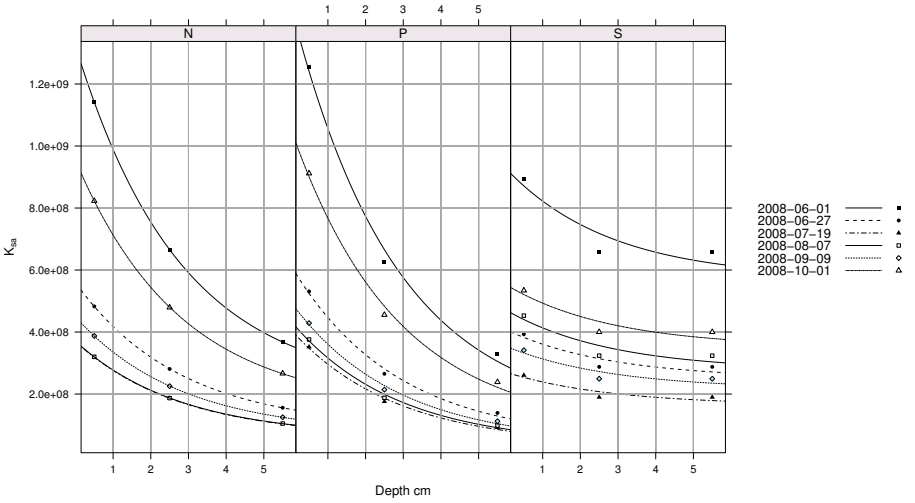

(b)

Figure S11: Temperature time series for air (at 1.8m above surface) and soil (at 0.1m below surface) for north and south facing stations respectively.

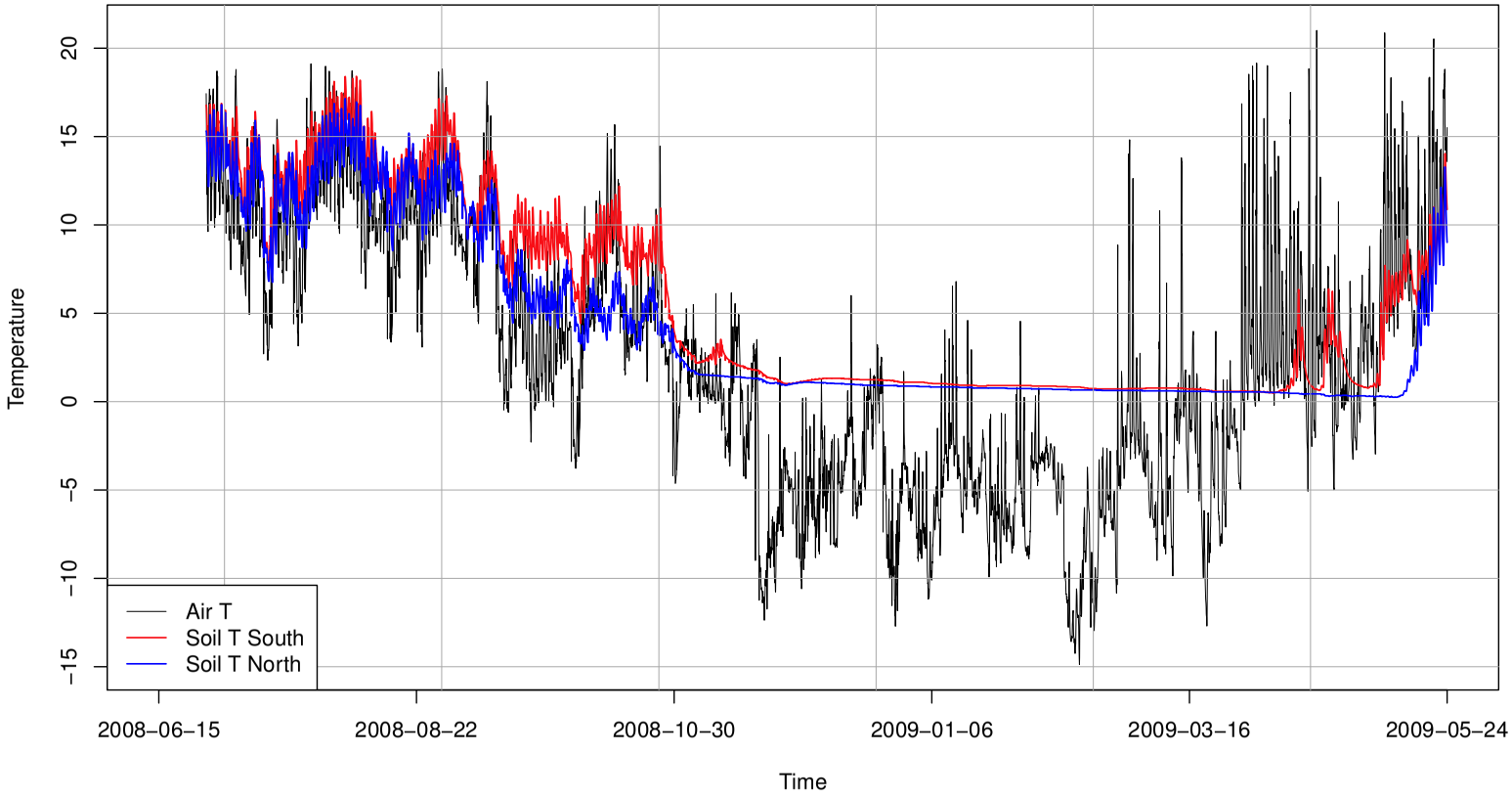

Chapter IV

Tremolada, P., Guazzoni, N., Smillovich L., Moia F., Comolli, R., 2012. The Effect of the Organic Matter Composition on POP Accumulation in Soil. Water, air and soil pollution 223, 4539−4556

Water Air Soil Pollut (2012) 223:4539–4556
DOI 10.1007/s11270-012-1216-3

The Effect of the Organic Matter Composition on POP Accumulation in Soil

Paolo Tremolada · Niccolò Guazzoni · Luisa Smillovich · Fabio Moia · Roberto Comolli

Received: 19 October 2011 / Accepted: 8 May 2012 / Published online: 2 June 2012

Abstract The effect of different humic fractions on polychlorinated biphenyl (PCB) contamination in soils was tested in the field by means of 53 soil samples from a high-altitude grassland plateau in the Italian Alps. Three humic fractions (humin, humic acids, and fulvic acids) were characterized in parallel by quantifying 12 PCB congeners to establish a direct relationship between PCB levels and humic fraction concentrations. Humin (the most hydrophobic fraction) appears to be the most closely correlated with the amount of PCBs in soil (R^2=0.83), while fulvic acid shows the lowest correlation (R^2=0.49). The idea of preferential sorption of hydrophobic compounds in the humin fraction is discussed, and the humin carbon content (f_{huminC}) is proposed as an improved parameter for evaluating the potential for POP accumulation in soils, replacing total organic carbon (f_{oc}). Congener studies revealed that penta- and hexa-substituted-CBs show the optimal combination of physicochemical properties for equilibrating with the humin content in soil. Moreover, $f_{\mathrm{huminC}}/f_{\mathrm{oc}}$ is conceptually equivalent to the empirical coefficients used in predictive K_{sa} equations. In our samples, the $f_{\mathrm{huminC}}/f_{\mathrm{oc}}$ was 0.55, a value in between the empirical coefficients proposed in the literature. In predictive equations, the use of f_{huminC} instead f_{oc} avoids the necessity of using an empirical parameter for a 'generic' condition by introducing an experimental parameter (f_{huminC}) that takes into account local conditions (organic matter composition).

Keywords Soil contamination · PCBs · Organic matter composition · Humic substances

P. Tremolada (✉) · N. Guazzoni · L. Smillovich
Department of Biology, University of Milan,
Via Celoria 26,
20133 Milan, Italy
e-mail: paolo.tremolada@unimi.it

F. Moia · R. Comolli
Department of Environmental and Land Sciences (DISAT),
University of Milan Bicocca,
Piazza della Scienza 1,
20126 Milan, Italy

1 Introduction

Soils are the main repository for hydrophobic persistent organic pollutants (POPs) such as polychlorinated biphenyls (PCBs) (Meijer et al. 2003), and soil organic matter (SOM) is a key parameter used in assessing the accumulation potential of POPs (Sweetman et al. 2005; Dalla Valle et al. 2005). Pignatello (1998)and Huang et al. (2003) have studied SOM and have shown that sorption occurs by a dual-mode mechanism (dissolution/partitioning and hole-filling mode). Though many authors have analyzed the importance of SOM composition on the sorption capacity (Rutherford et al. 1992; Piccolo et al. 1998; Chiou et al. 1998;Kohland Rice 1998; Ahmad et al. 2001; Doick et al. 2005; Kang and Xing 2005; Pan et al. 2006; Wen et al. 2007), whole organic carbon in soil (f_{oc}) is typically used as a directly proportional coefficient for predicting the

soil–air partition coefficient (K_{sa}) of semi-volatile persistent hydrophobic compounds (Hippelein and McLachlan 1998; Daly et al. 2007). Whole organic carbon is related to the accumulation capacity of hydrophobic compounds by means of the soil organic carbon/water partition coefficient (K_{oc})(Karickhoff 1981), even when consistent variability (Seth et al. 1999) and a non-linearity (Wen et al. 2007) exist in the K_{oc} determination for the same compound. Whenever POP distribution studies are performed in soils, a direct relationship between contaminant concentration (dry weight) and SOM is obtained but often with low regression coefficients. The main reason for this is that other variability factors affect the ability of SOM to predict the distribution of POPs in soil. Among these, the proximity of the contamination source can increase the POPs concentrations of by 1,000-fold between two soils having the same SOM content (Meijer et al. 2003). Differences in temperature with latitude (Meijer et al. 2002), altitude (Ribes et al. 2002), aspect (Tremolada et al. 2009), or season (Guazzoni et al. 2011) can also cause variation in contamination levels between soils with the same SOM content. Another factor that causes variability between soils with similar SOM content is related to past contamination events (Růžičková et al. 2008). Soils are not suitable for historical reconstruction of deposition events (in comparison with sediment and peat), but past contamination (prevailing deposition), in contrast to current net emission, is able to affect both concentration levels and vertical profiles (Armitage et al. 2006). In natural soils, POP contamination is concentrated at the surface because of the distribution of organic matter (Cousins et al. 1999; Krauss et al. 2000; Moeckel et al. 2008). Only arable soils affected by continuous mixing are able to transfer contaminants to different depths, reducing their volatilization back to the atmosphere (Armitage et al. 2006). Finally, vegetation type can act as an additional source of variability through the filter effect by which vegetation is able to efficiently accumulate POPs from the atmosphere, reducing the concentration in the air and transferring the contaminants to the soil at the end of a leaf cycle. Soils in forested areas show higher POP concentration levels than those with herbaceous vegetation, even after normalizing the concentrations to the SOM (Tremolada et al. 2008). All these elements affect POP contamination in soils to different degrees, surpassing the effect of the SOM and of its composition.

Despite the importance of SOM in determining the extent and distribution of POP contamination, the effect of SOM composition has not yet been widely considered. The preferential accumulation of non-ionic organic contaminants in specific SOM fractions has been reported by several authors, in particular, with regard to pesticides that are partially water-soluble (Piccolo et al. 1996, 1998; Ahmad et al. 2001), as well as highly hydrophobic compounds such as PCBs and PAHs (Chiou et al. 1998; Kohl and Rice 1998; Doick et al. 2005; Kang and Xing 2005; Pan et al. 2006; Wen et al. 2007). Chiou et al. (1998) explained that the elevated K_{oc} values of PCBs and PAHs in sediments as compared with soils is a result of the differences in their OM composition: Soils generally have higher combined fractions of *O*-alkyl and carboxyl-amide-ester components than do sediments, which results in a greater concentration of polar groups in their OM fraction. SOM is highly variable in its chemical composition; therefore, its sorption properties are expected to vary as well.

Traditionally, SOM is divided into humic and non-humic substances (Kononova 1966; Stevenson 1994; Andreux 1996; Stevenson and Cole 1999; Bleam 2011). Non-humic substances include simple organic molecules such as peptides, amino acids, and sugars. Humic substances are much more stable and abundant (up to 80% of the total) and can be defined as natural "heterogeneous polymers" of biogenic origin, characterized by color (yellow to black), high molecular weight, and refractoriness to the mineralization process (Hayes et al. 1989; Rice 2001; Albers et al. 2008).

The literature agrees on the preferential role of humin and especially its lipid components on the sorption of hydrophobic contaminants (Kohl and Rice 1998; Doick et al. 2005; Kang and Xing 2005; Pan et al. 2006; Wen et al. 2007). This conclusion is not surprising because it is expected that hydrophobic POPs be preferentially sorbed by the most hydrophobic component of the SOM (the humin fraction or some fraction of it), at least for sorption by partitioning. As the abundance of humin can vary greatly in soils, those with lower SOM but with a greater abundance of humin can be more effective in accumulating POPs than SOM-rich soils with a low humin fraction. The humin fraction can vary from 10% in spodosol to over 60% in vertisols (Andreux 1996). These differences, and in general the SOM composition, are expected to greatly affect the accumulation of POPs in soils. Until now, data have been obtained by

laboratory experiments relating K_{oc} with detailed humic substance characterization (elemental composition, Fourier transform infrared spectra, and ^{13}C NMR spectra), but no attempts have been made to directly relate SOM composition and contamination levels in the field. This work is aimed at comparing the content of humin, humic acids, and fulvic acids of 53 soil samples with their contents of several PCBs, which are representative of the PCB class. The analyzed soil samples came from a high-altitude plateau in the central Italian Alps.

2 Materials and Methods

2.1 Study Area and Sampling Sites

The study area is located on a high-altitude carbonatic plateau, 1 km wide and 5 km long, located at an altitude between 1,900 and 2,100 m asl (Andossi plateau near Splugen Pass, central Italian Alps). The general climatic conditions of the area were estimated from data gathered by a nearby weather station (Stuetta 1,850 m asl) over a 30-year time interval (1971–2000). The mean annual precipitation and mean annual temperature were 1170 mm year^{-1} and 2.7°C, respectively. The max-imum precipitation and temperature occur in the sum-mer (oceanic climate). Snow precipitation accounts for 45–50% of total precipitation and generally occurs from October to May (SISS 2007). The lithological substrate is made by marble and crystalline limestone, covered by acidic glacial deposit.

In 2008, soil sampling was performed on the plateau at approximately 1,930 m asl at three nearby sites (near 100 m distance) but with different aspects (North-, plain-, and South-facing sites). The different aspects were determined by small karstic reliefs (around 100 m high and 300 m wide) located irregularly on the plateau. The sampling sites were fenced (5 m× 5 m fences) to prevent the entry of cows that graze on the plateau (Fig. 1). Soil features and vegetation at the sampling sites were described in detail in Guazzoni et al. (2011) and in Tato et al. (2011), respectively. Briefly, the soil at the plain site, according to WRB (IUSS Working Group WRB 2006), is an epileptic cambisol (A-BA-Bw-C horizon sequence), with a topsoil pH_w of 3.6, having a thickness of 45 cm over a lithic contact (fractured marble). At the North

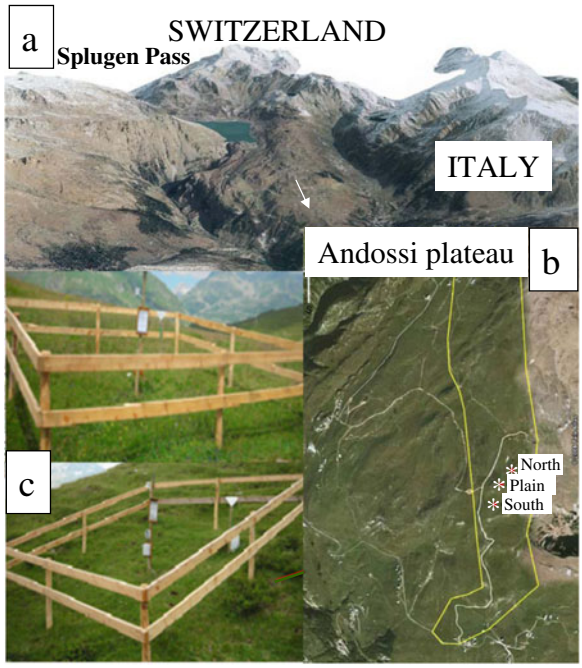

Fig. 1 Map of the Andossi plateau near Spluga Pass, central Italian Alps (**a**) with a detail of the sampling area (**b**) and of the sample sites (**c**)

site, the soil is again an epileptic cambisol (A-BAw1-BAw2), with a topsoil pH_w of 4.8, having a thickness of 42 cm over fractured marble. The South site soil is a rendzic phaeozem (A1–A2), with a topsoil pH_w of 5.1, having a thickness of 16 cm over a very fractured rock layer (C/R) with weathered marble pockets.

The vegetation present at the sampling sites and in general on the plateau is mainly determined by the grazing of cows during the summer, which maintains herbaceous species instead of the upper limit of coniferous woods. The composition and variability of grass species reflects two main factors: the grazing pressure and the local variability of the pedoclimatic conditions, which are determined mainly by substrate type, soil thickness, slope, and solar irradiation. In 2008, a detailed vegetation analysis was performed at the sampling sites, and a rich herbaceous community composed of 89 species belonging to 27 families was found (Tato L. unpublished data).

2.2 Soil Sampling

Soil samples were collected in 2008 on six dates spanning the period in which the soil was free from a

mantle of snow (T1-06/01/08, T2-06/27/08, T3-07/19/08, T4-08/07/08, T5-09/09/08, T6 10/01/08). Within every fence, three cubes (edge 10 cm) of soil were taken and separated into three layers: the O layer (0–1 cm depth), which is very thin in these Alpine grasslands, the A1 layer (1–4 cm depth), and the A2 layer (4–7 cm depth). The three sub-samples from each layer were homogenized (by manual mixing in situ) to reduce the local variability, wrapped in acetone-washed aluminium foil and enclosed in a sealed plastic bag. The samples were stored at −20°C until analyses were performed.

2.3 SOM Fractionation

The separation of humin and humic and fulvic acids was accomplished following the method described by Anderson and Shoenau (2008). The separation is based on the water solubility of the three fractions under different pH conditions. The following materials and reagents were used for the analytical procedure: lyophilizer (Edwards 1001, Edwards, Crawley, UK), sodium hydroxide and chloridric acid (Sigma-Aldrich, Steinheim, Germany), centrifuge (Sorvall), and elemental analyzer (Flash 1112, Thermo Scientific).

Two grams of lyophilized soil was suspended in a centrifuge tube with 20 mL of 0.5 M HCl for 1 h to solubilize the inorganic carbon. After centrifugation at 10,000 rpm for 15 min, the supernatant was eliminated, and 20 mL of distilled water was added to suspend the precipitate. After centrifugation at 10,000 rpm for 15 min, the supernatant was decanted, and the precipitate was suspended in 20 mL of 0.5 M NaOH (added under nitrogen flow) and shaken for 18 h on a rotary agitator in order to separate the humin fraction from the humic and fulvic acids that were extracted with the basic solution. After centrifugation at 10,000 rpm for 15 min, the precipitate, containing humin, was suspended with 10 mL of distilled water and then transferred to a pre-weighed beaker for lyophilization and for the gravimetric determination of the dry fraction.

The supernatant, containing humic and fulvic acids, was transferred to a new centrifuge tube and acidified with 6 M HCl to a pH between 1.5 and 1.1. The acidification causes the precipitation of the humic acids, while the fulvic acids remained in the acidic solution. After centrifugation at 10,000 rpm for 15 min, the supernatant, containing the fulvic acids, was transferred to a pre-weighed beaker for lyophilization and for gravimetric determination of the dry fraction. The precipitate, containing the humic acids, was suspended in 10 mL of 0.1 M NaOH and then transferred to a pre-weighed beaker for lyophilization and for gravimetric determination of its dry fraction.

The three dry fractions, containing humin, humic acids, and fulvic acids were analyzed for their carbon and nitrogen content with an elemental analyzer using aspartic acid as standard (36.09% and 10.52% of carbon and nitrogen, respectively). The C and N content in the samples was multiplied by the weight of every fraction extracted during the separation procedure, giving the amount of carbon and nitrogen in 2 g of soil, from which the amount in grams per kilogram was obtained.

The reproducibility of the carbon and nitrogen determination was confirmed by separating and analyzing nine samples in duplicate. The mean variability of the replicates was 4.7% and 6.6% for carbon and nitrogen, respectively. The accuracy of the analyses was indirectly evaluated by comparing the sum of organic carbon in the three fractions (humin, humic acids, and fulvic acids) with the total organic carbon measured for the whole sample (no separation). The mean difference between these results was 6.1%.

2.4 PCB Determination

The same soil samples were analyzed for their PCB content, measuring 13 congener concentrations (Guazzoni et al. 2011). The analyzed congeners included: CB-18, CB-31, CB-28, CB-44, CB-52, CB-101, CB-118, CB-138, CB-149, CB-153, CB-170, CB-180, and CB-194. The analytical procedure was as follows: sample lyophilization, extraction in a Soxhlet apparatus, digestion with sulphuric acid, cleaning on a multilayer column, and analysis using GC/MS/MS methodology. Complete information on the PCB quantification is available in Guazzoni et al. (2011).

2.5 Statistical Analyses

The software SPSS 18.0 was used to perform Kolmogorov–Smirnov tests (in order to verify the normal distribution of the data), linear correlations and regressions, generalized linear modelling (GLM), and Bonferroni post hoc tests.

3 Results and Discussion

3.1 SOM Composition of the Analyzed Soils

The separation method reported by Anderson and Schoenau (2008) is a traditional alkali extraction procedure, widely used, for separating humic fractions from soil (Hayes and Malcolm 2001; Rice 2001). It separates three main humic fractions: humin, humic acids, and fulvic acids; the definition of these mixtures derives from the method itself, as reported by Hayes and Clapp (2001): Humin is the OM-fraction insoluble at any pH; humic acids are the OM-fraction that precipitates at low pH (between 2 and 1), and fulvic acids are the OM-fraction soluble at all pH values.

The products obtained by the separation of the soil organic matter using the method reported by Anderson and Schoenau (2008) are shown in Fig. 2. So, different colors are typical of the three humic fractions (MacCarthy 2001). Each fraction has specific properties; one of these is the relative carbon and nitrogen content from which the C/N ratio is derived (Tan 2003).

For each soil sample and fraction, the carbon and nitrogen content was determined (Table 1). The evidence of the separation and conservation of the organic carbon in the three fractions is given by the comparison of the total organic carbon in the whole sample and that found after separation. For each sample, the sum of organic carbon in the three fractions accords very well with the total organic carbon in the whole sample (mean difference of 6.1%).

The mean concentrations and standard deviations of the organic carbon and nitrogen in the three fractions were 74±38, 37±15, and 24±4.4 g kg^{-1} for humin, humic acids, and fulvic acids, respectively, and those for nitrogen were 5.2±2.5, 3.2±1.3, and 2.2±0.35 g kg^{-1} for humin, humic acids, and fulvic acids, respectively. The mean C/N ratio (*w/w*) and its standard deviation in humin, humic acids, and fulvic acids were 14.3±1.1, 11.4±0.74, and 10.7±1.1, respectively. The C/N ratio decreases from humin to humic acids and fulvic acids. These C/N ratios were not far from values reported by Rice and MacCarthy (1991), which proposed representative data of the

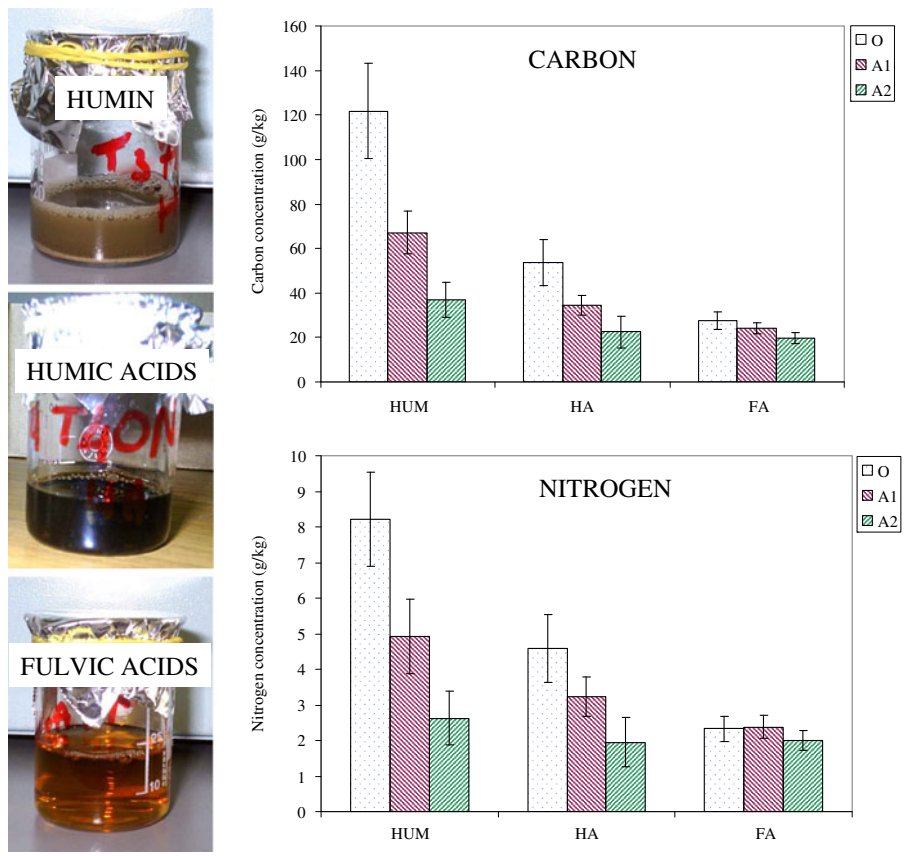

Fig. 2 Humin, humic acids and fulvic acids after separation (*left*) and mean carbon and nitrogen concentrations (*right*) in humin (*HUM*), humic acids (*HA*), and fulvic acids (*FA*) for the analyzed soil layers (O, A1, and A2). *Bars* indicate the standard deviation interval

Table 1 Carbon and nitrogen contents of the SOM fractions in the analyzed soils

Date	Layer	Aspect	Humin (g kg^{-1})		Humic acids (g kg^{-1})		Fulvic acids (g kg^{-1})	
			C	N	C	N	C	N
01 Jun 2008	O	North	111.4	7.7	46.6	4.4	27.4	2.4
01 Jun 2008	O	Plain	131.1	8.4	77.1	6.7	33.8	2.9
01 Jun 2008	O	South	89.9	6.3	43.1	3.7	26.0	2.4
01 Jun 2008	A1	North	84.1	6.6	43.8	4.4	28.7	2.9
01 Jun 2008	A1	Plain	67.1	5.0	37.4	3.7	26.3	2.6
01 Jun 2008	A1	South	78.8	6.5	38.5	3.8	22.8	2.4
01 Jun 2008	A2	North	37.2	2.6	19.7	1.8	19.6	2.0
01 Jun 2008	A2	Plain	28.4	1.9	16.5	1.4	18.9	2.0
01 Jun 2008	A2	South	48.4	3.7	37.0	3.3	22.3	2.2
27 Jun 2008	O	North	149.7	9.0	52.8	4.5	25.6	2.2
27 Jun 2008	O	South	95.0	6.0	46.6	3.8	25.4	2.1
27 Jun 2008	A1	North	76.0	6.2	35.1	3.7	26.7	2.9
27 Jun 2008	A1	Plain	75.2	5.9	38.6	4.1	29.2	3.1
27 Jun 2008	A1	South	74.2	6.4	34.9	3.1	22.3	2.1
27 Jun 2008	A2	North	36.6	2.5	17.4	1.5	19.0	2.0
27 Jun 2008	A2	Plain	27.0	1.8	15.9	1.4	18.3	1.9
27 Jun 2008	A2	South	43.7	3.3	31.2	2.8	22.6	2.2
19 Jul 2008	O	North	133.4	8.5	53.9	4.6	27.2	2.2
19 Jul 2008	O	Plain	152.6	10.6	74.8	6.6	35.6	2.9
19 Jul 2008	O	South	122.3	8.1	49.0	4.0	20.7	1.7
19 Jul 2008	A1	North	59.3	4.2	28.9	2.7	22.6	2.2
19 Jul 2008	A1	Plain	69.7	4.8	36.2	3.4	25.9	2.5
19 Jul 2008	A1	South	71.2	5.3	35.3	3.1	21.0	2.0
19 Jul 2008	A2	North	36.1	2.3	17.1	1.4	18.1	1.7
19 Jul 2008	A2	Plain	27.6	1.9	19.0	1.6	16.9	1.7
19 Jul 2008	A2	South	50.7	3.8	32.6	2.9	23.1	2.4
07 Aug 2008	O	North	137.9	9.6	56.7	5.0	29.8	2.4
07 Aug 2008	O	Plain	131.4	9.1	55.2	4.8	28.1	2.5
07 Aug 2008	O	South	107.9	7.7	46.4	3.8	24.5	2.0
07 Aug 2008	A1	North	55.2	3.9	25.5	2.4	24.1	2.4
07 Aug 2008	A1	Plain	49.6	3.5	26.2	2.4	21.7	2.1
07 Aug 2008	A1	South	80.0	5.8	36.6	3.1	21.1	1.9
07 Aug 2008	A2	North	32.2	2.1	15.8	1.2	19.0	1.9
07 Aug 2008	A2	Plain	25.8	1.7	15.7	1.3	14.2	1.5
07 Aug 2008	A2	South	49.2	3.8	33.3	3.0	23.3	2.4
09 Sep 2008	O	North	128.2	8.8	52.9	4.4	27.0	2.1
09 Sep 2008	O	Plain	138.8	10.1	50.2	4.2	30.9	2.6
09 Sep 2008	O	South	89.5	6.4	42.8	3.5	23.6	1.9
09 Sep 2008	A1	North	60.5	3.9	35.5	3.0	24.6	2.5
09 Sep 2008	A1	Plain	56.9	3.9	32.8	3.0	24.0	2.5
09 Sep 2008	A1	South	67.0	4.6	36.7	3.1	22.1	2.1
09 Sep 2008	A2	North	33.9	2.1	22.8	1.8	20.3	1.7
09 Sep 2008	A2	Plain	32.7	2.3	15.0	1.3	18.4	2.0

Table 1 (continued)

Date	Layer	Aspect	Humin (g kg^{-1})		Humic acids (g kg^{-1})		Fulvic acids (g kg^{-1})	
			C	N	C	N	C	N
09 Sep 2008	A2	South	42.3	3.3	28.1	2.5	21.9	2.3
01 Oct 2008	O	North	119.6	8.2	55.4	4.8	29.9	2.5
01 Oct 2008	O	Plain	143.4	8.4	66.0	5.7	32.7	2.7
01 Oct 2008	O	South	88.9	6.7	42.8	3.7	24.2	2.1
01 Oct 2008	A1	North	58.7	3.8	31.7	2.9	24.1	2.2
01 Oct 2008	A1	Plain	59.0	4.2	35.6	3.3	26.1	2.4
01 Oct 2008	A1	South	66.3	4.6	34.5	2.9	21.3	2.0
01 Oct 2008	A2	North	34.0	2.2	19.2	1.7	18.9	1.9
01 Oct 2008	A2	Plain	33.8	2.3	20.5	1.8	18.2	1.9
01 Oct 2008	A2	South	46.6	3.6	27.9	2.5	23.0	2.4

chemical composition of humic substances in soil (C/N ratio of 17.1, 15.1, and 15.8 for humin, humic, and fulvic acids, respectively). These values refer to a large data set of soil coming from all over the word, and, therefore, to a variety of soils, each one with their own C/N ratios. For this reason, these values must be taken as indicative, and do not match exactly with ours, which refer to a specific area on the Italian Alps. Another Italian site showed C/N ratios very similar to those calculated on our samples (n=30, C/N ratios of 16.6, 13.8, and 12.1 for humin, humic acids, and fulvic acids, respectively; Comolli R. personal communication). The observed decrease in C/N ratio from humin to humic acids and fulvic acids can be related to the age of the SOM: The C/N value decreases as decomposition proceeds (Stevenson and Cole 1999), and, following the Kononova (1966) suggestions for grassland soils, the humin is the first fraction to be formed, then the humic acids, and, finally, the fulvic acids are the most aged fraction. The observed C/N ratios also agree with the mean carbon-content of the three fractions, which decreases from humin to humic and fulvic acids, and this decrease is compensated principally by an increase in oxygen content (Kononova 1966; Bleam 2011). Therefore, the C/N ratio is higher in humin than in fulvic acids (where the carbon content decreases more than the nitrogen content).

The elemental composition of SOM remains controversial, especially for humin, but it has an important practical application in estimating the amount of organic matter (SOM) from the organic carbon content (SOC). Generally, for converting SOC in SOM, a multiplicative factor of 1.724 is used (Lyman 1990; Nelson and Sommers 1996). This factor corresponds to a mean carbon content of 58%. It is obvious that this value can change depending on the composition of the organic matter (different abundance and type of the three humic fractions). The carbon content in humic and fulvic acids is relatively well defined, and good agreement is present in the literature (Kononova 1966; Bleam 2011); on the contrary, the carbon content of humin is more variable and uncertain because of the higher heterogeneity of this fraction (Rice 2001; Wen et al. 2007). Therefore, starting from data in humic and fulvic acids proposed by Rice and MacCarthy (1991) and suggested recently by Bleam (2011) as reference values (mean OC content of 0.554 and 0.453 for humic and fulvic acids, respectively), and accepting an overall mean carbon content of 0.58 for the O layer (where most of the SOM is present), the mean carbon content in humin is obtained using the formula:

$$f_{\mathrm{OC-HUM}} = \frac{0.58 - (f_{\mathrm{OC-HA}} \cdot f_{\mathrm{HA}}) - (f_{\mathrm{OC-FA}} \cdot f_{\mathrm{FA}})}{f_{\mathrm{HUM}}} \quad (1)$$

where

f_{OC} Organic carbon content of humin (HUM), humic acids (HA), and fulvic acids (FA)

f Relative abundance of the three humic components

A mean carbon content in humin of 0.621±0.0054 was calculated for the O layer. This value agrees with

general indications of high carbon content in humin (OC > 60%; Kononova 1966), but it is higher than the mean values indicated by Rice and MacCarthy (1991). However, as suggested by the same authors, their mean carbon content in humin (0.561±0.026) can be considered less representative than those estimated for humic and fulvic acids, because it was calculated only from data on 26 different soils, while those of humic and fulvic acids on 215 and 127, respectively. Moreover, their mean C content in humin (0.561) together with those proposed for humic and fulvic acids (0.554 and 0.453) does not match with the overall mean carbon content in SOM (0.58) proposed by Lyman (1990) and Nelson and Sommers (1996) and generally accepted as reference value. For these reasons, the mean C content calculated in the present work (0.621) can be considered acceptable for humin, even if it is in the higher end of the interval proposed by Rice and MacCarthy (1991).

3.2 Spatial Variability of the SOM Fractions

The carbon and nitrogen content in the humin, humic acid, and fulvic acid fractions of the analyzed soils were highly variable (mean variability of 37% and 34% for carbon and nitrogen, respectively). The variability sources taken into account in the experimental plan are the soil layer (O, A1, and A2), the site (North, South, and plain aspect), and the sampling date (from June to October 2008). In such a short time interval (4 months), no consistent changes in the SOM content are expected for each site and layer because samples from each site and layer were taken close to one another, mixing several sub-samples. To confirm this assumption, we tested the sampling date, together with layer and aspect, using GLM: The date was significant neither for carbon (P>0.69) nor for nitrogen (P>0.33), while the layer was always found to have the highest level of significance (P≤0.001). Because the sampling date do not significantly affect the data, we tested the interaction of layer and aspect on carbon and nitrogen content in humin, humic acids, and fulvic acids using GLM and taking the six sampling dates as replicates (Table 2). As expected, layer has a great effect on the amount of both organic carbon and nitrogen in the three fractions: Both values decreased in all fractions as we moved from the surface (organic layer) to deeper layers (A1 and A2). As shown in Fig. 2, humin shows the greatest reduction (81% and 77% for its carbon and nitrogen content, respectively) compared with humic acids (54% for both carbon and nitrogen content) and fulvic acids (18 and 8%, respectively). The different degrees of change in the three fractions along the soil profile suggested a different SOM composition depending on the layer (Fig. 3). The greater presence of fulvic acids in deeper layers (its relative abundance is 14% in superficial layer and becomes 25% in A2) can be explained by different processes: (a) different parent materials (mainly epigean vegetal detritus in the surface layer and roots/elaborated organic detritus in deeper layers); (b) different physical properties of the SOM (mainly water solubility) that can generate a preferential vertical transport of the most soluble components of SOM (Stevenson 1994); (c) temporal diversity, according to the Kögel–Knabner theory (Kögel-Knabner 1993). Fulvic acids are generated at the final stage of the SOM elaboration and therefore are expected to be more abundant in deeper layers where the SOM takes time to appear.

Table 2 Statistical parameters of the GLM for the carbon and nitrogen content of the SOM fractions considering layer, aspect, and their interaction as factors

Fraction	Factor	Carbon			Nitrogen		
		DF	F	P value	DF	F	P value
Humin	Layer	2	405.4	<0.001***	2	238.3	<0.001***
	Aspect	2	1.3	0.29	2	0.068	0.93
	Layer×aspect	4	19.2	<0.001***	4	12.6	<0.001***
Humic acids	Layer	2	181.8	<0.001***	2	125.2	<0.001***
	Aspect	2	2.6	0.085	2	2.1	0.14
	Layer×aspect	4	17.7	<0.001***	4	15.3	<0.001***
Fulvic acids	Layer	2	91.2	<0.001***	2	17.5	<0.001***
	Aspect	2	6.7	0.003**	2	4.8	0.013*
	Layer×aspect	4	21.5	<0.001***	4	14.5	<0.001***

*P<0.05, significant level

**P<0.01, very significant level

***P<0.001, highly significant level

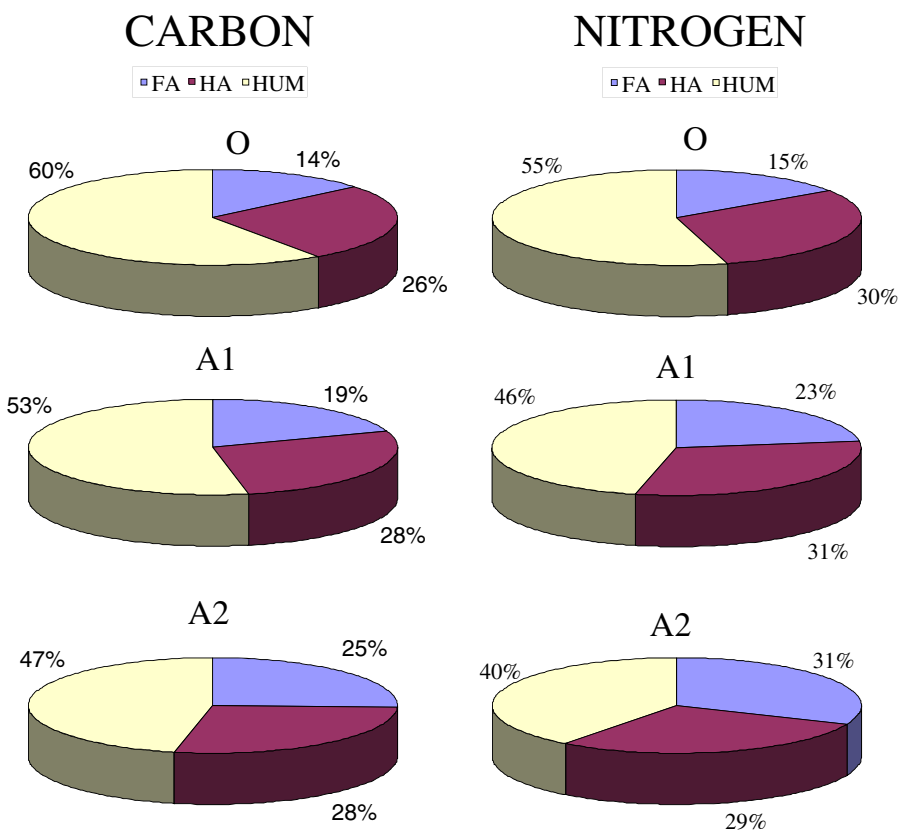

Fig. 3 Relative abundance of carbon and nitrogen in humin (*HUM*), humic acids (*HA*), and fulvic acids (*FA*) for the analyzed soil layers (O, A1, and A2)

Two further elements of SOM composition in the studied soils appear to be important: the aspect and the interaction between layer and aspect. From the GLM results reported in Table 2, the aspect factor has a significant effect only on fulvic acids, while the interaction between layer and aspect is always highly significant for both carbon and nitrogen. The first result means that the three sites were quite similar in their abundance and composition of the humic fractions, only fulvic acids were specifically more abundant in the North and plain sites than in the South. The other fractions were distributed independently of the aspect. On the contrary, the second result of the GLM analysis clearly shows that, depending on aspect, the abundance of the three fractions changes greatly among the layers. Both carbon and nitrogen in the three humic fractions in the O layer were higher in the North and plain sites in comparison to the South, while in the A2 layer the opposite trend was observed (the South site had higher amount of both carbon and nitrogen than the North and plain sites); the A1 layer showed an intermediate condition, acting as a transition layer (Table 3). The south site has the highest temperatures and the highest biological activity, with a greater consumption and transfer of SOM to deeper layers through bioturbation. Roots are also expected to penetrate the soil to great depths because of the higher demand for water in the South site in comparison to that of the plain and North sites.

3.3 Role of the SOM Composition on the POPs Contamination

In the analyzed soils, humin, humic acids, and fulvic acids were highly variable in both abundance and composition, especially among the three soil layers (O, A1, and A2): A higher SOM content with humin as the major component was found at the surface, while in deeper layers the abundance of the three humic fractions was lower overall, and fulvic acids showed preferential accumulation, reducing the dominance of the humin fraction (Fig. 3). This behavior can be taken into account in assessing the potential for POP contamination in soils because the three humic fractions may have different accumulation capacities for hydrophobic contaminants (Rutherford et al. 1992;

Table 3 Mean carbon and nitrogen contents and their 95% confidence intervals in the three humic fractions in the three layers (O, A1, and A2) depending on the site aspect (North, plain, and South)

Fraction	Layer	Aspect	Carbon (g kg^{-1})		Nitrogen (g kg^{-1})	
			Mean	95% Interval	Mean	95% Interval
Humin						
	O	South	98.9	91.5–106	6.9	6.2–7.5
	O	Plain	139	131–148	9.3	8.6–10
	O	North	130	123–137	8.6	8.0–9.3
	A1	South	72.9	65.5–80.3	5.5	4.9–6.2
	A1	Plain	62.9	55.5–70.3	4.5	3.9–5.2
	A1	North	65.6	58.2–73.0	4.7	4.1–5.4
	A2	South	46.8	39.4–54.2	3.6	3.0–4.2
	A2	Plain	29.2	21.8–36.6	2.0	1.4–2.6
	A2	North	35.0	27.6–42.4	2.3	1.7–3.0
Humic acids						
	O	South	45.1	41.0–49.2	3.8	3.3–4.2
	O	Plain	64.7	60.2–69.1	5.6	5.1–6.0
	O	North	53.0	49.0–57.1	4.6	4.2–5.0
	A1	South	36.1	32.0–40.2	3.2	2.8–3.6
	A1	Plain	34.5	30.4–38.6	3.3	2.9–3.7
	A1	North	33.4	29.3–37.5	3.2	2.8–3.6
	A2	South	31.7	27.6–35.8	2.8	2.4–3.2
	A2	Plain	17.1	13.0–21.2	1.5	1.0–1.9
	A2	North	18.6	14.6–22.7	1.5	1.1–2.0
Fulvic acids						
	O	South	24.1	22.6–25.5	2.0	1.9–2.2
	O	Plain	32.2	30.6–33.8	2.7	2.5–2.9
	O	North	27.8	26.3–29.3	2.3	2.1–2.5
	A1	South	21.8	20.3–23.2	2.1	1.9–2.3
	A1	Plain	25.5	24.0–27.0	2.5	2.4–2.7
	A1	North	25.1	23.7–26.6	2.5	2.3–2.7
	A2	South	22.7	21.2–24.2	2.3	2.1–2.5
	A2	Plain	17.5	16.0–19.0	1.8	1.7–2.0
	A2	North	19.2	17.7–20.6	1.9	1.7–2.0

Piccolo et al. 1998; Chiou et al. 1998; Kohl and Rice 1998; Ahmad et al. 2001; Doick et al. 2005; Kang and Xing 2005; Pan et al. 2006; Wen et al. 2007). Kohl and Rice (1998) reported preferential binding of PCBs and PAHs in humin and humic acids in comparison to that observed in fulvic acids, and Ahmad et al. (2001) found a strong relationship between aromaticity of SOM and K_{oc} for two non-ionic pesticides, while Wen et al. (2007) highlighted the relevant role of aliphaticity as well, because the most efficient part of humin for sorption (lipid fraction) also has the highest aliphaticity. These authors reported that the heterogeneous composition of humin is able to provide highly efficient and linear sorption isotherms in its lipid fraction and also non-linear sorption isotherms in its insoluble residues. Even if the sorption mechanisms are different, the two humin fractions (lipid and insoluble residue) showed high sorption efficiency for hydrophobic contaminants. Humic acids bound to humin (bound humic acids that are not recovered in the free humic acids fraction and therefore are found in humin) showed a lower sorption capacity than the other two humin fractions (lipid and insoluble residue), and K_{oc} values of the bound humic acids were similar to those of the free humic acids (Wen et al.

2007). This knowledge of the sorption properties of SOM for hydrophobic contaminants was obtained through laboratory experiments, but it can be difficult to transfer to field studies where more basic parameters are preferred. Despite the great heterogeneity of the humin fraction, the literature recognizes humin as the most important fraction for retaining hydrophobic contaminants in soils. Therefore, humin can be seen as a preferential component for the sorption of hydrophobic chemicals such as PCBs in soil, especially in comparison to fulvic acids.

In a preliminary experiment, the PCB content of the three humic fractions was measured after a separation procedure. The humin fraction contained from 97% to 99% of the total PCB content (sum of the PCBs measured in the three fractions), with further variation depending on the degree of chlorination. A higher degree of chlorination corresponded to a higher percentage in humin. Unfortunately, these results cannot be taken as representative of the actual sorption efficiency of the three fractions because they were highly affected by the separation procedure, which required the solubilization of the humic and fulvic acids at extreme pH conditions. In this case, the preferential partitioning of PCBs in humin was exaggerated by the partitioning between hydrophobic material (humin fraction) and a water solution in which humic and fulvic acids were forced to be soluble. In soils, the three organic fractions are not separated, but mixed in a complex form (humic substances are defined as an heterogeneous aggregates of macromolecules in which mineral components are present as well; Albers et al. 2008). By the partitioning sorption mechanism, lipophilic chemicals, such as PCBs, sorb to SOM and prefer the more lipophilic sites/areas of this complex matrix. Therefore, PCBs can be preferentially accumulated when the SOM present has more lipophilic properties, such as when the humin fraction is more abundant. Literature results support the conclusion that lipophilic chemicals are localized and preferentially accumulated in humin (Kohl and Rice 1998), even if other mechanisms related to sorption to the mineral fraction (Doick et al. 2005) or to sorption by the 'hole-filling mode' (Pignatello 1998) are possible.

Another suggestion of the importance of SOM composition comes from the predictive equations for calculating K_{oc} and K_{sa} from K_{ow} and K_{oa}, respectively. Karickoff proposes a coefficient of 0.411 for estimating K_{oc} from K_{ow} (Karickhoff 1981), reducing the sorption capacity of the SOC in relation to that of octanol by a factor 2.43. Seth et al. (1999) considered the high variability of the K_{oc} values for the same compound and proposed a coefficient of 0.33 (K_{oc}=0.33 K_{ow}), with an uncertainty interval between 0.14 and 0.89. For the same compound, they noticed that measured K_{oc} values typically varied as much as an entire order of magnitude, and they concluded that part of this variability lies in the complex and variable nature of the organic matter. The same suggestion is derived from the predictive equations for calculating K_{sa} values. Daly et al. (2007) proposed an empirical coefficient of 0.00075 $m^3\ kg^{-1}$ (equal to 0.75 $dm^3\ kg^{-1}$) to weight the role of SOC in relation to octanol. Hippelein and McLachlan (1998) proposed a lower coefficient (0.411 $dm^3\ kg^{-1}$) derived from that of Karickoff. These coefficients (lower than 1) indicate that the mean retention capacity of the SOC for hydrophobic contaminants is much lower than that of octanol. It is interesting to note that the mean humin abundance in our soils (0.55) is in between the coefficients used by Daly et al. and by Hippelein and McLachlan. Because SOM is a complex mixture of substances with different physico-chemical properties (heterogeneous complex), not all of the components contribute in retaining POPs with the same efficiency. We can hypothesize that only the most hydrophobic fraction of the SOM is preferentially involved in the sorption and retention of hydrophobic contaminants in soil; the empirical coefficients introduced in predictive equations account for this distinction between high-efficiency and low-efficiency sorption of hydrophobic contaminants to the different fractions of the SOM. If the humin fraction can serve to represent this distinction, it is possible to use it as an improved substitute of the total SOM.

3.4 PCB Concentrations in the Analyzed Soils

The same soil samples analyzed here for organic matter composition were previously analyzed for their PCB content (Guazzoni et al. 2011). This data set gives the opportunity to test the existence of preferential accumulation of PCBs in soils rich in humin in comparison to those more rich in humic and fulvic acids. To test this hypothesis, we correlated the PCB concentrations found in the analyzed soils to the different SOM fractions. However, in the analyzed area, the PCB concentrations did not depend only on SOM but also on other factors considered in the experimental plan (date, aspect, and

layer). As shown by Guazzoni et al. (2011), all of these parameters were statistically significant. The seasonal trend (date effect) was characterized by a concentration peak in June (at the beginning of the season). The marginal means of the ΣPCBs were 3.0, 1.3, 1.2, 1.2, 1.5, and 1.0 ng g^{-1} d.w. for T1, T2, T3, T4, T5, and T6, respectively (for the corresponding dates see paragraph "Soil Sampling"). The aspect effect was related to the mean temperature of the site, with higher concentrations in the North site (low temperature condition), intermediate concentra-tions in the plain site (intermediate temperature condi-tion), and lower concentrations in the South site (high temperature condition). The marginal means of the ΣPCBs were 1.9, 1.6, and 1.1 ng g^{-1} d.w. for the North, plain, and South sites, respectively. Finally, the layer effect was mainly interpreted as being related to the SOM content because the highest PCB concentrations were found in the surface layer where the highest amount of SOM was present. The A1 layer showed an intermediate condition, and the A2 layer had the lowest values of both SOM and PCB concentrations. The marginal means of the ΣPCBs were 2.3, 1.7, and 0.61 ng g^{-1} d.w. for O, A1, and A2 layer, respectively. This concentration profile is in agreement with that found by Weiss et al. (1993), Cousins et al. (1999), Krauss et al. (2000), Armitage et al. (2006), and Moeckel et al. (2008). Normalizing the PCB concentrations for the OM content of the soil, the concentration differences between layers were considerably reduced. Introducing SOC as covariate, the marginal means of the PCB concentrations in the O, A1, and A2 layer were 1.33, 1.81, and 1.36 ng g^{-1} d.w., respectively. This residual variability, not due to SOC, was still significant (P=0.030) and indicates a higher concentration in A1 than in the O and A2 layers. Normalizing the PCB concentration data for their organic carbon content (nanograms per gram OC) and analyzing them by date, aspect, and layer, similar results were obtained. The OM-normalized mean concentration in the surface layer (O) is lower than that found in the A1 layer, and this fact was mainly interpreted as depending on the net emission occurring during the summer, which preferentially depleted the surface burden as compared with the deeper layers. The reduced concentration in the A2 layer in relation to A1 was generally attributed to a non-equilibrium condition existing between the layers (Guazzoni et al. 2011).

3.5 Relationship Between SOM Composition and PCB Concentration

In the soils studied, the general relationship between PCB concentrations (nanograms per gram d.w.) and

Table 4 Regression parameters for the relationships between the SOM-residual variability factor of the PCB congeners and the carbon abundance of the three humic fractions in the analyzed soils

PCB	Humin (carbon g kg^{-1})				Humic acids (carbon g kg^{-1})				Fulvic acids (carbon g kg^{-1})			
Congener	a	b	R^2	P value	a	b	R^2	P value	a	b	R^2	P value
18	0.025	−0.48	0.63	<0.001	0.056	−0.79	0.59	<0.001	0.16	−2.43	0.41	<0.001
31+28	0.008	0.40	0.22	0.001	0.020	0.26	0.21	0.001	0.063	−0.49	0.19	0.002
52	0.018	−0.32	0.57	<0.001	0.039	−0.40	0.41	<0.001	0.10	−1.37	0.24	<0.001
44	0.017	−0.23	0.63	<0.001	0.039	−0.39	0.51	<0.001	0.11	−1.54	0.35	<0.001
101	0.014	−0.095	0.85	<0.001	0.033	−0.24	0.71	<0.001	0.092	−1.24	0.50	<0.001
149	0.014	−0.040	0.82	<0.001	0.032	−0.19	0.69	<0.001	0.092	−1.20	0.50	<0.001
118	0.018	−0.29	0.88	<0.001	0.042	−0.48	0.72	<0.001	0.12	−1.74	0.51	<0.001
153	0.014	−0.010	0.81	<0.001	0.032	−0.16	0.68	<0.001	0.088	−1.08	0.45	<0.001
138	0.013	0.015	0.82	<0.001	0.031	−0.15	0.71	<0.001	0.090	−1.13	0.51	<0.001
180	0.013	0.016	0.77	<0.001	0.032	−0.14	0.66	<0.001	0.088	−1.09	0.46	<0.001
170	0.015	−0.11	0.77	<0.001	0.036	−0.29	0.67	<0.001	0.099	−1.33	0.45	<0.001
194	0.014	0.005	0.66	<0.001	0.033	−0.17	0.58	<0.001	0.092	−1.17	0.41	<0.001
ΣPCBs	0.014	−0.036	0.83	<0.001	0.033	−0.20	0.70	<0.001	0.092	−1.19	0.49	<0.001

a slope of the regression line, *b* intercept of the regression line, R^2 regression coefficient, *P* significant level of the regression

total SOC (grams per kilogram) was highly significant (R^2=0.40; n=53; P<0.001), as was the relationship with humin, humic acids, and fulvic acids (P<0.001), with only small differences in their regression coefficients (0.38–0.40). These coefficients were similar to those found by Meijer et al. (2003) in their global survey, by Ribes et al. (2002) in a subtropical Atlantic island, and by Tremolada et al. (2008) in another mountainous area, confirming at both global and local scales the general and diffuse relationship between hydrophobic contaminant concentrations on a dry weight basis and SOM content. However, the quota variability explained by these relationships was limited (around or less than 50%) because other variability factors interfere with the PCB contamination levels. Including all the variability factors considered in the experimental plan (date, aspect, layer, and SOM), the overall explained variability rose to 81% (GLM using date, aspect, and layer as factors and SOM as covariate), and all factors were significant. To test the effect of SOM alone on the PCB contamination levels of the studied soils, it was necessary to extrapolate the residual variability due to the SOM alone. This was achieved by means of the ratio of each datum (that includes the SOM effect) with the expected PCB concentration based on the observed mean effect of date, aspect, and layer (excluding the effect of SOM). These observed mean effects were obtained by the marginal means of each factor calculated by GLM. In this way, we were able to obtain a residual variability factor relative only to the effect of SOM (RVF_{SOM}). Mathematically (Eq. 2), we divided each datum (PCB concentration in nanograms per gram d.w.) by three derived data, which together have the meaning of an expected PCB concentration (nanograms per gram d.w.). These derived data are: (1) the marginal mean of the PCB concentrations for the date factor; (2) the marginal mean of the PCB concentrations for the aspect factor divided by the overall mean; (3) the marginal mean of the PCB concentrations for the layer factor divided by the overall mean.

$$RVF_{SOM} = \frac{x_{i,j,k}}{\overline{x_i} \cdot \frac{\overline{x_j}}{\overline{x}} \cdot \frac{\overline{x_k}}{\overline{x}}} \qquad (2)$$

Where:

RVF_{SOM} Residual variability factor for the soil organic matter

$x_{i,j,k}$ Congener concentration for a ith date, jth aspect, and k th layer (each datum)

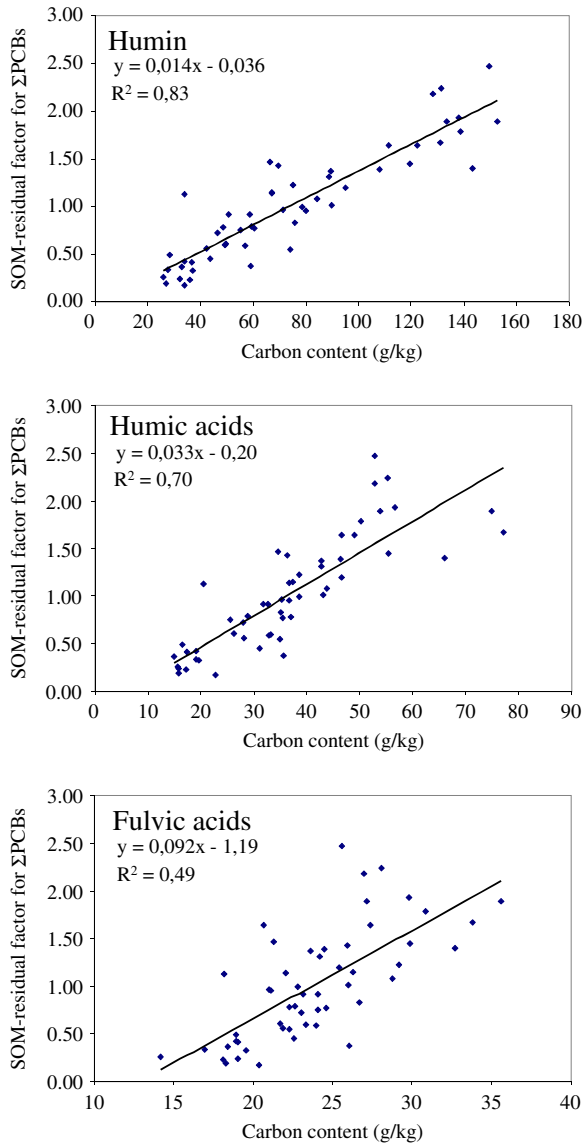

Fig. 4 Relationships between the SOM-residual variability factor for ΣPCBs and the carbon content in humin, humic acids, and fulvic acids for the analyzed soils

$\overline{x_i}$ Marginal mean of the PCB concentrations for the 'date' factor ('i') calculated by GLM

$\overline{x_j}$ Marginal mean of the PCB concentrations for the 'aspect' factor ('j') calculated by GLM

$\overline{x_k}$ Marginal mean of the PCB concentrations for the 'layer' factor ('k') calculated by GLM

$\overline{x}$ Mean of the marginal means of the PCB concentrations (overall mean).

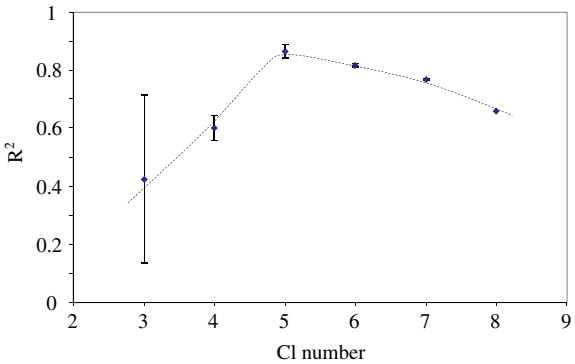

Fig. 5 Relation of the number of chlorine atoms of each congener vs. the mean regression coefficient for the relationship between the SOM-residual variability factor and the carbon content in humin for the analyzed soils

In this way, it was possible to exclude the effect of date, aspect, and layer (not due to SOM) on the data variability and evaluate only the effect of the SOM, separately testing the three humic fractions. Table 4 reports, for every CB congener separately and as a whole, the regression parameters of the relationship between the measured/expected concentration ratios and the carbon contents of each fraction. Similar results were obtained for the nitrogen content because of the stability of the C/N ratio within each fraction. For all congeners and, consequently, for their sum (ΣPCBs), the fraction most related to the PCB concentrations (residual variability due only to the SOM) was humin (R^2=0.83 for the ΣPCBs), then humic acids (R^2=0.70 for the ΣPCBs), and finally fulvic acids (R^2=0.49 for the ΣPCBs). The graphs in Fig. 4 allow comparison of the degree of association between the variables. Even if humin appears as the fraction most closely related to PCB contamination, humic and fulvic acids were also significantly related to the PCB contamination level for all of the congeners ($P \leq 0.002$) and for the ΣPCBs. This result might be considered in contrast with the hypothesis of a preferential POP accumulation in humin, but, in our case, it depends mainly on the inter-correlation of the abundance of the three humic fractions. Even if great differences were observed in the composition of the SOM among layers (see "Spatial Variability of the SOM Fractions"), the quantitative differences of the three humic fractions in the O, A1, and A2 layers were greater than those coming from their relative composition. In fact, the correlation coefficients between humic acids and humin and between fulvic acids and humin were high (0.94 and 0.82, respectively), as were those among humin, humic acids, and fulvic acids and total SOM (0.99, 0.97, and 0.87, respectively). Fulvic acids appear to be less related to humin, and when related to the level of PCB contamination, they appear to be only weakly associated. Only humin and, to a lesser extent,

Table 5 Regression parameters for the relationships between the SOM-residual variability factor of the PCB congeners and the relative carbon abundance of the three humic fractions in the analyzed soils

PCB	Humin (carbon%)				Humic acids (carbon%)				Fulvic acids (carbon%)			
Congener	a	b	R^2	*P* value	a	b	R^2	*P* value	a	b	R^2	*P* value
18	0.13	−5.60	0.46	<0.001	−0.027	1.96	0.003	0.71	−0.15	4.23	0.52	<0.001
31+28	0.036	−0.92	0.11	0.017	−0.006	1.18	0.001	0.87	−0.047	1.92	0.14	0.007
52	0.11	−4.81	0.52	<0.001	−0.11	3.90	0.080	0.041	−0.12	3.38	0.47	<0.001
44	0.097	−4.10	0.49	<0.001	−0.060	2.70	0.032	0.21	−0.11	3.25	0.51	<0.001
101	0.085	−3.56	0.76	<0.001	−0.054	2.44	0.052	0.10	−0.098	2.88	0.78	<0.001
149	0.083	−3.40	0.73	<0.001	−0.049	2.32	0.042	0.14	−0.096	2.88	0.76	<0.001
118	0.11	−4.65	0.76	<0.001	−0.075	3.10	0.062	0.072	−0.12	3.46	0.77	<0.001
153	0.081	−3.31	0.70	<0.001	−0.047	2.28	0.038	0.16	−0.095	2.88	0.74	<0.001
138	0.078	−3.16	0.70	<0.001	−0.042	2.15	0.034	0.19	−0.092	2.82	0.75	<0.001
180	0.080	−3.22	0.67	<0.001	−0.044	2.23	0.035	0.18	−0.093	2.85	0.72	<0.001
170	0.091	−3.79	0.67	<0.001	−0.049	2.36	0.032	0.20	−0.11	3.13	0.72	<0.001
194	0.080	−3.22	0.56	<0.001	−0.031	1.87	0.014	0.40	−0.097	2.92	0.63	<0.001
ΣPCBs	0.083	−3.42	0.72	<0.001	−0.047	2.31	0.039	0.16	−0.098	2.93	0.76	<0.001

a slope of the regression line, *b* intercept of the regression line, R^2 regression coefficient, *P* significant level of the regression

humic acids were able to explain a consistent quota of the residual PCB variability due to the SOM in the analyzed soils (83% and 70%, respectively), while fulvic acids explain only a limited amount of this variability (49%). These results agree with previous literature findings (Chiou et al. 1998; Kohl and Rice 1998; Doick et al. 2005; Pan et al. 2006; Wen et al. 2007) and highlighted the role of humin in the accumulation of hydrophobic contaminants in soil. Among the different congeners, penta-substituted PCBs were most strictly related to the humin content of soils (R^2>0.85), followed by the hexa-substituted (0.81<R^2<0.82), the hepta-substituted (R^2=0.77), the octa- and the tetra-substituted (0.57 <R^2 <0.66), and finally the tri-substituted congeners (0.22<R^2<0.63). This behavior is shown in Fig. 5, suggesting that there is an optimum degree of chlorination in determining a strict relationship with the humin content in soil; both tetra and octa-chlorinated congeners showed much lower regression coefficients than penta- and hexa-substituted ones. The association between PCB contamination and humin content seems to decrease for both the heaviest and the lightest congeners. The heaviest congeners, having low volatility, are very slow to reach equilibrium conditions with the SOM/humin content in soils once they are deposited. Wet and dry particle deposition does not depend on the organic matter/humin content of soils, while the soil–air equilibrium (K_{sa}), based on the SOM content of soil, requires efficient gas-phase exchanges, which for these congeners are very slow. The opposite can be observed for the lightest congeners, for which their greater volatility accounts for rapid exchange between soil and air to reach a physical equilibrium. However, for these congeners, rapid gas-phase exchange makes them highly sensitive to 'specific' climatic conditions that can affect the soil concentrations above or below the amount predicted by the mean climatic conditions and the organic matter/humin content. These congeners may be more dependent on the short-term climatic conditions than on the OM/humin content of soils, thus showing a lower association with the humin content, as shown in Fig. 5. Only penta- and hexa-chlorinated congeners have the optimum of physico-chemical properties to achieve equilibrium conditions between air and soil without strong dependence on the short-term meteorological conditions of the sampling period. Therefore, they give a higher degree of association with the humin content of soil (R^2>0.80) than the other congeners. Sweetman et al. (2005) reported similar behavior and considerations for the different PCB congeners in a model application, and the experimental data obtained by Meijer et al. (2002) are also in agreement.

To highlight the effect of the SOM composition on the PCB contamination in the analyzed soils, the relative abundance of the three humic fractions was considered. The relative abundances of the three humic fractions were much more different among the analyzed samples than was the absolute abundance. In fact, the relative

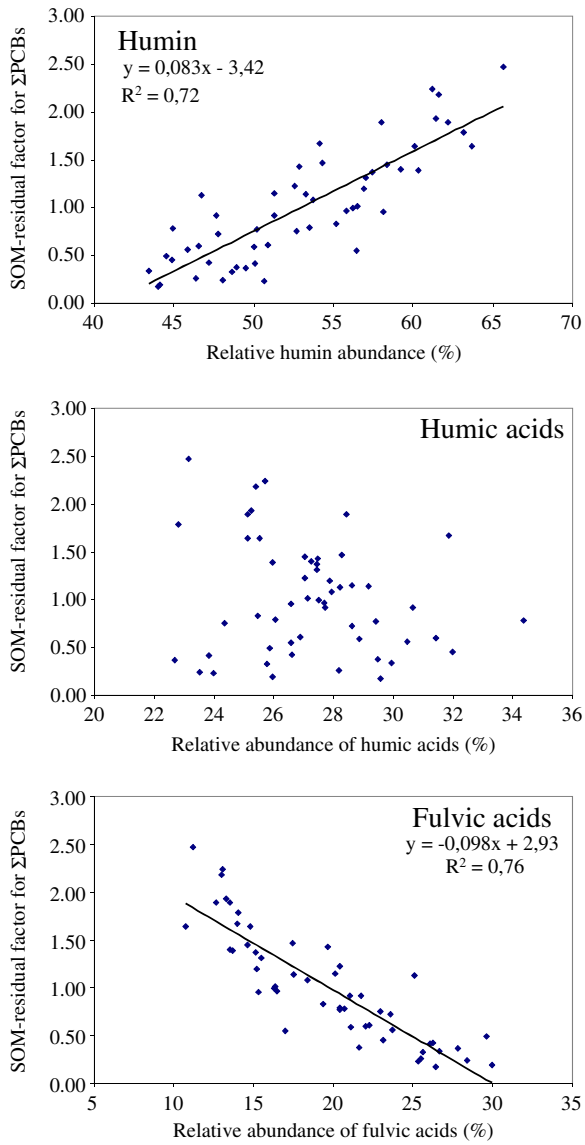

Fig. 6 Relationships between the SOM-residual variability factor for ΣPCBs and the relative carbon abundance in humin, humic acids, and fulvic acids for the analyzed soils

humic acid abundance was not correlated with that of fulvic acids (r=0.081; n=53; P=0.56), whereas the relative abundance of both humic and fulvic acids were inversely correlated to that of humin (r=−0.48; n=53; P<0.001, and r=−0.91; n=53; P<0.001, respectively). Table 5 reports the regression parameters of the relationship between the measured/expected concentration ratio of the PCB content and the relative carbon abundance in each fraction for the analyzed soils, and Fig. 6 shows the same relationship for the ΣPCBs. Very similar results were obtained using the relative nitrogen content, again because of the stability of the C/N ratio. In this form, the relationship between SOC fractions and PCB contamination is much more evident than was shown in Fig. 4. Considering the relative composition of the SOM in the analyzed soils, only humin has a strong and positive relationship with the PCB contamination (P<0.001); humic acids do not show any relationship (P=0.16), and fulvic acids revealed a significant negative relationship (P<0.001). These results clearly indicate that the residual variability of the PCB concentrations due to the SOM content alone is strictly associated with the relative abundance of the humin fraction and that it diverges from the most polar fraction (fulvic acids).

4 Conclusion

SOM composition can change not only among different soils (spatial variability) but also within the same soil with depth (vertical variability). The literature provides evidence of the different affinities of non-ionic organic contaminants for the different SOM fractions, mainly through laboratory experiments, while our work has provided additional evidence on this topic in the field. The humin fraction (the most hydrophobic) appears to be the most strictly related to the amount of PCBs in soil, while fulvic acids are the least correlated. This was observed by comparing the residual variability of the PCB concentrations due to the effect of the only SOM with the absolute amount of the three fractions and with their relative abundance. The indications coming from these data support the idea of a preferential accumulation of hydrophobic compounds in the humin fraction. Several consequences derive from this result:

1. Soils with the same SOM content may have different accumulation potentials for POPs;
2. Soils with a high humin content are highly efficient for accumulating POPs, and environmental conditions favoring humin accumulation increase the risk of POP contamination and retention;
3. The humin carbon content (f_{huminC}) can be taken as a better parameter for evaluating the accumulation potential for POPs than the total organic carbon (f_{oc}).

Although more research is needed, we suggest the use of the f_{huminC} instead of f_{oc} as a better estimator of the accumulation capacity of soil for hydrophobic contaminants. If f_{huminC} is used instead of f_{oc} in predictive equations, the use of empirical coefficients, used for reducing the accumulation capacity of the SOC in comparison to that of octanol, may be avoided. The mean f_{huminC} of our samples is 0.074, while the total organic carbon fraction is 0.135. The ratio between the mean f_{huminC} and mean f_{oc} in our soils represents the mean abundance of humin in the SOM and conceptually corresponds to an empirical coefficient that takes into account the most lipophilic fraction of SOM. In our experiments, this value is equal to 0.55, a value that is in between the empirical coefficients proposed by Daly et al. (0.75) and by Hippelein and McLachlan (0.411).

References

Ahmad, R., Kookana, R. S., Alston, A. M., & Skjemstad, J. O. (2001). The nature of soil organic matter affects sorption of pesticides. 1. relationships with carbon chemistry as determined by 13C CPMAS NMR spectroscopy. *Environmental Science and Technology, 35*, 878–884.

Albers, C. N., Banta, G. T., Jacobsen, O. S., & Hansen, P. E. (2008). Characterization and structural modelling of humic substances in field soil displaying significant differences from previously proposed structures. *European Journal of Soil Science, 59*, 693–705.

Anderson, D. W., & Schoenau, J. J. (2008). Soil humus fraction. In M. R. Carter & E. G. Gregorich (Eds.), *Soil sampling and methods of analysis* (pp. 675–680). Boca Raton: CRC Press.

Andreux, F. (1996). Humus in world soil. In A. Piccolo (Ed.), *Humic substance in terrestrial ecosystem* (pp. 45–100). Amsterdam: Elsevier.

Armitage, J. M., Hanson, M., Axelman, J., & Cousins, I. T. (2006). Levels and vertical distribution of PCBs in agricultural and natural soils from Sweden. *Science of the Total Environment, 371*, 344–352.

Bleam, W. F. (2011). *Soil and environmental chemistry*. Amsterdam: Academic Press.

Chiou, C. T., McGroddy, S. E., & Kile, D. E. (1998). Partition characteristics of polycyclic aromatic hydrocarbons on

soils and sediments. *Environmental Science and Technology, 32*, 264–269.

Cousins, I. T., Gevao, B., & Jones, K. J. (1999). Measuring and modeling the vertical distribution of semivolatile organic compounds in soil. 1: PCB and PAH soil core data. *Chemosphere, 39*, 2507–2518.

Dalla Valle, M., Jurado, E., Dachs, J., Sweetman, A. J., & Jones, K. C. (2005). The maximum reservoir capacity of soils for persistent organic pollutants: Implication for global cycling. *Environmental Pollution, 134*, 153–164.

Daly, G. L., Lei, Y. D., Castillo, L. E., Muir, D. C. G., & Wania, F. (2007). Polycyclic aromatic hydrocarbons in Costa Rican air and soil: A tropical/temperate comparison. *Atmospheric Environment, 41*, 7339–7350.

Doick, K. J., Burauel, P., Jones, K. C., & Semple, K. T. (2005). Distribution of aged ^{14}C-PCB and ^{14}C-PAH residues in particle-size and humic fractions of an agricultural soil. *Environmental Science and Technology, 39*, 6575–6583.

Guazzoni, N., Comolli, R., Mariani, L., Cola, G., Parolini, M., Binelli, A., et al. (2011). Meteorological and pedological influence on the PCBs distribution in mountain soils. *Chemosphere, 83*, 186–192.

Hayes, M. H. B., & Clapp, C. E. (2001). Humic substances: Considerations of compositions, aspects of structure, and environmental influences. *Soil Science, 166*, 723–737.

Hayes, M. H. B., & Malcolm, R. L. (2001). Structures of humic substances. In C. E. Clapp, M. H. B. Hayes, N. Senesi, P. Bloom, & P. M. Jardine (Eds.), *Humic substances and chemical contaminants* (pp. 3–40). Madison: Soil Science Society of America.

Hayes, M. H. B., MacCarthy, P., Malcolm, R. L., & Swift, R. S. (1989). *Humic substances II. Search of structure*. Chichester: Wiley.

Hippelein, M., & McLachlan, M. S. (1998). Soil/Air partitioning of semivolatile organic compounds. 1. Method development and influence of physical-chemical properties. *Environmental Science and Technology, 32*, 310–316.

Huang, W., Peng, P., Yu, Z., & Fu, J. (2003). Effects of organic matter heterogeneity on sorption and desorption of organic contaminants by soils and sediments. *Applied Geochemistry, 18*, 955–972.

IUSS Working Group WRB. (2006). *World reference base for soil resources 2006. World Soil Resources Reports No. 103*. Rome: FAO.

Kang, S., & Xing, B. (2005). Phenanthrene sorption to sequentially extracted soil humic acids and humins. *Environmental Science and Technology, 39*, 134–140.

Karickhoff, S. W. (1981). Semi-empirical estimation of sorption of hydrophobic pollutants on natural sediments and soils. *Chemosphere, 10*, 833–846.

Kögel-Knabner, I. (1993). Biodegradation and humification processes in forest soils. In J. M. Bollag & G. Stotzky (Eds.), *Soil biochemistry* (pp. 101–127). New York: Marcel Dekker Inc.

Kohl, S. D., & Rice, J. A. (1998). The binding of contaminants to humin: A mass balance. *Chemosphere, 36*, 251–261.

Kononova, M. M. (1966). *Soil organic matter. Its nature, its role in soil formation and in soil fertility*. Oxford: Pergamon Press.

Krauss, M., Wilcke, W., & Zech, W. (2000). Polycyclic aromatic hydrocarbons and polychlorinated biphenyls in forest soils: depth distribution as indicator of different fate. *Environmental Pollution, 110*, 78–88.

Lyman, W. J. (1990). Chapter 4. In W. J. Lyman, W. F. Reehl, & D. H. Rosenblatt (Eds.), *Handbook of chemical property estimation methods*. Washington, DC: American Chemical Society.

MacCarthy, P. (2001). The principles of humic substances. *Soil Science, 166*, 738–751.

Meijer, S. N., Steinnes, E., Ockenden, W. A., & Jones, K. C. (2002). Influence of environmental variables on the spatial distribution of PCBs in Norwegian and U.K. soils: Implications for global cycling. *Environmental Science and Technology, 36*, 2146–2153.

Meijer, S. N., Ockenden, W. A., Sweetman, A. J., Breivik, K., Grimalt, J. O., & Jones, K. C. (2003). Global distribution and budget of PCBs and HCB in background surface soils: Implications for sources and environmental processes. *Environmental Science and Technology, 37*, 667–672.

Moeckel, C., Nizzetto, L., Di Guardo, A., Steinnes, E., Freppaz, M., Filippa, G., et al. (2008). Persistent organic pollutants in boreal and montane soil profiles: Distribution, evidence of processes and implications for global cycling. *Environmental Science and Technology, 42*, 8374–8380.

Nelson, D.W & Sommers, L.E. (1996). Total carbon, organic carbon, and organic matter (pp 961–1010). In: J.M. Bartels et al. (Eds) Methods of soil analysis: Part 3 chemical methods (3rd ed). ASA and SSSA Book Series 5, Madison, WI.

Pan, B., Xing, B. S., Liu, W. X., Tao, S., Lin, X. M., Zhang, X. M., et al. (2006). Distribution of sorbed phenanthrene and pyrene in different humic fractions of soils and importance of humin. *Environmental Pollution, 143*, 24–33.

Piccolo, A., Celano, G., & Conte, P. (1996). Adsorption of glyphosate by humic substances. *Journal of Agricultural and Food Chemistry, 44*, 2442–2446.

Piccolo, A., Conte, P., Scheunert, I., & Paci, M. (1998). Atrazine interaction with soil humic substances of different molecular structure. *Journal of Environmental Quality, 27*, 1324–1333.

Pignatello, J. J. (1998). Soil organic matter as a nanoporous sorbent of organic pollutants. *Advances in Colloid and Interface Science, 76–77*, 445–467.

Ribes, A., Grimalt, J. O., Torres García, C. J., & Cuevas, E. (2002). Temperature and organic matter dependence of distribution of organochlorine compounds in mountain soils from the subtropical Atlantic (Teide, Tenerife Island). *Environmental Science and Technology, 36*, 1879–1885.

Rice, A. J. (2001). Humin. *Soil Science, 166*, 848–857.

Rice, A. J., & MacCarthy, P. (1991). Statistical evaluation of the elemental composition of humic substances. *Organic Geochemistry, 17*, 635–648.

Rutherford, D. W., Chiou, C. T., & Kile, D. E. (1992). Influence of soil organic matter composition on the partition of organic compounds. *Environmental Science and Technology, 26*, 336–340.

Růžičková, P., Klánová, J., Čupr, P., Lammel, G., & Holoubek, I. (2008). An Assessment of air-soil exchange of polychlorinated biphenyls and organochlorine pesticides across Central and Southern Europe. *Environmental Science and Technology, 42*, 179–185.

Seth, R., Mackay, D., & Muncke, J. (1999). Estimating the organic carbon partition coefficient and its variability for

hydrophobic chemicals. *Environmental Science and Technology, 33*, 2390–2394.

SISS-Società Italiana della Scienze del Suolo (2007). Escursione scientifica del convegno nazionale: 'La scienza del suolo nei territori montani e collinari'. Milano-Chiavenna, 9–13 Luglio.

Stevenson, F. J. (1994). *Humus chemistry: Genesis, composition, reactions*. New York: John Wiley and Sons.

Stevenson, F. J., & Cole, M. A. (1999). *Cycles of soil: Carbon, nitrogen, phosphorus, sulphur micronutrients*. New York: John Wiley and Sons.

Sweetman, A. J., Dalla Valle, M., Prevedouros, K., & Jones, K. C. (2005). The role of soil organic carbon in the global cycling of persistent organic pollutants (POPs): Interpreting and modelling field data. *Chemosphere, 60*, 959–972.

Tan, K. H. (2003). *Humic matter in soil and the environment*. New York: Marcel Dekker.

Tato, L., Tremolada, P., Ballabio, C., Guazzoni, N., Parolini, M., Caccianiga, M., et al. (2011). Seasonal and spatial variability of polychlorobiphenyls (PCBs) in vegetation and cow milk from a high altitude pasture in the Italian Alps. *Environmental Pollution, 159*, 2656–2664.

Tremolada, P., Villa, S., Bazzarin, P., Bizzotto, E., Comolli, R., & Vighi, M. (2008). POPs in mountain soils from the Alps and Andes: Suggestions for a 'precipitation effect' on altitudinal gradients. *Water, Air and Soil Pollution, 188*, 93–109.

Tremolada, P., Parolini, M., Binelli, A., Ballabio, C., Comolli, R., & Provini, A. (2009). Preferential retention of POPs on the northern aspect of mountains. *Environmental Pollution, 157*, 3298–3307.

Weiss, P., Riss, A., Hartl, W., Lorbeer, G., & Hagenmeier, H. (1993). Chlorinated hydrocarbons in soil profiles of two forest sites in the Linz area (upper Austria). *Organohalogen Compouds, 12*, 255–258.

Wen, B., Zhang, J.-J., Zhang, S.-Z., Shan, X.-Q., Khan, S. U., & Xing, B. (2007). Phenanthrene sorption to soil humic acid and different humin fractions. *Environmental Science and Technology, 41*, 3165–3171.

Chapter V

Tato, L., Tremolada, P., Ballabio C., Guazzoni, N., Parolini, M., Caccianiga, M., Binelli, A., 2011. Seasonal and spatial variability of polychlorinated biphenyls (PCBs) in vegetation and cow milk from a high altitude pasture in the Italian Alps. Environmental pollution 159, 2656−2664.

Environmental Pollution 159 (2011) 2656–2664

Contents lists available at ScienceDirect

Environmental Pollution

journal homepage: www.elsevier.com/locate/envpol

Seasonal and spatial variability of polychlorinated biphenyls (PCBs) in vegetation and cow milk from a high altitude pasture in the Italian Alps

Liliana Tato [a], Paolo Tremolada [a,*], Cristiano Ballabio [b], Niccolò Guazzoni [a], Marco Parolini [a], Marco Caccianiga [a], Andrea Binelli [a]

[a] Department of Biology, University of Milan, Via Celoria 26, Milan, I-20133, Italy
[b] Department of Environmental and Land Sciences, University of Milano-Bicocca, Piazza Della Scienza 1, Milan, I-20126, Italy

ARTICLE INFO

Article history:
Received 18 February 2011
Received in revised form
27 May 2011
Accepted 28 May 2011

Keywords:
Polychlorinated biphenyls
Seasonal trend
Vegetation
Cow milk
Mountain contamination

ABSTRACT

The seasonal and spatial variability of polychlorinated biphenyls (PCBs) in vegetation and cow milk was studied in a high altitude pasture in the Alps (1900 m a.s.l.). PCB contamination in vegetation shows a concentration peak in June, which is mainly interpreted as the consequence of a temporary PCB enrichment of the air layer above the ground due to net emission fluxes from the soil. A three compartment dynamic model was developed to test this hypothesis. The North/South enrichment factor in the vegetation was 1.5–1.6 for penta- and hexa-substituted congeners and 1.7 for hepta- and octa-PCBs, according to the effect of temperature on compounds having higher K_{oa} values. Milk concentrations followed the vegetation seasonal trend. The congener abundance in milk is in agreement with the biotransformation susceptibility, absorption efficiency and residence time of the different congeners in dairy cows.

1. Introduction

Polychlorinated biphenyls (PCBs) have been banned worldwide since 2001 by the Stockholm Convention. The PCB Elimination Network (PEN) was instituted to enforce the total elimination of PCBs remaining inside closed systems until 2028 (UNEP, 2009). As a consequence of their use and dispersion (Breivik et al., 2002) and because of their physical–chemical properties and persistence, PCBs are able to reach the most remote areas by long-range atmospheric transport (Wania and Mackay, 1993; Wania and Su, 2004). Air is the dominant medium of global transport and also the site of important degradation loss, whereas soils and sediments are the major reservoirs of PCBs globally (Wania and Daly, 2002).

Plants act as an efficient scavenging medium from the atmosphere (Thomas et al., 1998) and as major vectors of persistent organic pollutants (POPs) into terrestrial food chains (McLachlan, 1993). The contamination of plant leaves by lipophylic and semi-volatile organic compounds occurs primarily via air rather than via the soil-root system (Bacci and Gaggi, 1986; Paterson et al., 1994; Tolls and McLachlan, 1994; Trapp and Matthies, 1995; Welsh-Pausch et al., 1995; Polder et al., 1998; Böhme et al., 1999; Kömp and McLachlan, 2000). McLachlan (1999) pointed out that the plant uptake of lipophylic and semi-volatile organic compounds occurs via three processes: a) equilibrium partitioning between the vegetation and the gas phase for compounds having a Log K_{oa} range between 6 and 8.5; b) kinetically limited gaseous deposition for compounds having a Log K_{oa} range between 8.5 and 11; and c) particle-bound deposition for compounds having a Log K_{oa} above 11. Barber et al. (2004) reviewed the main factors affecting the air–vegetation transfer, such as exposure time, physicochemical properties of the compounds, environmental factors (temperature, wind speed, humidity and light conditions), and plant characteristics (functional type, leaf surface area, cuticular structure and leaf longevity).

This work mainly focuses on the seasonal variability of PCB contamination in grass vegetation and cow milk in a mountain pasture in the Alps. In the Alps at 1900 m a.s.l., great climatic changes occur over a short period. At the end of May, soils become free from snow and warm rapidly, producing flowering vegetation (June and July). At the end of September, snow again begins to cover the soil, and the vegetation disappears under the snow mantle. Recently, the importance of temporal variability in environmental distribution and bioaccumulation has been highlighted (Undeman et al., 2009). Increasing concentrations of PCBs during the growing season were observed by Nizzetto et al. (2008a) in different tree species at 1100 and 1400 m a.s.l., while decreasing seasonal trends were observed in mountain soils by Tremolada et al. (2009a) and Guazzoni et al. (2011). Typical seasonal cycles were described in air with higher concentrations in the summer

* Corresponding author.
E-mail address: paolo.tremolada@unimi.it (P. Tremolada).

0269-7491/$ – see front matter © 2011 Elsevier Ltd. All rights reserved.
doi:10.1016/j.envpol.2011.05.035

than in the winter (Halsall et al., 1995). On the contrary, Nizzetto et al. (2008b) reported that at 1800 m a.s.l., concentrations in the air seemed to be constant from May to October, at least for penta-, hexa- and hepta-chlorinated biphenyls. Different organochlorine compound concentrations were measured in the Alps during the summer and wintertime using semi-permeable membrane devices (Shen et al., 2009), and different soil–air fugacity ratios were measured for PCBs between July and November in several European countries (Ruzicková et al., 2008). Despite its importance, the seasonal variation of POP contamination in vegetation is not completely understood, and the roles of grass and tree vegetation have not been clarified.

2. Materials and methods

The study area (Andossi plateau) is a grassland plateau at 1900 m a.s.l. in the central Italian Alps (Fig. 1). Three different sampling sites were identified at the same altitude but with different aspects (North, South and intermediate). Intermediate conditions were found in a plain portion of the plateau. The North and South aspects were determined by small hills (around 100 m in height and 200 m in width). Vegetation samples were collected in 2008 during the growing period: T1-01/06/08, T2-27/06/08, T3-19/07/08, T4-07/08/08, T5-09/09/08 and T6-01/10/08. Milk samples were collected during the pasture period (mid-June to mid-September), and therefore, only four sampling campaigns were useful for milk (T2–T5). An integrated milk sample was collected for each date because samples taken from a single animal are subject to a great inter-variability due to many physiological factors (Sweetman et al., 1999). In addition, two other commercial milks bought in Milan (North Italy) were analysed for comparative purpose. Just two samples were analysed in order to have an indicative direct comparison between the PCB contamination in milk taken at high altitude on Alps and that coming from the Italian plain region at the bottom of the Alps, where almost all the commercial fresh milk, sold in Milan, is produced. The

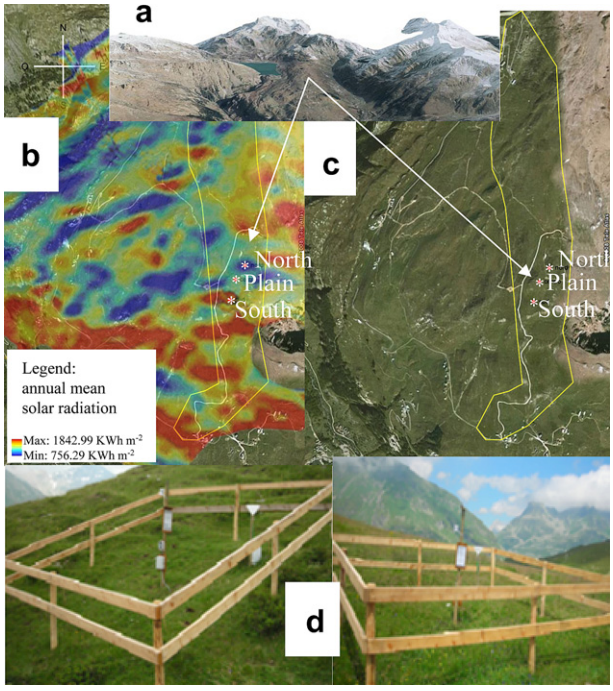

Fig. 1. (a) Map of the sampling area on the Italian side of the Spluga Pass (central Italian Alps); (b) annual mean solar radiation map of the Andossi plateau (sampling area) on which the sampling sites are marked by an asterisk; colours refer to solar radiation intensity as explained in the map legend. This map was obtained by the software SAGA taking into account the day length, zenith angle and orographic features, elaborated by DTM-digital terrain model obtained from airborne LIDAR-laser imaging detection and ranging data with 20-cm precision re-sampled at a height of 5 m; cloud influence is not included. The plot was constructed with ArcGIS 9.2, ESRI; (c) orthogonal image of the sampling area with the indication of the same sampling sites and the pasture area (yellow line). (d) fences enclosing North and intermediate experimental sites. (For interpretation of the references to colour in this figure legend, the reader is referred to the web version of this article.)

PCB congeners analysed in this work were chosen among those most frequently found in Italy in environmental samples and those having a wide range of chlorination degree (from tri- to octa-chlorinated congeners). The vegetation and milk samples were lyophilised, extracted by a Soxhlet apparatus, purified by concentrated sulphuric acid and a Silica–Florisil column and analysed by GC-MS–MS. A full description of the sampling sites, sampling modalities, analytical procedure and statistical analyses is reported in the Supplementary information (SI).

3. Results and discussion

3.1. PCBs in vegetation

The total PCBs (ΣPCBs) in the vegetation in the Andossi plateau varied over a 7-fold range (0.32–2.05 ng/g d.w.). The mean concentration (1.1 ± 0.50 ng/g d.w., mean ± standard deviation) is slightly lower than those reported by Nizzetto et al. (2008a) for other Italian mountain environments (1.2 ± 0.46, 1.4 ± 0.80, 1.5 ± 0.90 and 1.7 ± 0.50 ng ΣPCBs/g d.w. in spruce, beech, larch and mountain ash, respectively, mean ± standard deviation). Despite differences in space, time, altitude and plant species, the PCB concentrations measured in these two Alpine sites and their variability were very similar. On the Andossi plateau, CB-153 showed the highest concentrations and, together with CBs 138 and 180, constituted nearly 60% of the ΣPCBs. Congeners 101, 118, 149 and 170 gave an overall contribution of approximately 32%, while congeners 18, 31 + 28, 52, 44 and 194 accounted globally for less than 10% of the total PCB amount. This congener profile relates with the composition of the technical mixtures used in Europe (Breivik et al., 2002) and with the physicochemical properties and persistence determining high long-range transport potential (Klasmeier et al., 2006) and high mountain contamination potential (Daly et al., 2007). Whereas mean levels and congener composition accord to general background concentrations expected for mountain areas in Europe, the quite high variability of the PCB sum (7-fold range) was quite surprising for a such small area and short time interval.

3.1.1. Differences in vegetation contamination levels

Two main variability factors were analysed in this work: the small-scale space variability among sites with different aspects (North, plain and South) and the time-variability during the growing season (from June to September). By analysing the concentration data on a lipid base (Table 1) by General Linear Model, we found that the aspect and date factors were significant for almost all of the congeners and for their sum (Table 2). The lipid normalisation of the data was introduced in order to reduce the possible interference coming from the differences in the species composition and vegetative stage (vegetative grow, flowering and seed production) of the vegetation samples analysed in this work. The vegetation of the three experimental sites (North, plain and South) was analysed in detail and found to comprise a rich herbaceous community composed of 89 species belonging to 27 families. Our vegetation samples, including the entire vegetation on a prefixed area, result in site- and time-specific vegetation samples, characterised by a complex composition. This choice was preferred because it results in a higher ecological significance, even if inter-species differences in bioaccumulation were possible. However, we believe that the complex composition itself should be able to average those differences coming from species composition and vegetation stages. Barber et al. (2004) reported that inter-species variability was not simply related to the extractable lipid content because other plant characteristics, such as cuticle structure and composition, could be important. However, extractable lipid content may affect bioaccumulation in vegetation, being, at least partially, responsible for the physical partitioning of the compound between the air and the plant. The lipid content of our samples varied from 0.030 to 0.053 g lipid/g d.w. (mean content of 0.038 ± 0.0065 g lipid/g d.w.)

Table 1
PCB concentrations and lipid content of vegetation and milk samples.

Matrix	Date	Site	Lipid	PCB congener concentration (ng/g lipid)												
			g lip/g d.w.	18	31 + 28	52	44	101	149	118	153	138	180	170	194	∑ PCB
Veg	1 Jun	North	0.038	0.21	0.71	1.13	0.68	2.42	1.92	2.63	7.84	4.66	4.82	1.87	0.34	29.24
		Plain	0.053	0.04	0.28	0.30	0.17	0.64	0.68	0.55	1.77	1.11	1.04	0.49	0.09	7.17
		South	0.030	0.30	0.50	0.90	0.50	1.73	2.13	2.07	5.83	4.67	3.53	1.03	0.23	23.43
	27 Jun	North	0.043	1.44	1.14	2.09	1.05	3.42	2.86	3.16	9.74	7.49	8.63	2.35	0.88	44.26
		Plain	0.048	1.08	0.63	2.08	1.23	3.67	3.31	2.81	9.75	6.92	8.29	2.06	0.81	42.65
		South	0.045	0.87	0.67	1.02	0.84	3.00	2.38	2.33	7.78	5.76	6.24	1.69	0.27	32.84
	19 Jul	North	0.032	0.44	0.28	0.84	0.53	1.81	2.63	1.81	6.13	3.97	3.91	0.94	0.31	23.59
		Plain	0.034	0.26	0.09	0.53	0.26	1.06	1.41	1.12	2.79	2.21	2.21	1.06	0.21	13.21
		South	0.033	0.03	0.15	0.45	0.24	0.85	1.45	0.67	2.21	1.48	0.94	1.00	0.15	9.64
	7 Aug	North	0.033	0.06	0.39	0.73	0.33	2.33	3.52	3.36	7.64	6.30	6.03	3.09	0.70	34.48
		Plain	0.041	0.02	0.20	0.29	0.22	1.71	3.20	2.51	6.68	5.95	7.90	3.05	0.61	32.34
		South	0.038	0.03	0.29	0.39	0.29	1.71	2.58	2.24	5.21	4.66	5.08	1.89	0.55	24.92
	9 Sept	North	0.032	0.66	1.41	1.72	1.06	3.88	5.13	3.75	10.44	8.72	8.06	3.63	0.75	49.19
		Plain	0.036	0.11	0.64	0.69	0.72	1.94	3.25	2.50	7.25	5.58	4.78	2.17	0.44	30.08
		South	0.038	0.11	0.18	0.45	0.32	0.95	1.45	0.97	3.00	2.29	1.95	0.55	0.21	12.42
	1 Oct	North	0.030	0.27	0.67	1.20	0.67	3.23	4.30	3.47	9.60	7.48	6.60	1.97	0.73	40.18
		Plain	0.044	0.23	0.45	1.02	0.52	2.18	2.82	2.30	6.50	5.36	4.48	1.95	0.50	28.32
		South	0.038	0.24	0.53	1.18	0.55	2.55	3.53	3.76	8.08	6.39	5.32	2.16	0.74	35.03
Milk	27 Jun	Andossi	0.344		0.09			0.34	0.55	1.04	2.24	1.56	1.24	0.24	0.09	7.40
	19 Jul	Andossi	0.315		0.08			0.17	0.23	0.81	1.84	1.34	0.75	0.17	0.06	5.45
	7 Aug	Andossi	0.275		0.04			0.05	0.31	0.42	1.67	1.39	0.69	0.15	0.03	4.75
	9 Sept	Andossi	0.371		0.05			0.05	0.21	0.62	1.57	1.05	0.80	0.15	0.06	4.56
		Com 1	0.236		0.08		0.04	0.42	0.41	0.64	2.46	1.34	1.03	0.43	0.09	6.94
		Com 2	0.224		0.06		0.07	0.73	0.76	3.90	3.50	3.68	1.10	0.45	0.08	14.34

with a significant aspect effect ($F_{2;10} = 4.34$; $P = 0.044$) and a non-significant time effect ($F_{5;10} = 2.36$; $P = 0.12$). Marginal means of 0.035, 0.043 and 0.037 g lipid/g d.w. were obtained for the North, plain and South aspects, respectively. The highest value was obtained at the plain site and the second highest at the South site; these findings are in accord with the most favourable pedo-climatic conditions of these sites compared to those of the North site. Due to these differences, we decided to normalise the contamination data of each sample to its own lipid content, even if the statistical analyses repeated on a dry weight base gave very similar results.

3.1.2. Seasonal variability in vegetation

The seasonal trend of the mean concentrations (Fig. 2) shows a clear concentration peak at T2. The PCB levels at T2 were 2- to 10-fold higher than those at the beginning of the growing season (T1) or in the middle of July (T3). Seasonal trends of the PCB concentrations in vegetation were already reported by Nizzetto et al. (2008a) during the growing season in tree species at 1100 and 1400 m a.s.l. in the Alps, but with a different pattern. Nizzetto et al. (2008a) explained their seasonal pattern in vegetation mainly as an effect of temperature on the accumulation potential of vegetation, because they found mainly an increase in the PCB concentrations at the end of the growing season, when temperatures decreased while

Table 2
GLM results of the analysis of PCB concentrations in vegetation on a lipid base (ng/g lipid), considering the concentration as dependent variable and the aspect and time as factors.

PCB congener	Factors			
	Aspect		Time	
	$F_{2;10}$	P	$F_{5;10}$	P
18	4.27	0.046*	17.29	<0.001***
32 + 28	5.93	0.020*	3.72	0.037*
52	4.46	0.041*	5.18	0.013*
44	3.40	0.075	6.95	0.005**
101	5.98	0.020*	5.05	0.014*
149	3.44	0.073	3.01	0.065
118	4.64	0.038*	3.40	0.047*
153	6.09	0.019*	3.79	0.035*
138	4.32	0.044*	4.14	0.027*
180	4.50	0.040*	5.64	0.010*
170	2.94	0.099	2.86	0.074
194	4.20	0.047*	5.04	0.014*
ΣPCB	5.39	0.026*	4.20	0.026*

*Significant differences ($P < 0.05$).
**Very significant differences ($P < 0.01$).
***Highly significant differences ($P < 0.001$).

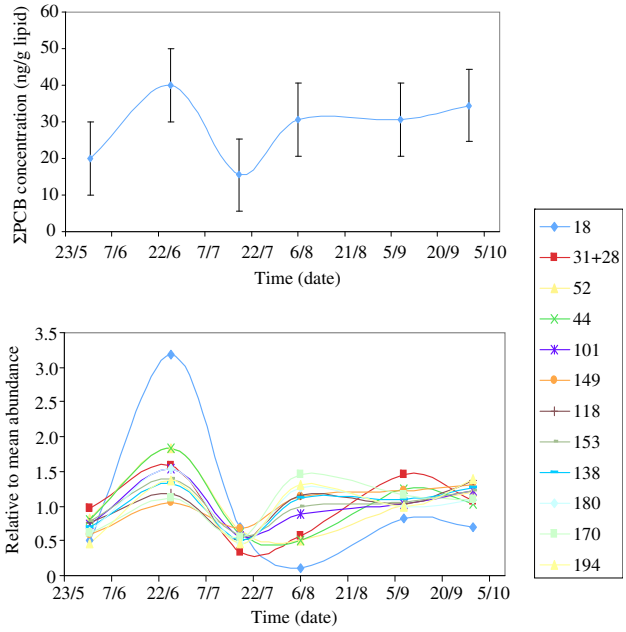

Fig. 2. Seasonal variation of PCB concentration in vegetation from the Andossi plateau during the 2008 growing season. The upper graph refers to the mean concentration of the PCB sum, and the lower graph refers to the abundance of each congener relative to its own mean. The mean concentrations were calculated by GLM (marginal means) and are reported with 95% confidence interval bars for the PCB sum.

the concentrations in the air maintained almost constant levels, at least until October and for penta-, hexa- and hepta-chlorinated biphenyls. Our concentration peak registered in the vegetation at the end of June (T2) cannot be easily related neither to a concentration peak in the air, because direct air measurements revealed great differences between winter and summer but not within summer (Nizzetto et al., 2008b; Lee and Jones, 1999; Halsall et al., 1999), nor to specific changes in environmental parameters such as temperatures. The effect of temperature considered by Nizzetto et al. (2008a) is not consistent with our data, because the highest and the lowest concentration were measured in two periods (end of June and the half of July) characterised by very similar temperature conditions (in situ measurements, Guazzoni et al., 2011). An effect of growth is also unlikely because at the end of June, when the concentration peak was registered, vegetation was still rapidly growing, determining a growth–dilution factor that was potentially able to decrease the concentrations rather than increase them. A possible explanation for the observed concentration peak could lie in the concentration data from the soil from the same area and time (Guazzoni et al., 2011). In the mean interval in which the PCB concentrations increased in the vegetation (1st of June–27th of June), concentrations in the soil significantly decreased by up to 3-fold; this decline was mainly interpreted as volatilisation (Guazzoni et al., 2011). The PCBs released from the soil during this interval could have temporarily increased the contamination level of the soil–air interface before passing to the air compartment above the grass, where they mix and dilute within a higher air volume. Meijer et al. (2003) showed a consistent gradient for several organochlorine pesticides in air between the heights of 3 cm and 150 cm above the soil, with higher concentrations in the soil–air interface of even more than one order of magnitude compared to those at 150 cm. A temporary PCB enrichment at the soil–air interface could not have been re-adsorbed by the soil itself because the increase of the soil temperatures during this period reduced its soil–air partition coefficient, K_{sa} (during the PCB release, the fugacity in the soil did not decrease: $2.7 \times e^{-12}$ and $3.2 \times e^{-12}$ Pa for congener 153 in T1 and T2, respectively). On the contrary, the vegetation may have intercepted this flux with the well-known 'filter effect'. Two elements could potentially contribute to this process: the uptake kinetics of pollutants into vegetation that depend on many parameters but can be also very rapid (see for example data of Mackay et al., 2006) and the peculiarity of the herbaceous vegetation characterised by a direct contact with the soil–air interface. In addition, plant cover is able to create a more stable air layer above the ground, reducing the wind speed and increasing the air–vegetation residence time. During period of net emission from soil, PCB concentrations in the 'stable' air layer at the ground level are expected to be order of magnitude higher than in the 'free' atmosphere, as predicted by the Fick's law. The net PCB emission from T1 to T2 was 97.4, 96.8 and 77.3 μg ΣPCBs m^{-2} for the North, plain and South aspects, respectively (data from Guazzoni et al., 2011), while the net uptake in vegetation was 0.38, 0.84, and 0.39 μg ΣPCBs m^{-2} for the same sites; therefore, the PCB fraction taken up by vegetation was 0.39, 0.87 and 0.50% of that lost by the soil for the North, plain and South aspects, respectively. The net uptake in vegetation was obtained by calculating the differences between the total PCB burden at the two dates (T1 and T2), refer-ring to 1 m^2 of surface, the biomass amount (g f.w. m^{-2}, SI section) and the d.w. fraction of each sample (g d.w./g f.w.). The emission fluxes from soil caused a PCB enrichment of the air inside the grass layer, determining also a temporary enrichment in the vegetation too. From the end of June, when the net emission from soil ceases, vegetation will start to equilibrate with the atmosphere above it, releasing the supplemental part of its contamination. To assess if the observed behaviour of the soil–plant system can be described by a theoretical model, we developed a suitable Ordinary Differential Equation (ODE) system which describes the dynamic of PCB mobility among the soil, the air layer above it and the vegetation.

3.1.3. Dynamic modelling of the PCB mobility in the soil–air–plant system

The full description of the model is reported in the Supplementary information. Conceptually, as the average temperature of soil increases the system will move from its initial state to a new equilibrium, to achieve which the soil will loose part of its adsorbed PCBs at a rate equal to $k_{sa}\Delta S$ until a new equilibrium is achieved. If soil temperature decreases the soil will start to absorb PCB with at a constant rate $k_{sa}A$. Local emission from the soil will not increase general atmospheric concentration, but only air concentrations just above the soil surface following Fick's diffusion law (to simplify the matter, we will consider that simple diffusion will create a PCB gradient in the first few decimetres). Consequently, the uptake of PCB from vegetation is function of two components: atmospheric concentration and net soil loss. In practice, plant surface will adsorb PCBs with at a velocity k_{ap} proportional to the atmospheric concentration plus the net soil loss of PCB.

The outcome of the ODE model for the CB-153 is shown in Fig. 3. The left hand graph (a) shows the variation of CB-153 content within the soil as a function of temperature change as simulated by ODE (black line) and the actual measured concentration of CB- 153 (black dots). The first measure of PCB concentration shows a concentration slightly higher than the one predicted by the model and could be due to either a measurement error or to some approximation of soil properties like soil density. As expected, soil CB-153 concentration falls quickly as temperature increases, until reaching a minimum value at the beginning of August. Theoretical minimum and the actual one are in almost perfect agreement. Nevertheless the general trend seems to be similar, at least to the degree one would expect from a model not taking into account many physical parameters (wind, rain, evapotranspiration, etc.) such as ours. The right hand graph (b) shows the trend of CB-153 within vegetation using the same graphical symbols. As previously stated, the model starts with a zero plant biomass and then follows the growth curve extrapolated from field data (Fig. S1). Thus there is a rapid increase of CB-153 concentration in the plant biomass as both soil PCB emissions and plant growth are quite conspicuous in June. The rapid growth of plant biomass ensures that the system does not reach saturation, while higher CB-153 availability, due to soil emissions, contributes to a rapid increase of PCB in the plant biomass. Then again, there seems to exist a good agreement between measured and simulated data, with the notable exception of the concentration measured in July. However, major differences between modelled and measured concentrations could be due to differences in estimated and actual temperatures, since plant temperatures were not measured, but rather estimated from air and soil's ones. Despite these discrepancies, the model elaboration applied to CB-153 is able to provide a quantitative and mathematical description of the observed soil–air–plant behaviour, supporting our interpretation of the data.

3.1.4. Small-scale spatial variability in vegetation

The second factor analysed in this work deals with the possible 'aspect effect' of the different temperature conditions of the sites, as they are close to each other but have different aspects (South, plain and North). Hourly air and soil temperatures were specifically monitored in the three experimental sites in 2008 (data shown in Supplementary materials). The air temperatures, measured 2 m above the ground, were similar in the three sites as a consequence of the small experimental area and the high air mixing (high wind speed). However, the soil temperatures in the South site significantly

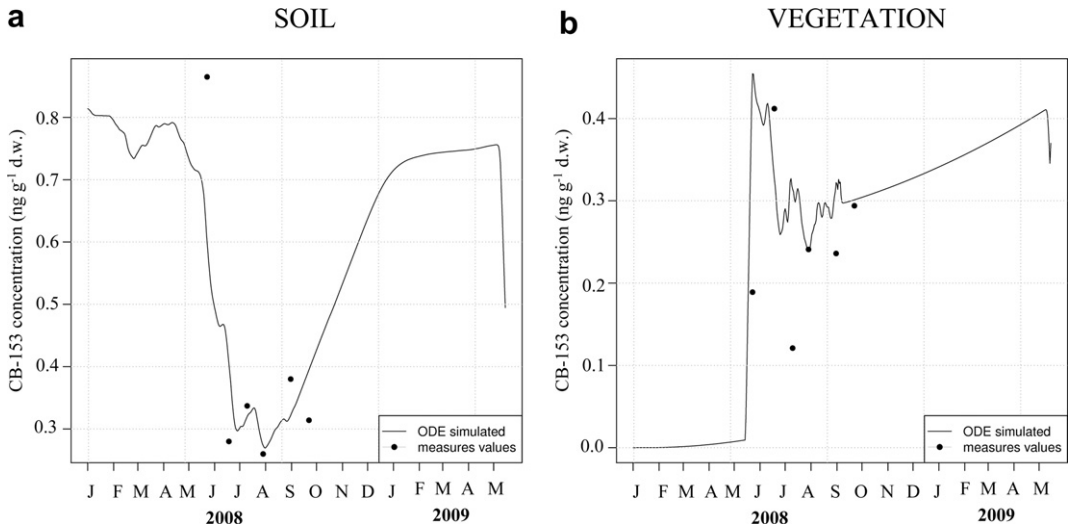

Fig. 3. Predicted (lines) and measured (dots) CB-153 concentrations in soil (a) and vegetation (b).

diverged during sunny days and during the daytime from those found at the North site by 4 °C or more. The plain site typically showed intermediate values. The same temperatures re-converged to similar values among the sites during night time and during rainy days, showing a direct and rapid surface soil response to the energy balance driven by net radiation. The high number of sunny days and the long solar irradiation during the summer were suffi-cient to often lead to higher daily mean temperatures in the South soils than in the North soils. These temperature differences were sufficient to cause large differences in the POP concentration in the soil with a North/South enrichment factor (N/S EF_s) of near 2-fold for PCBs (Guazzoni et al., 2011), for several polycyclic aromatic hydrocarbons (Tremolada et al., 2009b), and for chlorinated hydrocarbons (Tremolada et al., 2009a). Fig. 4 shows the 'aspect effect' for the analysed congeners and for their sum for vegetation. Concentrations in the North site were higher than those in the South site. Concentration differences ranged from 1.5 to 2-fold depending on the congener. These data and this interpretation can be affected by the 'growth dilution effect'; the lower concentrations found in the South site could be determined by a higher growth rate and therefore a higher dilution effect compared to the North site, where the higher concentrations could be determined by the lower observed growth rate (Fig. S1). However, the same effect (growth dilution) should also be present at the plain site, where the highest growth rate was observed (Fig. S1). The plain site did not show lower PCB concentrations than the South site (Fig. 4), but often intermediate concentrations between North and South sites. This consideration confirms the temperature-dependent interpretation of the North *vs.* South concentration difference in our results. These concentration differences in the vegetation were registered even though the air temperatures (measured 2 m above the ground) were equal among the three sites. If the energy balance among the three sites is different, because of the aspect, temperatures of the soil–air boundary layer are expected to be also different, because heat exchange also follows the Fick's law. Additionally, similarly to the soil also leaves have their own energy balance. Leaf temperature can be 5–10 °C different than air temperature. Leaves that receive smaller amount of short wave radiation (North aspect) are colder than those in the South aspect, therefore their accumulation capacity is higher, by means of the relationship between temperature and the plant–air equilibrium partition coefficient. North/South enrichment factors in vegetation (N/S EF_v) were calculated as the ratio of the marginal means of the PCB concentrations in the North and South sites (Table 3). Congeners with higher volatility (tri- and tetra-) showed the highest N/S EF_v values (up to 2.0) but also the highest variability and uncertainties, while the penta- and hexa-substituted congeners showed very similar calculated values (N/S EF_v of 1.5–1.6) with the lowest uncertainties Low chlorinated PCBs can reach the leaf–air equilibrium in few days, therefore their concentration in vegetation will greatly vary in accordance to short-term variability in temperature and air concentrations, giving higher differences of the North/South ratio due to effect of the specific conditions of the

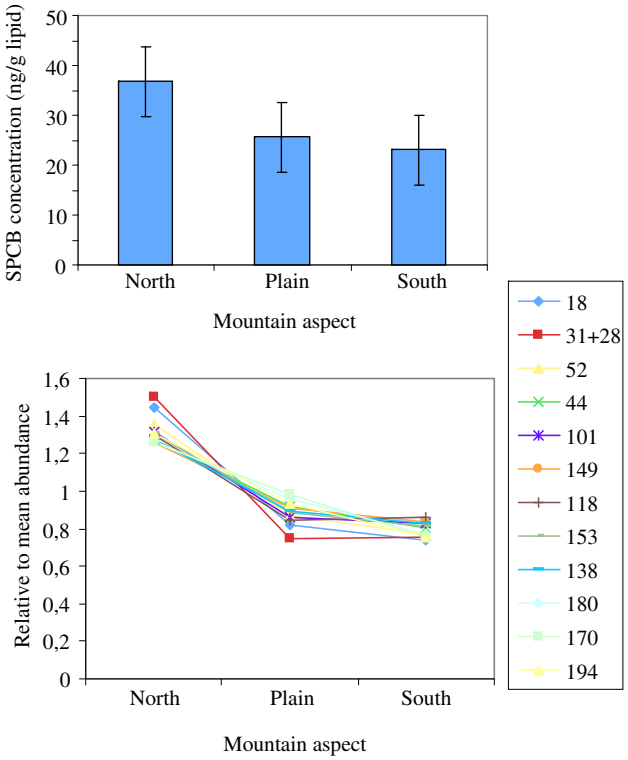

Fig. 4. PCB concentration in the vegetation from the Andossi plateau at the three sampling sites (North, plain and South). The upper graph depicts the mean concentration of the PCB sum, and the lower graph depicts the abundance of each congener relative to its own mean. Mean concentrations were calculated by GLM (marginal means) and are reported with 95% confidence interval bars for the PCB sum.

Table 3
North and South mean concentrations ± standard deviation in ng/g lipid and the resulting North/South Enrichment factor in vegetation (N/S EF_v). Mean concentrations are marginal means calculated by GLM.

PCB congener	Concentration (ng/g lipid)		N/S EF_v
	North	South	
18	0.51 ± 0.07	0.26 ± 0.07	2.0 ± 0.56
31 + 28	0.77 ± 0.09	0.39 ± 0.09	2.0 ± 0.52
52	1.3 ± 0.14	0.73 ± 0.14	1.8 ± 0.38
44	0.72 ± 0.07	0.46 ± 0.07	1.6 ± 0.30
101	2.9 ± 0.24	1.8 ± 0.24	1.6 ± 0.25
149	3.4 ± 0.33	2.3 ± 0.33	1.5 ± 0.26
118	3.0 ± 0.28	2.0 ± 0.28	1.5 ± 0.25
153	8.6 ± 0.71	5.4 ± 0.71	1.6 ± 0.25
138	6.4 ± 0.58	4.2 ± 0.58	1.5 ± 0.25
180	6.3 ± 0.59	3.8 ± 0.59	1.7 ± 0.30
170	2.3 ± 0.27	1.4 ± 0.27	1.7 ± 0.37
194	0.62 ± 0.07	0.36 ± 0.07	1.7 ± 0.36
ΣPCBs	36.8 ± 3.2	23 ± 3.15	1.6 ± 0.26

days before the sampling dates. On the contrary, less volatile PCBs takes months to reach equilibrium not because the kinetics are much slower but because the capacity of the leaf is order of magnitude higher than for low chlorinated congeners and the concentrations in air are generally lower. For these reasons the concentration of these compounds in the leaf is much less affected by the changes of the short-term conditions. The higher 'distance' from equilibrium of the high chlorinated congener in relation to short-term conditions plays a smoothing role of the concentration in vegetation.

The less volatile congeners (hepta- and octa-) had slightly higher N/S EF values (N/S EF_v of 1.7), according to the effect of temperature on compounds having higher K_{oa} values. The calculated values for vegetation were similar to those measured in the same area in the soil (Guazzoni et al., 2011) and correspond to an accumulation difference calculated for a ΔT of 3.5 °C between the North and South sites (using the Clausius–Clapeyron equation and ΔU_{oa} and K_{oa} values from Li et al., 2003). This ΔT between the South and North sites is in agreement with direct measurements in the soil but not in the air at 2 m above soil, suggesting that the vegetation/soil boundary layer is very 'stable'. Therefore molecular diffusivities in air specific for each compound can play their role in determining the kinetics of uptakes and explaining part of the observed variability.

3.2. PCBs in milk

The study area has been used for centuries as a summer pasture for dairy cows. PCB concentrations in the milk samples varied from 1.3 to 2.5 ng/g d.w. and from 1.6 to 3.2 ng/g d.w. for the mountain and the market milk, respectively (Table 1 shows data on ng g^{-1} lipid). Although only few samples were analysed, our results are in agreement with the diffuse PCB contamination of cow milk, as reported for Italy (Esposito et al., 2009) or for other European countries (Rappe et al., 1987; Focant et al., 2003; Rappolder et al., 2005; Petro et al., 2010). However, for the analysed PCB congeners, the concentrations found were well below the Italian legal threshold of 100 ng ΣPCB/g lipid (Rossi et al., 2010).

3.2.1. Seasonal trend of the contamination in milk

Fig. 5 shows the PCB seasonal trend in mountain milk observed during the pasture season on the same dates as the vegetation samples. A clear decreasing trend in contamination can be observed with some congener-specific differences. Higher-chlorinated congeners seem to have lower seasonal variations than lower-chlorinated congeners, which can be more subject to temporal changes in vegetation than the formers, because of the lower

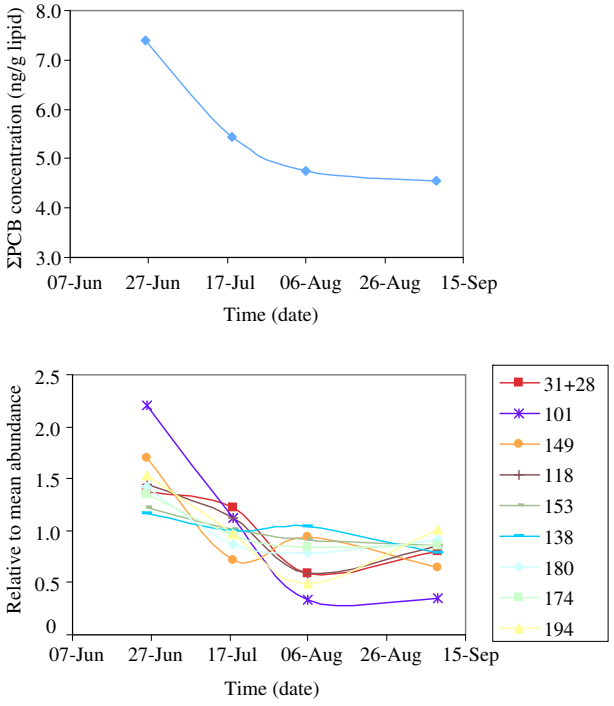

Fig. 5. Seasonal variation of PCB concentration in milk from the Andossi plateau during the 2008 growing season. The upper graph depicts to the concentration of the PCB sum, and the lower graph depicts the abundance of each congener relative to its own mean.

residence times in dairy cows (Thomas et al., 1999a). The concentration decrease in milk (1.6-fold for the ΣPCBs) temporarily follows the concentration decrease in vegetation, but with a lower fluctuation. Milk samples integrate partially the space- and time-variability of the PCB levels in vegetation, especially for the higher-chlorinated congeners that have longer residence times (Thomas et al., 1999a). When the amount of PCB stored in fat tissues is high, this stored amount serves as an additional PCB source for the circulating fluids (blood) when decreasing flux is coming from the vegetation to the intestinal tract. In fact, the time required to reduce the PCB contamination in milk coming from contaminated cows, when they are shifted to low-contamination feed, can be quite long (Rossi et al., 2010).

3.2.2. Contamination in milk in comparison to that in vegetation and soil

Fig. 6 reports the congener profile in milk in comparison to that in vegetation and soil. There is a high correspondence between the vegetation and soil profile, suggesting a common atmospheric origin of the contamination and a common congener-specific accumulation potential. On the contrary, greater differences are evident between vegetation and milk than between soil and vegetation, although PCBs arrive into milk mainly via vegetation (McLachlan, 1993; Thomas et al., 1999b; Rychen et al., 2008). Moreover, in pasture cows can ingest from 1% to 10% of the soil during their grazing activity, and this contribution to POP uptake may be important for contaminated soils (Mamontova et al., 2007). In our study area, the mean PCB contamination in the vegetation was 1.1 ± 0.50 ng ΣPCBs/g d.w. and that of the surface soil (0-1 cm) was 2.3 ± 1.2 ng ΣPCBs/g d.w. (Guazzoni et al., 2011). Supposing 14.9 g d.w. of ingested vegetation per kg of body weight per day (10 kg d.w. per day for an animal of 670 kg of body weight) and a 10% weight additional ingestion of soil (1.49 g per kg of body weight per day), the contaminant daily flux is 16.4 ng ΣPCBs per kg of body

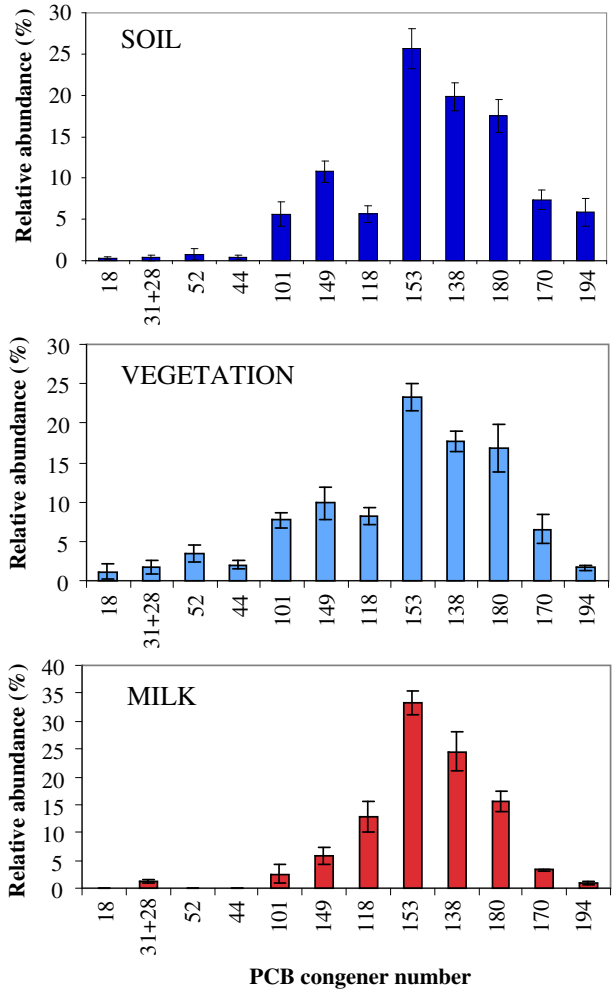

Fig. 6. The mean relative abundance of the studied congeners in soil (data from Guazzoni et al., 2011), vegetation and milk (data of this work) from the Andossi plateau in 2008. Bars in the graphs refer to the interval ± standard deviation.

weight per day and 3.4 ng ΣPCBs per kg of body weight per day from the vegetation and soil, respectively. In our conditions, the quantitative contribution of the soil to the overall PCB intake is limited and, in terms of congener abundance, very similar to that of vegetation. For these reasons, it was not further considered. Commercial cow food mainly made by meal cereals (2 kg per day) given to cows as integration feeding during milking was also neglected, because of the low PCB content of the analysed concentrate samples (0.10 ± 0.064 ng ΣPCBs/g d.w.) determining an additional intake contribution of 1.8%. Once ingested, PCBs are absorbed across the gastro-intestinal tract and pass into the blood; inside the body, they can be degraded, stored in body fat tissues or excreted mainly through milk (Sweetman et al., 1999). Different degradation susceptibility, absorption efficiency or transfer capability to milk may change the congener pattern in milk in comparison to that in food (Thomas et al., 1999a,b). The carry-over ratio from feed to milk summarises the entire process (McLachlan, 1993; Costera et al., 2006; Kierkegaard et al., 2009), while the absorption efficiency measures a specific step of the vegetation to milk transfer. Thomas et al. (1999b) observed that the absorption efficiency was very high (80% or above) for PCBs with a Log $K_{ow} < 6.5$, while for the conge-ners with higher K_{ow}, the absorption efficiency dropped to 50%or below. In our study, highly chlorinated congeners (hepta- and octa-CB; congeners 180, 170 and 194) having a Log $K_{ow} > 7$ were less present in milk than in vegetation (Fig. 6), and their carry-over ratios were lower (0.15–0.28) than for congeners 138 and 153 (carry-over ratio of around 0.45, Table 4).

The carry-over ratios calculated in the present study were lower than those reported in specific mass balance experiments under controlled conditions (Table 4). However, considering the absorption efficiencies measured by Thomas et al. (1999b), our values are in agreement with an efficient transfer capability. For example, an absorbed-milk transfer of near 80% was obtained for congener 118, considering a carry-over ratio of 0.54 (our data) and an absorption efficiency of 0.69 (Thomas et al., 1999b). The metabolism degree in cows for each congener was evaluated as in Thomas et al. (1999a) by the ratio of the concentration in milk (normalised on congener 153) to that absorbed in the gastro-intestinal tract (again normalised on congener 153) calculated by the absorption efficiencies reported by Thomas et al. (1999b). Congeners 118 and 138 appear as unmetabolised congeners in cows, having a ratio higher than 0.9 relative to congener 153, while congeners 18, 52 and 44 appear as largely

Table 4
Carry-over ratios from feed to milk calculated in this work and from the literature (Carry-over ratios, calculated as μg d^{-1} from milk/μg d^{-1} from vegetation), bioaccumulation factors in milk (BAF-milk, calculated as ng/g d.w. in milk/ng/g d.w. in vegetation), bioaccumulation factors in lipids (BAF-lipid, calculated as ng/g lipid in milk/ng/g lipid in vegetation) and bioaccumulation factors in cow (BAF-cow, calculated as ng/g f.w. in cow/ng/g f.w. in vegetation) for the PCB congeners studied and for their sum. All factors were calculated for the four dates in which the milk samples were collected (over the entire pasture season). Values reported are the means of the calculated data with their standard deviation.

PCB congener	Carry-over[a]	Carry-over	BAF-milk (g d.w./g d.w)	BAF-lipid (g lipid/g lipid)	BAF-cow (g f.w./g f.w)
	This study	Thomas et al., 1999b			
18	<0.04	0.03 ± 0.021	<0.2	<0.03	<0.4
31 + 28	0.30 ± 0.30	0.045 ± 0.33	1.8 ± 1.8	0.20 ± 0.19	2.8 ± 2.9
52	<0.01	n.d.	<0.1	<0.01	<0.1
44	<0.01	n.d.	<0.1	<0.01	<0.1
101	0.10 ± 0.09	0.05 ± 0.007	0.64 ± 0.52	0.07 ± 0.06	0.95 ± 0.80
149	0.17 ± 0.06	0.05 ± 0.019	1.0 ± 0.38	0.12 ± 0.05	1.5 ± 0.53
118	0.54 ± 0.36	1.09 ± 0.24	3.3 ± 2.2	0.37 ± 0.23	4.9 ± 3.5
153	0.45 ± 0.22	0.83 ± 0.14	2.8 ± 1.4	0.31 ± 0.13	4.1 ± 2.2
138	0.43 ± 0.26	0.74 ± 0.13	2.7 ± 1.6	0.30 ± 0.15	4.0 ± 2.5
180	0.28 ± 0.16	0.67 ± 0.10	1.7 ± 0.99	0.19 ± 0.09	2.5 ± 1.5
170	0.15 ± 0.08	0.65 ± 0.12	0.94 ± 0.51	0.11 ± 0.05	1.4 ± 0.78
194	0.21 ± 0.14	n.d.	1.3 ± 0.88	0.14 ± 0.09	1.9 ± 1.3
ΣPCBs	0.31 ± 0.17	0.27 ± 0.046	1.9 ± 1.0	0.21 ± 0.10	2.8 ± 1.6

[a] Carry-over factors were calculated assuming an ingestion of 10 kg d.w./d of grass and a production of 1.62 kg d.w./d, applying a mean calculated dry weight fraction of milk of 0.135 g d.w./g f.w. to a fresh weight milk production of 12 kg f.w./d. The grass ingestion and milk production values were taken from the literature, referring to indicative values of dairy cows in high altitude pastures in the Alps (Bovolenta et al., 2002).

metabolised congeners according to the finding that two adjacent hydrogen atoms, especially in the meta- and para-positions, increase the PCB biotransformation (Matthews and Dedrick, 1984).

3.2.3. Bioaccumulation factors in cow

The metabolic degradation and excretion efficiency into milk explain most of the PCB bioaccumulation values reported in Table 4, taking into account that bioaccumulation in cows occurs nearly completely via food, as reported by McLachlan (1993). In Table 4, the BAFs refer directly to milk (BAF-milk), to the vegetation and milk lipids (BAF-lipid) or to the whole animal (BAF-cow). The BAFs for cow tissues were calculated indirectly from the lipid-base concentrations in milk, based on the assumption that the lipid-base PCB concentrations in milk are a good indicator of the lipid-base PCB concentrations in the whole animal (Thomas et al., 1999a). Only the liver showed a specific lipid-base PCB enrichment; all other lipid-rich tissues showed a good level of equilibrium (Thomas et al., 1999b). Finally, to extrapolate a BAF for the entire cow (BAF-cow in Table 4), the values of 0.15 g lipid/g f.w. and 0.41 g d.w./g f.w. for a whole cow were considered, referring to the data of Gibb et al. (1992). The BAF for milk and cow were generally above 1 for most of the congeners, with maximum values for congeners 118, 153 and 138, according to the literature (Thomas et al., 1999b) and to the general increase of the concentrations of persistent lipophilic compounds along the food chain. Our result in milk and grass were similar to those found in other studies: for example Thomas et al. (1999b) reported an average ΣPCB content in forage (silage) of 1.5 ng/g d.w. and an average ΣPCB content in milk of 0.17 ng/g f.w. (our results are 1.1 ng/g d.w. and 0.24 ng/g f.w. for grass and milk, respectively). BAFs for milk and cow were 1.9 and 2.8 for the PCB sum, respectively (Table 4), showing that, on a dry and fresh weight base, these contaminants are subject to an actual increase of the concentrations along the food chain.

BAFs calculated on a lipid base (between 0.1 and 0.3 for most of the congeners and 0.2 for the PCB sum) give a completely different picture, because they are based on a fraction of the body weight and not to the whole organism. They cannot be representative of the bioaccumulation phenomenon, because they do not refer to the amount of PCB in the organism but to their concentration in a specific part (the lipid fraction) and therefore they depend on the dimension of this reservoir. PCBs were much more concentrated in the vegetation lipids than in cow lipids, because PCB in cow is diluted into a much larger volume of lipids metabolically produced for lactation and storage purposes.

4. Conclusions

Two different items were explored: (1) the seasonal variability of PCB contamination in vegetation at high altitude and (2) the space variability on a small scale. The 'aspect effect' on POP contamination was observed in vegetation. The higher contamination of the vegetation in the North site *vs.* that in the South one was mainly interpreted as a temperature-dependent event, allowing the calculation of a North/South enrichment factor in vegetation (N/S EF_v). Calculated N/S EF_v values correlated to a ΔT of 3.5 °C, which is near the typical temperature difference observed between North and South soils during sunny days and during the daytime (4 °C). Therefore, the observed N/S EF_v in vegetation correlates to direct measurements of ΔT in the soil between the South and North sites but not to those in the air at 2 m above the soil, suggesting the importance of micro-meteorological conditions of the air just above the soil and not of the mixed air layer above the vegetation. This item was also focused on interpreting the main seasonal trend observed in the vegetation. The concentration peak found at the end of June was interpreted as a temporary enrichment of the contamination of the air layer just above the soil caused by a PCB flux coming from the soil. Soils lose a consistent PCB amount because of a consistent temperature increase (mountain soils transition from around 0 °C after the melting of the snow to near 15 °C in a relatively short time). The emission from the soil causes a temporary PCB enrichment in the air layer above the soil and a temporary enrichment in the vegetation. When soils cease to emit PCBs, the contamination gradient in the air disappears, and the vegetation begins to equilibrate only with the general air compartment, losing this temporary over-contamination (concentration peak observed in T2). The model elaboration based on these assumptions supports this interpretation, allowing to calculate the concentration gradient in the air layer above soil during the period of net emission from soil (from T1 to T2) and the different diffusion parameters between soil and air and between air and vegetation.

The results presented in this paper have direct implications for milk contamination. In fact, milk reflects the contamination of cow fodder that may change spatially and seasonally in a relatively small and homogeneous area. Microclimatic conditions are able to affect the contamination status not only for soil but also for herbaceous vegetation, introducing a small-scale spatial and temporal variability that should be taken into account for contamination assessments and during sampling campaigns.

Acknowledgement

We would like to thank Mr. Donnino Della Bella and 'Consorzio Alpe Andossi' for their hospitality and contributions in setting up the sampling sites and for providing useful information.

Appendix. Supplementary material

Supplementary material associated with this article can be found, in the online version, at doi:10.1016/j.envpol.2011.05.035.

References

Bacci, E., Gaggi, C., 1986. Chlorinated pesticides and plant foliage: translocation experiments. Bulletin of Environmental Contamination and Toxicology 37, 850–857.

Barber, J.L., Thomas, G.O., Kerstiens, G., Jones, K.C., 2004. Current issues and uncertainties in the measurement and modelling of air–vegetation exchange and within-plant processing of POPs. Environmental Pollution 128, 99–138.

Böhme, F., Welsch-Pausch, K., McLachlan, M.S., 1999. Uptake of airborne semi-volatile organic compounds in agricultural plants: field measurements of interspecies variability. Environmental Science and Technology 33, 1805–1813.

Bovolenta, S., Saccà, E., Ventura, W., Piasentier, E., 2002. Effect of type and level of supplement on performance of dairy cows grazing on alpine pasture. Italian Journal of Animal Science 1, 255–263.

Breivik, K., Sweetman, A., Pacyna, J.M., Jones, K.C., 2002. Towards a global historical emission inventory for selected PCB congeners – A mass balance approach. 1. Global production and consumption. The Science of the Total Environment 290, 181–198.

Costera, A., Feidt, C., Marchand, P., Le Bizec, B., Rychen, G., 2006. PCDD/F and PCB transfer to milk in goats exposed to a long-term intake of contaminated hay. Chemosphere 64, 650–657.

Daly, G.L., Lei, Y.D., Teixeira, C., Muir, D.C.G., Castillo, L.E., Wania, F., 2007. Accumulation of current-use pesticides in neotropical montane forests. Environmental Science and Technology 41, 1118–1123.

Esposito, M., Cavallo, S., Serpe, F.P., D'Ambrosio, R., Gallo, P., Colarusso, G., Pellicanò, R., Baldi, L., Guarino, A., Serpe, L., 2009. Levels and congener profiles of polychlorinated dibenzo-p-dioxins, polychlorinated dibenzofurans and dioxin-like polychlorinated biphenyls in cow's milk collected in Campania, Italy. Chemosphere 77, 1212–1216.

Focant, J.F., Pirard, C., Massard, A.C., de Pauw, E., 2003. Survey of commercial pasteurised cow's milk in Wallonia (Belgium) for the occurrence of polychlorinated dibenzo-p-dioxins, dibenzofurans and coplanar polychlorinated biphenyls. Chemosphere 52, 725–733.

Gibb, M.J., Ivingst, W.E., Dhanoa, M.S., Sutton, J.D., 1992. Changes in body components of autumn-calving Holstein-Friesian cows over the first 29 weeks of lactation. Animal Production 55, 339–360.

Guazzoni, N., Comolli, R., Mariani, L., Cola, G., Parolini, M., Binelli, A., Tremolada, P., 2011. Meteorological and pedological influence on the PCBs distribution in mountain soils. Chemosphere. doi:10.1016/j.chemosphere.2010.12.043.
Halsall, C.J., Lee, R.G.M., Coleman, P.J., Burnett, V., Harding-Jones, P., Jones, K.C., 1995. PCBs in U.K. urban air. Environmental Science and Technology 29, 2368–2376.
Halsall, C.J., Gevao, B., Howsam, M., Lee, R.G.M., Ockenden, W.A., Jones, K.C., 1999. Temperature dependence of PCBs in the UK atmosphere. Atmospheric Environment 33, 541–552.
Kierkegaard, A., De Wit, C.A., Asplund, L., McLachlan, M.S., Thomas, G.O., Sweetman, A.J., Jones, K.C., 2009. A mass balance of tri-hexabrominated diphenyl ethers in lactating cows. Environmental Science and Technology 43, 2602–2607.
Klasmeier, J., Matthies, M., Macleod, M., Fenner, K., Scheringer, M., Stroebe, M., Le Gall, A.C., McKone, T., van de Meent, D., Wania, F., 2006. Application of multimedia models for screening assessment of long-range transport potential and overall persistence. Environmental Science and Technology 40, 53–60.
Kömp, P., McLachlan, M.S., 2000. The kinetics and reversibility of the partitioning of polychlorinated biphenyls between air and ryegrass. The Science of the Total Environment 250, 63–71.
Lee, R.G.M., Jones, K.C., 1999. The influence of meteorology and air masses on daily atmospheric PCB and PAH concentrations at a UK location. Environmental Science and Technology 33, 705–712.
Li, N., Wania, F., Lei, Y.D., Daly, G.L., 2003. A comprehensive and critical compilation, evaluation, and selection of physical–chemical property data for selected polychlorinated biphenyls. Journal of Chemical and Engineering Data 50, 742–768.
Mackay, D., Foster, K.L., Patwa, Z., Webster, E., 2006. Chemical partitioning to foliage: the contribution and legacy of Davide Calamari. Environmental Science and Pollution Research 13, 2–8.
Mamontova, E.A., Tarasova, E.N., Momontov, A.A., Kusmin, M.I., McLachlan, M.S., Khomutova, M.I., 2007. The influence of soil contamination on the concentrations of PCBs in milk in Siberia. Chemosphere 67, 571–578.
Matthews, H.B., Dedrick, R.L., 1984. Pharmacokinetics of PCBs. Annual Review of Pharmacology and Toxicology 24, 85–103.
McLachlan, M.S., 1993. Mass balance of polychlorinated biphenyls and other organochlorine compounds in a lactating cow. Journal of Agricultural and Food Chemistry 41, 474–480.
McLachlan, M.S., 1999. Framework for the interpretation of measurements of SOCs in plants. Environmental Science and Technology 33, 1799–1804.
Meijer, S.N., Shoeib, M., Jantunen, L.M.M., Jones, K.C., Harner, T., 2003. Air-soil exchange of organochlorine pesticides in agricultural soils. 1. Field measurements using a novel in situ sampling device. Environmental Science and Technology 37, 1292–1299.
Nizzetto, L., Pastore, C., Liu, X., Camporini, P., Stroppiana, D., Herbert, B., Boschetti, M., Zhang, G., Brivio, P.A., Jones, K.C., Di Guardo, A., 2008a. Accumulation parameters and seasonal trends for PCBs in temperate and boreal forest plant species. Environmental Science and Technology 42, 5911–5916.
Nizzetto, L., Jaevis, A., Brivio, P.A., Jones, K.C., Di Guardo, A., 2008b. Seasonality of the air-forest canopy exchange of persistent organic pollutants. Environmental Science and Technology 42, 8778–8783.
Paterson, S., Mackay, D., McFarlane, C., 1994. A model of organic chemical uptake by plants from soil and the atmosphere. Environmental Science and Technology 28, 2259–2266.
Petro, E.M.L., Covaci, A., Leroy, J.L.M.R., Dirtu, A.C., De Coen, W., Bols, P.E.J., 2010. Occurrence of endocrine disrupting compounds in tissues and body fluids of Belgian dairy cows and its implications for the use of the cow as a model to study endocrine disruption. The Science of the Total Environment 408, 5423–5428.
Polder, M.D., Hulzebos, E.M., Jager, D.T., 1998. Bioconcentration of gaseous organic chemicals in plant leaves: comparison of experimental data with model predictions. Environmental Toxicology and Chemistry 17, 962–968.
Rychen, G., Jurjaz, S., Toussaint, H., Feidt, C., 2008. Dairy ruminant exposure to persistent organic pollutants and excretion to milk. Animal 2, 312–323.
Rossi, F., Bertuzzi, T., Vitali, A., Rubini, A., Masoero, F., Morlacchini, M., Piva, G., 2010. Monitoring of the declining trend of polychlorobiphenyls concentration in milk of contaminated dairy cows. Italian Journal of Animal Science 9, 88–92.
Rappe, C., Nygren, M., Lindstrom, G., Buser, H.R., Blaser, O., Weuthrich, C., 1987. Polychlorinated dibenzofurans and dibenzo-p-dioxins and other chlorinated contaminants in cow milk from various locations in Switzerland. Environmental Science and Technology 21, 964–970.
Rappolder, M., Bruders, N., Schroter-Kermani, C., 2005. Comparison of congener patterns and TEQs in environmental and human samples. Organohalogen Compounds 67, 2086–2089.
Růžičková, P., Klánová, J., Čupr, P., Lammel, G., Holoubek, I., 2008. An Assessment of air-soil exchange of polychlorinated biphenyls and organochlorine pesticides across Central and Southern Europe. Environmental Science and Technology 42, 179–185.
Shen, H., Henkelmann, B., Levy, W., Zsolnay, A., Weiss, P., Jakobi, G., Kirchner, M., Moche, W., Braun, K., Schramm, K.-W., 2009. Altitudinal and chiral signature of persistent organochlorine pesticides in air, soil, and spruce needles (*Picea abies*) of the Alps. Environmental Science and Technology 43, 2450–2455.
Sweetman, A.J., Thomas, G.O., Jones, K.C., 1999. Modelling the fate and the behaviour of lipophilic organic contaminants in lactating dairy cows. Environmental Pollution 104, 261–270.
Thomas, G.O., Sweetman, A.J., Ockenden, W.A., Mackay, D., Jones, K.C., 1998. Air-pasture transfer of PCBs. Environmental Science and Technology 32, 936–942.
Thomas, G.O., Sweetman, A.J., Jones, K.C., 1999a. Metabolism and body-burden of PCBs in lactating dairy cows. Chemosphere 39, 1533–1544.
Thomas, G.O., Sweetman, A.J., Jones, K.C., 1999b. Input-output balance of polychlorinated biphenyls in a long term study of lactating daily cow. Environmental Science and Technology 33, 104–112.
Tolls, J., McLachlan, M.S., 1994. Partitioning of semivolatile organic compounds between air and *Lolium multiflorum* (Welsh ray grass). Environmental Science and Technology 28, 159–166.
Trapp, S., Matthies, M., 1995. Generic one-compartment model for uptake of organic chemicals by foliar vegetation. Environmental Science and Technology 29, 2333–2338.
Tremolada, P., Parolini, M., Binelli, A., Ballabio, C., Comolli, R., Provini, A., 2009a. Preferential retention of POPs on the northern aspect of mountains. Environmental Pollution 157, 3298–3307.
Tremolada, P., Parolini, M., Binelli, A., Ballabio, C., Comolli, R., Provini, A., 2009b. Seasonal changes and temperature-dependent accumulation of polycyclic aromatic hydrocarbons in high-altitude soils. The Science of the Total Environment 407, 4269–4277.
Undeman, E., Czub, G., McLachlan, M.S., 2009. Addressing temporal variability when modelling bioaccumulation in plants. Environmental Science and Technology 43, 3751–3756.
UNEP, 2009. Stockholm convention on persistent organic pollutants. In: Report of the Conference of the Parties of the Stockholm Convention on Persistent Organic Pollutants on the Work of its Fourth Meeting, Geneva 4–8 May, 2009.
Wania, F., Mackay, D., 1993. Global fractionation and cold condensation of low volatility organochlorine compounds in polar regions. Ambio 22, 10–18.
Wania, F., Daly, G.L., 2002. Estimating the contribution of degradation in air and deposition to the deep sea to the global loss of PCBs. Atmospheric Environment 36, 5581–5593.
Wania, F., Su, Y., 2004. Quantifying the global fractionation of polychlorinated biphenyls. Ambio 33, 161–168.
Welsh-Pausch, K., McLachlan, M.S., Umlauf, G., 1995. Determination of the principal pathways of polychlorinated dibenzo-p-dioxins and dibenzofurans to *Lolium multiflorum* (welsh ray grass). Environmental Science and Technology 29, 1090–1098.

SUPPLEMENTARY INFORMATION

Study area

The bedrock of the study area (Andossi plateau) consists of limestone with a discontinuous covering of glacial deposits. The general climatic conditions of the area were estimated from data gathered by a nearby weather station (Stuetta 1850 m a.s.l.) over a 30-year time interval (1971-2000). The mean annual precipitation and mean annual temperature were 1170 mm $year^{-1}$ and 2.7 °C, respectively. The maxima of precipitation and temperature occur in the summer. Snow accounts for 45 to 50% of the total precipitation and occurs generally from October to May (SISS, 2007).

The area lies within the Subalpine belt below the potential tree line. However, the present vegetation cover is represented by herbaceous communities due to cattle grazing and, to a lesser extent, mowing. The variability of grass species reflects two main factors: the grazing pressure and the local variability of the pedo-climatic conditions, determined by substrate typology, soil thickness, slope and aspect. The plant communities in the area are *Nardus stricta*-dominated grasslands (*Nardetum s.l.*) showing a very variable biodiversity level, *Poa alpina* and *Phleum alpinum* communities, which occur on nutrient-rich soil, and basophilic grasslands (*Seslerieto-Semperviretum*), which can be found on shallow soil. Subalpine heathlands (*Rhododendro-Vaccinietum*) occur only locally (SISS, 2007). In 2008, a detailed vegetation analysis was performed at the sampling sites (Tato L. unpublished data). Biomass growth was experimentally evaluated in the three experimental sites as a mean of three subplots (20 x 20 cm) for each site (Figure S1).

Sampling sites and sampling modalities

Three different sampling sites were identified at the same altitude but with different aspects (North, South and intermediate). Each sampling site was delimited by a 5 x 5 m fence to avoid disturbance and grazing by cows. Three field weather stations were located inside the fences. The North site had the lowest mean annual radiation amount and a typical vegetation typology of *Nardetum*. The South site had the highest mean annual radiation amount and presented more abundant vegetation.

Vegetation samples were collected in 2008 during the growing period from when the snowmelt was completed (end of May) until the beginning of October. Six sampling campaigns were conducted: T1-01/06/08, T2-27/06/08, T3-19/07/08, T4-07/08/08, T5-09/09/08 and T6-01/10/08. In each site and for every date, three samples (each one from a surface region of 20 x 20 cm) were obtained inside the fence by cutting all vegetation manually with a large clean steel knife at the soil level.

The three sub-samples taken from each site were immediately manually mixed. Therefore, three integrated samples were obtained for every sampling campaign, with care taken to avoid cross-contamination among sites. Each integrated sample was weighed, enfolded in aluminium foil and enclosed in a plastic bag. Samples were frozen as soon as possible at -20 °C. The vegetation samples from one sampling campaign to another were obtained as close as possible to maintain similar vegetation characteristics. The re-growth at that altitude is very slow.

Milk samples were collected during the pasture season, which usually starts in mid June and ends in mid September at that altitude. Therefore, only four sampling campaigns were useful for milk sampling (T2-T5). One integrated milk sample was collected for each date, because Sweetman et al. (1999) suggested integrate samples from the whole tank are preferred were simple models are used. Therefore, the integrated milk sample was taken from the common tank, where the milk from lactating cows is mixed. Milk was placed into a solvent-rinsed glass bottle and frozen as soon as possible at -20°C.

In addition to the milk samples from the Andossi plateau, two other commercial milks were analysed. They were bought in Milan in the same time period (summer 2008) and were high-quality labelled milks, meaning they were fresh products produced a few days earlier under high-quality standard conditions as defined by Italian legislation. Therefore, it is highly probable that these milk samples came from the wide agricultural area ("Padana" Plain) near Milan.

Meteorological data

In the study area a specific meteorological monitoring was performed by three meteorological stations specifically set up in the three experimental sites. Soil temperature (-5 cm and -10 cm) and air temperature (1.80 m) were gauged with a time step of 10 minutes. The placement of stations and instruments was carried out following the criteria established by the World Meteorological Organisation (WMO, 1996). Data collection started on June 28th. However, a nearby meteorological station, located approximately 5 km from the sampling sites, provided soil and air temperature data for the missing period. Because this latter station is nearly 100 m higher, a linear correlation model between the hourly mean temperatures of the two sites from June 28th to November 1st (R^2=0.94) was developed to obtain the missing air-temperature data. These latter data were then used to calculate the soil temperature for the missing period by applying a linear correlation between the soil temperature and the mean air temperature of two days earlier. This model, developed on data measured daily, is founded on the robust correlation observed for all soils (-5 and -10 cm for the three sites, with R^2 between 0.84 and 0.90). This model was used only for the time interval between the 10th and the 28th of June, because before this period, the soil temperatures were not correlated

with the air ones. Between the snow melt (19th of May) and the time in which the soil temperature reached almost the air temperature level (10th of June), the soil temperatures constantly increase (0.3836 °C day^{-1}) from near 1 °C (the constant temperature under the snow mantle) to near the air temperature. During this period a strong linear correlation between the number of days after the snow melt and the soil temperature was found (R^2=0.9816). These extrapolations permit to complete the meteorological dataset from May to October, in order to cover the complete vegetation sampling period. The daily mean air temperatures of the three stations and a comparison between the north and south daily mean soil temperatures (5 cm depth) are shown in Figures S2 and S3. Daily mean air temperatures were almost identical during the study period in the three sites (North, South and plain), while daily mean soil temperatures greatly diverge during sunny days according to the aspect. Hourly mean soil records (5 and 10 cm depth) for the two opposite aspects (North and South) are shown in Figure S4 for a 10 day interval, as an example. Figure S4 highlights the tendency of the soil temperature at different sites to significantly diverge during sunny days and during daytime (left part of the graph from the 26th of August to the 1st of September) and to re-converge during night time and during rainy days (right part of the graph from the 2nd to the 4th of September), following the effects of the energy balance driven by net radiation.

Analytical procedure

All glass materials used in the analytical procedure and instruments used in the sampling campaigns were previously rinsed with acetone and *n*-hexane (Sigma Aldrich, Steinheim, Germany) to avoid any external source of contamination. Frozen vegetation and milk samples were lyophilised (Instrument Edward 1001) for 24 h at a final temperature of 5 °C, and powdered milk and shattered vegetation were conserved in closed glass pots that had been previously rinsed with acetone and n-hexane.

Around 5 g of the lyophilised vegetation/milk samples was placed in cellulose thimbles (25 x 100 mm, Whatman, England) and then extracted using a Soxhlet apparatus (Falc Instruments, Lurano, Italy) for 12 h using 100 mL of acetone/n-hexane (1:1 v/v). A 10-μL aliquot of *p,p'*–DDE D8 (Dr. Ehrenstrofer, Ausburg, Germany) was added to the thimbles as a recovery standard before extraction to monitor analyte losses. The extract was concentrated in a rotary evaporator (RV 06-LR, IKA, Staufen, Germany) to a volume of 1 mL. Complete gentle evaporation was performed with a nitrogen flux until a constant weight was reached to determine the extracted lipid weight (g lipid/g d.w.). The dry extract was re-suspended in 3 mL of *n*-hexane and subjected to overnight digestion with 6 mL of 95-97% sulphuric acid to oxidise and dehydrate the organic matter. The supernatant was separated from the acid solution, brought to a volume of 1 mL and purified using a

two-layer column of 10 g of Silica gel with a 70-230 mesh (activated overnight at 130 °C and subsequently deactivated with water at 5% w/w) and 10 g of Florisil (activated for 16 h at 650 °C), both purchased from Sigma Aldrich, Steinheim, Germany. Columns were first washed with n-hexane/acetone/dichloromethane (8:1:1 v/v/v), and extracts were then loaded at the top. Elution was first performed with 50 mL of n-hexane and then with 50 mL of n-hexane/dichloromethane (1:1 v/v). A 1-mL aliquot of isooctane was added to the two fractions. The purified extracts were then concentrated to 1 mL using a rotary evaporator and nitrogen flow. All solvents used were from Sigma Aldrich, Steinheim, Germany.

GC-MS-MS analysis

An aliquot of 2 μL of the clean-up extract was injected into a gas chromatograph (Trace GC Ultra, Thermo-Electron, Texas Instruments, USA) equipped with a programmed temperature vaporiser injector (PTV) and coupled to a PolarisQ Ion Trap mass spectrometer that was equipped with an AS 2000 auto sampler (Thermo Electron). The chromatographic separation was performed with an Rtx-5MS capillary column with the following dimensions: 30 m length, 0.25 mm I.D., 0.25 μm film thickness (Restek, Bellafonte, PA, USA). The PCB congeners 18, 28+31, 52, 44, 101, 149, 118, 153, 138, 180, 170 and 194 were determined by EI MS/MS-SIM mode. The chromatographic and mass spectrometer conditions used for the PCB quantification were the same as those reported in Tremolada et al., 2009.

Quality assurance, quality control and limit of quantification of the analyses

Samples and blanks (one for 3 samples) were spiked with the recovery standard *p,p'* –DDE D8. All recoveries were over 85%. All blanks followed the same analytical procedure than samples, and no peaks above the quantification limit were found. The limits of quantifications (LOQ) ranged between 0.001 ng g^{-1} d.w. and 0.005 ng g^{-1} d.w., depending on the congener. Analytical variability, evaluated on replicate samples, was below 20%.

Statistical analysis

Statistical analysis was performed on the data using the parametric test (t-test) and general linear model (GLM) after the evaluation of the normal distribution of the data by the Kolomogorov-Smirnov test. Normal distribution can be assumed for all variables by the Kolomogorov-Smirnov test (P well above 0.05 for all variables). SPSS Version 17.0 software was used to perform all statistical analyses.

Model description

The mathematical model describing the PCB mobility among the soil-air-plant system is based on a three compartment system in which two compartments, soil and plant, are closed while atmosphere is open. The PCB mobility was described by a system of differential equations like:

$$\frac{dS}{dt} = k_{as} A - k_{sa} \Delta S \quad (1)$$

$$\frac{dP}{dt} = k_{ap}(A + dS) - k_{pa} \Delta P \quad (2)$$

Where ΔS is the mass of PCB in soil exceeding the equilibrium with the atmospheric concentration A at the local temperature, in the same way ΔP is the mass of PCB in the plant biomass exceeding equilibrium. The coefficients k_{as}, k_{sa}, k_{ap} and k_{pa} express transfer velocities between different compartments (namely: air to soil, soil to air, air to plant, plant to air).

ΔS and ΔP are defined as:

$$\Delta S(t) = S_{t-1} - K_{sa(t)} A \quad (2)$$

$$\Delta P(t) = P_{t-1} - K_{pa(t)} A \quad (3)$$

Where $K_{sa(t)}$ and $K_{pa(t)}$ are the time-dependent soil-air and plant air partition coefficients, defined and calculated as in Daly et al. (2007) and in Kömp and McLachlan (2000) for the soil-air and the plant-air partition coefficients, respectively. Physical chemical properties reported in Li et al. (2003) were used. These time-dependent coefficients were calculated for each time according to the temperature by the use of the Clausius-Clapeyron equation and the internal energy of octanol-air phase transfer (ΔU_{oa}).

Equations (3) and (4), in their initial state, take into account the PCB concentrations within soil and plant at time 0 ($S_{t=0}$ and $P_{t=0}$, respectively). The plant biomass is considered to have a negligible PCB content at the beginning of the vegetating season, due both to the small biomass present and to the relatively short age of the same biomass; therefore $P_{t=0}= 0$. The initial PCB concentration in soil is considered to be near to equilibrium with the atmosphere (as defined by K_{sa}); therefore initial values of $S_{t=0}$ have been chosen in the order of 0.9 $ng \cdot g^{-1}$. As the simulation starts well before the sampling dates, slightly higher or smaller concentrations do not change the ODE system trajectory as the system converges to the values defined by K. As such atmospheric concentrations are very small compared to plant's and soil's, otherwise the system becomes numerically unstable.

The soil to air transfer is described by Equation 1 where the air to soil kinetic is linear and soil to air is exponential. The difference in the kinetic is based on the consideration that PCB emission from the soil depletes soil reserve of PCB, thus emission must decrease at a rate proportional to concentration decrease. The air to soil kinetic is linear as the atmosphere is considered to have, at the mass scale of the study, an almost infinite mass; thus atmosphere will be never depleted of PCB.

Atmosphere to plant kinetic follows a similar path, however it should be noted that the uptake of PCB from vegetation is function of two components: atmospheric concentration and net soil loss. In practice, plant surface will adsorb PCBs with at a velocity k_{ap} proportional to the atmospheric concentration plus the net soil loss of PCB. The coefficient k_{ap} can be considered as the product of two sub-coefficients k_{pad} representing plant adsorbing efficiency (function of plant surface, shape and composition) and k_{diff} expressing the effect of diffusion on the vertical concentration of PCB. As concentration gradients were not measured in this study, the two k cannot be estimated singularly, but their combined effect can be modeled by fitting the coefficient of the differential equations system to empirical data.

The differential equations system can be solved with numerical methods like the Runge-Kutta algorithm which has been applied in this study. Variations of partition coefficients due K to changes in temperature were included as forcing functions in the model as has been the growth rate of vegetation.

References

Daly, G.L., Lei, Y.D., Castillo, L.E., Muir, D.C.G., Wania, F., 2007. Polycyclic aromatic hydrocarbons in Costa Rican air and soil: a tropical/temperate comparison. Atmospheric Environment 41, 7339-7350.

Kömp, P., McLachlan, M.L., 2000. The kinetics and reversibility of the partitioning of polychlorinated biphenyls between air and ryegrass. The Science of the Total Environment 250, 63-71.

Li, N., Wania, F., Lei, Y.D., Daly, G.L., 2003. A comprehensive and critical compilation, evaluation, and selection of physical-chemical property data for selected polychlorinated biphenyls. Journal of Physical and Chemical Reference Data 32, 1545-1590.

SISS – Società Italiana della Scienze del Suolo, 2007. Escursione scientifica del convegno nazionale: la scienza del suolo nei territori montani e collinari. Milano-Chiavenna: 9-13 July 2007.

WMO, 1996. Guide to meteorological instruments and methods of observation (WMO guide n. 8), Sixth edition, loose-leaf; updated by supplements when necessary, Geneva, CH.

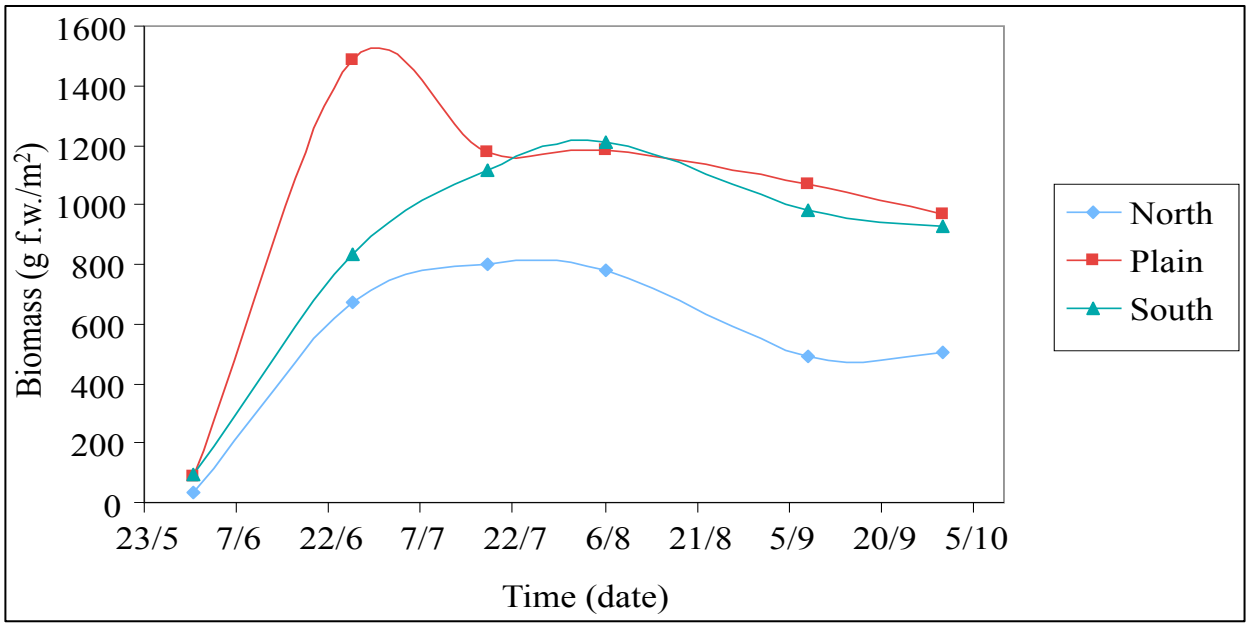

Figure S1: Growth curves of the herbaceous vegetation during the year 2008 at the three sampling sites (measured values).

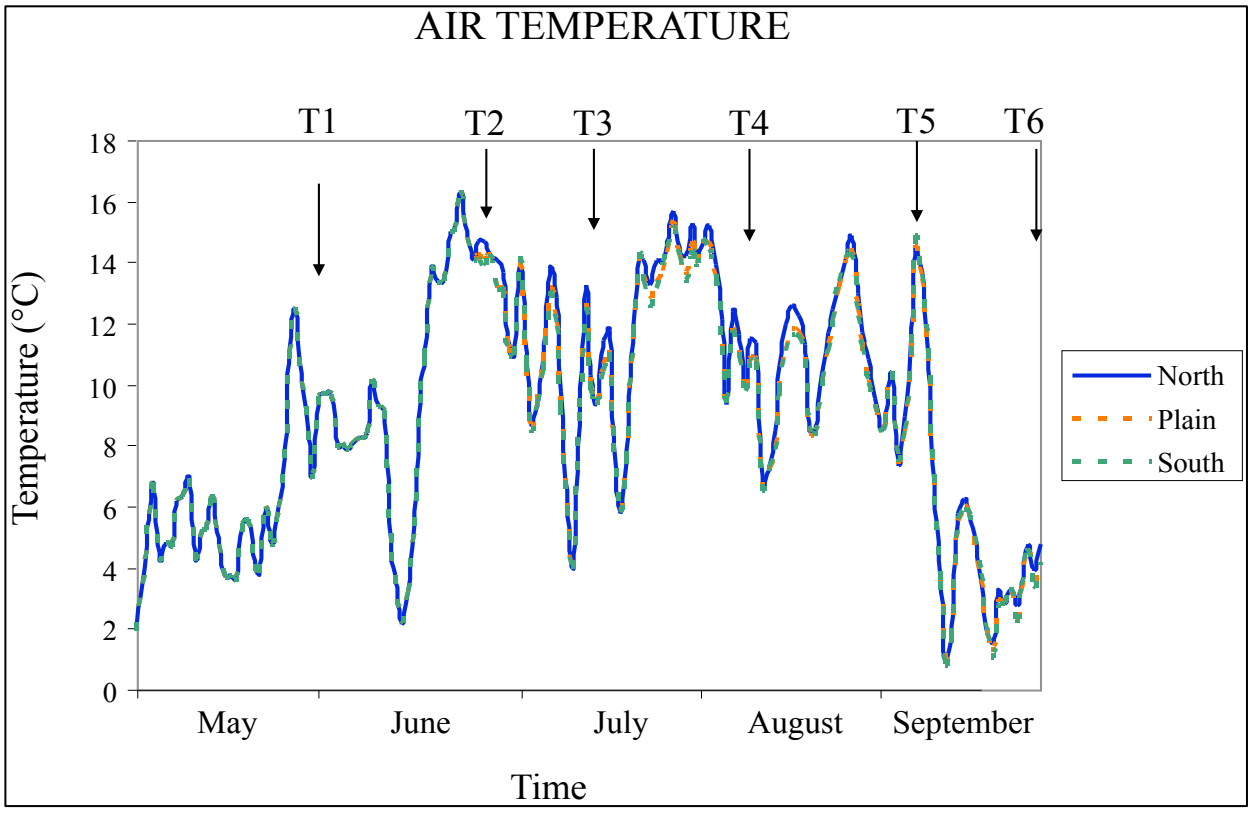

Figure S2: Daily mean air temperature in the three sites during the sampling period (May-October). Sampling times are indicated by arrows and by the same symbols used in the SI paragraph 'Sampling sites and sampling modalities', where the exact dates are reported.

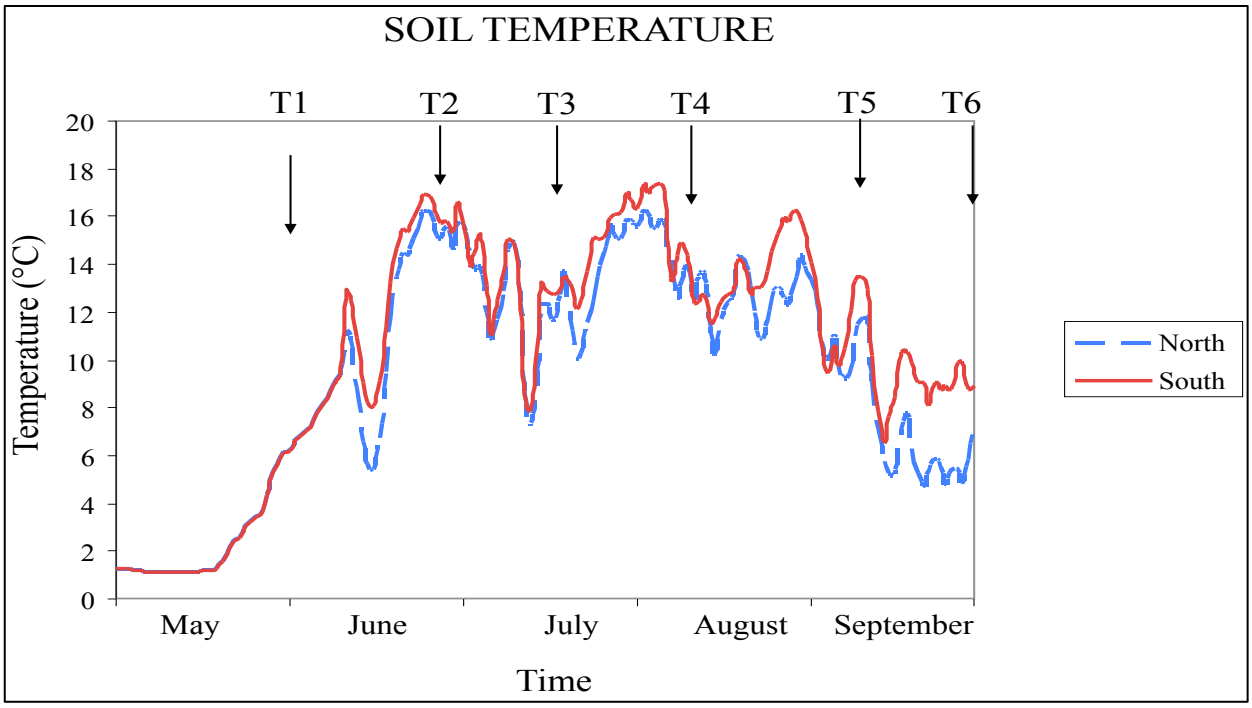

Figure S3: Daily mean soil temperature (5 cm depth) in the two opposite sites (North and South) during the sampling period (May-October). Sampling times are indicated by arrows and by the same symbols used in the SI paragraph 'Sampling sites and sampling modalities', where the exact dates are reported.

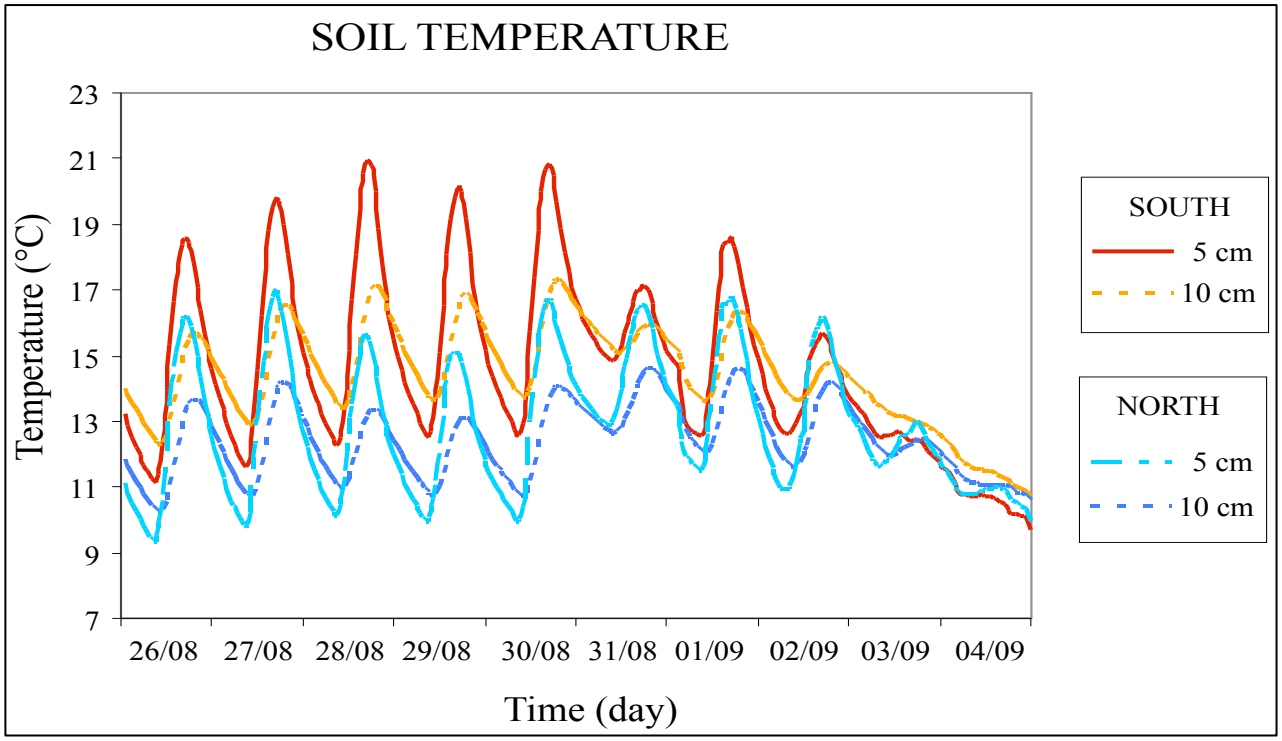

Figure S4: Hourly mean soil temperatures (5 and 10 cm depth) for the two opposite aspects (North and South) from the 26th of August to the 4th of September.

Chapter VI

Parolini, M., Guazzoni, N., Binelli, A., Tremolada, P., 2012. Polybrominated Diphenyl Ether Contamination in Soil, Vegetation and Cow Milk From a High-Mountain Pasture in the Italian Alps. Archives of environmental contamination and toxicology 63, 24−44

Arch Environ Contam Toxicol (2012) 63:29–44
DOI 10.1007/s00244-012-9753-8

Polybrominated Diphenyl Ether Contamination in Soil, Vegetation, and Cow Milk From a High-Mountain Pasture in the Italian Alps

Marco Parolini · Niccolò Guazzoni · Andrea Binelli · Paolo Tremolada

Received: 2 November 2011 / Accepted: 13 February 2012 / Published online: 9 March 2012

Abstract This study investigates contamination by 13 polybrominated diphenyl ether (PBDE) congeners in a high-mountain pasture located in the Italian Alps. The trend of PBDE contamination in three soil layers was investigated by a spring–summer sampling period to understand the importance of different environmental variables, such as seasonality, topographical aspect, and soil features. We also evaluated PBDE accumulation in grasses covering the plateau, and because the study area has been used for a pasture for a long time, we measured PBDE levels in milk from grazing cows. Overall, we found moderate PBDE contamination in Andossi soils, with differences depending on the layer, mountain side, and organic matter content. The vegetation of the plateau had greater PBDE concentrations than the soils and showed a grass/soil accumulation ratio between 2 and 12, indicating that deposition from the atmosphere is actually the dominant process in this area. Last, PBDE concentrations in milk followed similar seasonal trends as the vegetation but showed variations in congener abundance in agreement with the biotransformation susceptibility, absorption efficiency, and residence time of different BDEs in dairy cattle.

Polybrominated diphenyl ethers (PBDEs) constitute an important group of brominated flame retardants used as noncovalent additives in different kinds of resins, polymers, and textiles and in circuit boards, electrical components, panels, and coatings. Their use in Europe has increased during the last 30 years, with global annual production estimated at 436,800 tons in 2005 (CEFIC 2006). Three technical PBDE products have been or are still being used as additive flame retardants: penta-BDE, octa-BDE, and deca-BDE. Of global commercial BDE use, approximately 15% was penta-BDE, a mixture containing highly bioaccumulative compounds, whereas the major demand (approximately 80%) was for deca-BDE (Darnerud et al. 2001). Penta-BDE contains primarily tetra-BDE (BDE-47), penta-BDE (BDE-99 and -100), and hexa-BDE (BDE-153 and -154) congeners; octa-BDE contains primarily a hepta-BDE (BDE-183) plus hexa-BDES (BDE-153, -154) and octa-BDEs, whereas deca-BDE consists primarily of the fully brominated BDE-209 (La Guardia et al. 2006). Because flame retardant additives are not chemically bound to the products, PBDEs may be released into the environment during the production, use and disposal of PBDE-containing materials (de Wit 2002); high levels of several congeners have been found in ecosystems worldwide. These chemicals share similar molecular structures and physicochemical chemical-physical and toxicological features as other persistent organic pollutants (POPs; Watanabe and Sakai 2003): PBDEs are toxic and bioaccumulative and can undergo long-range atmospheric transport from polluted environments to pristine areas far from any anthropogenic activities. Of these bases, penta- and octa-BDE mixtures were banned from commercial products from European Union market (EU Decision 2002/95/EC) and from North America in 2004 because of their persistence and potential environmental and human health risks (Hale et al. 2006), although deca-BDE production is still allowed and used in most countries. However, according to the EU Directive restricting the use of

Electronic supplementary material The online version of this article (doi:10.1007/s00244-012-9753-8) contains supplementary material, which is available to authorized users.

M. Parolini (✉) · N. Guazzoni · A. Binelli · P. Tremolada
Department of Biology, University of Milan, 20133 Milan, Italy
e-mail: marco.parolini@unimi.it

certain hazardous substances in electrical and electronic equipment (RoHS Directive), manufacturers must substitute other compounds for PBBs and PBDEs in new equipment. Deca-BDE was exempted from this directive, but this exemption was challenged in the EU courts and recently overturned (April 1, 2008); thus the use of deca-BDE in the EU has been banned since July 1, 2008 (European Court of Justice 2008). Despite these regulations, PBDEs are continuously found in the environment, including remote regions that are prone to enrich lipophilic chemicals through global fractionation and cold condensation processes. Several studies in high-latitude polar regions have shown the widespread distribution of these chemicals in dissimilar matrices, both abiotic and biotic (de Wit et al. 2010). Similarly, high-altitude mountainous ecosystems have been considered the last pristine and ''untouched'' environments on our globe, although they have been found to be affected by the transport of POPs (Tremolada et al. 2009a, 2009b; Guazzoni et al. 2011). Moreover, recent studies have shown the PBDE contamination in soil from mountainous areas (Wang et al. 2009). The aim of this study was to investigate the levels of 13 BDE congeners in different matrices from the Andossi Plateau, a high-mountain pasture located in the Italian Alps. Previous studies have found moderate concentrations of different POPs in this area, including organochlorine compounds (DDTs, hexachlorobenzene, halogenated cyclic hydrocarbons, and polychlorinated biphenyls (PCBs; Tremolada et al. 2009a) and polycyclic aromatic hydrocarbons (PAHs; Tremolada et al. 2009b). However, to date, no data are available on the occurrence of PBDE in environmental samples from the Alps, although they have been detected in other European mountainous regions (Blais et al. 2006) and at low altitudes in Italy (Guzzella et al. 2008; Parolini et al. 2011). We investigated the trend of PBDE levels in three different soil layers during the spring–summer campaign to understand the importance of seasonality, topographical aspects, and soil features for contamination of this alpine environment. In addition, because plants are considered the major vectors of POPs in terrestrial food chains (McLachlan 1993) and that the Andossi plateau has been used as pasture for a long time, we evaluated PBDE levels in grasses that cover the plateau and in milk of cows grazing in this area. Our attention was mainly focused on common congeners composing the penta- and octa-formulations, which are considered to undergo long-range atmospheric transport (LRAT) and are considered to be the more hazardous PBDEs to the biocoenosis (Birnbaum and Staska 2004). Moreover, they are also on the proposed list of new chemicals to be included in the Stockholm Convention and the POPs Protocol to the United Nations ECE Convention on Long-Range Transboundary Air Pollution (de Wit et al. 2010). In this study, contamination by BDE-209 was not investigated because it is not considered highly susceptible to LRAT (Czub et al. 2008; Vonderheide et al. 2008) and because of its low volatility and high hydrophobicity (Tittlemier et al. 2002; Braekevelt et al. 2003). In fact, earlier studies have not detected BDE-209 in any analyzed soil samples from the Tibetan plateau (Wang et al. 2009).

Materials and Methods

Study Area and Sampling Method

Pasture samples (soil, vegetation, and milk) were taken from the Andossi plateau near Splugen Pass in the central Italian Alps during 2008 (for detailed information, see Guazzoni et al. 2011). Meteorological features of this area have been well documented and reported in Guazzoni et al. (2011). Soils were collected at approximately 1930 m a.s.l. at three closely spaced sites (approximately 100 m apart) with different aspects (north-, plain-, and south-facing). The northern and southern aspects in this small area are formed by small hills approximately 100 m high and 200 m long that are irregularly located on the plateau. Intermediate conditions between the southern and northern aspects were obtained on the flat portion of the plateau between the southern and northern sites. The sampling sites were fenced (5 × 5 m fences) to prevent the entry of cows grazing on the plateau. Vegetation of the Andossi plateau reflects the cows' grazing pressure and local variability in pedo-climatic conditions, which is determined by substrate typology, slope, and solar-radiation exposure. The main vegetational typology of this subalpine area is consistent with pure or mixed nardetum, principally on the northern aspects, although other associations are often found (especially in the plain site and on the south aspect), such as *Seslerieto-Semperviretum*, *Poetum*, and *Rhodoro-Vaccinietum* (SISS 2007). Samples were collected on six dates to cover the entire period during which the pasture is free from snow mantle (T1 = June 1, 2008; T2 = June 27, 2008; T3 = July 19, 2008; T4 = August 7, 2008; T5 September 9, 2008; and T6 = October 1, 2008). Within every fence, vegetation (grass) was cut and wrapped in clean tinfoil. Three cubes (edge 10 cm) of soil were taken and separated into three layers: the O layer (0–1 cm depth), which is rich in organic matter (OM); the A1 layer (1–4 cm depth); and the A2 layer (4–7 cm depth). Samples from each layer were homogenized by manual mixing to decrease local variability; wrapped in acetone-washed tinfoil; enclosed in a plastic bag; and labeled with the date (T1–T6), layer (O, A1, and A2) and mountain side (north, plain, and south). Vegetation litter and soil samples were quickly transported to the laboratory in cold bags and

stored at 20°C until analyses were performed. In addition, milk samples were collected during the pasture season, which at that altitude begins in mid-June and ends in mid-September. Therefore, there were only four milk sampling periods (T2–T5). One integrated milk sample was collected for each date because there was no relationship between any single cow and our experimental sites on the plateau because lactating cows graze over a wide area characterized by all of the different conditions of the plateau.

Reagents and Standards

All solvents used were pesticide grade. Florisil (100–200 mesh) and anhydrous sodium sulfate were obtained from Fluka (Steinheim, Germany). The silica gel for column chromatography (70–230 mesh) was supplied by Sigma-Aldrich (Steinheim, Germany). A BDE+ commonly occurring congener mixture (PBDE-COC) was purchased from AccuStandard (New Haven, CT). The 13 BDE congeners investigated in this study were as follows: BDE-17, -28, -71, -47, -66, -100, -99, -85, -154, -153, -138, -183, and -190. The total PBDE (Σ_{13} PBDEs) concentrations in samples were calculated as the sum of these congeners. Two $^{13}C_{12}$-labeled mixtures (PBDE-MXA and PDE-MXB) composed of $^{13}C_{12}$-labeled BDE-47, -99, and -153 and BDE-28, -154, and -183, respectively, were purchased from AccuStandard and used as internal surrogate standards.

Analytical Procedures

Before chemical analyses, all samples (soil, vegetation, and milk) were lyophilized, and each soil sample was analyzed for organic carbon (C) content by an elemental analyzer (Flash EA 1112 NC soil; ThermoFisher, Waltham, MA). The OM content was estimated from organic C content using a 1.724 multiplier constant as indicated in Nelson and Sommers (1996). Dry soil (approximately 20 g), vegetation (approximately 3 g), and milk (approximately 2 g) samples were spiked with 2 ng of two $^{13}C_{12}$-labeled recovery standard mixtures (PBDE-MXA and -MXB) before the 12 h extraction process. Extraction was performed using 100 mL of acetone/*n*-hexane (1:1 v/v) mixture in a cold Soxhlet apparatus (FALC Instruments, Lurano, Italy). Vegetation and milk extracts were dried in a rotating evaporator with nitrogen flow for the gravimetric determination of lipids. Clean-up was performed using a multilayer column (40 × 1.5 cm i.d.) made of 10 g of partially deactivated silica gel (activated overnight at 130°C, then deactivated with water [5% w/w]), 10 g of Florisil (activated for 16 h at 650°C), and 1 g of anhydrous sodium sulfate. The column was washed with 100 mL *n*-hexane/acetone/dichloromethane mixture (8:1:1 v/v). Two elutions were used to recover the analytes: The first contained 50 mL of *n*-hexane, and the second contained 50 mL of *n*-hexane/dichloromethane mixture (1:1 v/v). Isooctane (1 mL) was added to the final sample, which was subsequently concentrated by a rotary evaporator and then under a gentle nitrogen flow to produce a final volume of 1 mL. Amber glassware was used throughout the analytical procedure to avoid ultraviolet degradation of the PBDEs.

Instrumental Analysis

A 2 μL aliquot of each sample was injected twice into a gas chromatograph (TRACE GC; Thermo Electron, TX) equipped with a programmed temperature vaporizer injector and coupled with a PolarisQ Ion Trap mass spectrometer (Thermo Electron), using an AS autosampler (Thermo Electron). All of the analytes were separated by a Rtx-5MS (Restek, Bellefonte, PA) capillary column (30 m length, 0.25-mm i.d., 0.25 μm df) under the following conditions specified by Binelli et al. (2007): carrier gas helium at 1.2 mL/min; injection pressure of 120 kPa; transfer pressure of 240 kPa; injector temperature starting at 70°C and maintained for 1.2 min, then ramped to 280°C (held 1.2 min) at 14°C/s; initial oven temperature set at 70°C (held 1 min), then ramped to 220°C at 30°C/min (held 1 min), and finally to 290°C at 4°C/min (held 20 min). The samples were analyzed using tandem mass spectrometry under the following instrumental conditions: the electric ionization mode with standard electron energy of 70 eV was used, and the transfer line was maintained at 280°C, the damping gas at 2 mL/min, and the ion source at 260°C. Silanized glass liners (1 mL volume) were used. Quantitative analyses were performed with Excalibur software (Thermo Electron) and by external multilevel calibration curves ($r^2 > 0.97$).

Quality Control

A procedural blank was run in parallel with every batch of four samples using anhydrous sodium sulfate. No BDE congeners were detected in the blanks. The samples and blanks were spiked with 2 ng of internal $^{13}C_{12}$-labeled recovery standards (PBDE-MXA and -MXB) before the extraction procedures. Recoveries >80% were accepted and were (mean ± SD) as follows: 98 ± 3% for BDE-47, 97 ± 5% for BDE-99, 87 ± 7% for BDE-153, 90 ± 3% for BDE-28, 85 ± 5% for BDE-154, and 82 ± 4% for BDE-183. Limits of detection for each brominated class were quantified by the signal-to-noise ratio (3:1) and were 1 ng kg^{-1} dry weight for soil and vegetation and 0.8 ng kg^{-1} dry weight for milk.

Statistical Analysis

Data normality and homoscedasticity were tested by Kolmogorov–Smirnov test and Levene's test, respectively. A generalized linear model (GLM), followed by Bonferroni post hoc test, was used to evaluate the differences in PBDE contamination between the layers, slope aspects, and sampling dates. Statistical analyses were performed with Statistica 7.0 software.

Results and Discussion

PBDEs in Soils

Levels of PBDE in soil strata (O, A1, and A2 layers) from the Andossi plateau are listed in Tables 1, 2, and 3, respectively. Mean concentrations ± SD of the $\sum_{13}$PBDEs in the three layers were 1.55 ± 1.1, 0.72 ± 0.48, and 0.43 ± 0.27 ng/g dry weight (dw) for the O, A1, and A2 layers, respectively. $\sum_{13}$PBDE variability in each layer was quite similar, ranging from 0.310 to 3.853, 0.086 to 1.743, and 0.149 to 1.063 ng/g dw for the O, A1 and A2 layers, respectively. Mean $\sum_{13}$PBDE soil concentration (0.71 ± 0.83 ng/g dw) was in the middle of the range of the European background soils (0.065–12 ng/g dw; Hassanin et al. 2004), suggesting that the observed contamination is highly affected by the proximity of several European countries whose urban settlements represent consistent source areas. In fact, PBDE soil contamination of the Andossi plateau was greater than that found in more remote regions, such as the Russian Arctic (0.16–0.23 ng/g dw; de Wit et al. 2006) and the Tibetan Plateau (0.0043–0.0349 ng/g dw; Wang et al. 2009). Overall, the PBDE pattern of contamination was similar for each soil layer. By grouping single BDEs according to their bromination degree, tetra- and penta-BDEs were the main congeners of the fingerprint, accounting for approximately 95% (O) and 93% (A1 and A2) of the $\sum_{13}$PBDEs. Although lighter (tri-) and heavier (hexa- and hepta-) BDEs were found in all soil samples during the whole sampling period, they accounted for only 5–7% of the fingerprint. This is likely because lighter congeners could be more susceptible to frequent volatilization processes, which prevent their accumulation in soils. In contrast, heavier congeners have low volatility, which makes them less prone to undergo LRAT (Wang et al. 2009). Among the detected compounds (Fig. 1), BDE-99 was the main congener, accounting for >40% of the $\sum_{13}$PBDE (in detail: 43% of O, 42% of A1, and 51% of A2), followed by BDE-47 (37–43%) and BDE-100 (8–22%). The contamination pattern of Andossi soils, characterized by low-brominated congeners, was similar to that of the major components of the commercial penta-BDE product Bromkal 70-5DE (Sjödin et al. 1998), indicating that the penta- formulation could be the main BDE source. Considering the accounting of single congeners in the technical mixture, BDE-47 was expected to be the main congener in soils, whereas it was less abundant than BDE-99 in most of samples. BDE-47 could be degraded in soil relatively more rapidly than other BDEs, enhancing the relative proportion of BDE-99 (Hassanin et al. 2005). The presence of BDE-183, the marker congener of the octa-BDE formulation (Song et al. 2004), indicated a possible additional input of this mixture to the study area. However, the prediction of the contamination pattern is generally difficult for PBDEs because the ratio among congeners in environmental matrices can vary both according to the variability in the mixtures coming from source areas and the behavior of individual compounds in the ecosystem. Moreover, some BDEs can undergo debromination processes that transform the heavier congeners to lighter ones, which can also be degraded (Wang et al. 2009), thus complicating the characterization of the pollution pattern. Notwithstanding, no notable differences in the PBDE fingerprint were found between different layers or between mountain sides Table 2.

Effect of Layer, Mountain Side, and OM Content on PBDE Levels in Soils

Soil layer had a notable effect on $\sum_{13}$PBDEs in this high-mountain pasture ($F = 28.951$; $p < 0.01$). Overall, the average concentrations of brominated compounds in the O layer were two- to four-fold greater than those measured in A1 and A2 layers, respectively. Another important factor influencing the accumulation of PBDEs in soils is the mountain side (northern *vs*. southern). In north-facing slope soils, PBDE levels in the O layer were 2.2- and 3.8-fold greater than those measured in the A1 and A2 levels, respectively, whereas smaller differences were found in plain (2.7- and 3.2-fold greater, respectively) and, above all, in southern soils (1.6- and 2.5-fold greater, respectively). In contrast, the PBDE concentrations in the A1 and A2 layers showed lower differences (average 1.6 (range 1.2–1.8)) between north- and south-facing soils. The effect of mountain side on PBDE concentrations in the O, A1, and A2 layers was tested by GLM. There was a significant ($p < 0.01$) influence of mountain side in both the O and the A1 layers, whereas no differences ($p > 0.05$) were found in PBDE levels in the A2 layer among the northern, plain, and southern side. By considering dry weight–normalized values, the most contaminated soils were those exposed on the northern side of the mountain, which showed PBDE values up to fourfold greater than the southern ones. The contamination of plain soils was intermediate between the northern and the southern ones. Overall, $\sum_{13}$PBDEs in the

Table 1 Levels of 13 BDE congeners in the A1 soil layer (ng/g dw) from the Andossi plateau pasture measured at sampling periods (T1–T6) at three mountain sides (north, plain, and south)

O layer (ng/g dry weight)	T1			T2			T3			T4			T5			T6		
BDEs	North	Plain	South	North	Plain	South	North	Plain	South	North	Plain	South	North	Plain	South	North	Plain	South
BDE-17	0.009	0.023	0.001	0.009	Missing	0.003	0.001	0.009	<DL	0.001	0.003	0.001	0.007	0.007	0.002	0.010	0.001	0.001
BDE-28	0.041	0.032	0.015	0.015		0.008	0.011	0.008	0.004	0.004	0.002	0.003	0.031	0.022	0.016	0.008	0.006	0.002
BDE-71	<DL	<DL	<DL	<DL		<DL	<DL	<DL	<DL	<DL	<DL	<DL	<DL	<DL	<DL	<DL	<DL	<DL
BDE-47	1.701	2.480	1.104	1.275		0.341	0.279	0.277	0.235	0.425	0.356	0.295	0.444	0.790	0.384	0.259	0.113	0.116
BDE-66	<DL	<DL	<DL	<DL		<DL	<DL	<DL	<DL	<DL	<DL	<DL	<DL	<DL	<DL	<DL	<DL	<DL
BDE-100	0.731	0.691	0.175	1.583		0.055	0.321	0.304	0.169	0.465	0.645	0.105	0.045	0.000	0.075	<DL	<DL	<DL
BDE-99	0.986	0.280	0.661	0.932		0.537	0.372	0.548	0.380	0.168	0.595	0.372	0.545	0.509	0.283	0.879	0.981	0.148
BDE-85	<DL	<DL	<DL	<DL		<DL	<DL	<DL	<DL	<DL	<DL	<DL	<DL	<DL	<DL	<DL	<DL	<DL
BDE-154	0.034	0.011	0.013	0.005		0.002	0.005	0.015	0.001	0.004	0.005	0.002	0.040	0.009	0.012	0.017	0.034	0.010
BDE-153	0.003	0.027	0.012	0.007		0.002	0.003	0.006	0.002	0.005	0.007	0.001	0.005	0.005	0.001	0.024	0.009	0.004
BDE-138	0.006	0.002	0.003	0.011		0.006	0.002	0.008		0.003	0.004	0.002	0.003	0.023	0.003	0.010	0.017	0.014
BDE-183	0.007	0.018	0.002	0.008		0.003	0.004	0.003	0.001	0.006	0.006	0.005	0.006	0.008	0.003	0.030	0.009	0.012
BDE-190	0.012	0.009	0.018	0.007		0.003	0.002	0.013		0.006	0.005	0.004	0.011	0.006	0.009	0.002	0.011	0.001
Σ_{13}PBDEs	3.531	3.571	2.004	3.853		0.960	0.999	1.191	0.792	1.088	1.627	0.790	1.138	1.380	0.789	1.240	1.180	0.310

<*DL* lower than the detection limit

Table 2 Levels of 13 BDE congeners in the A2 soil layer (ng/g dw) from the Andossi plateau pasture measured at sampling periods (T1–T6) at three mountain sides (north, plain, and south)

A1 layer (ng/g dry weight)	T1			T2			T3			T4			T5			T6		
	North	Plain	South	North	Plain	South	North	Plain	South	North	Plain	South	North	Plain	South	North	Plain	South
BDE-17	0.007	0.004	0.007	0.001	0.001	0.001	<DL	0.001	0.002	0.002	<DL	0.002	0.001	0.001	0.001	0.001	0.001	0.002
BDE-28	0.020	0.018	0.018	0.008	0.003	0.002	0.002	0.001	0.003	0.003	0.003	0.004	0.007	0.004	0.002	0.006	0.001	0.004
BDE-71	<DL	<DL	<DL	<DL	<DL	<DL	<DL	<DL	<DL	<DL	<DL	<DL	<DL	<DL	<DL	<DL	<DL	<DL
BDE-47	1.056	0.792	0.827	0.142	0.025	0.074	0.090	0.138	0.107	0.231	0.088	0.167	0.813	0.135	0.414	0.087	0.050	0.238
BDE-66	<DL	<DL	<DL	<DL	<DL	<DL	<DL	<DL	<DL	<DL	<DL	<DL	<DL	<DL	<DL	<DL	<DL	<DL
BDE-100	0.203	<DL	0.182	0.274	0.024	0.150	0.193	0.360	0.076	0.078	0.073	0.048	0.038	0.036	0.029	<DL	<DL	<DL
BDE-99	0.303	0.875	0.307	0.440	0.023	0.292	0.377	0.297	0.199	0.094	0.083	0.082	0.273	0.231	0.326	0.473	0.231	0.104
BDE-85	<DL	<DL	<DL	<DL	<DL	<DL	<DL	<DL	<DL	<DL	<DL	<DL	<DL	<DL	<DL	<DL	<DL	<DL
BDE-154	0.005	0.016	0.011	0.004	0.003	0.001	0.004	0.006	0.009	0.002	0.003	0.001	0.004	0.013	0.007	0.007	0.017	0.004
BDE-153	0.005	0.014	0.005	0.002	0.002	0.002	0.001	0.002	<DL	0.002	0.002	0.001	0.004	0.015	0.005	0.014	0.006	0.008
BDE-138	0.003	0.004	0.003	0.001	0.001	0.002	0.001	0.007	0.005	0.002	0.005	0.002	0.007	0.013	0.016	0.005	0.009	0.011
BDE-183	0.005	0.012	0.005	0.005	0.003	0.004	0.006	0.001	<DL	0.001	0.002	0.001	0.002	0.006	0.005	0.006	0.002	0.006
BDE-190	0.023	0.008	0.005	0.005	0.001	0.004	0.009	0.002	0.004	0.002	0.007	0.004	0.011	0.013	0.003	0.001	0.002	0.012
Σ_{13}PBDEs	1.630	1.743	1.370	0.882	0.086	0.532	0.684	0.815	0.405	0.417	0.266	0.312	1.160	0.467	0.808	0.600	0.317	0.389

<DL lower than the detection limit

Table 3 Levels of 13 BDE congeners in the O soil layer (ng/g dw) from the Andossi plateau pasture measured at six sampling periods (T1–T6) at three mountain sides (north, plain, and south)

A2 layer (ng/g dry weight)	T1			T2			T3			T4			T5			T6		
BDEs	North	Plain	South	North	Plain	South	North	Plain	South	North	Plain	South	North	Plain	South	North	Plain	South
BDE-17	0.006	0.001	Missing	<DL	<DL	0.001	0.001	0.001	<DL	<DL	0.002	<DL	0.002	0.001	0.001	0.040	0.001	<DL
BDE-28	0.018	0.016		0.001	0.001	0.000	0.003	0.002	0.003	0.001	0.003	0.001	0.006	0.004	0.005	0.002	0.004	0.005
BDE-71	<DL	<DL		<DL	<DL	<DL	<DL	<DL	<DL	<DL	<DL	<DL	<DL	<DL	<DL	<DL	<DL	<DL
BDE-47	0.759	0.646		0.128	0.044	0.037	0.067	0.071	0.151	0.147	0.125	0.199	0.120	0.098	0.142	0.136	0.123	0.057
BDE-66	<DL	<DL		<DL	<DL	<DL	<DL	<DL	<DL	<DL	<DL	<DL	<DL	<DL	<DL	<DL	<DL	<DL
BDE-100	0.073	0.141		0.050	0.043	0.038	0.042	0.015	0.018	0.024	0.017	0.000	0.039	0.029	0.033	<DL	<DL	<DL
BDE-99	0.196	0.235		0.360	0.150	0.124	0.136	0.200	0.123	0.095	0.164	0.286	0.367	0.135	0.255	0.130	0.309	0.057
BDE-85	<DL	<DL		<DL	<DL	<DL	<DL	<DL	<DL	<DL	<DL	<DL	<DL	<DL	<DL	<DL	<DL	<DL
BDE-154	0.003	0.012		0.002	0.002	0.001	0.001	0.001	0.001	0.001	0.001	0.003	0.001	0.002	0.008	0.007	0.011	0.004
BDE-153	0.001	0.000		0.003	0.003	0.003	0.002	0.001	0.003	0.001	0.001	0.001	0.001	0.001	0.003	0.011	0.003	0.003
BDE-138	0.001	0.004		0.007	0.002	0.001	0.005	0.004	0.002	0.002	<DL	0.005	0.005	0.013	0.008	0.011	0.002	0.004
BDE-183	0.002	0.003		0.002	0.001	0.007	0.003	0.004	0.002	0.004	0.003	0.008	0.002	0.003	0.005	0.007	0.004	0.002
BDE-190	0.003	0.003		0.001	0.002	0.000	0.009	0.014	0.001	0.004	0.007	0.002	0.013	0.002	0.005	0.007	0.001	0.016
Σ_{13}PBDEs	1.063	1.060		0.553	0.248	0.212	0.268	0.312	0.304	0.278	0.324	0.504	0.554	0.288	0.465	0.349	0.459	0.149

<DL lower than the detection limit

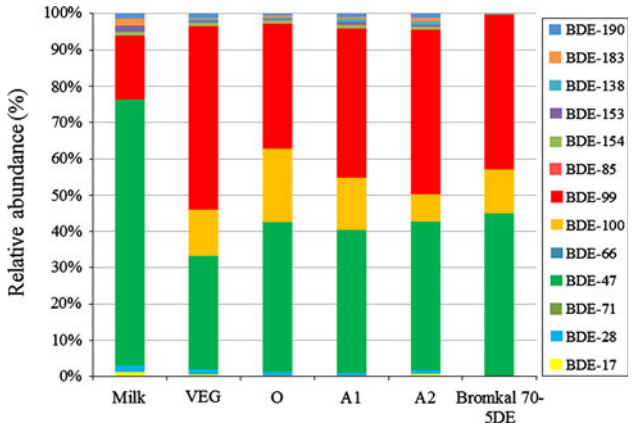

Fig. 1 PBDE patterns of contamination of the soil layers (O, A1, and A2), vegetation (*VEG*), and milk from a pasture on the Andossi plateau

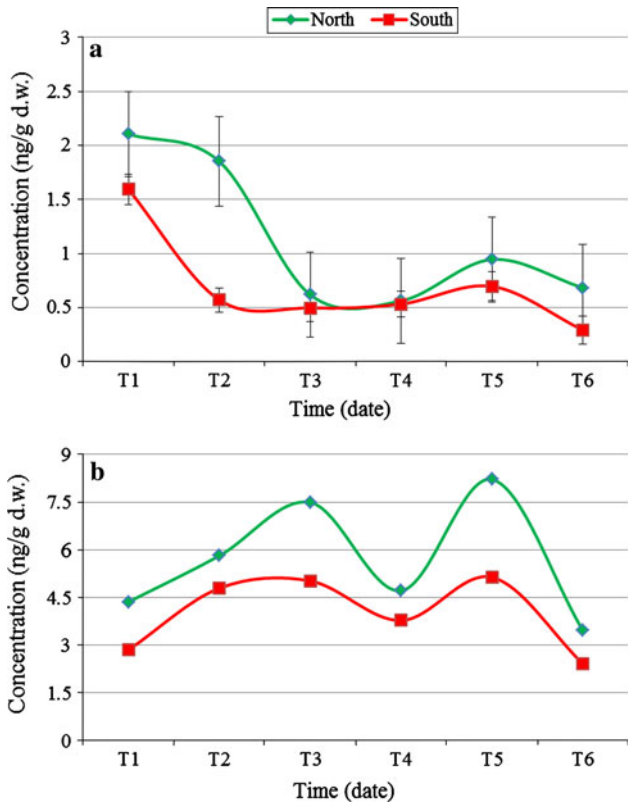

Fig. 2 Seasonal trends in $\sum_{13}$PBDE contamination in the northern and southern soils. **a** Mean of the concentration measured in (**a**) layers O, A1, and A2 (±SD; ng/g dw). **b** grass (mean ± SD; ng/g dw) samples from an Andossi plateau pasture

northern O and A1 layers were, respectively, 2.3 (range 1.3–4.0) and 1.5 (range 1.2–1.7) greater than that measured in the southern ones during the sampling period. A similar trend was found in the same area for chlorinated compounds (Tremolada et al. 2009a) and polycyclic aromatic hydrocarbons (PAHs; Tremolada et al. 2009b). The highest northern vs. southern differences measured in the O layer can be related to the difference in temperature (ΔT) between the two mountain sides, which could lead to different revolatilization rates and different PBDE-retention capabilities. As suggested by Guazzoni et al. (2011), differences in temperature (ΔT north/south [N/S] reaches 4–5°C in superficial soil during sunny days) and humidity (southern-facing soils tend to dry faster) lead to changes in the soil–air partition coefficient (K_{sa}) values between the northern and southern soils and, consequently, in the amount of PBDEs that volatilize back to the atmosphere. Hence, atmospheric variables, mainly temperature, affect PBDE accumulation in soils by changing the K_{sa} values of the different soils (Dalla Valle et al. 2005). K_{sa}, which describes the physical partitioning between the soil and the air, is a temperature-dependent parameter (Hippelein and McLachlan 2000): Low temperatures increase partitioning into the soil, thus increasing K_{sa} values of a compound. As explained by Tremolada et al. (2011), the ratio between the OM–normalized concentrations between two sites having the same air concentration but different temperatures is equal to the ratio between the OM–normalized K_{sa} values referred to those temperatures and to the ratio of the K_{oa} values referred to the same temperatures, considering near equilibrium conditions. Therefore, from temperature-specific K_{oa} values, a theoretical N/S enrichment factor (EF) can be calculated for BDEs. Basing on data of Harner and Shoeib (2002), we calculated K_{oa} values for −1 and 3.9°C (year mean temperatures of the northern and southern sites, respectively) for PBDEs, and from their ratio we obtained the K_{sa} EF of the northern vs. southern side, which ranged between 1.8 and 2.2 for the different congeners (see Supplementary material (Table S1)). As expected, N/S EF calculated for the O layer was the most affected by the temperature gradient between the northern and southern slopes (measured N/S EF for the Σ_{13}PBDEs in O layer was 1.8). Aside from meteorological effects, POP concentrations in soil is also determined by their high affinity to OM content (Meijer et al. 2003; Li et al. 2003). POPs are theoretically present in greater concentrations in soils with a greater percentage of OM, which was identified as a key variable in the contamination status of hydrophobic compounds (Bucheli et al. 2004; Sweetman et al. 2005). In the present study, OM content varied among the layers but also depended on mountain side. The OM content of the northern side soils was greater in the O layer and lower in the A2 layer, whereas there was no significant ($p > 0.05$) differences between the northern and southern OM content in the A1 layer. Similar to other pollutants (Tremolada et al. 2009a, 2009b), there was an overall significant ($p < 0.05$) correlation between soil OM and Σ_{13}PBDEs. To avoid the effects of variability in OM for the same area, altitude, and sampling time, we calculated the

Table 4 Levels of 13 BDE congeners in vegetation (ng/g dw) from the Andossi plateau pasture measured at six sampling periods (T1–T6) at three mountain sides (north, plain, and south)

Vegetation (ng/g dry weight)	T1			T2			T3			T4			T5			T6		
BDEs	North	Plain	South	North	Plain	South	North	Plain	South	North	Plain	South	North	Plain	South	North	Plain	South
BDE-17	0.020	0.002	0.033	0.015	0.022	0.017	0.006	0.015	0.004	0.011	0.015	0.006	0.125	0.060	0.051	0.005	0.007	0.013
BDE-28	0.073	0.014	0.007	0.023	0.047	0.033	0.021	0.021	0.023	0.046	0.013	0.032	0.413	0.128	0.102	0.034	0.047	0.016
BDE-71	<DL	<DL	<DL	<DL	<DL	<DL	<DL	<DL	<DL	<DL	<DL	<DL	<DL	<DL	<DL	<DL	<DL	<DL
BDE-47	1.511	0.554	1.082	2.385	3.597	2.293	2.622	0.585	1.373	1.763	2.131	1.494	1.965	0.963	1.044	1.577	1.036	0.753
BDE-66	<DL	<DL	<DL	<DL	<DL	<DL	<DL	<DL	<DL	<DL	<DL	<DL	<DL	<DL	<DL	<DL	<DL	<DL
BDE-100	0.249	1.357	0.209	1.045	0.447	0.733	0.679	0.144	0.705	0.760	0.606	0.476	1.106	1.009	0.602	<DL	<DL	<DL
BDE-99	2.289	1.357	1.394	2.220	3.240	1.610	4.062	0.844	2.849	2.105	1.888	1.731	3.730	1.630	3.253	1.726	2.554	1.538
BDE-85	<DL	<DL	<DL	<DL	<DL	<DL	<DL	<DL	<DL	<DL	<DL	<DL	<DL	<DL	<DL	<DL	<DL	<DL
BDE-154	0.006	0.013	<DL	0.020	0.005	0.012	0.005	0.018	0.011	0.003	0.013	0.003	0.511	0.042	0.011	0.004	0.022	0.010
BDE-153	0.012	0.018	0.008	0.003	0.012	0.010	0.023	0.007	0.011	0.007	0.008	0.007	0.151	0.040	0.018	0.018	0.017	0.012
BDE-138	0.023	0.008	0.015	0.010	0.007	0.032	0.013	0.006	0.016	0.003	0.003	0.009	0.039	0.031	0.011	0.033	0.070	0.022
BDE-183	0.018	0.019	0.013	0.009	0.030	0.021	0.031	0.014	0.002	0.006	0.005	0.004	0.016	0.020	0.022	0.033	0.023	0.017
BDE-190	0.156	0.058	0.080	0.078	0.041	0.025	0.029	0.039	0.025	0.008	0.040	0.010	0.157	0.049	0.021	0.024	0.041	0.027
Σ_{13}PBDEs	4.356	3.401	2.842	5.808	7.448	4.787	7.489	1.692	5.019	4.711	4.721	3.771	8.213	3.971	5.134	3.455	3.817	2.408

<*DL* lower than the detection limit

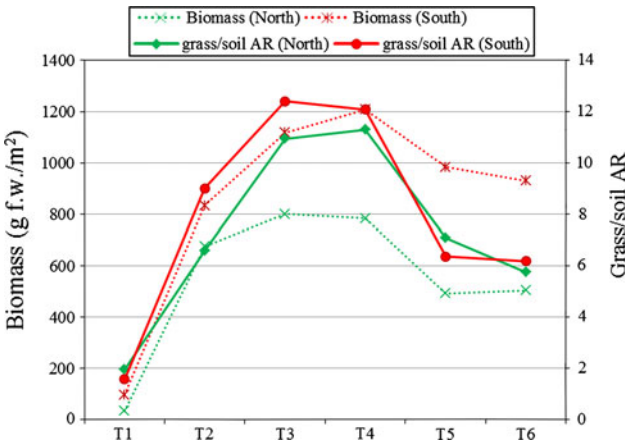

Fig. 3 PBDE grass–soil AR and above-ground biomass values (g fw/m^2; *dotted lines*) calculated for the north (*green*) and south (*red*) mountain sides from an Andossi plateau pasture (Color figure online)

OM-normalized N/S EF in northern and southern soils. OM normalization led to a 22% decrease in the N/S EF of the $\sum_{13}$PBDEs in the O layer, whereas no variations in A1 N/S EF were shown, suggesting that temperature, not OM content, was the main factor affecting PBDE accumulation in the northern soils. The OM-normalized N/S EF values were perfectly comparable with those measured using K_{sa} values, thus confirming the great influence of mountain side on PBDE accumulation in pasture soils.

Effect of Seasonality on PBDE Levels in Soils

The $\sum_{13}$PBDE level in soil of the Andossi plateau depended on the sampling date ($F = 13.601$; $p < 0.01$), suggesting that the behavior of BDE congeners is dynamic. Considering the seasonal variation (marginal means of the GLM), the PBDE contamination of O, A1, and A2 soils was at its maximum level during the first sampling period (June 1, 2008), which occurred few days after the complete snowmelt, showing levels significantly greater than those measured at the other sampling dates ($p < 0.01$). This peak of contamination could be related to the high scavenging rate of snow precipitation (Lei and Wania 2004). Hydrophobic pollutants associated with particles retained in the snowpack could be deposited in the soil during the last phase of the thaw (Meyer and Wania 2008). Moreover, it is also plausible that post-thaw soils are still cold and thus able to retain more pollutants than later in the growing season. After T1, PBDE concentrations in soils rapidly decreased on each mountain side and reached values on average twofold lower than those measured at T1, suggesting a relatively fast volatilization. After the thaw, the soils rapidly warm up, enhancing the revolatilization processes (Guazzoni et al. 2011). The rapid loss of brominated compounds between T1 and T2 may also be related to the strong wind that blows both over the plateau and the neighboring areas (ARPA 2010). Wind could enhance the volatilization of pollutants, particularly for heavy congeners and in soils with high organic-matter content (Koblizkova et al. 2009). From T3 to T6, there was no significant ($p > 0.05$) variation in $\sum_{13}$PBDEs on any mountain side, although an overall increase in contamination was found at T5. The PBDE concentration in A1 soils at T5 was up to threefold greater than at T4, whereas in the A2 layer it was up to twofold greater. The heavy rain that fell a few days before the fifth sampling date could have increased the air-to-soil fluxes (Guazzoni et al. 2011). In Fig. 2a, PBDE-seasonal PBDE trends of soils are shown separately for the opposite mountain sides. According to the differences in soil temperatures at the northern and southern sites, the decreasing concentration trend at the beginning of the Alpine summer was much faster for the southern side compared with the northern one, even if this gap was absent 20 days later. At the end of the Alpine summer (in September), PBDE concentrations in northern soils differed from those in the southern ones because of the lower solar height, which increases the shadow cone on them. This behavior highlighted once again the relationships among layer, season, and mountain side, thus confirming that they may consistently affect the soil contamination within the same year and over such a small area. In the GLM, the four factors (date, aspect, layer, and soil OM) explained 74% of the overall variability, and their relative contribution in decreasing order was date (49%), soil OM (30%) aspect (17%), and layer (4%). The date factor accounted for temperature and emission differences during the study period (from June to October); the mountain side effect accounted for temperature and humidity differences among soils; and the OM was the main factor explaining layer differences. Excluding the OM content of the three layers, the overall variability explained by the model decreases to 70%, but that of the layer factor greatly increases because it accounts for layer and OM variability together.

PBDEs in Vegetation

Levels of PBDE (ng/g dw) in vegetation from the Andossi plateau are listed in Table 4. Mean concentrations ± SD of Σ_{13}PBDEs in grass was 4.6 ± 1.8 ng/g dw (minimum maximum interval 1.7–8.2 ng/g dw). Measured concentrations were greater than those found in grass in a rural area in England (0.090–0.410 ng/g dw [Lake et al. 2011]). Grass samples in the current study had a different species composition among both sampling sites and date because they were characteristic of the pasture at that site and time. A rich herbaceous community, composed of 89 species belonging to 27 families, characterizes the Andossi pasture

(Tato et al. 2011). Therefore, our vegetation samples (which included all of the vegetation in the sampling area) had a site- and time-specific complex composition. This choice was preferred because it gives greater ecological relevance to our data even if interspecies differences in bioaccumulation were possible. However, the complex composition itself should be able to average both interspecies and vegetation-stage differences. Many plant characteristics could be important to explain the interspecies variability of the accumulation capacity of plants (Barber et al. 2004). Among these, lipid content may be an important factor affecting bioaccumulation in vegetation, and it is partially responsible for the physical partitioning of the compound between the air and the plant (Barber et al. 2004). For this reason, we took into account the specific lipid content of each sample. Overall, it was quite homogeneous, ranging between 0.030 and 0.053 g lipid/g dw (mean content 0.038 ± 0.0065), thus confirming the averaging effect of our sampling technique. Lipid weight–normalized PBDE concentrations showed similar trends to dry weight–normalized ones, but no significant correlation ($p > 0.05$) was found between lipid content and $\sum_{13}$PBDEs. Therefore, we decided to keep the dry weight–normalized data because they are most commonly used. Overall, the PBDE pattern of contamination overlapped that previously described for soils. Tetra- and penta-brominated congeners were the most represented compounds of the fingerprint, accounting for approximately 34 and 61% of the $\sum_{13}$PBDEs, respectively, whereas tri-, hexa-,and hepta-BDE congeners were found in negligible concentrations. BDE-99 was the main congener (Fig. 1), accounting for >49% of the $\sum_{13}$PBDEs, followed by BDE-47 (34%) and BDE-100 (12%). Focusing on the main congeners, we can use the BDE-47/BDE-99 ratio to identify the origin of the PBDE contamination. It was similar to that of Bromkal 70-5DE, which was the most commonly used technical formulation in Europe before its ban (La Guardia et al. 2006), as well as to the ratio previously described for soils. Considering that both matrices have a similar accumulation potential based on the octanol–air partition coefficient (K_{oa}) of congeners, the similarity of this ratio among vegetation and soil samples suggests a common source of contamination on the Andossi plateau, which can be traced to the penta-formulation. Plants may either take up chemicals from the air through their aboveground parts or from the soil through the roots (Trapp and Matthies 1995). Cousins and Mackay (2001) suggested that atmospheric uptake by particle-bound deposition is the dominant pathway for compounds with a log $K_{oa} > 9$. Considering that PBDEs have a log K_{oa} between 9.3 and 11.96 and a high affinity for particles (Harner and Shoeib 2002), the concentrations measured in grass can be assumed to be accumulated by atmospheric deposition. However, different PBDEs exhibit different behavior in the atmosphere (i.e., partitioning between the vapor phase and particulate material), and the impact of each of the deposition processes may vary between different congeners (Jin et al. 2008). By analyzing the PBDE fingerprint and the BDE-47/BDE-99 ratio, we can state that few differences exist in overall source-pathway transfer efficiencies for the investigated congeners despite notable variations in their physicochemical properties (Lake et al. 2011). Even if the contamination pattern between soil and vegetation was similar, the PBDE concentrations in grass samples were fivefold greater than those measured in each soil layer. The ratio between the PBDE concentration in grass and that in soil can be called the "grass–soil accumulation ratio" (AR) as an alternative to the term "biological concentration factor" already proposed by Wang et al. (2007). The grass–soil AR values calculated in this study showed that, on average, PBDE concentrations in grass were 2- to 12-fold greater than levels in soil. This ratio, calculated for both mountain sides in relation to the date of sampling (Fig. 3), followed a parabolic trend, showing the highest values at T3 and T4, with values ≤6-fold greater than those measured at T1. This trend coincided with the above-ground biomass experimentally measured at the same sites and time (Fig. 3). Our data agreed with those measured in other Alpine pasture (Boschetti et al. 2007) having similar altitude and vegetation facies: e.g., *Nardus stricta*-dominated grasslands and *Seslerieto-Semperviretum* in northern and southern sites, respectively. Net growth rates of the herbaceous community were 25 and 28 g fresh weight (fw) m^2/d for the northern and southern sites, respectively, in June and 6 and 13 g fw m^2/d for the northern and southern sites, respectively, in July. The maximum biomass was found between July (T3) and August (T4) and coincided with the highest PBDE levels in the herbage. A strong relationship between biomass and PBDE relative-to-soil contamination in grass was found. During the growing season (from the end of June to August), the temperatures were at their maximum, thus favoring vegetation growth (Fig. 3).

Effect of Temperature and Seasonality on PBDEs in Vegetation

The accumulation potential of vegetation was dependent on temperature as suggested by the concentration differences between northern and southern samples (Fig. 2b) during the entire season (N/S EF in vegetation (Tato et al. 2011)). Concentrations in grasses tend to be greater in the summer (higher temperature) than at the beginning or end of the growing season (lower temperatures) compared with the effects of temperature on the accumulation in vegetation and to the growth dilution effect, which both tend to

Table 5 Levels of 13 BDE congeners in cow milk (ng/g dw and ng/g lw) from the Andossi plateau pasture measured at the T2–T5 periods

BDEs	Milk (ng/g dw)				Milk (ng/g lw)				BAF (average T2–T5)
	T2	T3	T4	T5	T2	T3	T4	T5	
BDE-17	0.029	0.008	0.005	0.011	0.137	0.041	0.031	0.066	1.4
BDE-28	0.023	0.006	0.003	0.037	0.109	0.031	0.022	0.217	0.7
BDE-71	<DL	<DL	<DL	<DL	<DL	<DL	<DL	<DL	NC
BDE-47	1.232	0.596	0.485	0.471	5.796	3.100	3.147	2.778	1.1
BDE-66	<DL	<DL	<DL	<DL	<DL	<DL	<DL	<DL	NC
BDE-100	<DL	<DL	<DL	<DL	<DL	<DL	<DL	<DL	NC
BDE-99	0.152	0.115	0.084	0.345	0.715	0.596	0.548	2.039	0.2
BDE-85	<DL	<DL	<DL	<DL	<DL	<DL	<DL	<DL	NC
BDE-154	0.025	0.004	0.004	0.006	0.117	0.020	0.025	0.033	0.5
BDE-153	0.036	0.032	0.032	0.020	0.168	0.167	0.206	0.116	2.2
BDE-138	<DL	<DL	<DL	<DL	<DL	<DL	<DL	<DL	NC
BDE-183	0.021	0.006	0.018	0.034	0.098	0.030	0.114	0.199	3.9
BDE-190	0.057	0.040	0.028	0.101	0.270	0.207	0.182	0.596	0.8
Σ_{13}PBDEs	1.576	0.806	0.659	1.024	7.411	4.191	4.276	6.045	

<DL lower than detection limit, *NC* not calculable, *lw* lipid weight

The BAF was calculated for each single compound using mean dry weight–normalized BDE values from T2 to T5

decrease PBDE concentrations by dilution in the new biomass produced by growth. The seasonal PBDE behavior in vegetation can be explained only by increasing the PBDE concentration in the air and by a greater atmospheric deposition to the vegetation, which filter these contaminants before they reach the soil. The ability of grass to intercept atmospheric deposition is related to the leaf area index (LAI; m^2 of leaf/m^2 of ground surface), which tends to increase with vegetation growth. Thus, the maximum LAI in summer maximizes the ability of grass to "filter" the PBDEs from the atmosphere. LAI values were not experimentally measured, but their qualitative behavior can be evaluated by the above-ground biomass data (Röttgermann et al. 2000). In our experimental sites, above-ground biomass increased approximately one order of magnitude from the beginning of June to the middle of July, and a parallel LAI increase could be supposed in the same interval. Indicative LAI values for an Alpine grassland >2,000 m a.s.l. were in the range 1.2–2.7 depending on the mineral nutrient availability (Körner et al. 1997). We can conclude that grass is highly efficient in filtering atmospheric deposition of POPs (as already known) and that PBDE had a peak deposition, with some fluctuation, in the Andossi plateau during July and August. In fact, the seasonal trend (Fig. 2b) did not show a constant summer increase but rather a fluctuating trend, with two peaks in T3 and T5 (July and beginning of September). A possible source of PBDEs for atmosphere and vegetation can be found in PBDE emission from the soil of the same area by volatilization at the beginning of the growing season. The calculated net emission between T1 and T3 was 79 and 58 μg/m^2 for northern and southern soils, respectively, whereas the net uptake from vegetation in the same period, calculated according to Tato et al. (2011), was 1.5 and 1.3 μg/m^2 for northern and southern sites, respectively. Emissions from soil and uptake by vegetation at the northern site was slower than at the southern site (Fig. 2b), but the amount lost and taken up was greater because concentrations at the northern site were also greater. PBDEs released from the soils during this time period could have temporarily increased the contamination level of the soil–air interface before passing into the air compartment above the herbage. A temporary PBDE enrichment at the soil–air interface could not have been readsorbed by the soil itself because the increase of the soil temperatures during this period decreased its K_{sa}. In contrast, the vegetation may have intercepted this flux by the well-known "filter effect." Two elements could potentially contribute to this process: the uptake kinetics of pollutants into vegetation, which depend on many parameters and can also be rapid (Mackay et al. 2006), and the peculiarity of the herbaceous vegetation characterized by direct contact with the soil–air interface. PBDE emission from soil of the same area can be a possible explanation for the T3 peak in vegetation, at least partially, but not for that found at T5. This peak could have been due to the heavy rain that fell several days before that sampling, which could have increased the air-to-soil fluxes (Guazzoni et al. 2011). Although possible, it requires that PBDE levels in air are greater than those measured before and after the rainfall because precipitation and low temperature followed a similar trend but with a different intensity. The fifth

sampling was performed on September 9, and it was the first sampling after August (the main tourist period in the Italian Alps). The resident population in the valley where the experimental area is located is 24,696 inhabitants, which increased by 294,942 tourist arrivals (Istituto Nazionale di Statistica 2008). These data indicate that touristic activities and all of the anthropogenic-related emissions could provide a consistent pollutant input to the mountain ecosystems when tourism is high (December and August). Thus, our data seem to suggest that in August, a consistent PBDE emission to the atmosphere occurred in the valley, which determined the PBDE concentration peak in vegetation at T5. Similarly, in soil (Fig. 2a) a qualitative concentration peak is present during the same period, thus confirming the presence of consistent deposition events that were registered primarily by the vegetation and secondly by the soil (filter effect of the vegetation toward the atmospheric deposition).

PBDEs in Milk

The study area has been used for centuries as a summer pasture for dairy cows. The $\sum_{13}$PBDE concentration (Table 5) in the cow milk samples varied from 0.659 to 1.576 ng/g dw and was on the same order of magnitude as that of PCBs (Tato et al. 2011). A similar trend was also found in the lipid weight–normalized data (range 2.4–4.6 ng/g lipid) because the lipid content of the milk was similar throughout the pasture season (0.275–0.371 g lipid/g dw). Our results showed that PBDE contamination in milk from the Andossi plateau was much greater than that measured in milk samples collected from farms in other European countries (Gómara et al. 2006; Domingo et al. 2008; Fernandes et al. 2009). Surprisingly, the mean PBDE level (3.1 ± 1.0 ng/g lipid) was greater than that measured both in retail milk from Finland (0.1 ng/g lipid (Kiviranta et al. 2004)) and the United Kingdom (0.52 ng/g lipid (Food Standards Agency 2006)) and in cow milk from Spain (0.63 ng/g lipid (Bocio et al. 2003)), Ireland (0.4 ng/g lipid), and Switzerland (0.20 ng/g lipid (Gruemping et al. 2006)). When PBDE contamination in feed was also reported, such as in the study by Lake et al. (2011), the vegetation had much lower contamination levels than we found in our study area, indicating that high PBDE levels in grass was the main reason for the high levels in milk from the Andossi plateau. In fact, PBDE concentrations in milk followed a trend similar to vegetation (milk *vs*. vegetation regression shows an R^2 value of 0.80). Analyzing the PBDE congener ratio between milk and vegetation, great differences in fingerprint were found (Fig. 1), even if the accumulation of pollutants in milk mainly occurs by way of vegetation (Rychen et al. 2008). Moreover, the milk fingerprint was also different from the soil one, although cows can ingest from 1 to 10% of their diet as soil, thus contributing to POP uptake (Mamontova et al. 2007). Overall, according to vegetation and soil, tetra- and penta-BDE were the main congeners of the fingerprints and accounted for approximately 73 and 17% of the $\sum_{13}$PBDEs, respectively, whereas tri-, hexa-, and hepta-BDE congeners were found at negligible concentrations (2–3%). BDE-47 was the main congener, accounting for >73% of the $\sum_{13}$PBDEs, followed by BDE-99 (17%). Differences in the PBDE patterns among milk, vegetation, and soil could be due to the ability of lactating cows to degrade highly brominated compounds, thus favoring enrichment of the lighter ones. In fact, once ingested, PBDEs are absorbed across the gastrointestinal tract and pass into the blood; once inside the body, they can be degraded, stored in fat tissues, or excreted through milk and feces (Thomas et al. 1999). Different degradation susceptibility, absorption efficiency, or transfer capability to milk may change the PBDE pattern in milk from that in feed (Kierkegaard et al. 2007, 2009). Another possibility is that dietary absorption may differ between congeners. For example, hexa-brominated BDEs have a lower dietary absorption than tetra-brominated BDEs, and based on studies with other halogenated organics, dietary absorption can be expected to continuously decrease with increasing degree of bromination (Kierkegaard et al. 2009). Last, the differences in congener profiles could be due to reductive debromination after absorption: The effectiveness of this process was shown in cows and other vertebrates for high-brominated compounds (i.e., BDE-209; Kierkegaard et al. 1999; Huwe and Larsen 2005). Because of these issues, the interpretation of the debromination pathway is difficult because accumulation reflects both formation and resistance to further debromination. Unfortunately, at present, no data are available on the degradation of investigated BDE congeners in cows, although meta-debromination of BDE-183 and BDE-99 has been reported in carp (Stapleton et al. 2004). The metabolic degradation and excretion efficiency of PBDEs into milk explain most of the PBDE bioaccumulation and fingerprint, assuming that bioaccumulation in cows occurs nearly completely by way of food as reported by McLachlan (1993). The transformation of BDEs was not calculated directly in this study, but it can be indirectly evaluated by the relationship between intake and output of the native chemical (Kierkegaard et al. 2009). Hence, the bioaccumulation factor (BAF) on a dry weight–basis of individual congeners from feed (grass) to milk was calculated using the BDE average concentrations measured in the T2–T5 sampling periods (Table 5). The BAF for milk was often >1 for most of the congeners, with maximum values for congeners 183 (3.9), 153 (2.2), and 17 (1.4) according to a general increase in the concentrations of persistent lipophilic compounds in the food chain. In

contrast, the lower BAF value calculated for BDE-99 (0.2) and BDE-100 (<0.05) suggests that these congeners were efficiently metabolized by cows after ingestion because their absorption efficiency was greater than that of more highly brominated ones. For example, BDE-183 and BDE-153 have lower absorption efficiencies but much greater BAF values than BDE-99 or BDE-100. This is particularly true for penta-brominated compounds: The average concentration of BDE-99 and BDE-100 was notably greater in vegetation than in milk, suggesting a partial or complete degradation of the parent compound in lighter brominated congeners, which likely occurs after absorption by way of metabolism by the cow. Even if the behavior of BDEs in cows reported here is consistent with that of other studies (Kierkegaard et al. 2007, 2009), more investigations, including the analysis of a carryover rate and PBDE mass balance in cows, are necessary to confirm our present understanding of the vegetation-to-cow transfer of PBDEs.

Conclusion

Our data indicate that the Andossi plateau pasture was contaminated by PBDEs. Soils are effective reservoirs for these compounds, even if their concentrations in the different layers tend to have significant variations during the year. They show the highest levels soon after the spring thaw, followed by a fast decrease, probably due to volatilization processes. Even if most of the literature considers soils to be a stable environmental compartment, our data suggest that both climatic factors (e.g., seasonality and volatilization) and pedological characteristics (layer effects and OM content) lead to notable differences in PBDE contamination over space and time, suggesting that soil contamination is dynamic in Alpine ecosystems. Similarly, the vegetation of the Andossi plateau showed a seasonal variability in PBDE contamination and a spatial variability on a small scale. Physicochemical, topographic, and seasonal variables, as well as tourism, greatly influence PBDE levels in the Andossi herbage. Moreover, in further studies should be interesting to evaluate interspecies differences in PBDE herbage accumulation. PBDE contamination in vegetation has direct implications for the milk of the cows grazing in this pasture area. In fact, the relatively high contamination of the milk reflects the relatively high contamination in the herbage, which may change spatially and seasonally across a relatively small and homogeneous area. PBDE residues in cow milk could cause concern to local human health because it is habitually used for local cheese production. To date, we have no measurement of PBDE in dairy products from the Andossi plateau, so it is difficult to assess the potential hazard of these compounds to human health. In conclusion, given the unexpected occurrence of PBDEs in this alpine environment and the possible implications for human health, more emphasis, including toxicokinetics and toxicological studies, should be placed on their continuous monitoring.

References

ARPA (Regional agency for environmental protection) (2010) Rapporto sullo stato dell'ambiente in Provincia di Sondrio, anni 2007–2008. http://ita.arpalombardia.it/ita/dipartimenti/sondrio/index_so.asp

Barber JL, Thomas GO, Kerstiens G, Jones KC (2004) Current issues and uncertainties in the measurement and modelling of air-vegetation exchange and within-plant processing of POPs. Environ Pollut 128:99–138

Binelli A, Sarkar SK, Chatterjee M, Riva C, Parolini M, Bhattacharya B et al (2007) Concentration of polybrominated diphenyl ethers (PBDEs) in sediment cores of Sundarban mangrove wetland, northeastern part of Bay of Bengal (India). Mar Pollut Bull 54:1220–1229

Birnbaum LS, Staska D (2004) Brominated flame retardants: cause for concern? Environ Health Perspect 112:9–17

Blais JM, Charpentié S, Pick F, Kimpe LE, Amand AS, Regnault-Roger C (2006) Mercury, polybrominated diphenyl ether, organochlorine pesticide, and polychlorinated biphenyl concentrations in fish from lakes along an elevation transect in the French Pyrénées. Ecotoxicol Environ Saf 63:91–99

Bocio A, Llobet JM, Domingo JL, Corbella A, Teixido A, Casas C (2003) Polybrominated diphenyl ethers (PBDEs) in foodstuffs: human exposure through the diet. J Agric Food Chem 51: 3191–3195

Boschetti M, Bocchi S, Brivio PA (2007) Assessment of pasture production in the Italian Alps using spectrometric and remote sensing information. Agric Ecosyst Environ 118:267–272

Braekevelt E, Tittlemier SA, Tomy GT (2003) Direct measurement of octanol–water partition coefficients of some environmentally relevant brominated diphenyl ether congeners. Chemosphere 51:563–567

Bucheli TD, Blum F, Desaules A, Gustafsson Ö (2004) Polycyclic aromatic hydrocarbons, black carbon, and molecular markers in soils of Switzerland. Chemosphere 56:1061–1076

CEFIC (The European Chemical Industry Council) (2006) FR'2006 - 12th World Flame Retardant Conference, 14th–15th February - London. http://www.cefic-efra.com/images/stories/News/2006/FR2006summaryEFRA1-1_00.pdf

Cousins IT, Mackay D (2001) Gas-particle partitioning of organic compounds and its interpretation using relative solubilities. Environ Sci Technol 35:643–647

Czub G, Wania F, McLachlan MS (2008) Combining long-range transport and bioaccumulation considerations to identify potential arctic contaminants. Environ Sci Technol 42:3704–3709

Dalla Valle M, Jurado E, Dachs J, Sweetman AJ, Jones KC (2005) The maximum reservoir capacity of soils for persistent organic pollutants: implication for global cycling. Environ Pollut 134: 153–164

Darnerud PO, Eriksen GS, Johannesson T, Larsen PB, Viluksela M (2001) Polybrominated diphenyl ethers: occurrence, dietary exposure and toxicology. Environ Health Perspect 109:49–68

de Wit CA (2002) An overview of brominated flame retardants in the environment. Chemosphere 46:583–624

de Wit CA, Alaee M, Muir DCG (2006) Brominated flame retardants in the Arctic. Chemosphere 64:209–233

de Wit CA, Herzke D, Vorkamp K (2010) Brominated flame retardants in the Arctic environment–Trends and new candidates. Sci Total Environ 408:2885–2918

Domingo JL, Martí-Cid R, Castell V, Llobet JM (2008) Human exposure to PBDEs through the diet in Catalonia, Spain: temporal trend. A review of recent literature on dietary PBDE intake. Toxicology 248:25–32

Fernandes AR, Tlustos C, Smith F, Carr M, Petch R, Rose M (2009) Polybrominated diphenylethers (PBDEs) and brominated dioxins (PBDD/Fs) in Irish food of animal origin. Food Addit Contam Part B Surveill 2:86–94

Food Standards Agency (2006) Brominated chemicals: UK dietary intakes [report 10–06]. FSA, London

Gómara B, Herrero L, Gonzalez MJ (2006) Survey of polybrominated diphenyl ether levels in Spanish commercial foodstuffs. Environ Sci Technol 40:7541–7547

Gruemping R, Petersen M, Kuchen A, Tlustos C (2006) Levels of polybrominated diphenyl ethers in Swiss and Irish cow's milk. Organohalogen Compd 68:2147–2150

Guazzoni N, Comolli R, Mariani L, Cola G, Parolini M, Binelli A et al (2011) Meteorological and pedological influence on the PCBs distribution in mountain soils. Chemosphere 83:186–192

Guzzella L, Roscioli C, Binelli A (2008) Contamination by polybrominated diphenyl ethers of sediments from the Lake Maggiore basin (Italy and Switzerland). Chemosphere 73:1684–1691

Hale RC, La Guardia MJ, Harvey E, Gaylor MO, Mainor TM (2006) Brominated flame retardant concentrations and trends in abiotic media. Chemosphere 64:181–186

Harner T, Shoeib M (2002) Measurements of octanol–air coefficients (KOA) for polybrominated diphenyl ethers (PBDEs): predicting partitioning in the environment. J Chem Eng Data 47:228–232

Hassanin A, Breivik K, Meijer SN, Steinnes E, Thomas GO, Jones KC (2004) PBDEs in European background soils: levels and factors controlling their distribution. Environ Sci Technol 38:738–745

Hassanin A, Johnston AE, Thomas GO, Jones KC (2005) Time trends of atmospheric PBDEs inferred from archived U.K. herbage. Environ Sci Technol 39:2436–2441

Hippelein M, McLachlan MS (2000) Soil/air partitioning of semivolatile organic compounds. 2. Influence of temperature and relative humidity. Environ Sci Technol 34:3521–3526

Huwe JK, Larsen GL (2005) Polychlorinated dioxins, furans, and biphenyls, and polybrominated diphenyl ethers in a US meat market basket and estimates of dietary intake. Environ Sci Technol 39:5606–5611

Istituto Nazionale di Statistica (ISTAT) (2008) http://www.istat.it

Jin J, Liu W, Wang Y, Tang XY (2008) Levels and distribution of polybrominated diphenyl ethers in plant, shellfish and sediment samples from Laizhou Bay in China. Chemosphere 71:1043–1050

Kierkegaard A, Balk L, Tjarnlund U, De Wit CA, Jansson B (1999) Dietary uptake and biological effects of decabromodiphenyl ether in rainbow trout (Oncorhynchus mykiss). Environ Sci Technol 33:1612–1617

Kierkegaard A, Asplund L, de Wit CA, McLachlan MS, Thomas GO, Sweetman AJ et al (2007) The fate of higher brominated PBDEs in lactating cows. Environ Sci Technol 41:417–423

Kierkegaard A, de Wit CA, Asplund L, McLachlan MS, Thomas GO, Sweetman AJ et al (2009) A mass balance of tri-hexabrominated diphenyl ethers in lactating cows. Environ Sci Technol 43:2602–2607

Kiviranta H, Ovaskainen ML, Vartiainen T (2004) Market basket study on dietary intake of PCDD/Fs, PCBs, and PBDEs in Finland. Environ Int 30:923–932

Koblizkova M, Ruzickova P, Cupr P, Komprda J, Holoubek I, Klanova J (2009) Soil burdens of persistent organic pollutants: their levels, fate, and risks. Part IV. Quantification of volatilization fluxes of organochlorine pesticides and polychlorinated biphenyls from contaminated soil surfaces. Environ Sci Technol 43:3588–3595

Körner C, Diemer M, Schäppi B, Niklaus P, Arnon J (1997) The response of Alpine grassland to four seasons of Co2 enrichment: a synthesis. Acta Oecol 18:165–175

La Guardia MJ, Hale RC, Harvey E (2006) Detailed polybrominated diphenyl ether (PBDE) congener composition of the widely used penta-, octa- and deca-PBDE technical flame-retardant mixtures. Environ Sci Technol 40:6247–6254

Lake IR, Foxall CD, Fernandes A, Lewis M, Rose M, White O et al (2011) Effects of river flooding on polybrominated diphenyl ether (PBDE) levels in cow's milk, soil and grass. Environ Sci Technol 45:5017–5024

Lei YD, Wania F (2004) Is rain or snow a more efficient scavenger of organic chemicals? Atmos Environ 38:3557–3571

Li N, Wania F, Lei YD, Daly GL (2003) A comprehensive and critical compilation, evaluation, and selection of physical–chemical property data for selected polychlorinated biphenyls. J Chem Eng Data 50:742–768

Mackay D, Foster KL, Patwa Z, Webster E (2006) Chemical partitioning to foliage: the contribution and legacy of Davide Calamari. Environ Sci Pollut Res 13:2–8

Mamontova EA, Tarasova EN, Momontov AA, Kusmin MI, McLachlan MS, Khomutova MI (2007) The influence of soil contamination on the concentrations of PCBs in milk in Siberia. Chemosphere 67:571–578

McLachlan MS (1993) Mass balance of polychlorinated biphenyls and other organochlorine compounds in a lactating cow. J Agric Food Chem 41:474–480

Meijer SN, Ockenden WA, Sweetman AJ, Breivik K, Grimalt JO, Jones KC (2003) Global distribution and budget of PCBs and HCB in background surface soils: implications for sources and environmental processes. Environ Sci Technol 37:667–672

Meyer T, Wania F (2008) Organic contaminants amplification during snowmelt. Water Res 42:1847–1865

Nelson DW, Sommers LE (1996) Total carbon, organic carbon, and organic matter. In: Page AL et al (eds) Methods of soil analysis, part 2, 2nd edn. American Society of Agrongronomy, Madison, pp 961–1010

Parolini M, Binelli A, Marin MG, Matozzo V, Masiero L, Provini A (2011) New evidences in the complexity of contamination of the lagoon of Venice: polybrominated diphenyl ethers (PBDEs) pollution. Environ Monit Assess (in press)

Röttgermann M, Steinlein T, Beyschlag W, Dietz H (2000) Linear relationships between aboveground biomass and plant cover in low open herbaceous vegetation. J Veg Sci 11:145–148

Rychen G, Jurjaz S, Toussaint H, Feidt C (2008) Dairy ruminant exposure to persistent organic pollutants and excretion to milk. Animal 2:312–323

Sjödin A, Jakobsson E, Kierkegaard A, Marsh G, Sellström U (1998) Gas chromatographic identification and quantification of polybrominated diphenyl ethers in a commercial product Bromkal 70–5DE. J Chromatogr A 822:83–89

Società Italiana della Scienze del Suolo (SISS) (2007) Escursione scientifica del convegno nazionale: "La scienza del suolo nei territori montani e collinari." Milano-Chiavenna, Italy, July 9–13

Song W, Ford JC, Li A, Mills WJ, Buckley DR, Rockne KJ (2004) Polybrominated diphenyl esters in the sediments of the Great Lakes. Environ Sci Technol 38:3286–3293

Stapleton HM, Letcher RJ, Li J, Baker JE (2004) Dietary accumulation and metabolism of polybrominated diphenyl ethers by juvenile carp (Cyprinus carpio). Environ Sci Technol 23:1939–1946

Sweetman AJ, Dalla Valle M, Prevedouros K, Jones KC (2005) The role of soil organic carbon in the global cycling of persistent organic pollutants (POPs): interpreting and modelling field data. Chemosphere 60:959–972

Tato L, Tremolada P, Ballabio C, Guazzoni N, Parolini M, Caccianiga M et al (2011) Seasonal and spatial variability of polychlorinated biphenyls (PCBs) in vegetation and cow milk from a high altitude pasture in the Italian Alps. Environ Pollut 159(10):2656–2664

Thomas GO, Sweetman AJ, Jones KC (1999) Metabolism and body-burden of PCBs in lactating dairy cows. Chemosphere 39: 1533–1544

Tittlemier SA, Halldorson T, Stern GA, Tomy GT (2002) Vapor pressures, aqueous solubilities, and Henry's law constants of some brominated flame retardants. Environ Toxicol Chem 21: 1804–1810

Trapp S, Matthies M (1995) Generic one-compartment model for uptake of organic chemicals by foliar vegetation. Environ Sci Technol 29:2333–2338

Tremolada P, Parolini M, Binelli A, Ballabio C, Comolli R, Provini A (2009a) Preferential retention of POPs on the northern aspect of mountains. Environ Pollut 157:3298–3307

Tremolada P, Parolini M, Binelli A, Ballabio C, Comolli R, Provini A (2009b) Seasonal changes and temperature-dependent accumulation of polycyclic aromatic hydrocarbons in high-altitude soils. Sci Total Environ 407:4269–4277

Tremolada P, Comolli R, Parolini M, Moia F, Binelli A (2011) One-year cycle of DDT concentrations in high-altitude soils. Water Air Soil Pollut 217:407–419

Vonderheide AP, Mueller KE, Meija J, Welsh GL (2008) Polybrominated diphenyl ethers: causes for concern and knowledge gaps regarding environmental distribution, fate and toxicity. Sci Total Environ 400:425–436

Wang XP, Yao TD, Cong ZY, Yan XL, Kang SC, Zhang Y (2007) Distribution of persistent organic pollutants in soil and grasses around Mt. Qomolangma. China Arch Environ Contam Toxicol 52:153–162

Wang P, Zhang Q, Wang Y, Wang T, Li X, Li Y et al (2009) Altitude dependence of polychlorinated biphenyls (PCBs) and polybrominated diphenyl ethers (PBDEs) in surface soil from Tibetan Plateau, China. Chemosphere 76:1498–1504

Watanabe I, Sakai S (2003) Environmental release and behavior of brominated flame retardants. Environ Int 29:665–682

Supplementary Material
Table S1.

Congener	$logK_{oa}$	A[a]	B[a]		$logK_{oa}$ at −1°C	$logK_{oa}$ at 3.9°C	N/S EF
17	9.3	-3.45	3803		10.524	10.277	1.766637
28	9.5	-3.54	3889		10.750	10.497	1.789519
47	10.53	-6.47	5068		12.152	11.823	2.134796
100	11.13	-7.18	5459		12.879	12.524	2.263427
99	11.31	-4.64	4757		12.839	12.530	2.037724
85	11.66	-6.22	5331		13.369	13.022	2.220487
154	11.92	-4.62	4931		13.499	13.178	2.091477
153	11.82	-5.39	5131		13.464	13.130	2.155017
183	11.96	-3.71	4672		13.457	13.153	2.01197

[a]Regression coefficients (A and B) are for equation logKoa = A + B/T from Harner and Shoeib (2002)

Chapter VII

Guazzoni, N., Comolli, R., Binelli, A., Tremolada, P., 2012. Environmental variables affecting POPs distribution on Mt. Meru, Tanzania. Submitted to Ambio

Environmental variables affecting POPs distribution on Mt. Meru, Tanzania

Niccolò Guazzoni[1*], Roberto Comolli[2], Andrea Binelli[1] and Paolo Tremolada[1]

[1] Department of Biology, University of Milan, Via Celoria 26, 20133 Milan, Italy

[2] Department of Environmental and Land Sciences (DISAT), University of Milan Bicocca, Piazza della Scienza 1, 20126 Milan, Italy

*Corresponding author. Tel.: +39 02 50314715; fax: +39 02 50314713. E-mail address: niccolo.guazzoni@unimi.it

Abstract

The knowledge of POPs presence and distribution is fundamental to understand where they tend to reside and how they move along the planet. In the "global fractional distillation" theory Tanzania, as an equatorial country, should be a source zone for POPs, but this scenario could be different in mountainous areas like our sampling site, the Mount Meru, a 4566 m a.s.l volcano situated in the Rift Valley. We took samples along an altitudinal transect up to the top of the volcano and obtained data on POPs contamination and pedological and vegetation features. Our work gives the first data about the POPs contamination on the Meru slopes. Contamination pattern in Mt.Meru shows level slightly higher than those of other remote places for DDX (that evidenced a descending historical thread of the Metabolites/DDT ratio), PCBs and HCHs and extremely low levels of HCB. Distribution of POPs shows strong correlation with soil organic matter and vegetation. SOM-normalization evidenced an altitudinal dependence according to cold condensation for PCB and HCH, while DDX are more present in the agricultural area at the volcano foot. OM-normalised concentrations suggested also a possible role of the OM composition on the POPs distribution and that of the mineral nano-porosity of volcanic ashes in permitting an efficient POPs sorption when the soil organic matter is very low. This paper helps to evidence the different role of the pedological, climatic and vegetation variables in determining the POPs distribution in a mountain environment in an equatorial zone.

Keywords: POPs; Tanzania; Altitudinal transect; Environmental variables; Metabolites/DDT

1 - Introduction

Organochlorine POPs are still a problem for environmental and human health. The knowledge of their presence and distribution is fundamental to understand where they tend to reside and how they move along the planet. In this frame there is a wide amount of work about contamination in environmental matrices in North America and Europe (e.g. Moeckel et al., 2008; Gasic et al., 2010), also with a modeling approach, based on the "global fractional distillation" and "fugacity" concepts (e.g. Van Jaarsveld et al., 1997; MacKay and Arnot, 2011).

African contamination is still poorly understood in comparison to the worldwide knowledge, despise the fact that a great gamma of these substances are still used (AGENDA, 2006; Stadlinger et al., 2011), or stockpiled (AGENDA, 2005) in the African continent. A wide arrange of POPs, banned in the industrialized countries, has been sold to developing countries or stockpiled in African nations, often causing leaks and ecological damages (Frey, 1995). Only in the last decade an increasing number of papers were published referring to a specific nation (e.g. Kishimba et al., 2004 for Tanzania) or to continental monitoring studies (Klanova et al. 2009). As in many African countries, in Tanzania there is an historical DDT contamination due to malaria control. Moreover, in this country there is nowadays a continuative use of dangerous pesticides (in some cases expressly recommended by the government; Nyambo, 2009). In literature there are some works about contamination in Tanzania (Paasivirta et al., 1988; Tremolada et al., 1993; Mwevura et al., 2002; Kishimba et al., 2004; Bettinetti et al., 2011) but there are few information about pollution in soils. In the "global fractional distillation" theory (Wania and MacKay, 1996) Tanzania, as an equatorial country, should be a source zone for POPs, but this scenario could be different in mountainous areas according to the maximum reservoir capacity theory (Dalla Valle et al., 2005) that points that step gradients of accumulative capacity could be found in mountains. Since the Ksa (the partition coefficient between soil and air) is influenced by the temperature, (He et al., 2009) it is expected that pollutants will tend to condensate more at high altitude also in low latitude environments (Calamari et al., 1991). Moreover mountains tend to have a contamination gradient due to the effect of precipitation that overlaps to the cold condensation one (Offenthaler et al., 2009). These climatic features are completed by the effect of the different vegetation cover by the "forest filter effect" (Nizzetto et al., 2006).

The first aim of this study is to produce first data about DDX, HCH, HCB and PCB contamination in the area of Mt. Meru (Tanzania), which is the second highest mountain of Africa. The second aim is to further investigate the effect of altitude and cold condensation in soils in an equatorial environment, in relation to soil properties and vegetation cover.

2 - Materials and methods

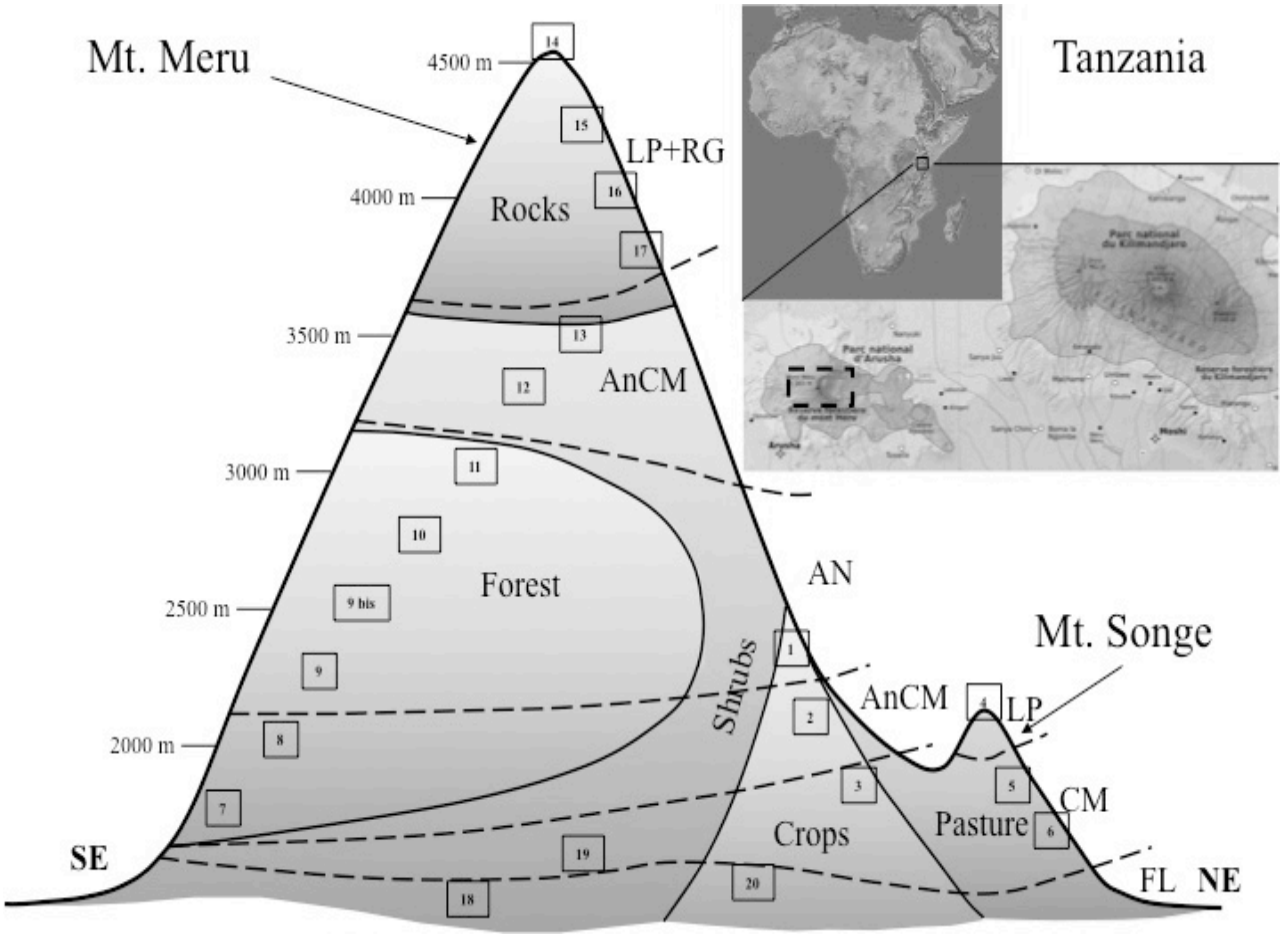

Figure 1: Figure 1 - Graphical representation of our transect along Meru slopes. Number represents our sampling sites. Solid lines outline the different vegetation categories (crops, pasture, shrubs, forest and rocks), dashed lines outlines pedological classification (FL=Fluvisol, CM=Cambisol, LP=Leptosol, AN=Andosol, RG=Regosol). In the top-right corner: location of Mt.Meru

2.1 - Study area

Mount Meru (height 4566 m a.s.l.) is an active volcano in the North of Tanzania, in the Arusha district (Figure 1). The altitudinal transect crosses a wide range of biome from the agricultural and pasture area near the bottom of the volcano and in the adjacent Mount Songe to the savannah, forest, high altitude shrubs and herbaceous vegetation biotopes along the slopes of the volcano till its top. The climate in this region (North of Tanzania) is characterized by two main rainy periods (in October-December the long rains "Masika"; in March-May the short rains "Vuli") intercalated by dry periods (OECD, 2003). Our sampling occurred in February, at the end of the short dry season, and was conducted to include the vegetation categories typical of the area. The soils in our sampling sites are strictly conditioned by parent material and climate (Veldkamp, 2001; Mlingano Agric. Res. Inst., 2006). Complete description of vegetation categories

and soil taxonomy is available in the S.I. (Text S1)

2.2 - Sample collection

For each sampling site, three sub-samples of soil (litter was removed) were manually homogenized to reduce the site variability. The samples were enveloped in a tin foil and enclosed in plastic bags to avoid pollutant loss. As soon as possible they were frozen (-20 °C) until analysis.
Vegetation cover was evaluated for every site by characterizing grass, shrub and tree layers, according to Braun-Blanquet method (Braun-Blanquet et al., 1932). Graphical representation of the distribution of our samples in different vegetation and pedological categories is shown in Figure 1. The distribution of vegetation and pedological categories in our transect is shown the S.I. (Table S2), along with the position and altitude of each sampling site.

2.3 - Methodology and analysis

Samples were lyophilized to remove water by sublimation and extracted in a Soxhlet apparatus with a solution of acetone and n-hexane (1:1 v/v) for 12 hours. The extract was digested with sulphuric acid and purified with a Silica-Florisil column. Samples were analysed by GC/MS/MS in order to quantify DDX (p,p'-DDT and its isomer and metabolites), polychlorobiphenils (CB-18, CB-31+28, CB-44, CB-52, CB-101, CB-138, CB-149, CB-153, CB-170, CB-180, CB194), isomers of hexachlorociclohexane (α-HCH, β-HCH, γ-HCH, δ-HCH) and hexachlorobenzene (HCB).
Extensive description of analytical procedures, quality assurance and quality control are available in the S.I. (Text S1).
Each soil sample was analysed for organic carbon (OC) and total N content by an elemental analyser (Flash EA 1112 NC soil, ThermoFisher, Waltham, MA, USA). The organic matter content (OM) was estimated from the organic-C content using a 1.724 multiplier constant, as indicated in Nelson and Sommers (1996). Soil pH was measured in a soil:water = 1:2.5 suspension. Soil bulk density was obtained sampling with a 100 cm^3 metallic cylinder and calculating the mass after oven drying at 105 °C for 8 hours.

3 - Results and Discussion

3.1 - Taxonomy of sampled soils and soil characteristics

The sampled soils show different characteristics, as they belong to very different soil types: from a taxonomic point of view, using the WRB system (IUSS Working Group WRB, 2007), the following altitudinal sequence exists from low areas to the Mt. Meru summit: Haplic Fluvisols, Haplic and Endosalic Cambisols, Andic Cambisols, Melanic Andosols, Andic and Vitric Cambisols, Tephric Regosols, Lithic Leptosols. There is an altitudinal belt favourable to andosolization (1700-3200 m); this pedogenic process reaches its top below the forest vegetation.

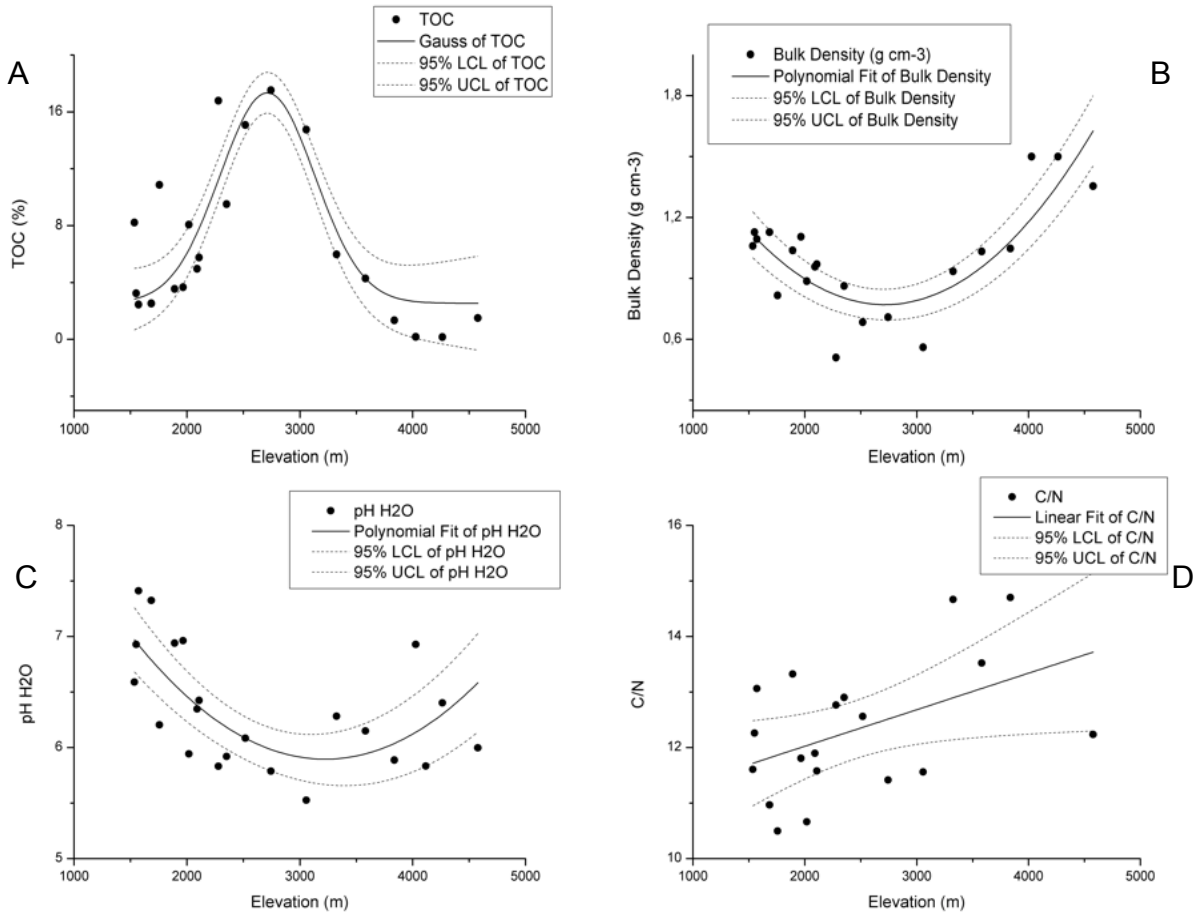

Figure 2: Distribution of pedological variables along altitudinal transect. A: Total organic carbon in soils (% = g OC g^{-1} d.w.*100). B: Bulk density of soils (g cm^{-3}). C: pH measured in a soil:water suspension (1:2.5). D: Ratio between Total Organic Carbon and Total Nitrogen. All regression lines were fitted with the best function, shown with 95% confidence interval.

OC content, N content, bulk density and pH of each sample is available in S.I. (Table S2). The OC distribution is strictly linked to climate (especially rain), soil type, vegetation type (higher valued under forest) and cover (that is biomass accumulation). OC content was very high (15-18%) in the 2300-3100 m belt, where the andosolization process is more developed, while decreased at upper and lower elevation, according to a normal curve distribution (Figure 2A). Two samples at high elevation were particularly low in SOM (below 0.5%), but the soil type was Tephric Regosol, unconsolidated and not pedogenized soil made by lapilli and volcanic ash, with limited grass vegetation. Other low OC content values were found in rocky areas on the top of the mountain, where pedogenic processes slow down and soils (Leptosols) are subject to erosion and can be retained only inside pockets between the rocks or when protected by sparse herbaceous vegetation.

The bulk density (BD) of the soil has an altitudinal trend (Figure 2B) opposite to the previous one: at low elevation (Fluvisols, Cambisols) BD values are around 1.0-1.1 g cm^{-3}, the same found at higher elevations (Andic Cambisols); values significantly lower (0.5-0.7 g cm^{-3}) correspond to the true

Andosols belt, whereas higher values (up to 1.5 g cm^{-3}) are found among Tephric Regosols near the summit. Soil BD is closely related (r = -0.90***) to OM content.
The pH in water has a very similar trend, compared to elevation (Figure 2C), to that of BD: values are near neutrality (pH 6.5-7.5) at low altitudes, subacid (up to pH 5.5) in the Andosols belt, subacid-neutral (up to pH 6.9) at higher altitudes. The reasons are to be searched in rainfall amount, which varies with altitude, and leads to some acidification in the central forest belt. The pH in water is significantly correlated (r = -0.62**) to OM content.
The C/N ratio has a positive trend with altitude (Figure 2D), statistically significant but less marked than the previous. In any case, this parameter is interesting because it's a qualitative indicator of the OM type: the three fractions that compose OM (fulvic acids, humic acids and humin) are characterized by different C/N ratios (greater for humin, smaller for fulvic acids; Stevenson and Cole, 1999). Moreover, the C/N ratio has a negative correlation (r = -0.49*) with the vegetation cover.

3.2 - POPs contamination of the Meru area.

Ranges of contamination in the area (extensive data are shown in the S.I. Table S3) showed low concentrations of every residue analyzed, comparable with those found in others remote or semi-remote areas (Meijer et al., 2003; Tremolada et al., 2007, 2010; Whang et al., 2009; Guazzoni et al., 2011; Zheng et al., 2012) confirming the indirect POPs contamination of the Mt. Meru area. A possible factor contributing to low concentration could be also the sampling time (sampling was performed at the end of a dry season). Kishimba et al. (2004) have demonstrated that contamination values in an area near the Meru are consistently higher during wet seasons than during dry ones, so it is possible that there is a seasonal variation of contamination like the one found in other areas (Guazzoni et al., 2011) but with two contamination peak (wet seasons) and two low contamination period (dry seasons). This behaviour with one or two distinct wet seasons must be better investigated.
The obsolete POPs storage site of Vikuge (AGENDA, 2005; Marco and Kishimba, 2005), a putative source area for the northern Tanzanian environment (Bettinetti et al., 2011), seems nonetheless too far (~400 Km) to severely influence the Meru area. Nevertheless the fact that we found measurable concentrations of every residue we searched for in almost every sample means that POPs reach the Meru area by means of atmospheric transport from both global and regional sources (e.g. Vikuge or other local diffuse sources such as agricultural areas for DDX and HCH or urban sites with electric equipment for PCB).
To summarize the distribution of POPs in the area we used box plot graphs (Figure 3), which show a great variability between categories and between samples inside every category in terms of concentration (ng g^{-1} of d.w.). Nevertheless it is possible to find some qualitative differences specific for each class.

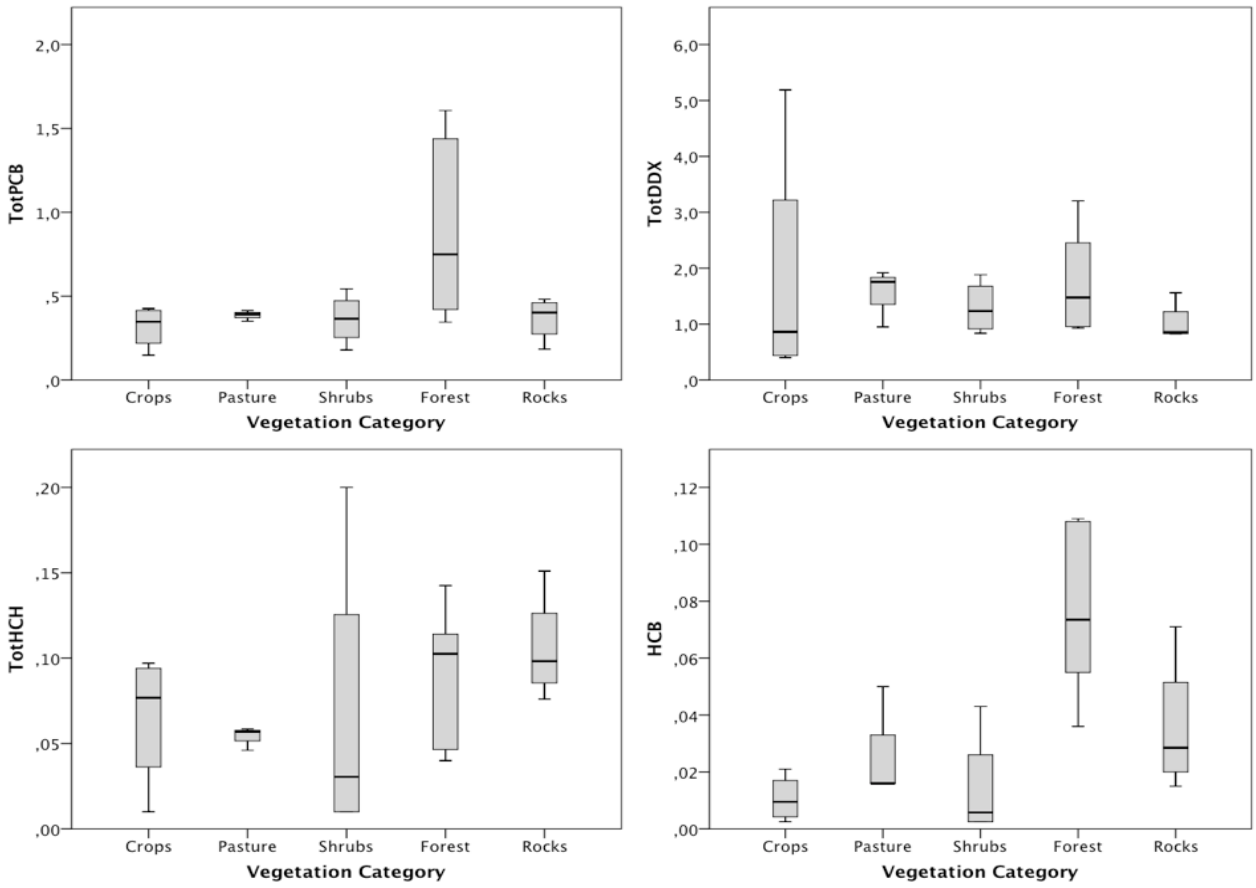

Figure 3: Figure 3 - Box plots of concentrations of POPs among vegetation categories. Data in ng g^{-1} dry weight.

PCB concentrations, as sum of 12 congeners, ranges from 0.15 to 1.61 ng g^{-1} of d.w. with levels that seems to point a remote contamination. Levels detected are 3-fold lower than those found in Italian Alps (Tremolada et al., 2007, 2010: Guazzoni et al., 2011) but 10 times higher than those found in the Tibetan Plateau (Whang et al., 2009; Zheng et al., 2012) and in Peruvian Andes (Tremolada et al., 2007). With those comparison we could speculate that, since PCB are industrial pollutants, the Meru area is probably affected by minor local sources of PCB located somewhere around. Putative source area could be the town of Arusha that is a big town with more than 250.000 inhabitants located at the foot of mount Meru and has a local market of pesticides and obsolescent electric material (TANESCO, 2005; AGENDA, 2006). Tanesco (Tanzanian energy service company limited) reports few electrical gears still containing PCB oil, but also report lack of knowledge on the disposal of old dielectric fluids that could be released in the environment (TANESCO, 2005).

Higher values were found in the forest environment and this can be interpreted as depending on the "forest filter effect" (Nizzetto et al., 2006). A qualitative association between PCB levels and vegetation categories (also related to OM in soils) is shown in the S.I. (Image S4). The congener specific analyses show a prevalence of penta- and hexa-chlorinated biphenyls with relative concentrations according to

those found in commercial mixtures of PCB (Frame et al., 1996; Breivik et al., 2002).

HCH contamination shows extremely low values (some isomers were below quantification level) with concentrations ranging from 0.04 to 0.2 ng g^{-1} of d.w. These levels are at least 50 times lower than the levels found some agricultural area in Tanzania where an HCH usage can be supposed at least in the recent past. Kishimba et al. (2004) reports high HCH levels in Tanganyika sugar cane plantations soils (~70 km from Mt.Meru) both in dry and wet season (mean of 5 and 9 ng g^{-1} respectively), while Kihampa et al. (2010) found average levels of ~200 ng/g of Lindane in tomato fields of Ngarenanyuki (at the foot of the volcano). Both those areas are located nearby the Meru but levels found in agricultural category of Songe area sampling indicate that HCH are not currently used in local agriculture probably since several years. Nevertheless data from sugarcane and tomato plantation nearby seems to suggest those areas as possible contamination sources for Mt. Meru area.
Along the altitudinal transect, higher HCH values could be found in high altitude rocky areas and below forests. This confirm both "forest filter effect" and the "mountain contamination potential" (Dalla Valle et al., 2005). Since HCH are the most volatile compounds in this study it is possible that their low levels, also in the analysed agricultural soils, are due to a fast volatilization from these hot equatorial soils. In addition, the condition of temperature and soil organic matter found in the Meru area are not enough to permit a massive deposition at the top of the volcano (Mt.Meru as a grasshopper step for HCH). Contamination fingerprint shows a prevalence of γ-HCH (Lindane), that denote as a primary source for this area the use of Lindane as a pesticide in agriculture and/or as a medicament for human ectoparasites, rather than the old technical HCH (rich in α-HCH) (Willett et al., 1998). HCB concentrations range was between 0.01 and 0.11 ng g^{-1} of d.w., with the higher levels in the forest areas. These values are in the low end of worldwide background concentration (Meijer et al., 2003), pointing out that the Meru area is a remote place for hexachlorobenzene.

DDX were measured in every sample with a concentration range from 0.4 to 5.2 ng g^{-1} d.w. DDX levels show slightly higher concentrations in the low altitude samples (agricultural area). It is conceivable that the DDX found are the residues of past DDT use in agricultural practice. Anyway, the contamination appears to be not severe, in fact levels found in the Meru area are lower than those detected, for example, in the Alps where a direct contamination can be excluded (Tremolada et al., 2007, 2010). The non recent use of DDT in Songe area, is deduced also by the comparison of our data with those found in nearby sugarcane and tomato plantations where levels 50 to 100 times higher were detected (Kishimba et al., 2004; Kihampa et al., 2010). The DDX

contamination of the Meru transect could be thereafter due to volatilization from intensive agriculture area and a residue of our agricultural sampling zones. The most abundant residue is p,p'-DDE giving the 98% of the total DDX contamination. The metabolites/DDT ratio (~162/1) strongly indicates an old/remote contamination. As shown in Figure 4 the metabolites/DDT ratio found in this study update an already increasing temporal trend of the metabolites/DDT ratio in Tanzania. It is obvious that this elaboration contains possible uncertainties because data used in the figure refer to different matrices and come from different areas in Tanzania, yet the trend seems to point out a strong tendency to the DDT transformation without new fresh DDT inputs. DDT was legally used in agricultural practices since it was finally banned in 1991 in Tanzania and in 1985 in Kenya (Bettinetti et al., 2011). The ban, along with fast volatilization and degradation of the parent compound could lead to the high metabolites/DDT ratio and to the low concentrations seen nowadays.

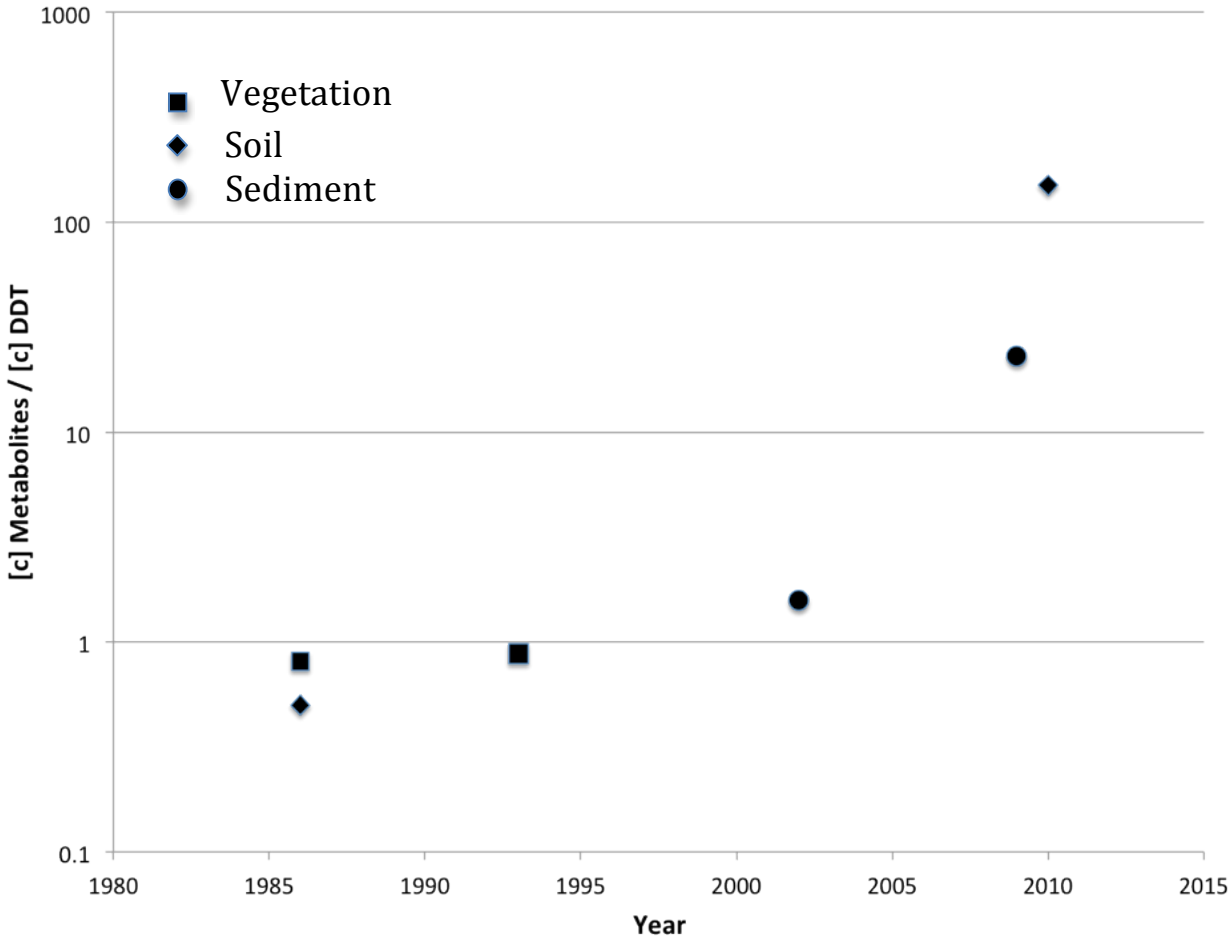

Figure 4: Figure 4 - Trend of the metabolites / DDT ratio in historical data in logarithmic scale. Data from: Paasivirta et al., 1986; Tremolada et al., 1993; Mwevura et al., 2002; Bettinetti et al., 2009 and this paper, 2010.

3.3 - OM-normalized POPs concentrations and altitudinal gradient.

OM-normalized concentrations of pollutants in soil represent better the part of variability due to meteorological factors, summarized by the altitude, and minimizing pedological interferences on the concentrations levels measured in soils. Moreover OM-normalized data eliminates from our data set also the eventual effect due to different sampling depth, as different studies have demonstrated (e.g. Armitage et al., 2006; Guazzoni et al., 2011). Normalized data (ng g^{-1} of OM) show an abnormally high OM-normalized concentration for every compound in samples 15 and 16 (complete data are available in the S.I. Table S3). These samples came from the high altitude rocky area near the top of the volcano and have an extremely low level of organic matter: their OM content is one order of magnitude less even than that of the other two samples that are comparable in terms of altitude (sample 14 and 17). For this reason, their OM-normalised concentrations appear to be abnormally high. We think that this overestimation of the contamination of samples 15 and 16 is an artefact of the OM-normalisation. Although, these samples are rich in volcanic ashes, that are very rich in nano-porosity (Wilson et al., 2002; Arnalds et al., 2007). This feature could act as a substitute of organic matter in permitting an efficient POPs sorption in soils (Farrell and Reinhard, 1994) by the hole-filling model (Pignatello, 1998). In these samples, with very low OM but high mineral nano-porosity, the POPs sorption could be done by the nano-porosity of the volcanic ashes. This is just a hypothesis that suggests further researches. It is clear that the OM-normalization of these soils lead to an overestimation of their contamination burdens and a misleading representation of their contamination level, therefore we decided to remove sample 15 and 16 from the data pool when we calculated the correlation between altitude and OM-normalized concentration. However these data are a qualitative indication of a high accumulation capacity of these soils.

With the data of the remaining 19 samples we proceeded to analyze correlations between OM-normalised contamination levels and altitude with Pearson correlation. We found a positive and significant correlation between the concentration of PCB and HCH and the altitude (PCB: $r=0.528$, $n=19$ $P=0.020$; HCH: $r=0.466$, $n=19$ $P=0.044$). HCB shows a positive correlation with a P-value of 0.071. On the contrary, DDX do not show any positive relationship with the altitude, because the highest concentration values were observed in the agriculture areas at the lowest altitude. DDX were the only class among the analyzed ones, probably used in the area in the past years, even if any evidence of a heavy and recent DDT pollution was found. However, the majority of the analysed POPs shows a positive relationship with the altitude, making us to assume that they come from medium/long range atmospheric transport giving a typical altitudinal gradient due to the condensation effect at the highest altitudes.

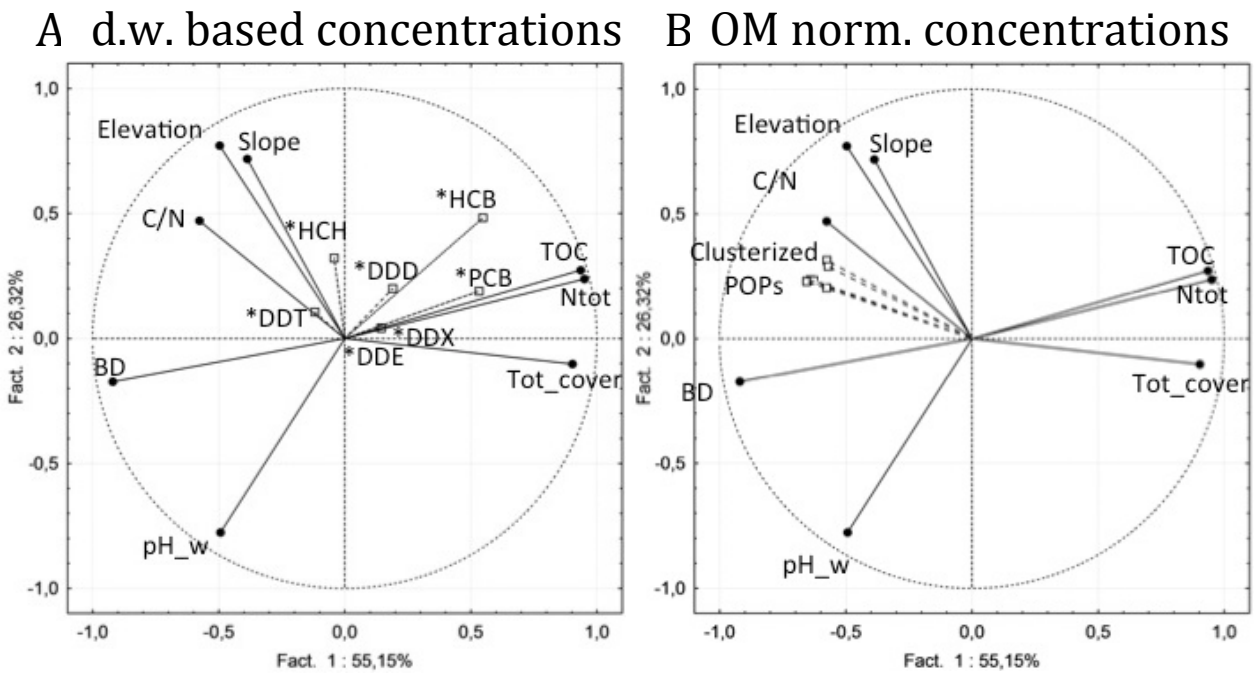

Figure 5: PCA of environmental variables with the addition of POPs concentrations as non active variables. In both figures (A; B) black dots represent the active variables used to perform the PCA. Elevation: altitude in m a.s.l.; Slope: inclination of the sampling zone in %; BD: Bulk density of soils (g cm^{-3}); TOC: total organic carbon of soil (% = g OC / g d.w*100); Ntot: Total Nitrogen of soil (% = g N g^{-1} d.w*100); C/N: Total Organic Carbon / Total Nitrogen; pH_w: pH measured in a soil:water suspension (1:2.5); Tot_cover: Braun-Blanquet index of cover percentage. White dots represent the position in the factorial plane of the POPs concentration levels in ng g^{-1} d.w. (A) and in ng g^{-1} OM (B). In figure B, all POPs concentrations are clustered together and single class position is not shown.

3.4 - PCA of the contamination in relation to the environmental variables

The relative importance of environmental variables on the POPs contamination in Mt. Meru area was analysed by PCA with dry-weight and OM-normalised data (Figure 5A and 5B). Total nitrogen (N tot), total organic carbon (TOC), carbon-nitrogen ratio (C/N), pH, bulk density (BD) and slope were considered as pedological features. Elevation was the only variable representative the climate, because direct meteorological data were unavailable. However, altitude summarizes different meteorological features like the temperature gradient, the precipitation gradient and several local meso-climatic effects. The last variable considered was the vegetation cover (Tot_cover), this variable can be considered related to biomass production and the organic detritus that can reach the soil. In Figure 5A the variability explained by the first and second axes reaches the 80% and indicates, as most important environmental variables on the first axis, the total amount of carbon and nitrogen and the vegetation cover (highly related in general) to which the BD is opposed (effect of the organic matter on the soil density). On the second axis the elevation and the slope (highly related for these samples) are

the most important variables to which is opposed the pH (generally at high altitude the soil organic matter is higher and the pH is lower). When POPs classes were added as dry-weight concentrations, HCB and PCB appear to be associated mainly with the OM (TOC and N tot) and then with elevation (second axis). DDTs seems to be independent from all variables, while HCH shows a limited association with elevation on the second axis. DDX and HCH are the compounds with a higher historical use and thus they have a more localised contamination, more dependent on historical use than on environmental features. Nonetheless HCH are more volatile than DDTs and therefore are more related to elevation. Even between HCB and PCB, HCB is more volatile than the majority of the PCB congeners; according to this it appears more related to elevation (this results were not confirmed by direct relationship between altitude and OM-normalised concentrations). Among DDX, DDE and DDD, that derive from an older contamination than the parent compound, seem to be more related to OM indicating a distribution nearer to equilibrium than for DDT, which appear as the most independent compound in relation to the environmental variables. By analysing the behaviour of OM-normalised concentrations (Figure 5B) we found that all POPs group together, loosing, as expected, the relation with the OM, but maintaining that with elevation. An interesting result of this analysis is the association of POPs with C/N variable. This suggests that, eliminating the gross effect of OM on concentrations, a secondary relationship appears with the quality of the OM (C/N depends on the composition of organic matter). The main humic fractions, that compose the majority of the soil organic matter, have different C/N ratios: the highest C/N are measured in humin. It is known that POPs tend to have a preferential association with humin than with humic and fulvic acids (Kohl and Rice 1998; Ahmad et al. 2001; Doick et al. 2005) and the association of POPs with C/N variable seems to confirms this feature. Higher C/N ratio, which indicates a higher relative abundance of humin, lead to higher POPs amount. This interesting result underlines once more the possible role of the OM composition on POPs distribution.

4 - Conclusion

Our work gives the first data about the contamination of several POPs in the Meru area. DDX levels and a metabolites/DDT ratios confirm the abandonment of this compound in agricultural practices at least in this area, and the general low concentration levels of all analyzed POPs indicate that this area is comparable with other remote/semi-remote ones. All the analysed POPs show contamination levels lower than those found in European mountains, but higher than those of other remote places such as some areas in the Tibetan plateau and Andes. For the HCH group it is conceivable a usage of Lindane. The DDX contamination, which is the most severe among the residues we searched for, seems to be affected by direct

usage area as the intensive plantation nearby the volcano. However both levels and DDT/metabolite ratio indicate a past use. For PCB the most probable 'surrounding source' is the Arusha town with its obsolescent electrical gears.

Regarding to the relationship between contamination and environmental variables, the soil organic matter seems to be the most important features for the POPs distribution in this mountain area. SOM is able to summarize many environmental characteristics: SOM content depends fundamentally from the vegetation detritus and thus to the vegetation density covering the soils and it accumulates in soils depending on the substrate (pH) and the climate (mainly temperature and humidity). Therefore SOM is able to group both pedological and climatic characteristics, and only eliminating it, other interesting items were evidenced. First at all, the significant correlation found between the SOM-normalised concentrations of PCB and HCH and the altitude point out again the mountain contamination potential and the importance of the condensation/precipitation effect in determining the distribution of POPs in mountain areas. Secondly, PCA suggests the relationship between POPs concentrations and the SOM composition throughout the C/N variable. This parameter, that is very easily measured, could be proposed for characterizing the SOM in POPs distribution studies.

Another interesting result, derived by the SOM-normalised concentrations, is the abnormally high concentrations found in samples 15 and 16. This finding suggests an important role of the mineral nano-porosity, which could act by the hole-filling model in permitting an efficient POPs sorption when the soil organic matter resulted inefficient because of the scarcity.

5 - Bibliography

AGENDA(2005): Water and Sediments Analysis in Vikuge POPs Contaminated Site in Tanzania. http://www.ipen.org/ipepweb1/library/ipep_pdf_reports/6urt%20vikuge%20water%20and%20sediments.pdf

AGENDA(2006): A CASE STUDY ON TRADE AND UTILIZATION OF PESTICIDES IN TANZANIA: Implication to Stockpiling. http://www.pan-uk.org/archive/Projects/Obsolete/14.%20Babati%20Case%20Study_Tanzania.pdf

Arnalds, Ó., Bartoli, F., Buurman, P., Óskarsson, H., Stoops, G., García-Rodeja, E., 2007. Soils of Volcanic Regions in Europe. Springer Berlin Heidelberg, NY.

Bettinetti, R., Quadroni, S., Crosa, G., Harper, D., Dickie, J., Kyalo, M., Mavuti, K., Galassi, S., 2011. A Preliminary Evaluation of the DDT Contamination of Sediments in Lakes Natron and Bogoria (Eastern Rift Valley, Africa). Ambio. 40, 341-350.

Braun-Blanquet, J., Fuller, G.D. Conrad, H.S. 1932 Plant Sociology: The Study of Plant Communities. McGraw-Hill Inc., New York, NY, USA.

Breivik, K., Sweetman, A., Pacyna, J.M., Jones, K.C., 2002. Towards a global historical emission inventory for selected PCB congeners – a mass balance approach. 1 Global production and consumption. Sci. Total Environ. 290, 181–198.

Dalla Valle, M., Jurado, E., Dachs, J., Sweetman, A.J., Jones, K.C., 2005. The maximum reservoir capacity of soils for

persistent organic pollutants: implication for global cycling. Environ. Pollut. 134, 153–164.

Farrell, J., Reinhard, M., 1994: Desorption of halogenated organics from model solids, sediments, and soil under unsaturated conditions 1.Isotherms. Environ. Sci. Technol. 28, 53-62.

Frame, G.M., Wagner, R.E., Carnahan, J.C., Brown, J.C., May, R.J., Smullen, L.A., Bedard, D.L., 1996. Comprehensive, quantitative, congener-specific analyses of eight aroclors and complete PCB congener assignments on DB-1 capillary GC columns. Chemosphere 33, 603–623.

Frey, S.R., 1995. The international traffic in pesticides. Technol. forecast. soc. chang. 50, 151-169.

Gasic, B., MacLeod, M., Klanova, J., Scheringer, M., Ilic, P., Lammel, G., Pajovic, A., Breivik, K., Holoubek, I., Hungerbuhler, K., 2010. Quantification of sources of PCB to the atmosphere in urban areas: A comparison of cities in North America, Western Europe and former Yugoslavia. Environ. pollut. 158, 3230-3235.

Guazzoni, N., Comolli, R., Mariani, L., Cola, G., Parolini, M., Binelli, A., Tremolada, P., 2011. Meteorological and pedological influence on the PCB distribution in mountain soils. Chemosphere. 83, 186-192.

He, X., Chen, S., Quan, X., Zhao, Y., Zhao, H., 2009. Temperature-dependence of soil/air partition coefficients for selected polycyclic aromatic hydrocarbons and organochlorine pesticides over a temperature range of -30 to +30 °C. Chemosphere. 76, 465-471.

IUSS Working Group WRB, 2007. World Reference Base for Soil Resources 2006, first update 2007. World Soils Resources Report No. 103, FAO, Rome.

Kihampa, C., Mato, R. R., Mohamed, H., 2010. Residues of organochlorinated pesticides in soil from tomato fields, Ngarenanyuki, Tanzania. J. Appl. Environ. Manage. 14, 37-40.

Kishimba, M.A., Mwevura, L.H.H., Mmochi, A.J., Mihale, M., Hellar, H., 2004. The status of pesticide pollution in Tanzania. Talanta. 64, 48-53.

Mackay, D., Arnot, J.A., 2011. The Application of Fugacity and Activity to Simulating the Environmental Fate of Organic Contaminants. J. Chem. Eng. Data. 56, 1348-1355.

Marco, J.A.M., Kishimba, M.A., 2005. Concentrations of pesticide residues in grasses and sedges due to point source contamination and the indications for public health risks, Vikuge, Tanzania. Chemosphere. 61, 1293-1298.

Meijer, S.N., Ockenden, W.A., Sweetman, A., Breivik, K., Grimalt, J.O., Jones, K.C., 2003. Global distribution and budget of PCB and HCB in background surface soils: implication for sources and environmental process. Environ. Sci. Technol. 37, 667-672.

Mlingano Agric. Res. Inst., 2006. Soils of Tanzania and their Potential for Agriculture Development. Ministry of Agric., Food Security and Co-operatives, Tanga, Tanzania.

Moeckel, C., Nizzetto, L., Di Guardo, A., Steiness, E., Freppaz, M., Filippa, G., Camporini, P., Benner, J., Jones, K.C., 2008. Persistent organic pollutants in boreal and montane soil profiles: distribution, evidence of process and implication for global cycling. Environ. Sci. Technol. 42, 8374–8380.

Mwevura, H., Othman, O.C., Mhehe, G.L., 2002. Organochlorine pesticide residues in sediments and biota from the coastal area of Dar es Salaam city, Tanzania. Marine pollut. bulletin. 45, 262-267.

Nelson, D.W., Sommers, L.E., 1996. Total carbon, organic carbon, and organic matter. In: Page, A.L. et al. (Eds.), Methods of Soil Analysis, 2nd ed., Part 2, Agronomy, vol. 9 Am. Soc. of Agron., Inc., Madison, WI, pp. 961–1010.

Nizzetto, L., Cassani, C., Di Guardo, A., 2006. Deposition of PCB in mountains: The forest filter effect of different forest ecosystem types. Ecotoxicol. Environ. Saf. 63, 75–83.

Nyambo, B., 2009. Integrated pest management plan. Dar es Salaam, Tanzania http://www.google.it/url?sa=t&rct=j&q=ipmp%20plan%20tanzania&source=web&cd=1&ved=0CB0QFjAA&url=http%3A%2F%2Fww

w.kilimo.go.tz%2Fpublications%2Fenglish%2520docs%2FIPMP%2520Plan.pdf&ei=0VPKTsGYOY7pOZO11MUP&usg=AFQjCNHp2mWbsI5tfd1_B6eNdXNnEby8hw&cad=rja

OECD: Organisation for Economic Co-operation and Development, 2003: Development and climate change in Tanzania: focus on mount Kilimanjaro. www.oecd.org/dataoecd/47/0/21058838.pdf

Offenthaler, I., Bassan, R., Belis, C., Jakobi, G., Kirchner, M., Krauchi, N., Moche, W., Schramm, K.W., Sedivy, I., Simoncic, P., Uhl, M., Weiss, P., 2009. PCDD/F and PCB in spruce forests of the Alps. Environ. Pollut. 157, 3280-3289.

Paasivirta, J., Palm, H., Paukku, R., Akhabuhaya, J., Lodenius, M., 1988. Chlorinated insecticide residues in Tanzanian environment. Tanzadrin. Chemosphere. 17, 2055-2062.

Pignatello, J.J., 1998. Soil organic matter as a nanoporous sorbent of organic pollutants. Adv. Colloid Interface Sci. 76-77, 445-467.

Stadlinger, N., Mmochi, A.J., Dobo, S., Gyllback, E., Kumblad, L., 2011. Pesticide use among smallholder rice farmers in Tanzania. Environ. Dev. Sustain. 13, 641-656. Stevenson F.J., Cole M.A., 1999. Cycles of soil: carbon, nitrogen, phosphorus, sulphur micronutrients. Wiley, New York.

TANESCO, 2005. Reinforcement and upgrade of Dar Es Salaam, Kilimanjaro and Arusha transmission and distribution system project, Final report. http://www-wds.worldbank.org/servlet/WDSContentServer/WDSP/IB/2006/03/02/000160016_20060302114823/Rendered/PDF/E650VOL10410PAPER.pdf

Tremolada, P., Calamari, D., Gaggi, C., Bacci, E., 1993. Fingerprints of some chlorinated hydrocarbons in plant foliage from Africa. Chemosphere. 27, 2235-2252.

Tremolada, P., Villa, S., Bazzarin, P., Bizotto, E., Comolli, R., Vighi, M., 2007. POPs in mountain soils from the Alps and Andes: suggestions for a "precipitation effect" on altitudinal gradients. Water air soil pollut. 188, 93-109.

Tremolada, P., Comolli, R., Parolini, M., Moia, F., Binelli, A., 2010. One-Year Cycle of DDT Concentrations in High-Altitude Soils. Water air soil pollut. 217, 407-419.

Van Jaarsveld, J.A., Van Pul, A.J., De Leew, F.A.A.M., 1997. Modelling transport and deposition of persistent organic pollutant in European region. Athmos. Environ. 31, 1011-1024.

Veldkamp, W.J., 2001. Zonation and integrated plant nutrient management strategies and options in Tanzania. Vol. II. Soil types and soil groups, Tanzania National Soil Service.

Wania, F., MacKay, D., 1996. Tracking the Distribution of Persistent Organic Pollutants. Environ. sci. technol. 30, 390-396.

Whang, P., Zang, Q.H., Wang, Y.W., Wang, T., Li, X.M., Li, Y.M., Ding, L., Jiang, G.B., 2009. Altitude dependence of polychlorinated byphenyls (PCB) and polybrominated diphenyl ethers (PBDEs) in surface soil from Tibetan Plateau, China. Chemosphere, 76, 1498-1504.

Willett, K.L., Ulrich, E.M., Hites, R.A., 1998. Differential Toxicity and Environmental Fates of Hexachlorocyclohexane Isomers**.** Environ. Sci. Technol. 32, 2197–2207.

Wilson, M.A., Lee, G.S.H., Taylor, R.C., 2002. Benzene displacement on Imogolite. Clay and clay minerals. 50, 348-351.

Zheng, X., Liu, X., Jiang, G., Wang, Y., Zhang, Q., Cai, Y., Cong, Z., 2012. Distribution of PCB and PBDEs in soils along the altitudinal gradients of Balang Mountain, the east edge of the Tibetan Plateau. Environ. pollut. 161, 101-106.

Materials and Methods. Supplementary information (Text 1)

Vegetation categories in sampling sites

In the Songe area we sampled in the "crops" category that includes *Zea mais* fields and the "pasture" category including grazing areas for the local cattle and goats (1500-2500 m a.s.l). In the Meru area we could found the "shrubs" category which includes the savannah bushes at low altitude (1500 m a.s.l) and the vegetation of the ericaceous zone with *Philippia* and *Erica* as the dominant genus at 3200-3600 m a.s.l. It is obvious that savannah and ericaceous zone has different ecological features, but the vegetation density is similar. Then we crossed the "forest" category (1700-3200 m a.s.l.) that includes a wide arrange of forest areas following the increment of altitude (dry mountain forest, dominated by *Juniperus procera* trees; moist mountain forest with trees of the *Croton* genus; upper mountain forest with *Hagenia abyssinica* as the main tree). Again we put together ecological areas that are different, but characterized by multi layered forest cover. Above 3600 m a.s.l. there is the afroalpine zone, characterized by freezing and thawing cycles and by very little precipitation that support only desert-like grasses of the genus *Pentaschistis,* which survive in pockets of soil inside rock fractures and volcanic ashes.

Soil taxonomy in sampling sites

In the lower dry plains, Cambisols are widespread, with Salic and Sodic features, showing strong evapotranspiration and salt accumulation in the upper soil horizons. These soils show alkaline or strong alkaline reaction. In the alluvial plains also Fluvisols are present, often with Sodic features. Going up the slopes, Cambisols acquire Andic characteristics, due to the presence of pyroclastic materials (due to the past eruptive activity of Mt. Meru) in the substrate. In a central altitude belt, that for the eastern side of Mt. Meru is between about 2000 and 3100 m, the abundant rain and the thick pyroclastic cover allow the formation of true Andosols, rich in organic matter and with Melanic features (their pH is acid-subacid). Higher, in a belt till about 3600 m, Andic Cambisols appear again. At higher elevation they leave space to Regosols with Tephric characteristics, rich in pyroclastic material with little weathering, and to Lithic Leptosols, very shallow over hard rock.

Chemicals and instruments

All solvents used were pesticide grade. Florisil adsorbent for chromatography (100–200 mesh) was obtained from Fluka (Steinheim, Germany). Silica gel for column chromatography (70–230 mesh) was supplied by Sigma–Aldrich (Steinheim, Germany). The p,p’-DDE D8 (deuterated p,p’-DDE) used as an internal recovery

standard was purchased from Dr. Ehrenstorfer (Augsburg, Germany).

A GC chromatograph (TRACE GC, Thermo-Electron, Austin, Texas, USA) equipped with a Programmed Temperature Vaporizer injector (PTV) and an AS 2000 autosampler (Thermo Electron) was used coupled with a PolarisQ Ion Trap mass spectrometer. A Rtx-5MS (Restek, Bellefonte, PA, USA) capillary column (30 m length, 0.25 mm I.D., 0.25 μm film thickness) was used for the chromatographic separation. Helium for gas-chromatographic analyses was purchased from Sapio, Monza, Italy.

Extraction and cleanup procedure

Samples (~20 g) were lyophilised and extracted for 12 h using 100 mL acetone/n-hexane (1:1 v/v) in a soxhlet apparatus (FALC Instruments, Lurano, Italy). Samples were then concentrated to the final volume of 3 mL initially by a rotary evaporator (RV 06-LR, IKA, Staufen, Germany) and then by a gentle nitrogen flow. Organic matter was digested adding 6 mL of sulfuric acid 95% and digesting overnight. The supernatant solution of acetone and hexane was then concentrated with gentle nitrogen flow to the volume of 1 mL.

Cleanup was performed using a multilayer column (40 cm x 1.5 cm I.D.) composed of 10 g of silica gel (activated overnight at 130 °C, then deactivated with water, 5% w/w), followed by 10 g of Florisil (activated for 16 h at 650 °C). The phase-filled columns were washed with n-hexane/acetone/ dichloromethane (8:1:1 v/v). Elution was carried out first by collecting 50 mL of n- hexane and then 50 mL of 1:1 n-hexane/dichloromethane (v/v). 1 mL of isooctane was added to the fractions that were then concentrated by rotary evaporator to 10 mL and then to 1 mL under gentle nitrogen flow.

Quantification conditions

Samples were analysed using GC/MS/MS methodology under the following instrumental conditions: PTV in solvent split mode with split flow of 20 mL min^{-1} and splitless time at 2 min; carrier gas helium at 1 mL min^{-1}; EI mode with standard electron energy of 70 eV; transfer line at 270 °C; damping gas at 1 mL min^{-1} and ion source at 250 °C. Chromatographic separation of the PCB congeners was obtained by the following conditions: initial oven temperature starting at 100 °C and maintained for 1 min, then ramped to 180 °C (no hold time) at 20 °C min^{-1}, to 200 °C (no hold time) at 1.5 °C min^{-1}, to 250 °C (no hold time) at 3 °C min^{-1} and finally to 300 °C (held 5 min) at 30 °C min^{-1}. Chromatographic separation of DDX, HCHs and HCB was obtained by the following conditions**:** initial oven temperature starting at 70°C and maintained for 1 min, then ramped to 220 °C at 8 °C min^{-1} and finally to 300 °C (held 7 min) at 20 °C min^{-1}. DDX, PCB, HCH and HCB quantification was

performed by external standard calibration curves, ranging from 1 to 100 pg μL^{-1} for each compound.

Quality assurance (QA) and quality control (QC)

Samples and blanks were spiked with 10 μL of the deuterated recovery standard p,p'-DDE D_8 (and so with 5 ng of DDE-D_8) prior to solvent extraction to monitor methodological analyte losses, as in Sarkar *et al*. (2008). Recoveries over 80% were accepted. The suitability and the stability of deuterated standard response were evaluated as in Sarkar *et al*. (2008). A procedural blank was run in parallel with every batch of three samples and then extracted in a manner identical to that of the samples. No significant concentrations of analysed compounds were found in blanks. LODs (limits of detection) were estimated by the signal-to noise ratio (3:1) and ranged between 0.15 and 0.35 pg (injected amount) depending on the compound. Considering 20 g of extracted soil and the ratio 1:1000 or 1:500 of the injected vs. sample volume, LOQs (limits of quantification) are not higher than 0.001 ng g^{-1} d.w. for PCB and DDX, while it's non higher than 0.005 ng g^{-1} d.w. for HCH and HCB.

Statistical analysis

All statistical elaboration of our data (Box plots, GLM analysis, PCA) were performed with the SPSS 19 software pack and the STATISTICA software pack

Bibliography

S. K. Sarkar, A. Binelli, C. Riva, M. Parolini, M. Chatterjee, A. K. Bhattacharya, B. D. Bhattacharya and K. K. Satpathy (2008): Organochlorine Pesticide Residues in Sediment Cores of Sunderban Wetland, Northeastern Part of Bay of Bengal, India, and Their Ecotoxicological Significance. Archives of Environmental Contamination and Toxicology, 55, 358-371.

Table S2: position, altitude, exposition, slope and distribution of vegetation and pedological categories of each sampling site.

Sample	Coordinates		Altitude	Exposition	Slope	Vegetation	Vegetation cover (%)			
	Lat.	Long.	m a.s.l.		%	Category	Grass	Shrubs	Trees	Total
1	-3.170	36.766	2351	N	80	Crops	50	0	0	50
2	-3.161	36.774	2090	NNE	40	Crops	60	0	0	60
3	-3.157	36.779	1965	-	0	Crops	70	0	0	70
4	-3.146	36.794	2108	-	0	Pasture	90	0	0	90
5	-3.141	36.796	1891	NE	100	Pasture	90	10	0	100
6	-3.138	36.798	1684	N	30	Pasture	60	30	10	100
7	-3.248	36.838	1756	E	20	Forest	100	50	100	250
8	-3.243	36.821	2018	ENE	20	Forest	80	70	10	160
9	-3.233	36.811	2279	ESE	15	Forest	90	70	80	240
9 bis	-3.229	36.799	2517	SE	50	Forest	100	30	0	130
10	-3.226	36.794	2745	ESE	50	Forest	100	50	10	160
11	-3.225	36.786	3057	ESE	60	Forest	100	60	50	210
12	-3.220	36.780	3325	ESE	50	Shrubs	50	90	0	140
13	-3.218	36.773	3581	-	0-2	Shrubs	40	30	0	70
14	-3.244	36.750	4577	O	80	Rocks	5	0	0	5
15	-3.233	36.749	4263	NO	90	Rocks	7	0	0	7
16	-3.226	36.755	4027	N	80	Rocks	10	0	0	10
17	-3.222	36.765	3838	NNE	80	Rocks	25	0	0	25
18	-3.222	36.858	1535	-	0	Shrubs	90	60	10	160
19	-3.131	36.804	1571	SE	2	Shrubs	50	20	10	80
20	-3.128	36.812	1550	-	0	Crops	100	0	0	100

Sample	Sampling Depth cm	Soil type (WRB)	BD g cm-3	pH H2O	TOC %	tot N %	C/N
1	0-10	Melanic Andosol	0.86	5.92	9.51	0.74	12.9
2	0-10	Andic Cambisol	0.96	6.35	4.96	0.42	11.9
3	0-10	Haplic Cambisol	1.11	6.96	3.66	0.31	11.8
4	0-10	Mollic Leptosol	0.97	6.42	5.76	0.50	11.6
5	0-10	Haplic Cambisol	1.04	6.94	3.55	0.27	13.3
6	0-10	Haplic Cambisol	1.13	7.32	2.52	0.23	11.0
7	0-5	Andic Cambisol	0.82	6.21	10.87	1.04	10.5
8	0-5	Andic Cambisol	0.89	5.94	8.07	0.76	10.7
9	0-5	Melanic Andosol	0.51	5.83	16.79	1.32	12.8
9 bis	0-5	Melanic Andosol	0.68	6.08	15.08	1.20	12.6
10	0-5	Melanic Andosol	0.71	5.79	17.53	1.54	11.4
11	0-5	Melanic Andosol	0.56	5.52	14.76	1.28	11.6
12	0-5	Andic Cambisol	0.94	6.28	5.98	0.41	14.7
13	0-5	Vitric Cambisol	1.03	6.15	4.28	0.32	13.5
14	0-3	Nudilithic Leptosol	1.35	6.00	1.50	0.12	12.2
15	0-5	Haplic Regosol (Tephric)	1.50	6.40	0.16	0.01	13.7
16	0-4	Haplic Regosol (Tephric)	1.50	6.93	0.18	0.01	13.5
17	0-5	Lithic Leptosol (Tephric)	1.05	5.89	1.33	0.09	14.7
18	0-5	Haplic Fluvisol	1.06	6.59	8.22	0.71	11.6
19	0-5	Endosalic Cambisol	1.09	7.41	2.45	0.19	13.1
20	0-5	Haplic Fluvisol	1.13	6.93	3.23	0.26	12.3

Table S3 (Part 1): Complete PCBs Data

Sample ng/g d.w.	CB18	CB31+28	CB52	CB44	CB101	CB149	CB118	CB153	CB138	CB180	CB170	CB194	∑PCBs
1	0.021	0.046	0.010	0.010	0.026	0.039	0.015	0.101	0.056	0.045	0.042	0.016	0.426
2	0.018	0.023	0.010	0.009	0.026	0.032	0.041	0.108	0.052	0.052	0.026	0.007	0.404
3	0.020	0.019	0.007	0.007	0.018	0.031	0.025	0.046	0.037	0.042	0.026	0.011	0.290
4	0.037	0.020	0.010	0.008	0.024	0.032	0.028	0.069	0.040	0.043	0.034	0.007	0.351
5	0.016	0.037	0.016	0.011	0.027	0.040	0.037	0.080	0.070	0.046	0.030	0.003	0.414
6	0.017	0.035	0.016	0.012	0.030	0.029	0.034	0.093	0.064	0.048	0.012	0.004	0.392
7	0.019	0.016	0.058	0.020	0.080	0.074	0.040	0.144	0.083	0.104	0.023	0.005	0.666
8	0.021	0.015	0.098	0.038	0.170	0.157	0.092	0.374	0.265	0.165	0.039	0.003	1.438
9	0.133	0.025	0.157	0.075	0.237	0.135	0.083	0.298	0.201	0.203	0.054	0.007	1.607
9 bis	0.164	0.025	0.025	0.014	0.082	0.058	0.056	0.162	0.117	0.090	0.036	0.004	0.833
10	0.034	0.002	0.023	0.011	0.042	0.036	0.018	0.074	0.041	0.040	0.021	0.003	0.345
11	0.024	0.002	0.031	0.019	0.048	0.050	0.026	0.105	0.043	0.053	0.019	0.002	0.421
12	0.042	0.018	0.042	0.026	0.066	0.055	0.031	0.124	0.069	0.057	0.013	0.001	0.543
13	0.047	0.070	0.018	0.014	0.042	0.023	0.027	0.079	0.042	0.030	0.009	0.001	0.403
14	0.081	0.039	0.014	0.006	0.025	0.017	0.021	0.067	0.039	0.038	0.014	0.003	0.364
15	0.020	0.007	0.008	0.002	0.020	0.012	0.014	0.045	0.024	0.023	0.008	0.001	0.184
16	0.023	0.011	0.025	0.012	0.045	0.040	0.024	0.087	0.066	0.086	0.019	0.002	0.440
17	0.046	0.043	0.036	0.023	0.065	0.035	0.012	0.068	0.055	0.074	0.019	0.005	0.482
18	0.020	0.023	0.031	0.010	0.038	0.030	0.015	0.053	0.036	0.048	0.021	0.001	0.327
19	0.007	0.006	0.012	0.005	0.017	0.014	0.012	0.053	0.029	0.020	0.002	0.001	0.179
20	0.018	0.007	0.011	0.006	0.020	0.015	0.011	0.026	0.013	0.014	0.006	0.001	0.148

Sample ng/g OM	CB18	CB31+28	CB52	CB44	CB101	CB149	CB118	CB153	CB138	CB180	CB170	CB194	∑PCBs
1	0.126	0.278	0.059	0.064	0.157	0.240	0.092	0.615	0.340	0.272	0.257	0.096	2.596
2	0.209	0.275	0.121	0.108	0.303	0.378	0.477	1.264	0.611	0.606	0.299	0.080	4.730
3	0.312	0.308	0.105	0.117	0.286	0.499	0.394	0.732	0.593	0.661	0.413	0.178	4.600
4	0.368	0.199	0.104	0.079	0.241	0.322	0.283	0.694	0.407	0.431	0.338	0.072	3.539
5	0.266	0.606	0.261	0.186	0.444	0.656	0.603	1.302	1.141	0.747	0.492	0.054	6.758
6	0.382	0.797	0.363	0.284	0.686	0.657	0.772	2.133	1.476	1.108	0.270	0.085	9.015
7	0.102	0.085	0.309	0.109	0.428	0.392	0.213	0.769	0.445	0.554	0.122	0.024	3.553
8	0.149	0.107	0.707	0.276	1.219	1.129	0.664	2.688	1.908	1.189	0.279	0.024	10.338
9	0.459	0.086	0.541	0.260	0.818	0.466	0.286	1.030	0.695	0.701	0.187	0.024	5.552
9 bis	0.630	0.095	0.098	0.054	0.315	0.224	0.216	0.622	0.448	0.348	0.139	0.015	3.203
10	0.112	0.007	0.076	0.038	0.140	0.120	0.059	0.244	0.136	0.132	0.068	0.009	1.140
11	0.093	0.009	0.121	0.073	0.190	0.195	0.101	0.414	0.169	0.210	0.074	0.007	1.656
12	0.404	0.177	0.409	0.248	0.636	0.536	0.302	1.202	0.664	0.553	0.129	0.008	5.269
13	0.641	0.943	0.249	0.187	0.569	0.316	0.368	1.073	0.568	0.410	0.124	0.015	5.464
14	3.120	1.516	0.529	0.235	0.959	0.671	0.810	2.596	1.496	1.480	0.555	0.116	14.083
15	7.199	2.543	2.888	0.848	7.070	4.440	5.194	16.323	8.816	8.190	2.881	0.381	66.774
16	7.372	3.699	8.089	3.757	14.362	12.887	7.643	28.154	21.222	27.676	6.246	0.634	141.741
17	2.006	1.864	1.587	1.005	2.838	1.524	0.537	2.983	2.393	3.206	0.826	0.234	21.003
18	0.139	0.166	0.218	0.070	0.271	0.209	0.107	0.376	0.251	0.340	0.149	0.009	2.305
19	0.170	0.139	0.282	0.115	0.411	0.338	0.287	1.264	0.687	0.475	0.054	0.013	4.236
20	0.330	0.131	0.200	0.103	0.352	0.273	0.197	0.462	0.240	0.244	0.102	0.005	2.640

Table S3 (Part 2): Complete DDX data. < LOQ = Concentration < to limit of quantification

Sample ng/g d.w.	o,p'-DDE	p,p'-DDE	o,p'-DDD	p,p'-DDD	o,p'-DDT	p,p'-DDT	∑DDX
1	0.012	1.227	< LOQ	0.004	< LOQ	< LOQ	1.243
2	0.014	5.146	< LOQ	0.003	0.008	0.019	5.190
3	0.008	0.465	< LOQ	0.002	0.001	0.002	0.477
4	0.013	0.926	< LOQ	0.008	0.002	0.000	0.950
5	0.011	1.897	0.002	0.007	0.001	0.002	1.918
6	0.008	1.730	< LOQ	0.011	0.002	0.003	1.754
7	0.007	0.912	< LOQ	0.008	0.001	0.001	0.928
8	0.013	3.173	0.002	0.004	0.002	0.012	3.205
9	0.011	1.896	0.004	0.019	< LOQ	0.007	1.936
9 bis	0.010	2.413	0.004	0.015	0.004	0.008	2.455
10	0.011	0.994	< LOQ	0.002	0.001	0.002	1.010
11	0.006	0.944	0.002	0.002	< LOQ	< LOQ	0.953
12	0.008	1.446	0.002	0.004	0.003	0.011	1.474
13	0.015	1.851	< LOQ	0.011	0.003	0.002	1.882
14	0.008	1.506	0.003	0.014	0.009	0.021	1.561
15	0.010	0.812	< LOQ	0.006	0.002	0.004	0.834
16	0.003	0.814	< LOQ	0.008	< LOQ	0.001	0.826
17	0.006	0.869	0.001	0.003	0.000	0.001	0.881
18	0.004	0.814	< LOQ	0.007	0.003	0.007	0.835
19	0.009	0.980	< LOQ	0.003	0.001	0.002	0.995
20	0.006	0.383	0.002	0.002	0.001	0.006	0.400

Sample ng/g OM	o,p'-DDE	p,p'-DDE	o,p'-DDD	p,p'-DDD	o,p'-DDT	p,p'-DDT	∑DDX
1	0.071	7.486	< LOQ	0.024	< LOQ	< LOQ	7.582
2	0.161	60.184	< LOQ	0.034	0.099	0.220	60.697
3	0.120	7.374	< LOQ	0.025	0.013	0.032	7.564
4	0.131	9.326	< LOQ	0.084	0.021	0.002	9.565
5	0.178	30.990	0.025	0.115	0.009	0.025	31.342
6	0.180	39.823	< LOQ	0.251	0.052	0.078	40.384
7	0.038	4.866	< LOQ	0.041	0.004	0.004	4.954
8	0.090	22.806	0.011	0.028	0.013	0.088	23.037
9	0.037	6.551	0.013	0.064	< LOQ	0.023	6.689
9 bis	0.040	9.283	0.015	0.057	0.014	0.032	9.442
10	0.035	3.288	< LOQ	0.008	0.004	0.008	3.343
11	0.022	3.708	0.007	0.009	< LOQ	< LOQ	3.746
12	0.082	14.023	0.023	0.038	0.028	0.106	14.300
13	0.201	25.087	< LOQ	0.144	0.043	0.028	25.503
14	0.322	58.237	0.104	0.526	0.360	0.830	60.377
15	3.651	294.194	< LOQ	2.061	0.806	1.556	302.268
16	1.118	262.163	< LOQ	2.478	< LOQ	0.376	266.134
17	0.279	37.912	0.043	0.121	0.010	0.044	38.409
18	0.029	5.747	< LOQ	0.050	0.019	0.047	5.892
19	0.222	23.209	< LOQ	0.061	0.019	0.055	23.567
20	0.110	6.886	0.029	0.038	0.023	0.103	7.187

Table S3 (Part 3): Complete HCHs and HCB data. < LOQ = Concentration < to limit of quantification

Sample ng/g d.w.	α-HCH	β-HCH	γ-HCH	δ-HCH	∑HCH	HCB
1	0.029	0.023	0.033	0.012	0.097	0.021
2	0.010	0.011	0.062	0.007	0.091	0.013
3	0.005	0.033	0.022	< LOQ	0.060	0.006
4	0.009	0.034	< LOQ	0.013	0.056	0.016
5	0.021	0.009	0.017	0.009	0.057	0.050
6	0.010	0.022	0.011	0.004	0.046	0.016
7	0.017	0.006	0.012	0.005	0.040	0.036
8	0.014	< LOQ	0.005	0.025	0.044	0.066
9	0.049	0.042	0.013	0.010	0.114	0.109
9 bis	0.017	0.019	0.104	< LOQ	0.140	0.055
10	0.021	0.009	0.004	0.059	0.093	0.081
11	0.013	0.011	0.012	0.076	0.112	0.108
12	0.020	0.005	0.015	0.011	0.051	0.009
13	< LOQ	< LOQ	< LOQ	< LOQ	< LOQ	< LOQ
14	0.007	0.007	0.114	0.023	0.151	0.025
15	0.007	0.018	0.028	0.023	0.076	0.032
16	0.005	0.008	0.081	0.000	0.095	0.015
17	< LOQ	0.029	0.034	0.036	0.099	0.071
18	< LOQ	< LOQ	< LOQ	< LOQ	< LOQ	< LOQ
19	0.016	0.085	0.082	0.017	0.200	0.043
20	< LOQ	< LOQ	< LOQ	< LOQ	< LOQ	< LOQ

Sample ng/g OM	α-HCH	β-HCH	γ-HCH	δ-HCH	∑HCH	HCB
1	0.176	0.142	0.204	0.071	0.592	0.130
2	0.121	0.134	0.729	0.081	1.065	0.149
3	0.082	0.516	0.354	< LOQ	0.951	0.095
4	0.087	0.346	< LOQ	0.133	0.566	0.163
5	0.347	0.153	0.272	0.154	0.925	0.824
6	0.229	0.501	0.258	0.081	1.069	0.363
7	0.090	0.032	0.064	0.028	0.214	0.192
8	0.104	< LOQ	0.034	0.177	0.316	0.473
9	0.170	0.146	0.046	0.034	0.395	0.376
9 bis	0.065	0.072	0.402	< LOQ	0.539	0.212
10	0.069	0.030	0.015	0.194	0.307	0.268
11	0.050	0.043	0.047	0.300	0.440	0.426
12	0.197	0.044	0.148	0.110	0.499	0.088
13	< LOQ	< LOQ	< LOQ	< LOQ	< LOQ	< LOQ
14	0.285	0.272	4.402	0.886	5.845	0.981
15	2.379	6.402	10.286	8.489	27.556	11.580
16	1.599	2.488	26.290	0.136	30.512	4.829
17	< LOQ	1.262	1.483	1.591	4.336	3.095
18	< LOQ	< LOQ	< LOQ	< LOQ	< LOQ	< LOQ
19	0.391	2.018	1.935	0.399	4.742	1.021
20	< LOQ	< LOQ	< LOQ	< LOQ	< LOQ	< LOQ

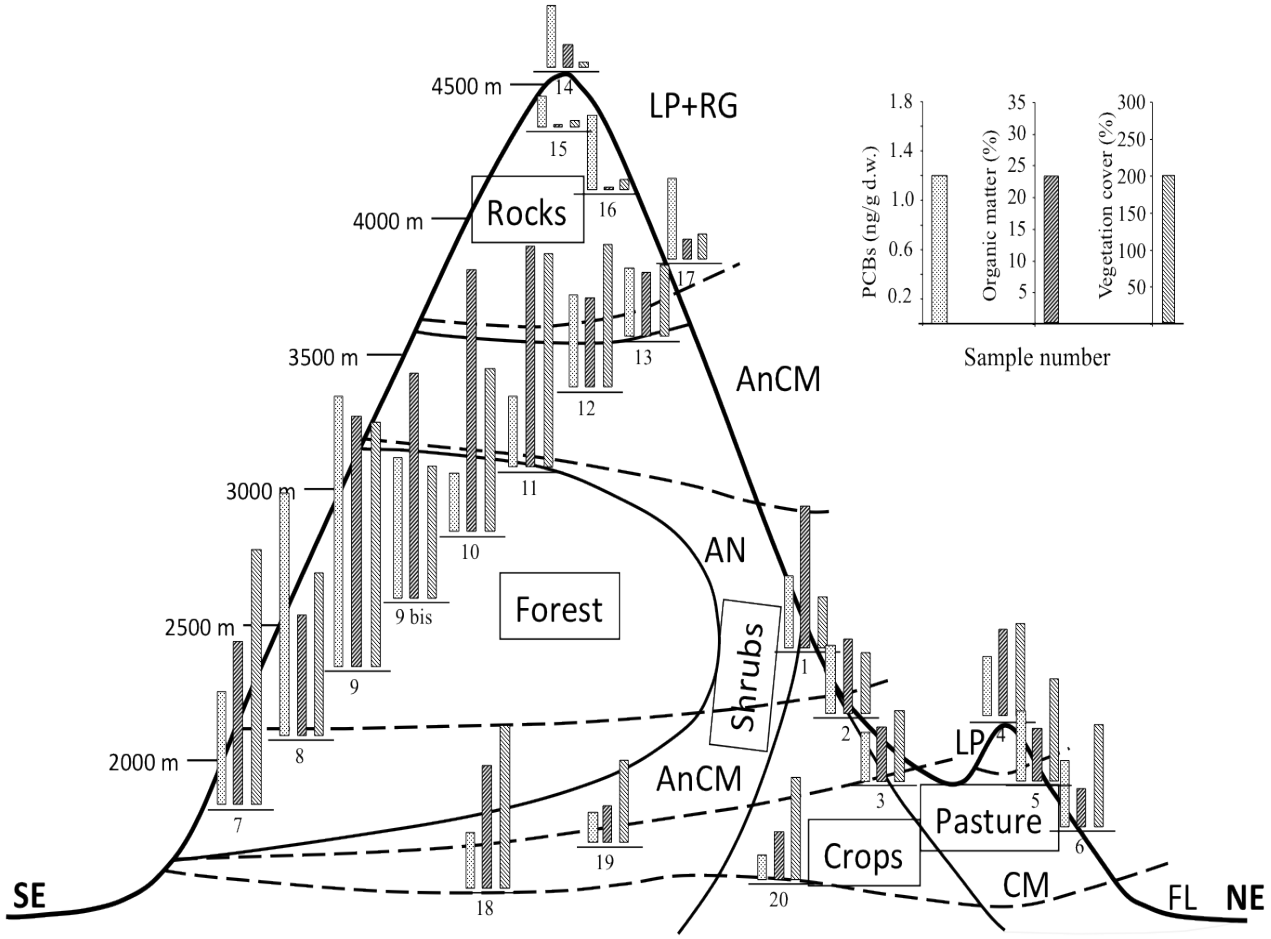

Figure S4: qualitative association between PCBs levels, organic matter and vegetation categories in our sampling sites.

Chapter VIII

Conclusion

VIII - Conclusions and future development

In this work some of the main factors that influence the partition and distribution of POPs in mountain environments and the behaviour of pollutants inside a pasture environment are evidenced. The variability of contamination at a local scale has been deeply analyzed in the main study area of the Andossi plateau, giving some useful information about the dependence of contamination from seasonality, soil and meteorological features.

With the findings of chapter II (which gave a good definition of the horizontal, vertical and seasonal variability of contamination at local scale) and the modeling of chapter III it is possible to integrate a set of simple data (about OM content and soil temperatures) with concentration data from few samples to obtain detailed maps of potential contamination and release in a mountain environment. These methods need obviously further validation and refining but could become useful tools to evaluate POPs concentrations with a high spatial and temporal definition, that may increase the accuracy of exposure and risk assessment based only on few experimental data and general environmental features. By knowing the local variability with a high definition it is possible to draw realistic pictures of concentration into complex alpine environments and evaluate exposure risk for the local fauna or for the domestic animals grazing on alpine pastures. Future work on this topic will be made to include the air contamination to better understand the factors affecting the air-soil fluxes for the definition of actual sink and/or emission areas.

In chapter IV it is reported the first field work about the different retention potential of humic substances. OM is generally considered in POPs distribution papers as a whole indistinct component of soil and its effect is only viewed as quantitative (general direct relationship between OM content and POPs concentration), but the

different retention potential of humin, humic acids and fulvic acids may change this view. Moreover the three humic substances have different behaviour in terms of mobility and general ability to distribute vertically and horizontally within the soil affecting the transport of the pollutants adsorbed. The effect of the quality of OM on the POPs distribution needs to be better assessed with future studies (not only into OM-rich alpine pasture soils but also into forest and plain soils with less organic matter content and different humic fraction composition).

Further research on these topics could lead to a better understanding of soil distribution but still gives few information about exposure for domestic animals and human beings. Our main research area was settled inside a pasture also to assess the transfer rates between the soil-air long range transport system and the vegetation-cow-milk system, which represent an important way also for human exposure. In chapters V and VI the distribution into biotic matrices has been evaluated, evidencing a strict relation between soil and vegetation contamination (taking also into account local variability due to different solar exposition) and also a good relation between POPs concentration in vegetation and milk. Seasonality of contamination and grazing location could lead to different intake of contaminants by cows and so higher or lower milk contamination. With some further work abut this topic and with the application of the contamination maps developed in chapter III it may be possible to reduce milk contamination by selecting grazing times and places that are less prone to contamination by the soil-air long range transport system.

The first POPs contamination data in the Mt.Meru area have been reported in chapter VII and some of the findings about regional scale distribution factors have been confirmed in an equatorial area. The forest filter effect and the "cold condenser effect" due to the altitude gradient were found into a mountain environment located into a zone that have the climatic characteristics of a "source" zone for POPs. The data presented in the chapter report the interesting finding of an high contamination

level in the soils near the top of the mountain that have very low OM content. The low temperature of that altitude have certainly favoured the condensation of the contaminants but it has been hypothesised that those soils have an adsorption mechanism alternative to the partitioning in the OM, typical of the volcanic ashes and probably depending by the ‘hole filling’ mode. This point need further consideration in order to reconsider the soil capacity for POPs accumulation not only in function to the OM content and composition but even in function to the mineral matter in particular the volcanic ash content and nano-porosity.